Preparation and evaluation of sorbitan monopalmitate and sunflower oil based biphasic formulation as matrices for controlled delivery

A thesis submitted in partial fulfilment

for the award of the degree of

DOCTOR OF PHILOSOPHY

IN

BIOTECHNOLOGY AND MEDICAL ENGINEERING

by

BEAUTY BEHERA

(510BM103)

Under the guidance of

Supervisor

Dr. Kunal Pal

Co-supervisor

Prof. A.K. Srivastava

Department of Biotechnology and Medical Engineering

NATIONAL INSTITUTE OF TECHNOLOGY

Rourkela-769008, Odisha, India

2014

National Institute of Technology-Rourkela

CERTIFICATE

This to certify that the thesis entitled "Preparation and evaluation of sorbitan monopalmitate and sunflower oil based biphasic formulation as matrices for controlled delivery" being submitted by Miss Beauty Behera for the award of the degree of Doctor of Philosophy in Biotechnology & Medical Engineering of NIT Rourkela, is a record of bonafide research work carried out by her under my supervision and guidance. Miss Beauty Behera has worked for more than four years on the above problem in the Department of Biotechnology & Medical Engineering, National Institute of Technology Rourkela and her work has reached the standard for fulfilling the requirements and the regulation relating to the degree. The contents of this thesis, in full or part, have not been submitted to any other University or Institution for the award of any degree or diploma.

Place: Rourkela
Date:

(Dr. Kunal Pal)
Assistant Professor
Dept. of Biotechnology & Medical Engineering
NIT-Rourkela

TABLE OF CONTENTS

ACKNOWLEDGEMENT

At this moment of accomplishment, it is easy to recognize that many people have helped me to achieve such an important stage of my life. Herein, I express my deep gratitude to all of them who have supported me throughout these years.

Foremost, I would like to express my sincere gratitude to my advisor, Prof. Kunal Pal, for his relentless encouragement, constructive guidance and words of motivation throughout the duration of my research study and moreover for the inspiration he provided to ensure the completion of this work. His expertise, availability to discuss the ideas and willingness to give of his knowledge were instrumental in my research. For this, I will be eternally grateful to him. I thank my co-advisor Prof. A. K. Srivastava for his valuable guidance and help.

I gratefully thank my Doctoral Scrutiny Committee (DSC) members, Prof. S. Paul, Prof. Amit Biswas Prof. B. C. Ray and Prof. B. K. Pal. I also acknowledge the help provided by Prof. Krishna Pramanik and her research group in the Department of Biotechnology and Medical Engineering for their valuable suggestions.

Many thanks go in particular to Prof. Sirsendu Ray, Prof. B. P. Nayak, Prof. Mukesh Gupta, Prof. A. Thirugnanam, Prof. Indranil Banerjee, and Prof. Devendra Verma for their support during the research period. Heartiest thanks to technical assistants Haladhar Behera and Rabindra Kumar Moharana, Department of Biotechnology and Medical Engineering for their help and support.

Collective and individual acknowledgments are owed to research group members and other Ph.D. scholars of the department and institute who helped me in accomplishing my research work. I gratefully acknowledge the financial support provided by the NIT, Rourkela to conduct research in the doctoral program.

I also thank my friends Sangamitra, Kanti, Mausami, Samir, Satyendra, Deepak, Chanda, Bhisham, Silu and Babita for their true and best support. Finally, I convey my heartiest thanks to my loving parents Sj. Krushna Chandra Behera and Smt. Aratibala Behera, sister Sweety, brothers Shuvrajyoti, Aditya and Pradeep for their support and love throughout my career.

Finally, I offer my sincerest gratitude and salutations at the holy feet of Paramahansa Swami Nigamananda Saraswati Dev and Shri Shirdi Saibaba for their blessings towards the work and a blissful life.

Abstract

The flexible properties of the gels make them superior candidates for the delivery of bioactive agents in cosmetics, medicine, biomaterials and food technologies. The aim of the present study was to develop bigels from the oleogel of sunflower oil and sorbitan monopalmitate for the delivery of metronidazole. The bigels were prepared by mixing oleogel with the polymer solution. Natural (proteins and polysaccharides) and synthetic polymers were used to alter properties of the bigels. Fluorescence microscope was used to study the microstructure of the bigels. The molecular interactions amongst the components of the bigels were studied by FTIR spectroscopy. The mechanical behavior of the bigels was determined using viscometer and static mechanical tester. Gel disintegration studies were carried out at pH 7.4. The thermal and electrical properties of the bigels were analysed using differential scanning calorimeter (DSC) and phase-sensitive multimeter, respectively. Goat blood and HaCaT cells were used to test the hemocompatibility and the cytocompatibility of the bigels, respectively. The antimicrobial efficacy of the drug (metronidazole) loaded bigels was studied against *E. coli*. The efficiency of the bigels as controlled delivery formulations was evaluated *in vitro*. Iontophoretic delivery of the drugs was carried out by injecting an AC current (peak current of 96.44 μA). The micrographs suggested the formation of an oleogel-in-hydrogel type of bigels. The particle size of the bigels containing proteins was smaller (4-5 μm) than the bigels containing natural polysaccharides and synthetic polymers. Hydrogen bonding was the major driving force in the formation of the bigels. The mechanical properties of the polysaccharide based bigels were better as compared to the other bigels. The firmness of starch bigels and maltodextrin bigels was found to be highest 729.4421 ± 3.1471 g and 1000.7623 ± 1.8211 g, respectively. All the bigels exhibited pseudoplastic flow and were viscoelastic in nature. The disintegration time of the bigels was dependent on the property of the polymer used. The melting endotherm of the bigels was ~46 °C. The bigels were biocompatible in nature. The drug loaded bigels showed equivalent inhibitory zones against *E. coli* as compared to the marketed formulations. The application of AC current increased the *in vitro* drug release. In conclusion the results of the study suggested that the release of metronidazole was controlled by various types of polymers and also greatly influenced by the physical and mechanical properties of the bigels.

Keywords: Oleogels, bigels, fluorescence, pseudoplastic, viscoelastic, thermal, resistance, metronidazole, iontophoresis.

LIST OF FIGURES

CHAPTER 8

CHAPTER 9

LIST OF TABLES

LIST OF ABBREVIATIONS AND SYMBOLS

Abbreviations

AC	Alternating current
ANOVA	Analysis of Variance
CMC	Carboxymethyl cellulose
CFR	Code of federal regulations
DC	Direct current
DMEM	Dulbecco's modified Eagle's medium
DPBS	Dulbecco's phosphate buffer saline
DSC	Differential scanning calorimeter
EDTA	Ethylene diamine tetra acetate
FBS	Fetal Bovine Serum
FDA	Food and Drug administration
FTIR	Fourier Transform Infra Red
ICH	International conference on harmonisation
MTT	3-[4,5-dimethyltriazol-2-y1]-2,5-diphenyl tretrazolium
MW	Molecular weight
NCCS	National centre for cell science
NCIM	National collection of industrial microorganisms
OD	Optical density
PBS	Phosphate Buffer Saline
PVA	Polyvinyl alcohol
PVP	Polyvinyl pyrrolidone
SD	Standard deviation
UV	Ultraviolet
USP	United states of pharmacopoeia

Symbols

η	Shear viscosity
γ	Shear rate
τ	Relaxation time
ω	Angular frequency
σ_{dc}	DC conductivity
A	Constant
s	Exponential factor

k_1	Rate of relaxation
k_2	Extent of stress relaxation
F^*	Asymptomatic force
F_r	Residual stress
F_0	Initial stress
S^*	Area under curve of normalized force-time plot
P(t)	Stress or force at time ‘t’
P_0	Residual stress
P_1, P_2 and P_3	Pre-exponential constants
τ_1, τ_2 and τ_3	Relaxation times in seconds
R_c	Cup radii
R_p	Probe radii
v_p	Probe velocity
C_1	Instrument constant
η_w	Dynamic viscosity of water
η_{app}	Apparent viscosity

CHAPTER 1

INTRODUCTION

1.1 Background and significance of study

A substantial amount of drug should be absorbed from the site to obtain a desired therapeutic response. An effective therapeutic response of the drug can be attained by controlling the release rate of the drug from the dosage form, rate of absorption to the site and achieving a site specific delivery [1]. These factors can be well tailored by using controlled drug delivery systems (CDDS). These systems ideally release the drug at a constant rate over an extended period of time. CDDS initially release a part of the dose from the formulation so as to attain a rapid therapeutic concentration. The remaining part is then released in a definite pattern to maintain the desired drug level [2]. The term controlled drug release implies both sustained delivery of the drug for days/weeks/months/years and also for one time delivery [3]. Various types of dosage forms like tablets, capsules, gels, suspensions are used in CDDS. Amongst all these above types, gels are getting widespread attention for the preparation of CDDS. Gels are typically classified into oleogels and hydrogels based on the nature of liquid phase entrapped [4]. Apart from oleogels and hydrogels, bigels are also used as CDDS. Bigels are often defined as composites of organogels and hydrogels. These systems appear structurally as emulsions [5]. These are a new class of biphasic soft solids whose both the phases are semi-solid in nature. The existence of these systems was first predicted by lattice Boltzmann simulations in the year 2005. Recently, bigels are gaining widespread application in topical and transdermal delivery. One such study reported increased release of diltiazem hydrochloride from bigels as compared to the hydrogel and organogel formulations [5]. The bigels of carbopol hydrogels and oleogels of sorbitan monostearate-sweet almond oil and cholesterol-liquid paraffin have also been explored [6]. As bigel contains both hydrophilic and hydrophobic phases, it acts as an efficient delivery vehicle for both lipophilic and hydrophilic bioactive agents. The synergistic effect of hydrogels and oelogels can be achieved in bigels.

Bigels of vegetable oil and sorbitan esters have been explored for topical and transdermal applications. Vegetable oils are being used in the preparation of various foods, pharmaceutical, and cosmetic products. Apart from vegetable oil, fish oil has also been used for the preparation of these types of biphasic gels [7]. This is mainly due to the functional and beneficial properties of vegetable oils apart from their inherent physical stability [8]. Vegetable oil, such as sunflower oil, is rich in vitamins and polyunsaturated fatty acids which make it an excellent candidate for drug delivery applications. Sorbitan esters are widely used in formulating pharmaceutical formulations, emulsions, solutions, oral and injectable

suspensions. The acceptable daily intake, as per FDA is about 25 mg a day [9]. Sorbitan monopalmitate (Span-40) is a sorbitan ester and has been studied as an organogelator for the preparation of organogels. It is non-ionic in nature with an HLB value of 6.7 [10]. Sorbitan monopalmitate can help in the preparation of semi-solid formulations by immobilizing apolar liquids e.g. hexane, isopropyl myristate, etc. [11].

Apart from the presence of these stabilizing agents, the effectiveness of the vigil system has been evaluated by adding various proteins, polysaccharides as well as synthetic polymers. Proteins like gelatin and whey powder have been used in many pharmaceutical and nutraceutical preparations. Gelatin, a protein, that is obtained from the hydrolysis of collagen obtained from the skin, connective tissues and bones of animals. Its biocompatibility and biodegradability make it a suitable candidate for the preparation of scaffolds in tissue engineering. Whey protein is a by-product of the food industry. It has been used as a stabilizer in the preparation of different types of emulsions. Amongst the polysaccharides, sodium alginate, sodium carboxymethyl cellulose, maltodextrin, soluble starch, xanthan gum, guar gum and gum arabic were chosen as representative polysaccharides for the preparation of the bigel. Polysaccharides such as alginates and cellulose are biochemically similar to the extracellular matrix components of the human body and hence are biocompatible. Apart from biocompatibility, these polysaccharides have easy availability. They are low-cost materials due to their abundance in nature, which in turn, makes them suitable for bigel preparation. All these polysaccharides are water soluble and are used as binders, emulsifiers, solubilizers and stabilizers in many pharmaceutical formulations. Due to these advantages, they were selected as suitable candidates for the preparation of bigels. Synthetic polymers, on the other hand, provide good mechanical stability. The synthetic polymers such as polyvinyl pyrrolidone (PVP) and polyvinyl alcohol (PVA) are non-ionic and have good hydrophilicity and biocompatibility. PVP is a biocompatible polymer that has been used in the preparation of temporary skin covers and wound dressings [12]. It is not biodegradable in the body, but may be eliminated by renal filtration if the molecular weight is not very high [13]. PVA has a good stabilizing property for various multiphase systems enabling them to be used as a physical property modifier.

So far, little information is available on these bigels for the delivery of antibiotics. Their use as matrices for iontophoresis has been studied. The current study proposes the development of bigel formulations for the delivery of metronidazole. Metronidazole is a partial hydrophilic nitroimidazole agent that inhibits anaerobic microorganisms and protozoan infections. Its poor solubility in water (10 mg/ml) makes it a candidate for prolonged delivery [14]. The

prolonged release of this drug from bigels is preferable for reducing application frequency and improving patient compliance [15].

Bigels as drug carriers for iontophoresis were also studied in-depth. Conventional iontophoretic setup uses direct current (DC) for the delivery of drugs, but it is associated with many side effects. The main disadvantage of using DC is the polarization of the electrodes which causes a tingling sensation and subsequently pain during the iontophoresis process [16]. Though the efficiency of the DC in the transportation of drug is much higher than the AC iontophoresis, the procedure is limited to a short duration (10-15 min) due to the electrochemical burns caused by the formation of hydrogen and hydroxide ions generated during DC iontophoresis. AC iontophoresis enables a longer duration of drug delivery with a negligible polarization of the electrodes and the associated disadvantages [17]. The iontophoresis usually employs a current density up to 0.5 mA/cm^2 [18]. Keeping the above facts in mind, the developed bigels were tested as matrices for iontophoretic drug delivery applications. These bigels were thoroughly characterized using various techniques. The microstructural analysis of the bigels was carried out by a light and fluorescence microscope. The physical properties were evaluated by a viscometer and a static mechanical tester. Electrical and thermal characterizations of the prepared bigels were studied in-depth. The antimicrobial efficiency of these bigels was tested against *E. coli*.

CHAPTER 2

LITERATURE REVIEW

2.1 Overview

Technology using CDDS is nowadays used both for the temporal and the spatial placement of the drugs. The objectives behind the development of the CDDS usually depend on the type of drug used and the pathophysiology of the disease (acute or chronic). CDDS is intended for those drugs with short biological half-life. The use of CDDS prevents first pass metabolism of drugs, maintains the plasma drug concentration within the therapeutic window and improves the patient compliance. There have been many formulations that have been used for CDDS. Examples of such types of formulations are tablets, gels, implants, and devices. The primary mechanisms that control the release of drugs are membrane and matrix diffusion, osmosis and biodegradation.

Use of gels in CDDS is gaining significant attention. A gel is defined as a semisolid system, containing a solvent, either hydrophobic or hydrophilic, immobilized within the spaces available in a three-dimensional network structure [19]. The tunable mechanical properties of the gels make them superior candidates for the delivery of bioactive agents in cosmetics, medicine, biomaterials and food technologies [20]. Gels also act as good moisturizing agents for skin [21]. According to the nature of the liquid phase, gels may be differentiated into hydrogels and organogels (oleogels). In a hydrogel, the liquid phase is aqueous, whereas, in an oleogel the liquid is lipophilic. Besides hydrogels and oleogels, some other types of gels (figure 2.1), such as emulgels, bigels and aerogels are also reported for dermal application of drugs. The present review discusses the different types of the gels with an emphasis on bigels and their applications in various fields.

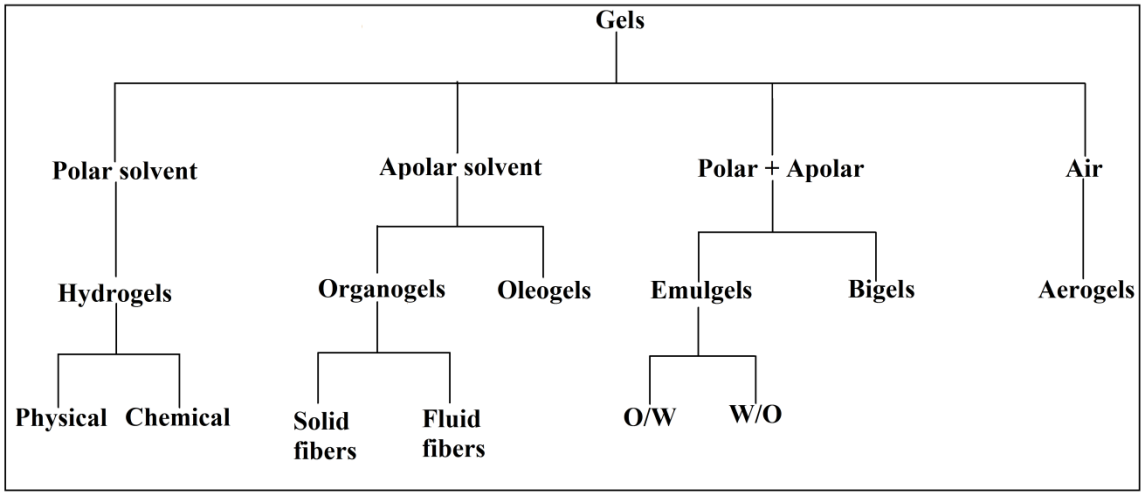

Figure 2.1: Classification of gel

2.2 Organogels

Organogels or oleogels are gels containing apolar (e.g. chloroform, alcohol, dimethyl sulfoxide, hexane, etc.) liquids or oil (e.g. cod-liver, olive, groundnut, castor oil, etc.), respectively, as the liquid phase. The liquid is entrapped within a three-dimensional solid network structure. The solid-like network is formed from either low-molecular-weight components (LMOG) or polymers, which are collectively known as organogelator. Apart from these, many waxes including candelilla wax, rice bran wax, carnauba wax and sugarcane wax have also been investigated as organogelators for transdermal delivery of lipophilic drugs [22]. Apart from the above gelators, lecithin (phospholipids obtained from egg yolks) has also been used for the preparation of organogels. These organogels are biocompatible and are thermodynamically stable. The thermoreversible nature, resistance to microbial contamination and insensitivity to moisture make these organogels a suitable carrier for drug delivery [23].

The interactive forces that govern the formation of the three-dimensional network in the organogels include hydrogen bonding, van der Waals (hydrophobic) and π-stacking interactions. Organogels are usually formed by two mechanisms (figure 2.2). The first mechanism involves the formation of organogels by a solid fiber gelator network. In this method, the gelator is heated in an apolar solvent until it is completely solubilized. The temperature is then decreased below the crystallization temperature of the gelator. The gelator molecules start precipitating and self-assemble by physical interaction to form solid aggregates. These aggregates form a 3D network which immobilizes the solvent. In the second mechanism, organogels are obtained from the fluid-filled structures. In this method, the organogels are formed by the addition of polar solvents to the surfactant solution in apolar solvents that leads to the formation of reverse micelles. The reverse micelles form structures of different shapes which undergo aggregation to form 3D networks, to immobilize the solvent. Both of these mechanisms cause the formation of networks by non-covalent interactions. The major difference between these types of the organogels lies in the stability of the formulations. Organogels of solid fibers are usually strong, as compared to fluid filled structure organogels, due to the presence of large junction points.

The release of drug from the organogels occurs mainly by diffusion and surface erosion. The diffusion of the drug from these organogels is further controlled by many other factors like pH, temperature, electric field, light, etc. One such type of mechanism of drug release was observed from the stearyl-acrylate organogels. When these organogels were heated above

their melting temperature, there was a reversible transformation from ordered crystalline structure to disordered amorphous structure. This type of reversible transformation further allows the release of drugs by diffusion [24]. The release of drug from Eudragit L based organogels was dependent on the surface erosion of the matrices [25]. The erosion may occur either from the bulk or from the surface. The erosion makes the matrices more porous, thereby, allowing the easier passage of the drugs across the matrices [26]. The absorption of the drugs through the stratum corneum from the organogels is a sequential process. The surfactants and phospholipids present in the organogels get absorbed into the stratum corneum and increase the tissue hydration. The hydration of the tissues consequently increases the drug permeation [27].

Organogels have a wide area of application in the pharmaceutical field. The major advantage of using organogels in the drug delivery application is their ability to enhance the drug penetration through stratum corneum. This may be explained by the presence of various components, e.g., fatty acids, glycols, surfactants and terpenes, which are established chemicals to promote permeation of drugs through the skin.

Sorbitan monostearate isopropyl myristate-water organogel has been used for *in vitro* nasal delivery of propanolol hydrochloride [25]. Organogels are also used for parenteral administration of drugs [28]. One such study was conducted where tyrosine-based organogels was used for the delivery of rivastigmine to treat Alzheimer's disease[29]. Oleogels using N-stearoyl L-alanine methyl ester organogelator in safflower oil was used for subcutaneous delivery of rivastigmine [30]. Gelatin based w/o microemulsion based organogels was used to deliver cyclosporine (immunosuppressant drug) [31]. Some literature has proposed the preparation of organogel-based niosomal gels for the delivery of lipid soluble vitamins and antigens [32]. Lecithin organogels have been used for the topical delivery of many therapeutically active molecules such as hormones, NSAIDS, amino acids, local anesthetics, antifungal agents, peptides and vitamin A and C [33].

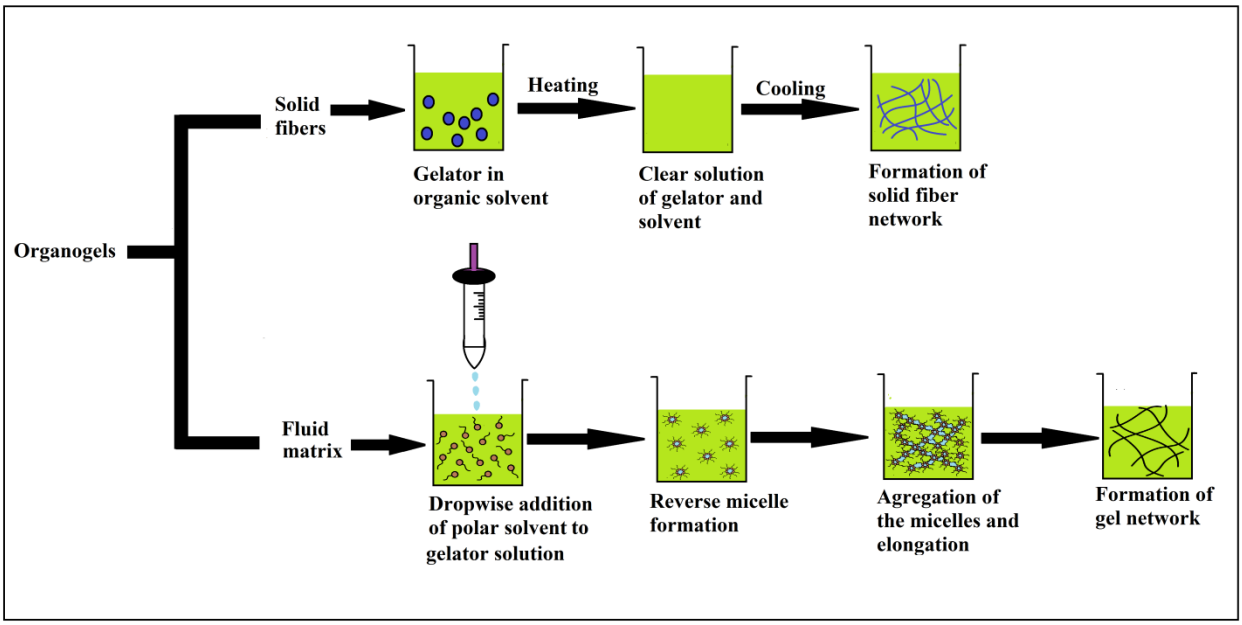

Figure 2.2: Types of organogels and their mechanism behind formation

2.3 Hydrogels

Hydrogels contain an aqueous dispersion medium, gelled with a suitable hydrophilic gelling agent. They include three-dimensional hydrophilic polymer network that can absorb large quantities of water [34]. In CDDS, hydrogels have been used as smart delivery systems. Hydrogels may be designed to alter their microstructure by giving either physical or chemical stimuli. The physical stimuli include electric and magnetic field, temperature, light, sound and pressure. The chemical stimuli that influence the hydrogel working include pH, enzyme, ions and molecular recognition events.

The mechanism of hydrogel formation involves chemical or physical crosslink of the gelator molecules. The gelators for hydrogel preparation are hydrophilic. Hydrogels formed from physical crosslinks are known as ‘reversible’ or ‘physical’ hydrogels (figure 2.3). The physical hydrogels include crosslinks such as entanglements, crystallites, van der Waals interactions or hydrogen bonding. Hydrogels formed from chemical crosslink are known as ‘‘chemical’’ or ‘‘permanent’’ gels which are formed via covalently bonded crosslinked networks [20]. The chemical hydrogels differ from the physical ones in many aspects. Chemical hydrogels as compared to the physical hydrogels have a low swelling capability and a high crosslink density.

The release from the hydrogels occurs mainly by two different mechanisms, i.e., diffusion and chemical stimulation. Diffusion of the drug occurs across the polymer matrix. It is usually dependent on the concentration gradient of the drug built inside the hydrogel and the

environment. The release of the drugs may also occur by bulk erosion of the hydrogel matrix. In the case of chemically stimulated gels, swelling is the primary factor that governs the release of drugs. Swelling of hydrogels occurs in response to external conditions like temperature, pH or by enzymatic action [35]. This kind of release is well accepted for targeted drug delivery. In general, drug release via diffusion is more common for localized and non-specific drug release whereas drug release by chemical stimulation is applied mainly for oral drug delivery system [34].

There is a progressive increase in the application of hydrogels in biomedical sciences, i.e. in cell encapsulation, tissue repair and in the controlled delivery of growth factors. The discovery of hydrogels prepared from acrylated poloxamine, poloxamine hydrogels, and polymerized oligolactides led to a significant application in drug delivery as well as tissue engineering [36]. pH and temperature sensitive hydrogels have been used for the controlled delivery of proteins and calcitonin. Some examples of pH and temperature sensitive hydrogels are PAA (polyacrylamide) and PMA (polymethacrylate) hydrogels. These types of hydrogels were used for the development of colon-specific drug delivery systems. pH-sensitive hydrogels of N-isopropylacrylamide have been used for the delivery of antithrombotic agents [37]. Hydrogel-based niosomes and proniosomes have been studied as potential carriers for transdermal delivery of drugs [38].

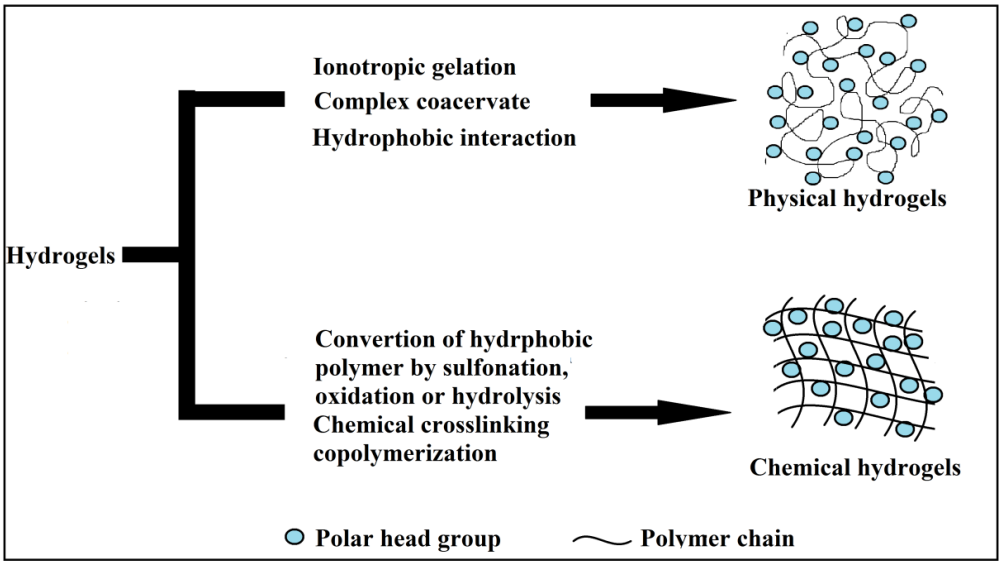

Figure 2.3: Various methods in the formation of physical and chemical hydrogels

2.4 Aerogels and xerogels

Aerogels and xerogels are also known as inorganic gels because both these gels are composed of silica [39]. Both aerogels and xerogels are prepared by sol-gel process. Xerogels are

obtained by drying wet silica gel under normal pressure. Aerogels, on the other hand, are formed by supercritical fluid technology. In this process, the liquid within the hydrogel or lyogel (polysaccharide gels based on organic solvents) is replaced with air or other gases. The supercritical fluid technology works by raising the pressure of the liquid within the gel above the vapour pressure of the liquid leading to the formation of gels with little shrinkage and high porosity [40]. Aerogels are more flexible in terms of their structure, pore size and surface area than xerogels. As xerogels are prepared by a normal drying process, these gels have a changed morphology as compared to the aerogels (figure 2.4). Drying under normal condition causes shrinkage and results in the formation of a dense matrix. These materials have small pore size as compared to other gels.

Apart from silica aerogels, organic polysaccharide aerogels have been reported by some authors [41]. The commonly used polysaccharides for the preparation of aerogels are cellulose, nitrocellulose and agar [41]. Aerogels and xerogels as delivery systems have the capability to enhance the solubility of the drugs and their bioavailability by manipulating their release kinetics [42]. They have been used in the form of device or disc in CDDS. The mechanism of prolonged delivery of drugs from these formulations is diffusion mediated [43].

Silica aerogels have a high drug loading capacity due to their large surface area [44]. Aerogels of silica have been used for the dermal delivery of dithranol. Polyethylene glycol hydrogel coated aerogels have been used for the controlled delivery of ketoprofen [45]. Hydrophilic aerogels of silica have been tried for the delivery of ketoprofen and griseofulvin. The adsorption of these drugs led to an increased dissolution rate [46].

Aerogels have several advantages. The drug release kinetics can be tailored by modifying the surface of the aerogel [47]. The volume and pore size of the aerogel can be easily changed. Their biocompatibility and nontoxic nature make them suitable systems for enzyme immobilization, waste treatment, biosensors and drug release [48]. Apart from the above aerogels also allow faster dissolution of drugs [49]. Researchers have shown that ionically cross-linked multi-membrane alginate aerogels increased the loading as well as prolonged the release of nicotinic acid [50]. Silk fibroin aerogels have been reported to extend the release of ibuprofen [51]. Alginate aerogels have shown to increase the release of poorly soluble drug in the upper gastrointestinal tract [52]. Mechanically stable whey protein aerogels were found to have pH controlled swelling behavior and sustained the release of ketoprofen in both stomach and intestine [53]. Highly porous aerogels from nanofibrillar cellulose were prepared for the

delivery of beclomethasone dipropionate. The study revealed that the release of the drug was controlled by altering and modulating the structure as well as the matrix of the aerogel, respectively [54].

Xerogels are porous, resorbable materials that have been used for the delivery of low molecular weight antibiotics like vancomycin [55]. Xerogels are non-toxic and biocompatible in nature [56]. Silica xerogels have been studied in subcutaneous drug delivery, where they have been evaluated as drug implants [57]. The discs of silica xerogels have shown to sustain the release of toremifene citrate for 42 days [58]. Studies have shown that the drug release of dexamethasone was controlled in silica xerogel [59]. Silica xerogels loaded with gentamicin for the elimination of Salmonella from liver and spleen delayed the release of drug for 5 days [60]. Implants of silica xerogels were found to be non-toxic in liver and kidney thus making them a suitable candidate for the sustained delivery of drugs [61]. The drug release from these type of xerogels can be controlled by altering the precursor, concentration of catalyst and also the drying temperature [62]. A study was reported where it was found that lidocaine hydrochloride release can be easily controlled by substituting tetraethoxysilane with organosilanes [63]. Studies have also indicated that the biological activity of heparin was retained after its encapsulation within silica xerogels [64]. Xerogels of sodium diclofenac prepared by sol-gel method were found to be resistant to gastric pH [65]. Chitosan-silica xerogels have been used as a membrane material for the bone regeneration. These xerogels were found to have good mechanical properties and cellular response apart from the higher rate of bone regeneration in rats [66].

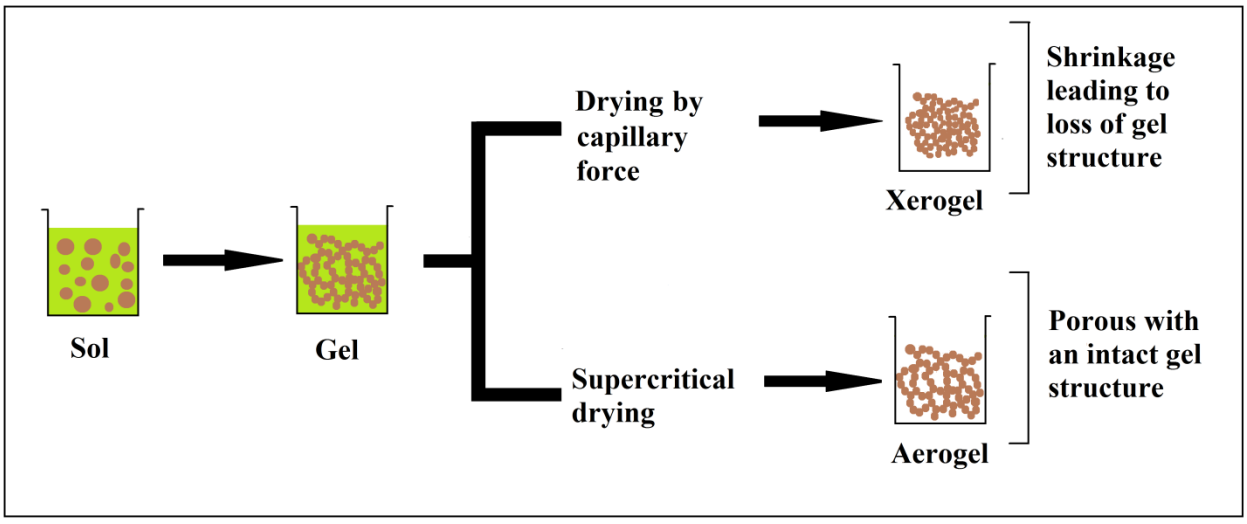

Figure 2.4: Effect of drying on aerogel and xerogel structure

2.5 Emulgels

Emulsions gels (emulgels) are highly viscous, elastic biphasic systems which have been widely used in the areas of food, pharmaceutical, cosmetic, paint and petroleum industries. The stability of the emulsions is enhanced by the addition of substances known as emulsifiers. The emulsifiers prevent the coalescence or coarsening of the droplets (dispersed phase) by reducing the interfacial tension. The commonly used emulsifiers in food and pharmaceutical industries include proteins, surfactants, and solid particles [67]. The emulsifiers are amphiphilic in nature which get adsorbed at the liquid-liquid interface to form a protective layer. The size of the solid particles used as emulsifiers usually range from nanometer to micrometer. These types of emulsions are termed as pickering emulsions. These types of solid-stabilized emulsions provide more mechanical rigidity to the droplet as compared to the other emulsions [68]. Another form of an emulsion is the emulgel. Most of these gel systems contain a high amount of surfactant and are anisotropic. The gelled emulsion are highly concentrated systems with a high internal phase volume ratio (0.74) [69]. These are comprised of tightly packed droplets of the dispersed phase. The radii of the droplets are few microns. These droplets are separated by a thin film of the continuous phase. Emulsion gels are prepared by mixing oil, water, non-ionic surfactant and a gelling agent [70].

The formation of emulsion gels is influenced by the property of the non-ionic surfactants. The properties of non-ionic surfactants are dependent on the temperature. These surfactants form micelles at low temperature, and at higher temperature there is a transformation to reverse micelles. At the transition temperature, the surfactant phase coexists both with the water and the oil phase and results in the formation of soft emulsion gels [71]. The mechanism of protein based emulsion gels also occurs in a similar manner. The gels of proteins are formed by heating the protein stabilized emulsions above a certain temperature. This method causes the adsorbed proteins to unfold partially and expose some reactive amino acids, which are inaccessible in native (folded) proteins. These reactive amino acids then participate in the formation of crosslinks between proteins present in the interfacial film and that in the aqueous phase. These crosslinks consist of both physical and chemical bonds. The chemical bond responsible for the crosslink formation includes disulfide linkages. The physical crosslinks are formed by electrostatic, hydrophobic and hydrogen bonding. These crosslinks help in tailoring the mechanical properties of the interfacial film and also hinders

coalescence. The other advantage is that these crosslinks enable the formation of a 3D solid network that helps in the formation of textured emulsions [72].

There are two classes of emulsion gels depending on the dispersed and continuous phase, one being the water-in-oil (W/O) and the other oil-in-water (O/W). The emulgels can also be classified into adhesive and non-adhesive depending on the forces acting between the droplets of dispersed phase. Adhesive emulgels are those emulsions that do not relax and maintain a high degree of packing due to the presence of attractive forces between droplets. The non-adhesive emulgels, on the other hand, relax in such a way that the emulsion dilates to the state of non-deformed droplets [73]. The emulgels have widespread application in pharmaceutical, cosmetic, and food industry.

The mechanism of drug release from these systems is also governed by diffusion. The internal phase of the emulgels acts as a reservoir for the active compounds, which slowly releases the drug into the external phase. The drug finally permeates through the skin by both intercellular and intracellular penetration.

Emulgels were introduced to overcome the problem associated with the delivery of the hydrophobic drugs. Emulgels are prepared by the addition of the gelling agent in the external phase, thereby, converting a classical emulsion into an emulgel. These emulgels have several favorable dermatological properties. They are thixotropic in nature, and their greaselessness, spreadability, removability, emollient properties, long shelf-life and a pleasing appearance make them preferable over the other gel systems [74]. Emulgels have a high patient acceptability. Studies reported that emulgels from carbopol and HPMC were easy to prepare and had a high diffusion as well as absorption rates [75]. Emulgels are excellent vehicles for skin care products for protection against ultraviolet A and B (UVA/UVB radiation) [76]. Table 2.1 summarizes the characteristic features and the available commercial products of the above-discussed gels.

Table 2.1: **Summary of types of gels and their major feature with examples of commercial products**

Formulation types	Characteristic feature	Indications	Commercial products	Refer--ences
Organogels/ Oleogels	Organic solvent or oil entrapped in the 3D network of organogelator	Skin care-Acts as emollient bases, moisturizing agents	Gilugels, Phlogel organic (lecithin organogel)	[77]
Hydrogels	3D network of hydrophilic gelling agents containing water	Antimicrobial	Aursta, transgel	[78]
Aerogels	Inorganic gels of silica produced by supercritical drying	No pharmaceutical preparation are currently available	Aerosil	[79]
Emulgels	Comprises of a hydrogels or oleogels with any emulsion type and a surfactant	Anti-inflammatory, and antifungal	Voveran, Voltaran, Miconaz-H	[80]

2.6 Bigels

Bigels consists of two immiscible fluid phases which are individually stabilized by independent gelators. The immobilization of the liquid phase causes a marked reduction in the interfacial free energy [81]. Due to the microarchitecture of the bigels, the bigels can thus be regarded as biphasic gels. Bigels have several other features that make them a suitable candidate for various applications in pharmaceutical and biomedical industries. As compared to the major drawbacks of the listed gels in Table 2.2, the bigels have better acceptability. One important reason for choosing bigels is to provide a synergistic effect of both hydrogels and oleogels. Due to the combination of hydrogels and oleogels, bigels can be used as vehicles for simultaneous delivery of both hydrophilic and lipophilic drugs. Their easy

method of preparation prevents the high cost incurred during the development of other CDDS such as nanoparticles, liposomes, etc.

Table 2.2: Advantages and drawbacks of different kinds of gels

Advantages	Drawbacks	Reference
Organogels		
❖ There is an absence of polymorphic transformation. ❖ A large amount of lipophilic drug can be incorporated into organogels.	❖ The delivery of hydrophilic compounds is difficult. ❖ Their poor washability and oily texture make them poor vehicles for cosmetic application.	[24, 82-83]
Hydrogels		
❖ Hydrogels are an ideal candidate for the preparation of soft biotissue and scaffolds. ❖ The water content of these systems makes them a suitable candidate for cell culturing.	❖ Hydrogels of polysaccharide origin are prone to microbial contamination. ❖ They are difficult to sterilize. ❖ Act as good delivery systems for hydrophilic agents. ❖ They possess a low mechanical strength.	[20, 84]
Aerogels		
❖ They are highly porous.	❖ Poor mechanical and thermal stability. ❖ High cost of preparation.	[85-87]
Emulgels		
❖ They have a good consistency. ❖ They are easily spreadable, greaseless and have emollient properties.	❖ They cause skin irritation. ❖ Bubble formation during the preparation of emulgels.	[88-89]

Bigels are prepared by suspending the gelator in a single-phase of a two immiscible fluid mixture. The single phase is obtained by increasing the temperature of the liquid mixture to a critical temperature, where the fluid pair is miscible. The temperature is then lowered (quenched) to induce phase separation, commonly known as spinodal decomposition. During quenching to low temperatures, the spinodal decomposition increases and separates the liquid

mixture. This decreases the interfacial area due to phase coarsening (caused by interfacial tension). The spinodal decomposition process results in the deposition of the gelator particles at the interface of the two immiscible phases and causes the arresting of droplet coalescence. These types of the systems have the ability to withstand unequal stresses and form a stable structure having different anisotropic shapes [90]. The gel structures, formed after the arresting of the coalescence, are made up of two interpenetrating gels. The structure of a bigel is difficult to predict as it results from an out of equilibrium process.

As reported earlier in the literature, bigel formation occurs when there is an equal volume ratio of the two liquids. Formation of pickering emulsions occurs when one fluid is present in the majority [91]. Pickering emulsions usually contain unconnected particle stabilized droplets distributed in a second continuous fluid phase while the bigels show an interface between the two continuous fluid phases, which is covered by particles [92]. Although there is a slight difference in the bigel and pickering emulsions, some authors have also reported that bigels are a type of pickering emulsions [93]. Another class of bigels is reported in the literature. They are known as bridged bigels. Bridged bigels are rich and complex multiphase systems. These bigels differ from the conventional bigels in their bicontinuous spinodal-like structure, which is stabilized mechanically by jamming at the spinodal interface. The droplets tend to form bridges in one liquid phase [94]. The mechanism of formation of bridged bigels is based on double demixing of the different phases present in the system (figure 2.5). The figure explains the demixing of two fluids after spinodal decomposition. During the demixing of the fluids the colloidal particles partition in the respective fluids resulting in the formation of a network like structure. These types of systems have introduced new intriguing observations, for future research.

The mechanism behind the formation of the biphasic gels of oleogel and hydrogel mixture is not yet well identified. In some literature, it has been reported that bigels result from high shear mixing of oleogels and hydrogels [7]. The high shear mixing tends to break up one phase into droplets and disperses it into another phase.

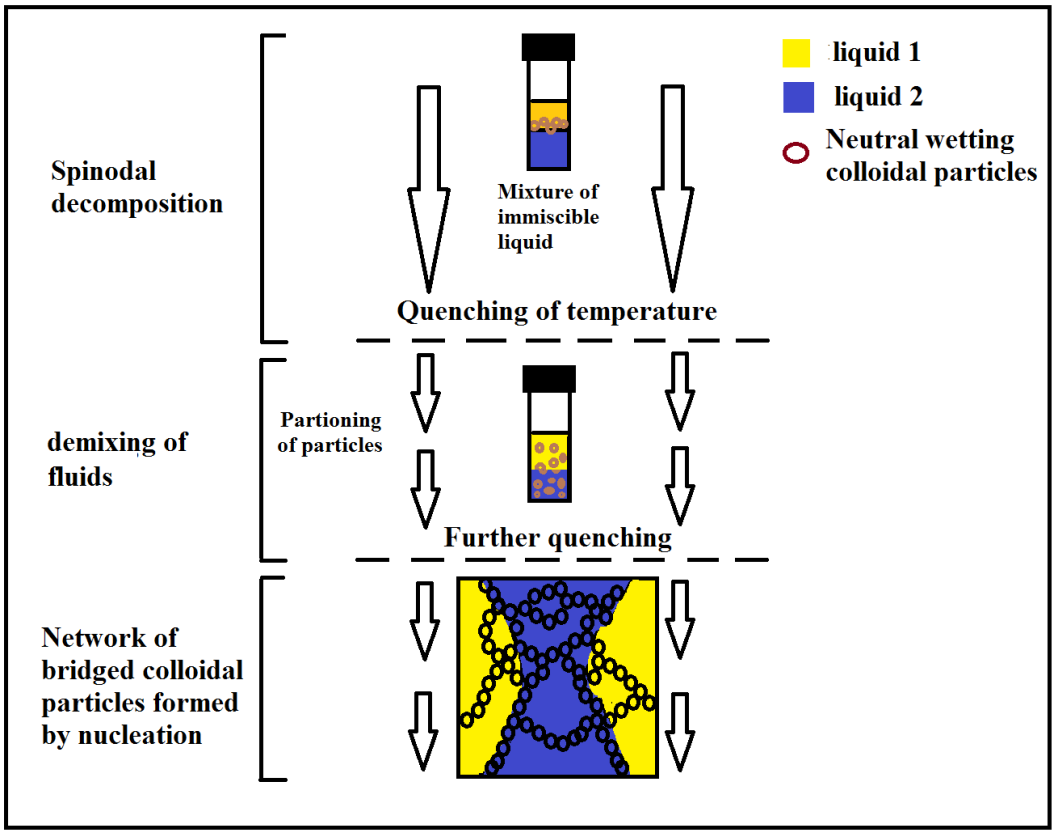

Figure 2.5: Mechanism of formation of bridged bigels

2.7 Advantages of bigels

There are several advantages of bigels. The shear modulus of the bigels can be varied over a wide range of frequency by changing the process parameters and the concentration of the gelator. The networks formed by the particles are stable over a long period. As reported earlier in literature, the bigels are more resistant to strain as compared to the other gels when prepared in same volume fraction of the two phases. This can be attributed to the fact that in one component gel, the stress relaxes easily with respect to bigels where the stress remains constant [95]. These classes of gels have highly tunable elasticity [96]. Bigels have a cooling and moisturizing effect. They are easily spreadable and provide enhanced hydration of the stratum corneum. The easy water washability of these formulations makes them suitable for topical delivery of bioactive agents.

The mechanism of drug penetration into the skin from the bigels occurs in a similar manner as that of hydrogels and oleogels. The mechanism of drug release through the bigels usually is a combination of diffusion from the hydrogels as well as penetration enhancement due to the presence of fatty acids in the oleogels or organogels [97]. Some authors have used bigels for the preparation of stimuli-responsive material. These gels contained two layers, one being

controlled layer that was sensitive to the environment stimulus and the other being the non-responsive substrate layer [98].

As bigels are composed of both organogels and hydrogels, they contain a gelator for the organogel and a gelling polymer that is usually used in the hydrogel phase. The polymers employed in the preparation of the bigels may be of natural or synthetic origin. The synthetic polymers that have been used for the preparation of bigels are carbopol, polyvinyl pyrrolidone, polyvinyl alcohol, etc. Bigels of carbopol polymers have gained wide attention. Many authors have prepared carbopol bigels from the oleogels of sweet almond oil and liquid paraffin. The bigels were physically stable and provided a cooling effect on the human skin. These gels also showed good emollient property [97].

The natural polymers that have been used in the preparation of bigels are mainly comprised of celluloses. Examples of cellulosic polymers that have been used in the preparation of the bigels are xanthan gum and sodium carboxymethyl cellulose. The use of polysaccharide based bigels has been explored for probiotics delivery [99]. Apart from natural and synthetic polymers, proteins have been used for the preparation of bigels. Amongst the proteins available, gelatin has been widely used. Its biodegradability, biocompatibility, low cost of production as well as its commercial acceptability makes it a suitable candidate for the preparation of the bigels.

2.8 Pharmaceutical applications of bigels

Recently bigels are gaining widespread use in topical as well as transdermal delivery. Bigels were reported to increase the release rate of diltiazem hydrochloride as compared to the hydrogel and organogel preparation of the same drug [5]. The developed bigels showed a higher permeation across the rabbit skin than the corresponding organogels of the same drug. The bigels of carbopol hydrogels along with oleogels of span 60-sweet almond oil and cholesterol-liquid paraffin have also been explored [6]. These bigels enhanced the moisturizing effects, thus making them promising candidates for topical application. Bigels of various polysaccharides have been reported to increase the viability of the probiotics. The bigels of N-isopropylacrylamide (NIPAAm) gel and polyacrylamide (PAAM) gels were prepared for the development of polymer gel actuator. These gels were used to study the adhesion by the silica particles [100]. Recently, edible bigels have been developed from gelatin and maltodextrin for the first time. These edible bigels contained various strains of microorganisms like yeast and *L. bulgaricus*. The study revealed that the presence of microbes altered the rheological properties of the gels to a larger extent [101]. Bigels of

testosterone are commercially available as anti-inflammatory and antimicrobial formulation [102]. The bigels are suited for the preparation of the crosslinked polymer scaffold by the selective polymerization of one continuous phase [103]. Bigels have potential applications in catalysis of chemical reaction [104]. Bigels have been used in the development of templates comprising of macroporous and composite materials [105].

CHAPTER 3

SCOPE AND OBJECTIVE

The present study focuses on the preparation of bigels using sorbitan monopalmitate/sunflower oil oleogels for controlled delivery applications. The present investigations included:

(a) To study the effect of polymers (proteins: whey protein, gelatin; polysaccharides: maltodextrin, starch, sodium alginate, and sodium carboxymethyl cellulose: synthetic polymers: polyvinyl alcohol and polyvinyl pyrrolidone) on the physical and mechanical properties of bigels,
(b) To ascertain the biocompatibility of the bigels,
(c) To determine the ability of the bigels to be used as delivery matrices for drugs (e.g. metronidazole), and
(d) To evaluate the ability of these bigels for iontophoretic drug delivery.

CHAPTER 4

MATERIALS AND METHODS

4.1 Materials

Sorbitan monopalmitate (FDA approved 21 CFR), xanthan gum and PVP K30 (MW-40000) were purchased from Loba Chemie, Mumbai, India. Edible grade sunflower oil, (Gold winner®) was procured from NCS Industries Pvt. Ltd, Kakinada, India. Whey powder was obtained as a gift from V.R.S. foods, Malanpur, Sahibabad, India. Sodium carboxymethyl cellulose and acacia gum were obtained from RFCL Limited, New Delhi, India. Gelatin, sodium alginate (Viscosity-1% w/v solution, 25 °C: 5.5 ± 2 cps), maltodextrin (dextrose equivalent, DE 20%), PVA (MW-115000), rhodamine B, nutrient agar, and broth were purchased from Hi-media laboratories, Mumbai, India. Starch soluble and guar gum were procured from Merck Specialities Pvt. Limited, Mumbai, India. Fluorol yellow 088 was purchased from Sigma-Aldrich, USA. Metronidazole was obtained as a gift from Arti drugs, Mumbai, India. All the chemicals were used as received.

Microbial culture of *E. coli* was obtained from NCIM, Pune, India. Dulbecco's phosphate buffer saline (1X DPBS), and Trypsin-EDTA solution 1X were procured from Hi-media laboratories, Mumbai, India. HaCaT cell lines were procured from NCCS, Pune, India. Absolute alcohol was purchased from Changshu Yangyuan Chemical, China.

For sanitization purposes, 70% (v/v) alcohol was used wherever necessary. Double distilled water was used throughout the study.

Detailed specifications of the materials used have been provided in Annexure 1.

4.2 Preparation methods

The preparation methods of the bigels are described in the respective chapters.

4.3 Characterization of the gels

4.3.1 Evaluation of microstructure

Light and fluorescence microscopy

The microscopic analysis of the oleogels and emulgels was carried out using an LEICA-DM 750, compound optical microscope, Germany.

The bigels were observed under fluorescence microscope (Optika, model XDS-3FL, Italy). Rhodamine B 1% (w/w) and fluorol yellow 088 1% (w/w) were dissolved in water and oil phases, respectively, during the preparation of the bigels.

Particle size distribution

The droplet size distribution of all the bigels was calculated from the micrographs using ImageJ software v 1.43 (NIH, USA). The span of the distribution was calculated from the following equation 4.1:

$$\text{Span} = \frac{d_{90} - d_{10}}{d_{50}} \quad (4.1)$$

where, d_{90}, d_{10} and d_{50} are the average diameter of 90%, 50% and 10% droplet population

4.3.2 Physico-chemical, thermal, electrical and mechanical evaluation

FTIR spectroscopy

The bigels were analyzed physicochemically using an ATR-IR spectrometer (AlphaE ATR-FTIR, Bruker, Germany) in the range of 450-4000 cm^{-1}.

Viscosity analysis

A controlled stress cone-and-plate viscometer (Bohlin Visco 88, Malvern, UK) with a cone angle of 5.4° and plate diameter of 30 mm was used to determine the viscosity of the freshly prepared formulations. The gap between the cone and the plate was set to 0.15 mm. A solvent trap was used to prevent the moisture loss. All the measurements were carried out at room temperature (20-23 °C). Ostwald-de Wale power law mathematical model (equation 4.2 and equation 4.3) was used to analyze the flow behavior of the gels.

$$\eta = k\gamma^{n-1} \quad (4.2)$$

Taking log on both sides the above equation becomes

$$\log \eta = \log k + (n\text{-}1) \times \log \gamma \quad (4.3)$$

where, η=shear viscosity, K=consistency index, n=power law index and γ = shear rate.

n-1 is the slope and k is the intercept on y-axis for log η vs. log γ profile.

Mechanical analysis

The mechanical analysis of the bigels was carried out using a TA-HD plus Texture Analyzer (Stable Micro Systems Ltd, Surrey, UK). Mechanical parameters of the gels (such as firmness, stickiness, work of cohesion, work of adhesion and gel strength) were analyzed from the resultant force vs. time plots. The parameters of the tests conducted have been listed in Table 4.1.

Table 4.1: Texture parameters and test condition for gels

Type of Fixture	**Parameters**	**Testing conditions**			**Mode of study**
		Pre test speed (mm/sec)	**Test speed (mm/sec)**	**Post test speed (mm/sec)**	
HDP/SR spreadability rig with 45° conical perspex probe	Firmness Stickiness Spreadability	-	1	1	Button (20 mm)
	Stress relaxation	1	0.5	10	Auto force (5g, 5mm)
Backward extrusion	A/BE back extrusion rig	-	1	1	Button mode (20 mm)

Firmness, work of shear, stickiness, and work of adhesion were the parameters that were used to differentiate the products. Firmness was measured in terms of maximum force (g) required to compromise the integrity of the gels. Stickiness is the maximum force that is necessary to overcome the attractive forces between the surface of the sample, and the surface of the probe, while in contact with one another. This is an important textural property of many confectionery or gelled products such as jams and cheese.

The work of shear was calculated in terms of total force required to carry out the shearing process and is a characteristic feature of semisolid preparations. It is a measurement of the

spreadability of the samples. Spreadability is defined as the ability of the product to spread and deform with ease and uniformity. As reported earlier in literature, work of shear is also the reciprocal of spreadability.

The viscoelastic properties were determined using stress relaxation studies. For this, Peleg and Normand model (equation 4.4) was used.

$$\frac{(F_0\text{-}F(t))t}{F_0} = k_1 + k_2 t \tag{4.4}$$

where, F_0 is the maximum force and F (t) represents the force at a particular time. k_1 and k_2 represent the rate and extent of stress relaxation, respectively.

According to this model, solid materials have k_2 values close to unity. An in-depth analysis of the viscoelastic parameters was carried out by calculating S^* and F^*. F^* is the asymptotic residual force. Equation 4.5 was used to calculate the S^* values and quantify the decay in the force with respect to time. The S^* value, in other words, was the area under the curve, obtained after normalization of the force-time plot of the stress relaxation study.

$$S^* = \int_a^b P(t).dt \tag{4.5}$$

where, 'a' and 'b' are the lower and upper limits of the time, respectively

$$F^* = \frac{F_r}{F_0} \tag{4.6}$$

where, F_r= Residual stress and F_0= Initial stress

The percent stress relaxation of the gels was calculated from the following equation 4.7.

$$\%\ \text{Stress relaxation} = \left(\frac{F_0\text{-}F_r}{F_0}\right) \times 100 \tag{4.7}$$

The stress relaxation study was fitted to Maxwell Weichert model (figure 4.1) in order to know the change in stress with time. This model contains Maxwell elements, a spring and a dashpot that are connected in series (the exponential terms). The spring was connected in parallel to the Maxwell elements (asymptotic residual stress at a long time) [106-107]. The equation 4.8 was used to define the Maxwell model.

$$P(t) = P_0 + P_1 e^{\frac{-t}{\tau_1}} + P_2 e^{\frac{-t}{\tau_2}} + P_3 e^{\frac{-t}{\tau_3}} \tag{4.8}$$

where, P(t) represents the stress or force at time 't'

τ_1, τ_2 and τ_3 are the relaxation times in seconds, P_0 represents the residual stress (fraction of original stress) and P_1, P_2 and P_3 are pre-exponential constants so that, $P_0 + P_1 + P_2 + P_3 = 1$.

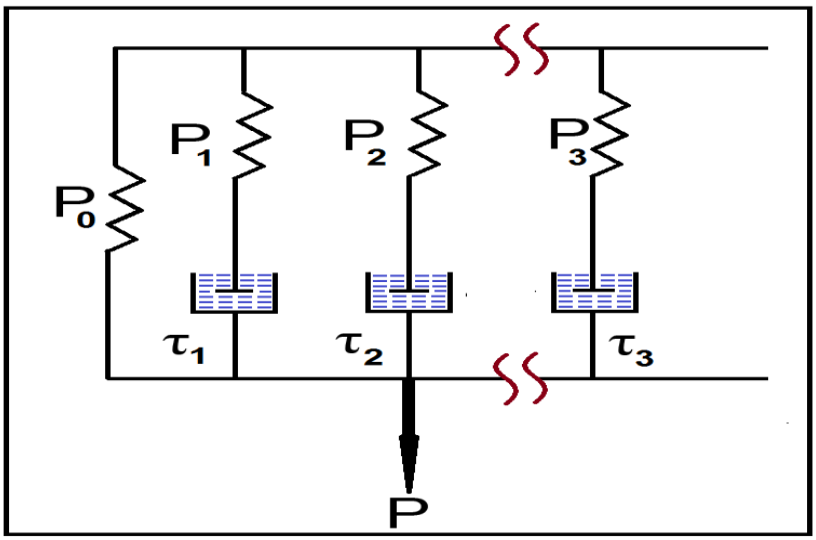

Figure 4.1: Weichert model describing the springs and dashpots

The backward extrusion study was conducted at 30 ^{o}C to calculate the apparent viscosity (η_{app}) of the polymer sols (equation 4.9). The viscosity of water (η_w) was taken as a standard. The η_{app} of the molten polymer sols at 30 ^{o}C was calculated as per the equation 4.10 [108].

$$\eta_{app} = \frac{R_c^{\,2} - R_p^{\,2}}{2\pi R_c^{\,2} C_1 v_p} \times \left(df / dx \right) \tag{4.9}$$

$$\eta_{app} = \eta_w . K \times \frac{\left(df_a / dx_a \right)}{\left(df_b / dx_b \right)} \tag{4.10}$$

where,

$$K = \frac{R_c^{\,2} - R_p^{\,2}}{2\pi R_c^{\,2} C_1 v_p}$$

The df_a/dx_a and df_b/dx_b is the slope of the force *vs.* distance curve of the hydrogels and water, respectively, as the probe moves out of the sample. The R_c and R_p cup and probe radii v_p is the probe velocity and C_1 is the instrument constant. The η_w of water was taken as 0.000798 Pas at 30°C.

Gel disintegration studies

The disintegration of the bigels was studied in phosphate buffer (pH 7.4). The test was carried out in a USP disintegration apparatus. 2 g of the bigels was used for the study. To

simulate the GIT conditions, bigels are subjected to intestinal pH 7.4 at 37 ± 2 °C. Disintegration time for the bigels does not provide any details about the stability of the bigels. This is a study to estimate the duration of the solubilisation of the gel in a particular liquid. The time recorded for the complete disintegration and solubilisation of the bigels were noted. Solubilisation here refers to the complete dissolution of the gel in the media. The solubilisation was assessed by visual examination of the buffer turning milky white.

Thermal analysis

The thermal properties of the emulgels and the bigels were evaluated using differential scanning calorimeter (DSC-200F3, MAIA, Netzsch, Germany) over a temperature range of 25 °C and 120 °C at a heating rate of 1 ºC/min. 10-15 mg of bigels was used for the study. The analysis was performed under inert N_2 atmosphere.

Electrical analysis

A phase-sensitive multimeter (PSM 1735, Numetriq, UK) was used to study the electrical properties of the bigels in a frequency range from 0.1 Hz to 1.0 MHz. The bigels were first sealed in vials of capacity 1.5 ml, and an AC voltage of 100 mV was applied. All the measurements were conducted at room temperature. The variation of the AC conductivity σ' (ω) of the gels with frequency (ω) was expressed using Jonscher's power law model. This is also known as AC universal law (equation 4.11)

$$\sigma'(\omega)=\sigma_{dc}+A\omega^{s} \qquad (4.11)$$

where, ω is the angular frequency, σ_{dc} is the frequency independent conductivity (DC conductivity). A and s are constants and exponential factor, respectively.

4.3.3 *In vitro* cytotoxicity of dialyzed formulation components

The *in vitro* cytotoxicity of dialyzed formulation components of the gels was checked by hemocompatibility and cytotoxicity studies.

Hemocompatibility studies

The gels, placed in a dialysis tubing (MW cut-off = 12kda), were equilibrated in 50 ml of saline at 37 °C for 30 min. 0.5 ml aliquots of the extracts were mixed with 0.5 ml of citrated goat blood diluted with normal saline (prepared in 4:5 ratio), followed by the addition of normal saline (9 ml). The positive control (+ve) was prepared by adding 0.5 ml of 0.1 N hydrochloric acid to 0.5 ml of diluted blood, whereas, the negative control (-ve) was prepared by adding 0.5 ml of saline to 0.5 ml of diluted blood. The final volume was made up to 10 ml

using saline. Thereafter, the test, the +ve control, and the –ve control were incubated at 37 °C for 1 h. After incubation, the samples were subsequently centrifuged at 3000 rpm for 10 min. The supernatant was siphoned off and analyzed at 545 nm using UV-visible spectrophotometer (UV 3200 double beam, Labindia). % hemolysis was calculated from the following equation 4.12:

$$\% \text{ Hemolysis} = \frac{OD_{Test} - OD_{Negative}}{OD_{Positive} - OD_{Negative}} \times 100 \qquad (4.12)$$

where, OD_{Test} = Optical density of test sample, $OD_{Positive}$ = Optical density of +ve control and $OD_{Negative}$ = Optical density of -ve control.

***In vitro* cytotoxicity studies**

HaCaT cell lines were used to carry out the cytocompatibility tests. HaCaT cells are non-tumorigenic keratinocyte cell-lines that retain their differentiation potential. These cells can be easily grown and passaged indefinitely. These cells have been used as a model for many cytotoxicity studies [109]. The cells were maintained at 5% CO_2, 95% humidity and 37 °C in DMEM supplemented with 10% fetal bovine serum. The cells were washed with 1X Dulbecco's Phosphate Buffer Saline and Trypsin-EDTA solution during passaging. After washing, the cells were harvested. Trypan blue dye exclusion test was used to assess the viable cell density in the harvested culture. The cells were then seeded onto 96 well plates in a concentration of 5 x 10^4 cells/ well and the seeded plate was kept under incubation for 12 h to promote the adherence. The leachants, at a concentration of 10 µg/ml were added to the cells and further incubated for 24 h. The cell viability was determined using MTT Assay. The assay is based on the principle of MTT reduction (3-[4, 5-dimethylthiazol-2-yl]-2, 5-diphenyltetrasodium bromide) to a dark-blue formazan crystal in the presence of active mitochondria of living cells.

4.3.4 Applications of the bigels

***In vitro* antimicrobial studies**

The antimicrobial efficacy of the bigels was studied against *E. coli*, model gram-negative bacteria. The antimicrobial activity was determined by agar diffusion assay. Firstly, 1.3 g of nutrient broth was dissolved in distilled water and sterilized at 121 °C, 15 psi for 15 min in an autoclave. The autoclaved broth was then allowed to cool to room temperature in laminar air flow. Fresh colonies of bacterial strains (1 ml) were inoculated into 100 ml of nutrient broth

and incubated overnight at 37 °C ± 1 °C in a shaker incubator. The final volume was adjusted to 5 × 10^5 CFU/ml. Thereafter, 28 g of nutrient agar was dissolved in 1000ml of distilled water sterilized under the same condition as nutrient broth. 10 ml of the media was poured into petri plates (diameter of 10 cm) and allowed to set in laminar air flow. Inoculums of 100 µl was spread on the agar plates with a sterilized spreader. Wells of diameter 5 mm were bored with a borer and then filled with 0.1 g of the bigels. Wells containing marketed formulation of metronidazole were used as positive control. The culture plates were incubated at 37±1 °C for 24 h. The zone of inhibition was measured using a ruler or vernier caliper. Marketed preparation of metronidazole Metrogyl® (Dosage form-1% gel, Dose-Apply, and rub in a thin film of Metrogyl gel twice daily to affected areas after washing) was used as a reference.

Solubility determination of metronidazole:

1.5 g of the drug was weighed and added to a volumetric flask containing 50 ml of phosphate buffer (pH 7.4). The flask was kept on overnight stirring (100 rpm) at 37±1 °C. The solution was filtered the next day, and the amount of drug dissolved was analyzed spectrophotometrically at λ_{max} = 321 nm using a UV-vis spectrophotometer (UV-3200, LabIndia, Mumbai, India) [110].

***In vitro* drug release studies**

The effect of the polymers on the metronidazole release from the gels was studied. 1.5 g of the gels was tied in dialysis tubing and dipped in the receptor compartment, which contained 50 ml of phosphate buffer (pH 7.4). The whole setup was maintained at 37 ± 1 °C and 100 rpm**.** To maintain the sink condition, the entire receptor fluid was replaced with fresh phosphate buffer (pH-7.4) at predetermined intervals. The amount of metronidazole released was measured spectrophotometrically at λ_{max} = 321 nm using a UV-vis spectrophotometer (UV-3200, LabIndia, Mumbai, India). Marketed formulation of metronidazole Metrogyl® (Dosage form-gel, Dose-Apply, and rub in a thin film of Metrogyl gel twice daily to affected areas after washing) was used as a reference.

Iontophoretic application of the bigels

The bigels were tested as matrices for iontophoretic delivery applications. The iontophoretic drug release studies were performed using a modified Franz's diffusion cell designed in -house. Stainless steel electrode (diameter = 1 cm) was used for the study. The electrode was connected to the donor, containing drug loaded bigels. The donor and the receptor chambers

were separated using a pre-activated dialysis membrane. The receptor contained 30 ml of phosphate buffer. The iontophoretic driver circuit injected an AC current having a peak current of 96.44 μA. This resulted in the peak current density of 0.122 μA/cm^2. The study was conducted for 2 h. 3 ml of the receptor volume was sampled at regular intervals of time (15 min). The receptor fluid was replaced with 3 ml of fresh phosphate buffer. The samples were then analyzed spectrophotometrically.

4.4 Statistical analysis

All the experiments were performed in triplicate. Data was prepared as the mean ± standard deviation (S.D.). Significant differences between them were determined using ANOVA single factor. The $p < 0.05$ was considered to be a statistically significant difference.

CHAPTER 5

Preparation and characterization of emulgels from sorbitan monopalmitate and sunflower oil based oleogels

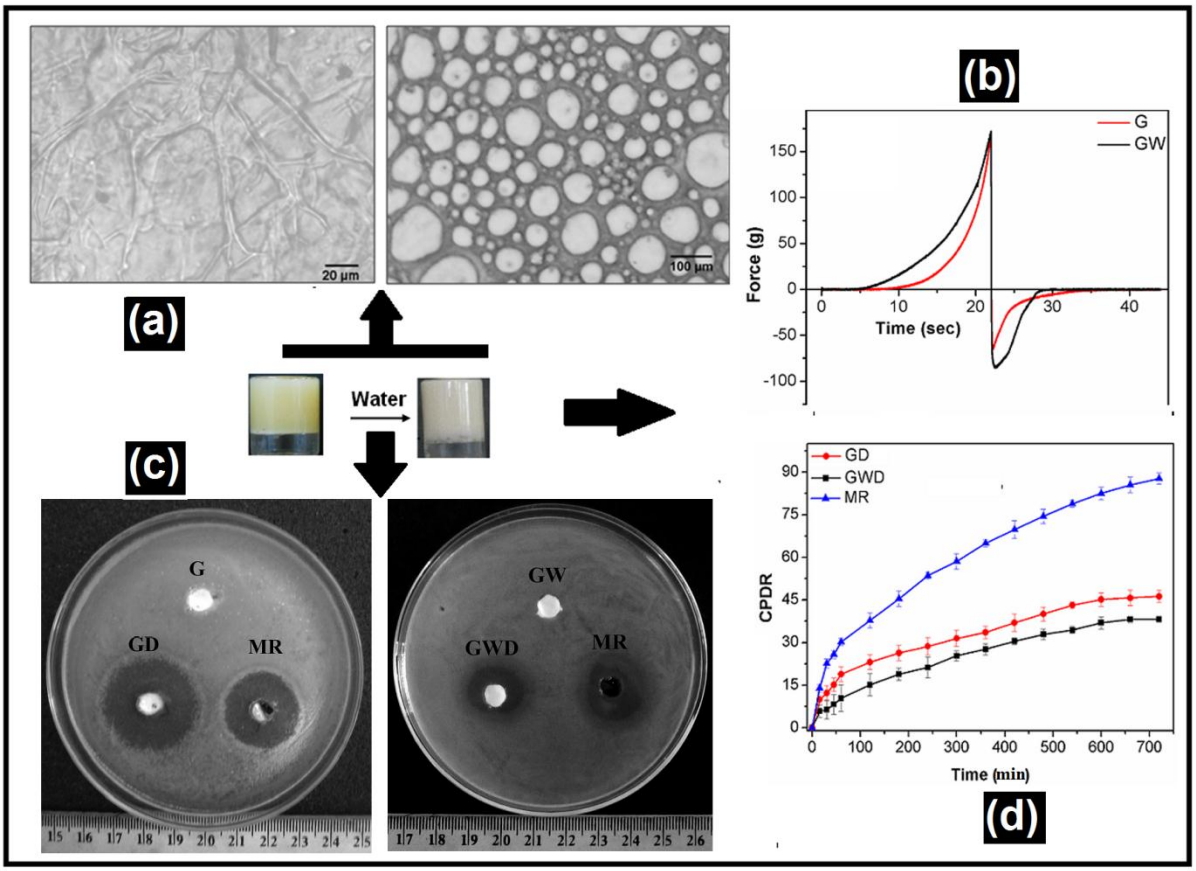

Graphical outline: (a) Fluorescence micrographs, (b) firmness (c) antimicrobial efficiency and (d) *in vitro* release properties of oleogels, and emulgels

Overview

Oleogels and emulgels of sunflower oil and sorbitan monopalmitate were prepared for the delivery of metronidazole. The emulgels were prepared by adding water dropwise to the sunflower oil-sorbitan monopalmitate mixture at 50 °C and subsequently cooling the mixture to room temperature. The microstructural analysis of the gels was carried out using a bright field and fluorescence microscope. The molecular interactions within the oleogels and emulgels were studied using FTIR spectroscopy. The mechanical properties of the gels were evaluated by a static mechanical tester. The gel disintegration studies were carried out at pH 7.4. A differential scanning calorimeter and phase sensitive multimeter were used to study the thermal and electrical properties of the gels, respectively. The *in vitro* cytotoxicity of the gels was checked using HaCaT cells. *E. coli* was used to test the antimicrobial efficiency of the drug loaded gels. The *in vitro* release studies were conducted in phosphate buffer (pH 7.4). The oleogels (G) were found to be pale yellow in color while the emulgels (GW) were white in color. Both types of gels were thermoreversible in nature. The microscopic analysis revealed the presence of rod-shaped tubules, responsible for the formation of G. GW showed the presence of oil droplets distributed uniformly in the aqueous phase. FTIR studies indicated the presence of intermolecular hydrogen bonding, responsible for gel formation. The firmness of emulgels (172.1127 ± 4.1175 g) was higher than oleogels (170.1043 ± 2.9867 g). All the gels showed pseudoplastic flow behavior. The disintegration time of GW (57 ± 1.54 min) was slightly higher than G (55 ± 2.22 min). The melting endotherm of both G and GW was observed at ~47 °C. The conductivity of GW was higher than G. Metronidazole-loaded gels showed good antimicrobial properties against *E. coli*. The drug release was slightly lowered in emulgels (38.18%) than the oleogels (43.12%). The p values of the antimicrobial studies and *in vitro* drug release profile between the marketed and the test preparations were less than 0.05. Based on the preliminary results, the developed gels may be tried as delivery vehicles for various bioactive agents.

5.1 Introduction

Of late, there has been an increased use of vegetable oils for the production of various food, cosmetic, and pharmaceutical products. This is mainly due to the functional and beneficial properties of vegetable oils apart from their inherent physical stability [8]. One such product is thermo-reversible organogels, a semi-solid product having apolar phase as the continuous phase. They are often also known as lipogels or oleogels [111]. They are usually prepared by dissolving low molecular weight gelators (MW < 3000), in concentration above critical gelation concentration (CGC), in hot apolar liquids followed by lowering the temperature of the hot gelator solution below the sol-to-gel transition temperature ($T_{sol\text{-}to\text{-}gel}$) [112]. These gels are viscoelastic in nature. The properties of these gels have been found to be dependent on the composition of the oils and fats used [113]. Though various studies on the use fatty acid esters as organogelators have been reported, unfortunately not much emphasis has been paid to the use of sorbitan monopalmitate as an organogelator. Sorbitan monopalmitate, a fatty acid derived ester (figure 5.1), is a non-ionic emulsifier having an HLB of 6.7, which makes it a good candidate to promote water-in-oil emulsion [10]. It has been reported that sorbitan monopalmitate can help developing semi-solid formulations by immobilizing apolar liquid [11].

Sunflower oil is highly rich in vitamin E and omega- 6 polyunsaturated fatty acids (prone to oxidative degradation). The degradation may be reduced by converting them into highly cohesive gel matrix [114]. Due to this property, sunflower oil has been often used in devising matrices for controlled delivery of bioactive agents [115].

Taking inspiration from the above, attempts have been made to develop oleogels using sorbitan monopalmitate as the organogelator and sunflower oil as the apolar liquid. Further attempts were also made to improve the stability of the sorbitan monopalmitate-sunflower oil oleogels by incorporating water into the gelled structure.

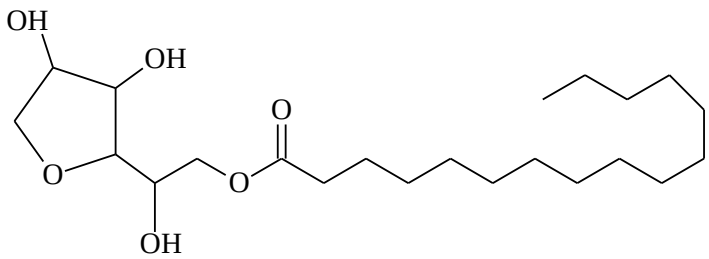

Figure 5.1: Structure of sorbitan monopalmitate

5.2 Experimental

5.2.1 Preparation of the emulgel

A homogeneous solution of sorbitan monopalmitate in sunflower oil was prepared by stirring the mixture at 50 °C. The transparent solution was subsequently cooled to room temperature for 2 h. The concentration of sorbitan monopalmitate was varied from 1% (w/w) to 25% (w/w) to find out the critical gelation concentration (CGC). CGC is the minimum concentration of sorbitan monopalmitate required to immobilize sunflower oil. The CGC was found to be 18% (w/w), and the sample was regarded as G. The gelation of the sunflower oil was confirmed by inverted-tube method (figure 5.2) [116]. The effect of water on the properties of organogel was studied by adding 5 g of water to 5 g of G. The mixture was kept on stirring (12000 rpm) at 50 °C. The samples were cooled to room temperature for 2 h and were regarded as GW. No significant differences in the pH of the formulations were observed. The pH of GW was found to be 6.7.

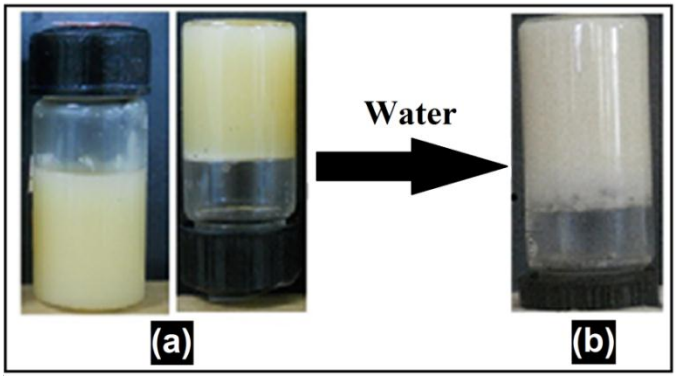

Figure 5.2: Inverted-tube method showing the gel formation (a) G and (b) GW

5.3 Results and discussion

5.3.1 Microscopy and microstructural analysis

The light micrographs revealed that individual tubules of sorbitan monopalmitate join to form a networked structure. A similar mechanism of self-assembly of the organogelators to form tubules has been reported earlier in the literature [117]. Figure 5.3 shows the micrographs of the formulations as the concentration of gelator increased during the determination of CGC. The micrographs of the formulations containing 2% (w/w) gelator showed the presence of circular structures. The formulations containing 5% (w/w) gelator showed clusters of particles of sorbitan monopalmitate having variable size and shape. As the concentration of the gelator increased to 10% (w/w), needle-shaped crystals were observed. Further increase in the gelator concentration to CGC, these needle-shaped crystals grew and formed

interconnecting networked structures. These interconnected networked structures were responsible for the immobilization of the apolar phase. This was attributed to the surface active interactions amongst the gelator and apolar phase [118].

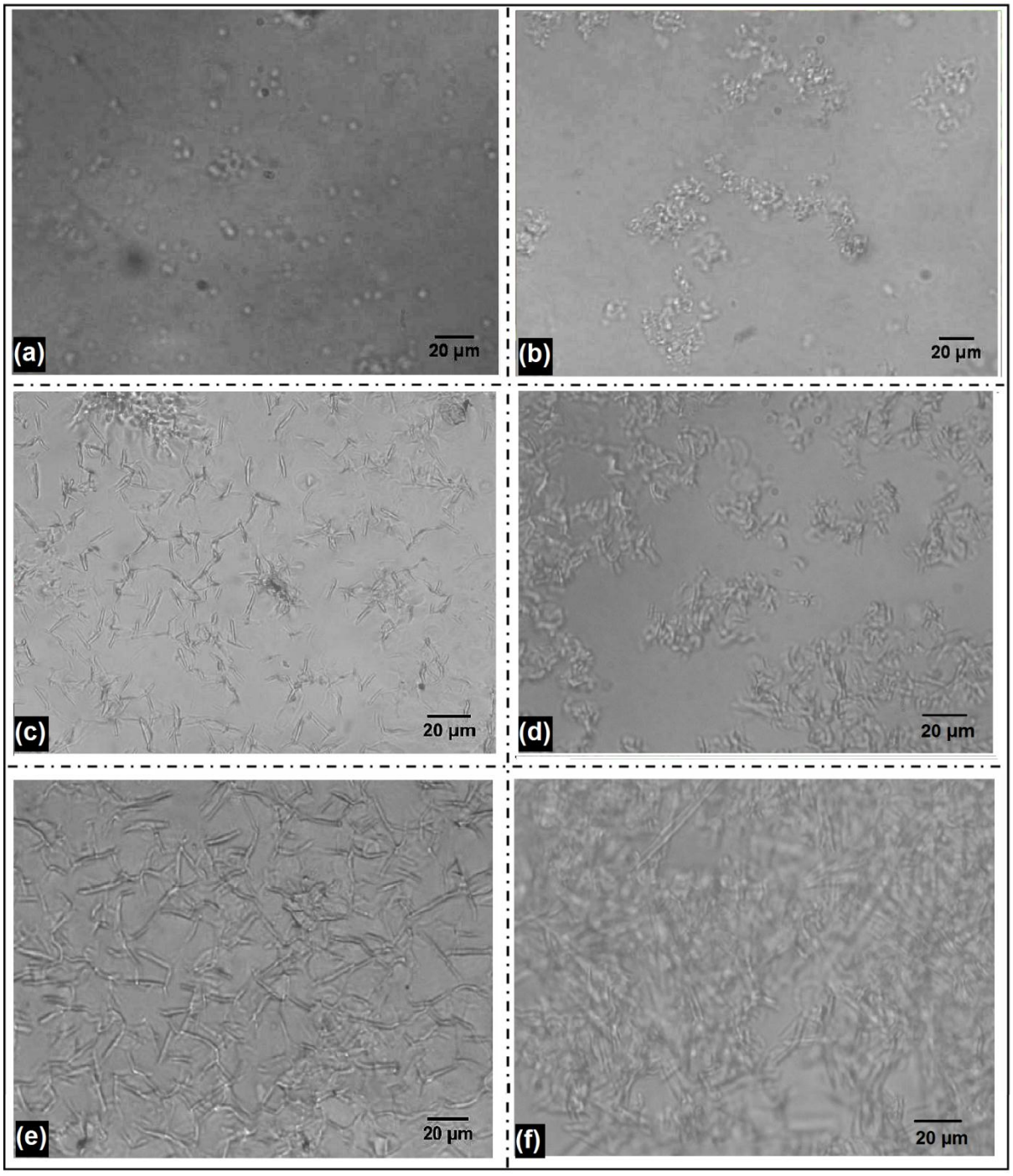

Figure 5.3: Light micrographs of oleogels showing the mechanism of gelation with the increase in the concentration of the gelators (a) 2%, (b) 5%, (c) 10% (d) 15% (e) 18% and (f) 20% of gelator

The gelator molecules formed fiber-like structures which entangled with each other to form a 3D networked structure. This phenomenon was seen in figure 5.4a. The GW emulgel showed a uniform distribution of oil droplets (figure 5.4b). The aqueous phase was distributed as droplet indicating the formation of O/W emulgels which was confirmed from the fluorescence micrographs of the emulgels (figure 5.4c).

The GW emulgels showed a broad size distribution (figure 5.5d). The average droplet size of GW was found to be 3.32 ± 0.81µm.

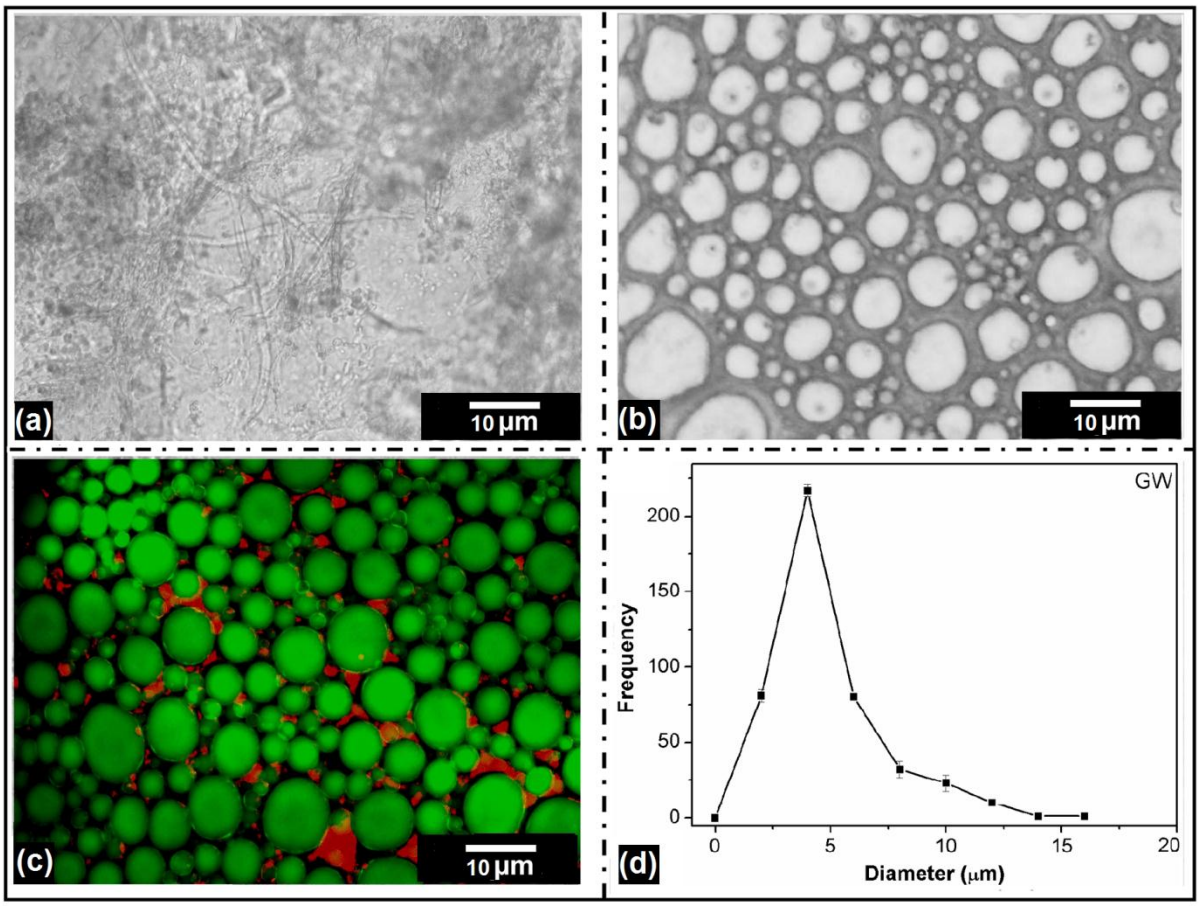

Figure 5.4: Light micrographs of (a) G, (b) GW, (c) fluorescence micrographs of GW and (d) size distribution of GW

5.3.2 FTIR analysis

FTIR studies give information about the nature of chemical interactions (figure 5.5). Sunflower oil showed an absorption peak at ~3008 cm^{-1}, which may be was associated with the stretching vibration of cis olefinic, C=H present in fatty acids [119]. The absorption peaks at ~2920 cm^{-1} and ~2850 cm^{-1} were due to CH asymmetric and symmetric stretch in CH_2 and CH_3, respectively [120]. This indicated the presence of highly ordered trans zig-zag conformation of aliphatic hydrocarbon chain in the sunflower oil [121]. Absorption at ~1743

cm^{-1} indicated the presence of stretching vibration of CO in the ester group of triglycerides present in sunflower oil [122]. The CH_2 and CH_3 scissoring vibrations were observed at ~1460 cm^{-1} and 1373 cm^{-1} [123]. Absorption at ~1733 cm^{-1} in sorbitan monopalmitate indicated the carbonyl absorption of ester group [124]. Sorbitan monopalmitate showed an absorption peak at ~1172 cm^{-1} that may be attributed to the CO symmetric stretching vibration due to the sugar group present in sorbitan monopalmitate. Intramolecular hydrogen bonding amongst the sorbitan monopalmitate molecules was confirmed by the presence of the absorption peak at ~3391 cm^{-1} [125]. The gels also showed peaks at ~3391 cm^{-1}, which indicated the presence of the intermolecular hydrogen bonding amongst the gel components. A shift to the higher wavenumber (~2922 cm^{-1} and ~2853 cm^{-1}) of CH asymmetric and symmetric stretch in CH_2 and CH_3, respectively, in gels, showed the presence of gauche conformers in the hydrocarbon chain often associated with the high degree of disorderliness [126].

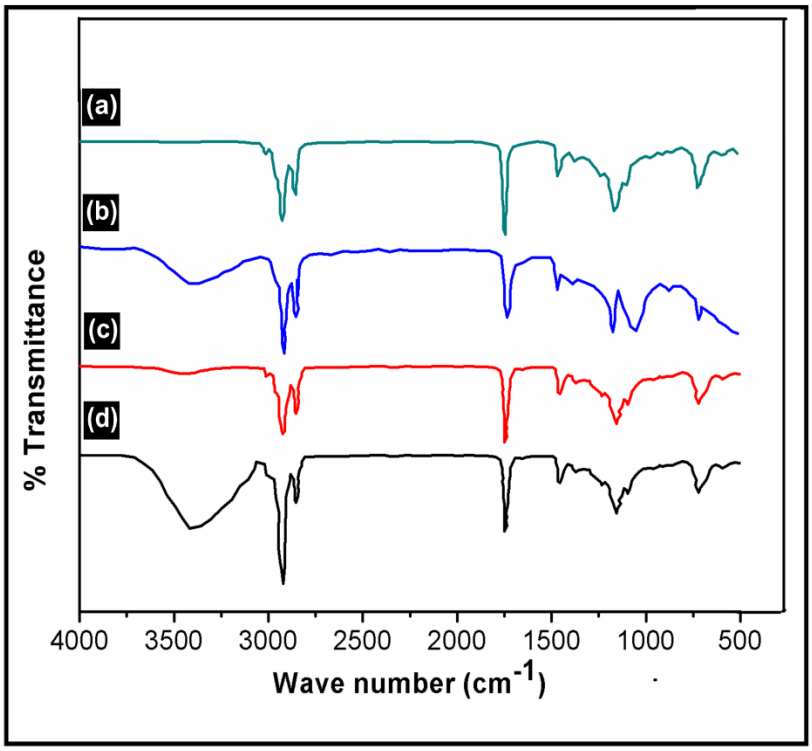

Figure 5.5: FTIR of (a) sunflower oil, (b) sorbitan monopalmitate, (c) G and (d) GW

5.3.3 Viscosity analysis

The gels showed shear-thinning property, i.e., the viscosity of the gels decreased as the shear rate was increased (figure 5.6a). Gels intended for topical pharmaceutical and cosmetic applications are expected to have shear thinning property. This property ensures the formation of a thin layer of the formulation over the skin surface, which is necessary for

efficient delivery of bioactive agents [127]. Apart from the above, a higher viscosity at low shear rates ensures long term stability during storage, as the higher viscosity of the formulation reduces the chances of phase separation. FTIR results suggested the formation of hydrogen bonding during gelation. Comba and Sethi (2009) reported that these interactions are progressively disrupted under the influence of increased shear stress, which is responsible for the flow of the gels at higher shear rates [128]. The viscosity of the GW was higher than G. This may be attributed to the formation of a more ordered structure as water was incorporated in G. The ordered structure can be explained by the ordering of the water molecules (clathrates) at the oil-water interface. The power law indices (n) were calculated in the shear rate range of 13.07-97.42 s^{-1} (Table 5.1, figure 5.6b). The results showed that n < 1, indicating the pseudoplastic rheological behavior of the gels [129].

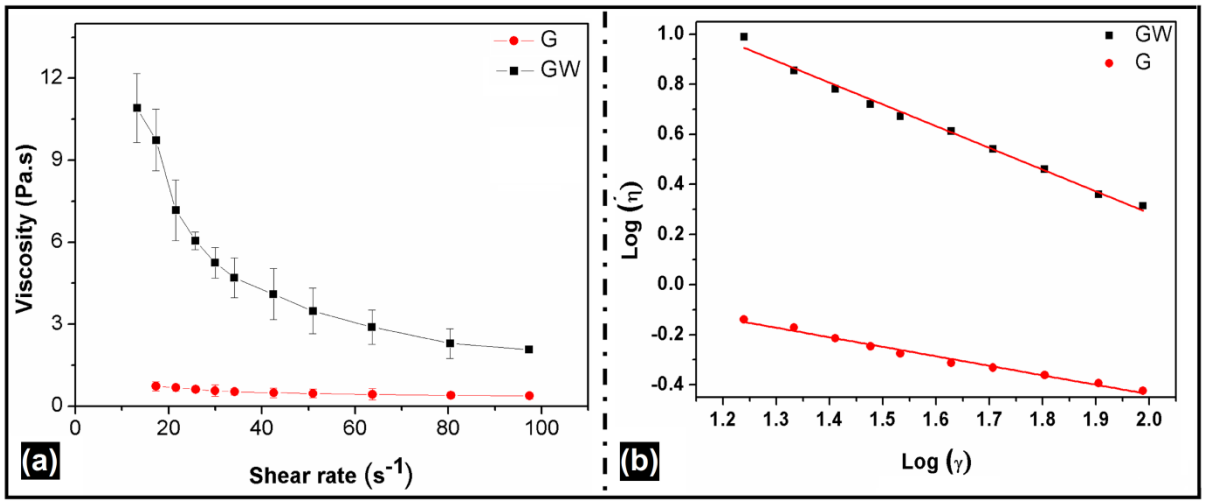

Figure 5.6: Flow behavior (a) viscosity profile and (b) power law fit

Table 5.1: Power law parameters

Gels	Power law index (n)	Correlation coefficient
G	0.6321	0.9845
GW	0.1423	0.9911

5.3.4 Mechanical analysis

The firmness of the gels was calculated from the spreadability profiles (figure 5.7a). It was observed that GW had a little higher firmness as compared to G. These results were in agreement with the viscosity study. The stickiness of the GW was greater than the G oleogel. The spreadability of the formulations was calculated. It was observed that addition of water to the oleogel decreased the spreadability of the formulations. Spreadability of G was higher than GW.

The stress relaxation profile of the emulgels is shown in figure 5.7b. Table 5.2 tabulates the stress relaxation parameters of the gels. There was a decrease in the force (F^*) to an equilibrium value instead of 0 in both the gels. The S^* values for all the gels were found to be less than 1 suggesting the viscoelastic property of the gels. The S^* of the gels were found to be closer to 1. The rate of relaxation (k_1) calculated from the normalized force vs. time graph was calculated (figure 5.7c). It was observed that k_1 was higher in the case of GW emulgels. The extent of relaxation (k_2) could not be quantified as it was less than 0.

It was observed that the percent stress relaxation of GW was higher than G. This suggested the solid viscoelastic nature of the gels. The low percent relaxation of the G may be due to the higher hydrophobic interactions in the organogelator molecules.

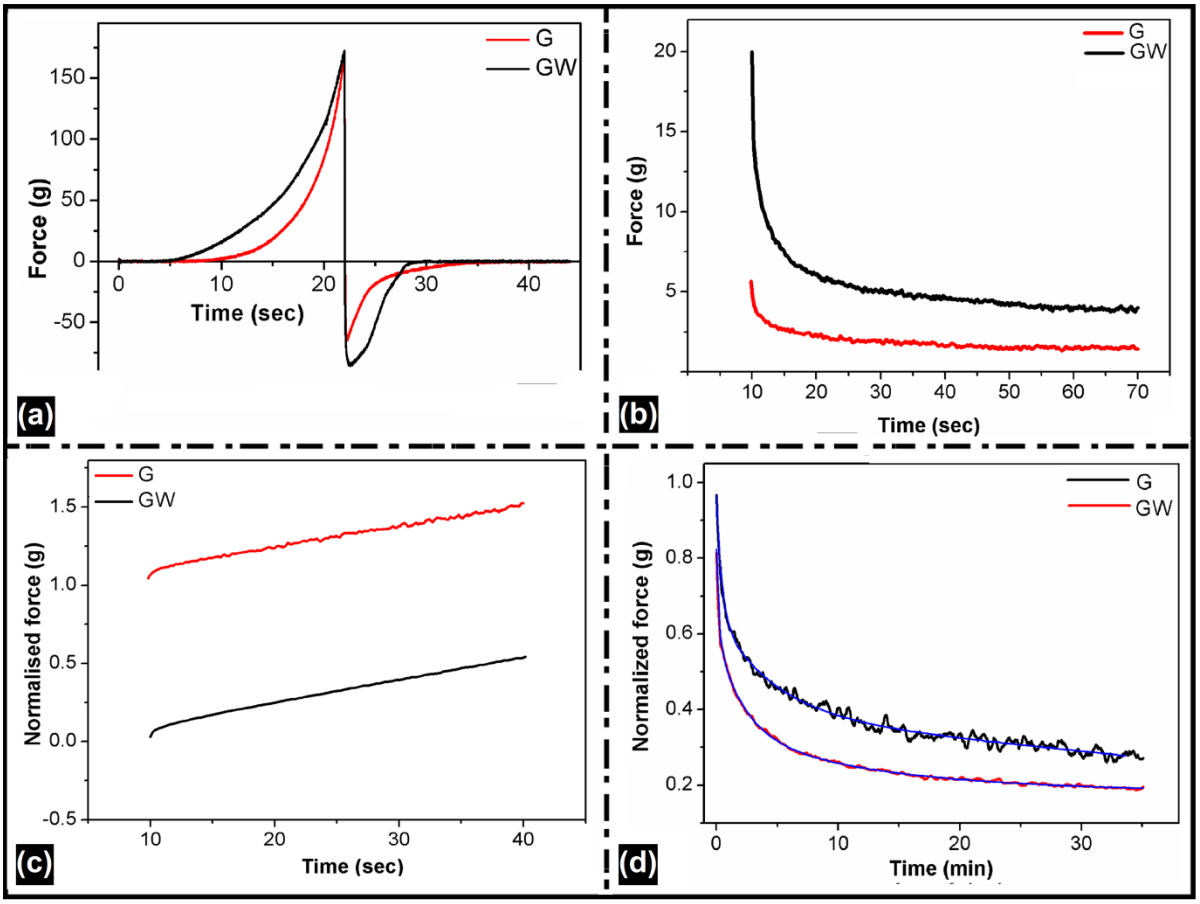

Figure 5.7: Mechanical properties of G and GW gels (a) spreadability, (b) stress relaxation, (c) normalized force vs. time and (d) Weichert model

Table 5.2: Mechanical properties and stress relaxation parameters of the G and GW gels

Studies		G	GW
Mechanical Properties	Firmness (g)	170.1043 ± 2.9867	172.1127 ± 4.1175
	Stickiness (g)	68.0025 ± 5.1238	84.9208 ± 4.1854
	Spreadability $(g.sec)^{-1}$	0.0023 ± 0.0005	0.0009 ± 0.0001
Stress relaxation Parameters	F^* (g)	0.2499	0.1761
	K_1 (g)	0.0659	0.0964
	S*	0.8598	0.8573
	Percent stress relaxation	75.0200	82.3862

The Weichert model (figure 5.7d) was used to describe the stress decay as a function of time. This model describes the viscoelastic properties in details. The Weichert model parameters for G showed the residual stress value below 0 indicating a fluid nature. The Weichert model parameters for GW are listed in Table 5.3. The relaxation times (τ) were in the order of $\tau_1 < \tau_2 < \tau_3$ and were in acceptance with the literature [107]. The sum of P_0, P_1, P_2 and P_3 was found to be 1 indicating a good fit. The coefficients of viscosity of the dashpots for GW are listed in Table 5.4. The coefficients of viscosity of the dashpots increased with the relaxation time.

Table 5.3: Weichert model parameters of G and GW gels

Sample code	**τ_1**	**τ_2**	**τ_3**	**r^2**
G	0.2732	2.0327	16.1467	0.9880
GW	1.0946	6.8146	9.8146	0.9986
		Pre-exponential factors		
Sample code	**P_0**	**P_1**	**P_2**	**P_3**
G	0.2057	0.2685	0.2683	0.2191
GW	1.0946	0.2730	0.2430	0.2830

Table 5.4: Stress relaxation model fitting using Wiechert model

Formulations	Stress relaxation model	Coefficient of viscosity of the dashpots
G	$P(t) = 0.2057 + 0.2685e^{\frac{-t}{0.2732}} + 0.2683e^{\frac{-t}{2.0327}} + 0.2191e^{\frac{-t}{16.1467}}$	0.0733, 0.5453, 3.5377
GW	$P(t) = 1.0946 + 0.2730e^{\frac{-t}{1.0946}} + 0.2430e^{\frac{-t}{6.8146}} + 0.2830e^{\frac{-t}{9.8146}}$	0.2988, 1.6559, 2.7775

5.3.5 Gel disintegration studies

The disintegration times of G and GW were 55 ± 2.22 min and 57 ± 1.54 min, respectively. No significant differences in the disintegration time of the formulations were observed in G and GW gels.

5.3.6 Thermal analysis

The thermal behavior of the gels was analyzed by DSC analysis (figure 5.8). The DSC profiles of the gels showed an endothermic peak at ~47 °C. This endothermic peak was associated with the melting of sorbitan monopalmitate molecules in the gels. An additional endothermic peak at ~100 °C in GW was observed. This endothermic peak may be associated with the evaporation of the water in the emulgel. The addition of water also influenced the enthalpy (ΔH) values of the endothermic peak at ~47 °C. The ΔH values for G and GW were found to be -4.739 J/g and -0.412 J/g, respectively. This decrease in the ΔH in GW may be explained by the presence of water. It has been reported earlier that addition of water increases the kinetic energy of the molecules during heating [130].

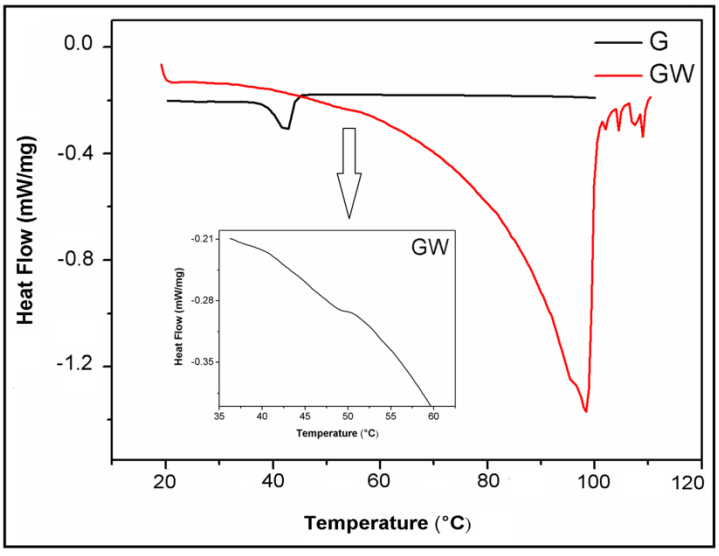

Figure 5.8: DSC curves of G and GW

5.3.7 Electrical analysis

Figure 5.9a shows the Nyquist plot depicting the electrical properties of the oleogel and emulgel. The formation of a semicircle in the high-frequency region provides information about the bulk properties of the materials. A spike in the lower frequency region is associated with the formation of an electrical double layer at the electrode/sample interface. The oleogel showed a higher bulk resistance as compared to GW. Incorporation of water increased the conductivity of the emulgel. The variation of dielectric constant (ε) with frequency is shown in figure 5.9b. The ε value of GW was higher at low frequencies which decreased at the higher frequencies. This phenomenon is associated with the polar dielectric material. This behavior was not prominent in the oleogel.

Figure 5.9c shows the variation of AC conductivity with frequency. The AC conductivity was very less for oleogel as compared to GW. The AC conductivity of the GW increased with the rise in the frequency. A plateau was obtained in oleogel at higher frequencies which give information about the DC conductivity of the gels.

The s-values obtained from the equation for G and GW were found to be 0.48 and 0.60, respectively. This study showed that the addition of water to the oleogel highly influenced the electrical properties of the oleogel. The presence of higher conductivity relaxation in GW (figure 5.9d) indicated better forward and backward motion of the electrons. On the contrary, the oleogel showed a low conductivity relaxation. The conductive property of GW can be attributed to the formation of conducting aqueous channels in the system [131]. The preliminary results indicated that GW may be tried as a matrix for iontophoretic drug delivery.

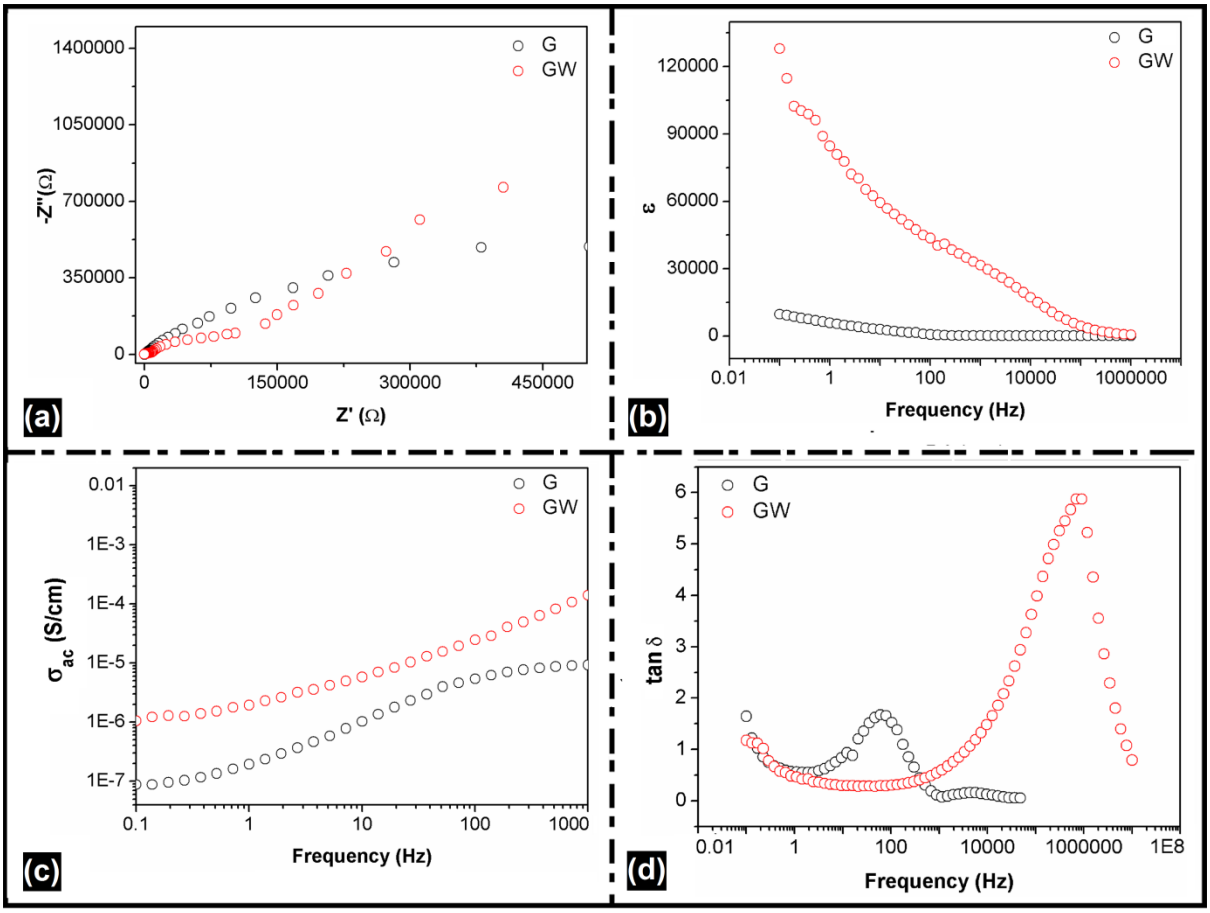

Figure 5.9: Electrical properties (a) Nyquist plot, (b) variation of ε with frequency, (c) AC conductivity vs. frequency and (d) tan δ profile of G and GW gels

5.3.8 *In vitro* cytotoxicity of dialyzed formulation components

The result of *in vitro* cytotoxicity studies is shown in figure 5.10a and figure 5.10b. The absence of hemolysis is an indication of good hemocompatibility. The percent hemolysis indicates the extent of lysis of red blood cells when kept in contact with blood. Both the samples were found to be acceptable as blood compatible (percent hemolysis < 5) and may be regarded as biocompatible based on the preliminary study. The percent hemolysis of the GW was less as compared to G. The cell viability index of GW was slightly higher than that of G. These studies suggested that addition of water to the oleogels increased the overall biocompatibility of the gels. The p values for all the tests were less than 0.05 indicating a statistically significant difference. The HaCaT cells maintained their structure in the presence of the bigels (figure 5.11).

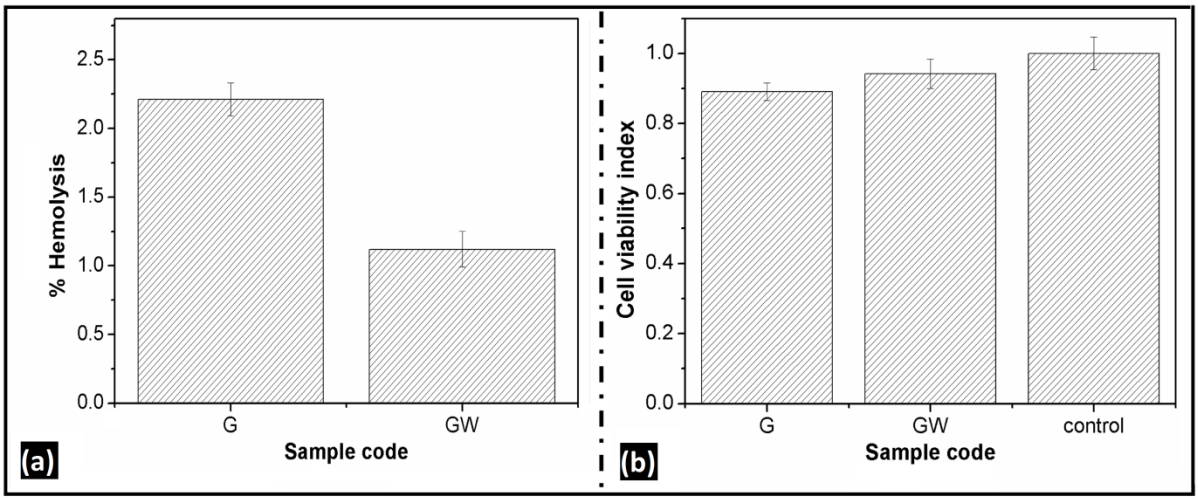

Figure 5.10: *In vitro* cytotoxicity studies (a) percent hemolysis and (b) cell viability index

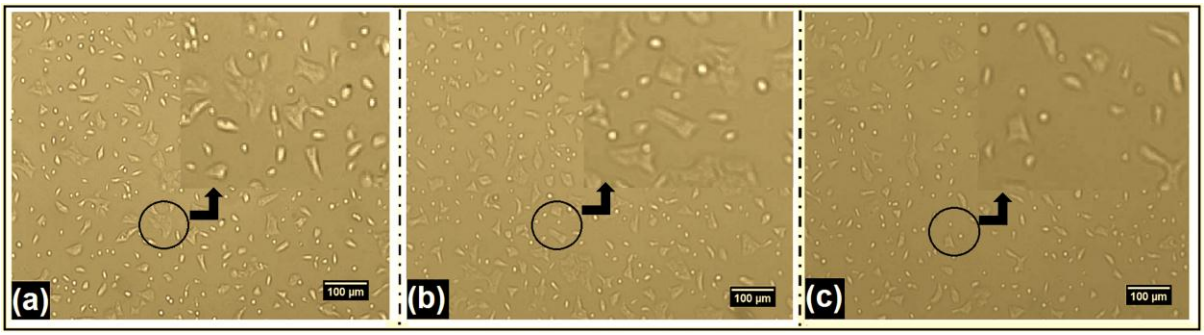

Figure 5.11: Micrographs of HaCaT cells (a) control, in the presence of leachates (b) G and (c) GW

5.3.9 *In vitro* antimicrobial study

The results of antimicrobial study are shown in table 5.5 and figure 5.12. Marketed formulation of metronidazole Metrogyl® (Dosage form-gel, Dose-Apply, and rub in a thin film of Metrogyl gel twice daily to affected areas after washing) was used as a reference. The study showed that GD (organogels containing drug) and GWD (emulgel containing drug) had comparable activity against *E. coli* with respect to Metrogyl® (MR). Also, the drug loaded gels were able to restrict the growth of the microorganisms in the surrounding area of the formulation and did not allow the growth of microorganisms even after 24 h. GWD showed a lower zone of inhibitions as compared to GD and marketed formulation. The p values were < 0.05 indicating a significant difference. 1000 µg of the drug dose was used in all the cases for the test as well as for reference.

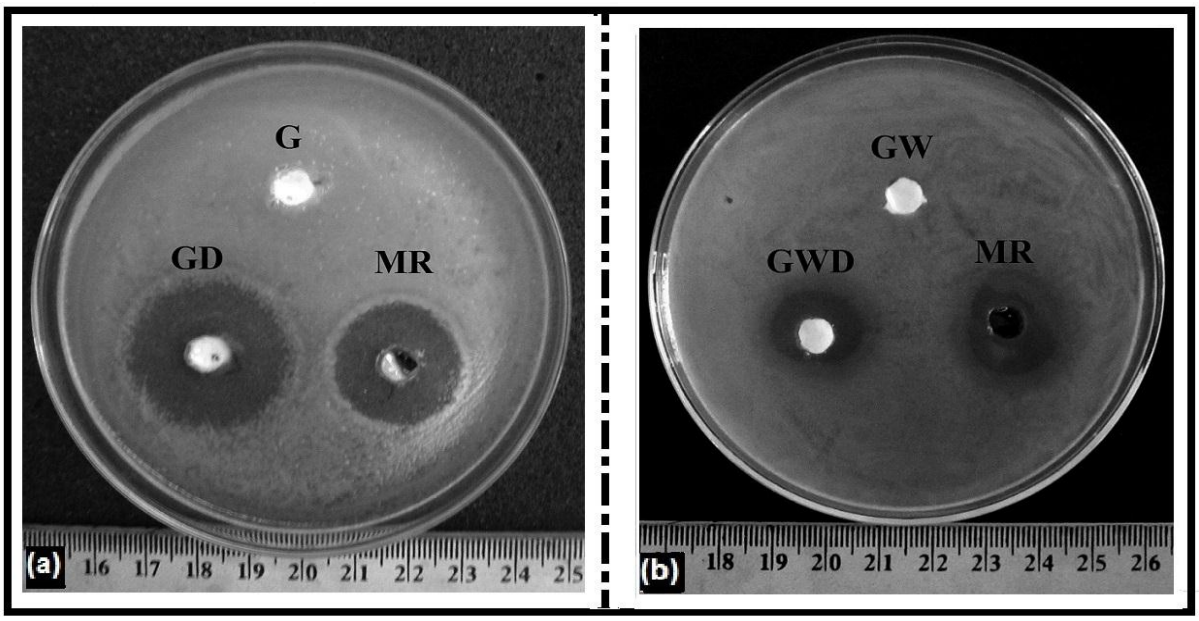

Figure 5.12: Antimicrobial activity of the formulations against *E. coli.* (a) GD and (b) GWD. MR-Marketed formulation

Table 5.5: Zone of inhibitions of GD and GWD gels

Sample code	Zone of inhibitions (cm) *E. coli*		
	Test	**MR**	**Blank**
GD	2.5 ± 0.11	2.5 ± 0.55	-
GWD	2.0 ± 0.17	2.6 ± 0.68	-

5.3.10 *In vitro* drug release studies

The solubility of metronidazole in phosphate buffer (pH 7.4) was found out to be 19.4286 ± 4.3764 mg/ml.

The cumulative percentage drug release (CPDR) profile of the gels is shown in figure 5.13. A level of statistical significance was found between the samples ($p < 0.05$). The GD, GWD, and MR showed 43.12%, 38.18%, and 90.44% release of metronidazole at the end of 12 h, respectively. It was observed from the graph that GD and GWD were able to control the release of the drug as compared to the marketed formulations. The incorporation of water in G slightly decreased the drug release. This may be associated with the higher viscosity and firmness of GW, which hindered the solvent diffusion into the matrix and also the drug release. The release mechanism from the oleogels and emulgels followed Higuchian kinetics (Table 5.6). The Higuchian kinetics is a common phenomenon and is observed in the matrix type delivery systems [132]. The mechanism of diffusion was further evaluated from the 'n'

value (release exponent) of Korsmeyer-Peppas model. A value greater than 0.5, but less than 1, it indicates non-Fickian diffusion. The results showed n ≤ 0.5 indicating a Fickian release of metronidazole from the bigels [133]. Marketed formulation of metronidazole Metrogyl® (Dosage form-gel, Dose-Apply, and rub in a thin film of Metrogyl gel twice daily to affected areas after washing) was used as a reference.

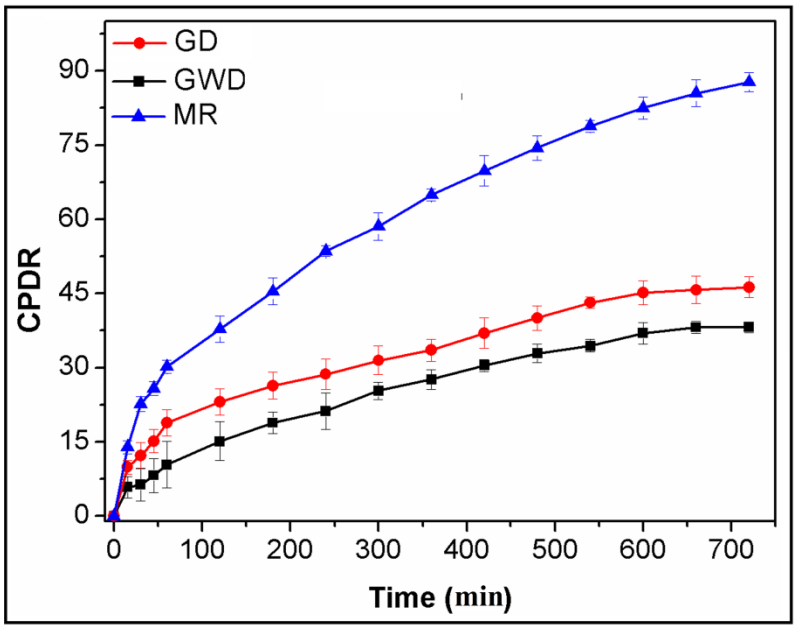

Figure 5.13: *In vitro* drug release profile of metronidazole from GD, GWD, and Metrogyl® (MR)

Table 5.6: *In vitro* drug release kinetics of metronidazole

Sample code	Zero order r^2	Higuchi r^2	Best fit model	KP model		Mechanism of release
				r^2	n value	
GD	0.9812	0.9923	Higuchi	0.9872	0.4500	Fickian
GWD	0.9954	0.9956	Higuchi	0.9812	0.4700	Fickian
MR	0.9885	0.8872	Zero order	0.9174	0.4700	Fickian

5.4 Major Outcomes

- The incorporation of water into the organogel produced mechanically stronger emulgel.
- The emulgel exhibited a higher viscosity.
- The conductivity of these gels may allow them to be used as an efficient vehicle for iontophoretic drug delivery systems.
- The emulgel can be used as a vehicle for the delivery of hydrophilic, lipophilic and amphiphilic agents.
- The use of edible oil rich in unsaturated fatty acid in gel formation can serve as a substitute for many food supplements.

CHAPTER 6

Preparation and characterization of protein-based bigels using emulgels of sunflower oil and sorbitan monopalmitate

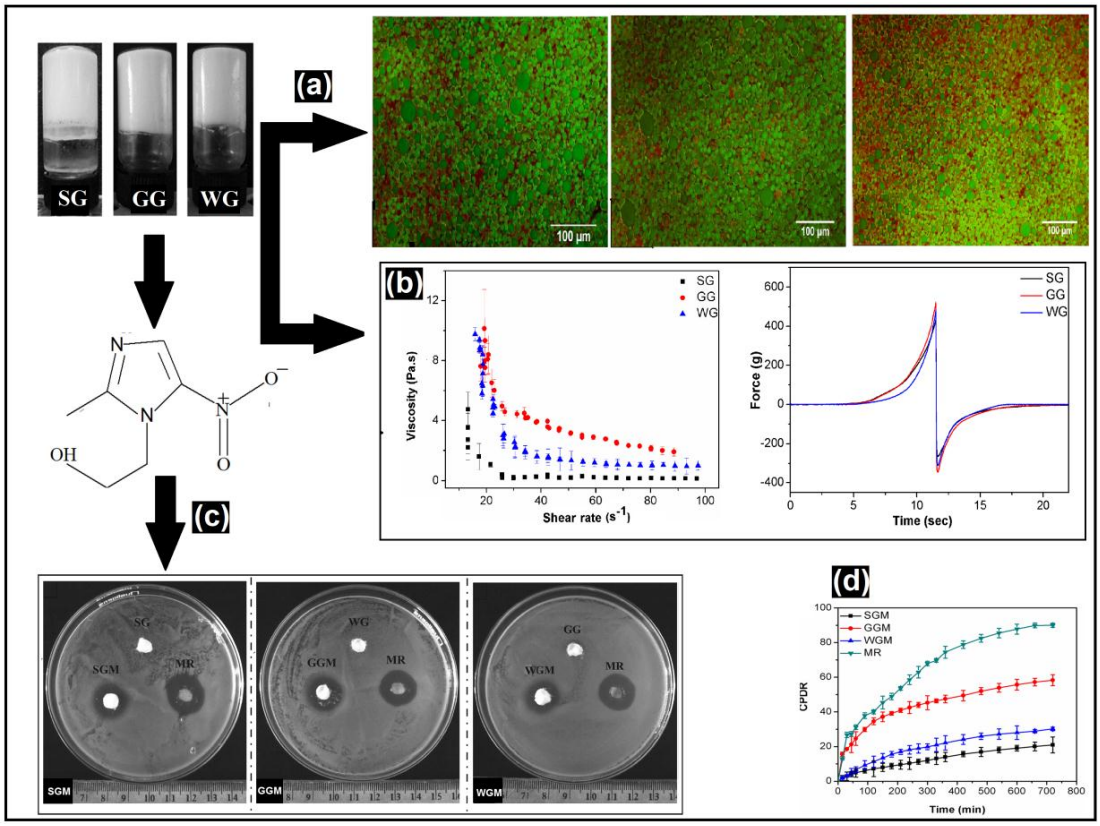

Graphical outline: (a) Fluorescence micrographs, (b) Mechanical properties, (c) antimicrobial efficiency, and (d) *in vitro* release profile of protein based bigels.

Overview

Sunflower oil and protein (gelatin and whey powder) based bigels for were prepared and characterized drug delivery applications. Sorbitan monopalmitate was used as an organogelator for the preparation of the bigels. The bigels were characterized by fluorescence microscopy, FTIR, and viscometer. The mechanical properties of the bigels were evaluated by a static mechanical tester. The thermal and electrical properties of the bigels were determined using DSC and phase sensitive multimeter, respectively. Goat blood RBC and HaCaT cells were used to check the *in vitro* cytotoxicity of the bigels. The micrographs showed that the droplets were apolar in nature (oleogels) while the continuum phase was polar in nature (protein hydrogel matrix). Incorporation of the proteins improved the stability of the bigels. Intermolecular hydrogen bonding was the major driving force behind the bigel formation. The bigels exhibited shear thinning behavior. Bigels containing gelatin showed higher firmness as compared to the other bigel. The melting endotherm of the bigels was observed at ~47 °C. The whey powder based bigels disintegrated faster as compared to other bigels. The melting endotherm of the bigels was observed at ~47 °C. The bulk resistance of the gelatin based bigel was lower than that of whey powder based bigels. The bigels were biocompatible in nature. The drug loaded bigels showed good antimicrobial efficiency against *E. coli*. The addition of proteins resulted in the controlled release of metronidazole. The release was diffusion mediated.

6.1 Introduction

A gel is an elastic, semisolid and solvent rich system. Gel is reported to form interconnected assembled structures of macromolecules or colloidal particles. The gels are classified depending upon the nature of the networked structure. If the network structure arises from crosslinked polymer molecules, the gels are known as polymer gels. If aggregated colloidal particles are involved in the network formation, then the gels are known as particle gels [134]. Major classes of gels that have been used for the topical and transdermal delivery applications are broadly classified as organogels and hydrogels. Organogels are semisolid systems that contain apolar phase entrapped within the 3D matrix of the gelator. The organogels prepared from edible oils, such as sunflower oil, have been tried as matrices for many biomedical applications like the controlled release of pharmaceuticals. The commonly used gelators for the preparation of organogels include low molecular weight organogelators and polymeric surfactants with non-ionic, anionic and cationic structures. On the contrary, hydrogels are defined as the polymer networks in which water/ aqueous phase has been imbibed and entrapped. The amount of water absorbed may be up to thousand times the dry weight of the polymer structure. Gelatin is a natural protein obtained from the controlled hydrolysis of the collagen. The main advantages of gelatin include biodegradable and biocompatible properties. Also, it is available at low cost. Whey powder, on the other hand, is a byproduct of the food industry. It is available in three forms-whey protein isolate, concentrate, and hydrolase [135]. Whey powder is also low cost and is readily available. It has poor film forming properties. Proteins get adsorbed at the oil-water interface and tend to form stabilizing layers around the droplets. In this chapter, this advantage of proteins has been explored to formulate bigels for the controlled release of metronidazole. Metronidazole belongs to a class of azole group and is poorly soluble in water and pharmaceutical oils[15]. The available aqueous gel compositions are limited to a concentration of 0.75% because of the poor solubility of the drug in water. This results in the increased dosing frequency of the formulation which, in turn, reduces the patient compliance. The problems associated with these kinds of drugs can be eliminated by loading them in bigels rather than single-phase aqueous gels.

6.2 Experimental

6.2.1 Preparation of proteins based bigels

0.9g of sorbitan monopalmitate was dissolved in sunflower oil (50 °C). To the above solution, phosphate buffer (pH 7.4; 50 °C) was added dropwise with continuous stirring. After the addition of the specified volume of phosphate buffer, the solution mixture was vigorously mixed using a high-speed vortex (12000 rpm) for 30 min and cooled to room temperature to induce gelation. Bigels of gelatin and whey powder were prepared and regarded as GG and WG, respectively (Table 6.1). Drug loaded bigels were prepared in a similar manner. Metronidazole was first dissolved in sunflower oil. Rest of the procedure was same.

Table 6.1: Composition of the proteins based bigels

Formulation Code	Composition, % (w/w)					
	Sorbitan monopamitate	Sunflower oil	Phosphate buffer	Gelatin	Whey Powder	Metronidazole
SG	9.0	41.0	50.0	-	-	-
GG	9.0	41.0	49.0	1.0	-	-
WG	9.0	41.0	49.0	-	1.0	-
SGM	9.0	41.0	49.0	-	-	1.0
GGM	9.0	41.0	48.0	1.0	-	1.0
WGM	9.0	41.0	48.0	-	1.0	1.0

6.3 Results and discussion

6.3.1 Preparation of protein based bigels

The viscosities of the gelatin and whey powder sols, obtained from the backward extrusion study (figure 6.1), were 0.0081 ± 0.0011 Poise and 0.0080 ± 0.0021 Poise, respectively. The sols followed Newtonian flow behavior. The mechanism of formation of whey protein based bigel is a consequence of its complex structure. Lactoglobulin, α-lactalbumin, bovine serum albumin (BSA) and the immunoglobulins are the essential components of whey protein [136]. As the bigel formation requires a heating process, whey protein undergoes denaturation process. A fraction of the denatured whey proteins undergoes irreversible aggregation at the initial point of gel formation, thus forming a primary spatial structure of the gel. After the gel point, the remaining proteins are incorporated into the gel network [137]. The phenomenon of aggregation of these globular proteins is a combination of conformational changes, chemical

reactions and physical interactions. The conformational changes during the denaturation step are reversible. The irreversible aggregation occurs via non-covalent and covalent interactions. The non-covalent bonds are van der Waals attractive forces, electrostatic interactions, hydrogen bonds and hydrophobic interactions. The covalent bonds are intermolecular disulphide bonds, formed during sulphydryl-disulphide exchange reactions and in sulphydryl-sulphydryl reactions These sulphydryl groups are exposed from β-lactoglobulin and BSA on heating whey protein [138]. A somewhat similar mechanism works behind the formation of gelatine based bigels. The fundamental unit of gelatin is collagen, a triple helical protein structure. The triple helical structure is composed of three α-chains with continuous repeated units of Gly–X–Y- sequence. The X is proline and Y is hydroxyproline. Gelatin consists of varying amounts of 18 amino acids [139-140]. Gelatin above 40°C exists as flexible, isolated, and usually lightly cross-linked, chains.The gelatin present in the bigels on tend to gel as cooling occurs by the formation of ordered quasi-crystalline triple helical junction zones [141].

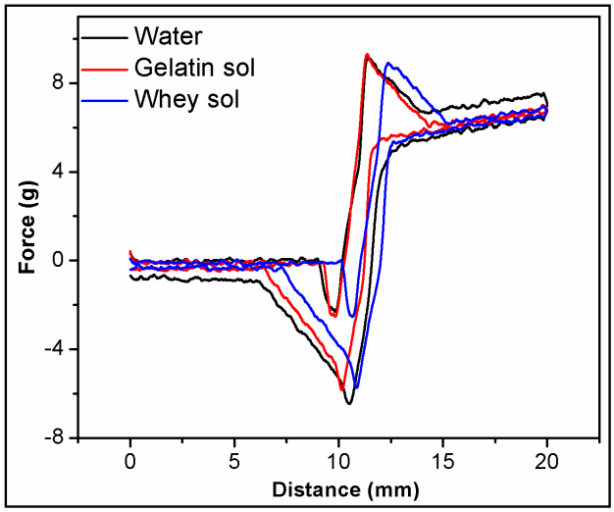

Figure 6.1: Backward extrusion of water, gelatin and whey sol

Figure 6.2 shows the pictographs of the bigels. The white color of the formulations is often associated with the biphasic nature. Diffraction of light from the interface of the oleogel-hydrogel mixture can explain the appearance of the white color. The bigels prepared were smooth and soft. All the bigels were in the pH range of 6 and 7. The bigels were stable for > 10 + months when incubated at 30 °C ± 2 °C/65% RH ± 5% RH.

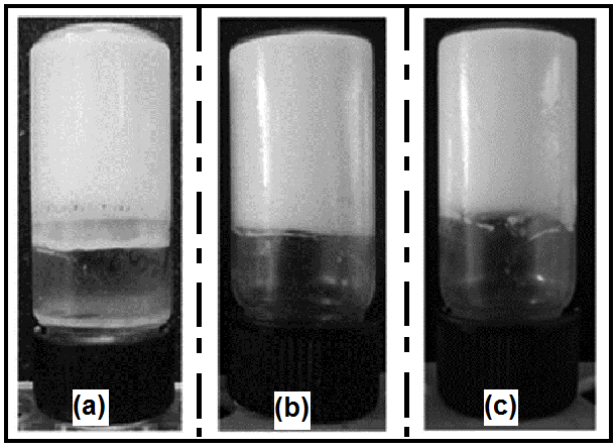

Figure 6.2: Inverted-tube method for the formation of bigels (a) SG, (b) GG and (c) WG bigels

6.3.2 Microscopy and microstructural analysis

The micrographs (figure 6.3a) showed the presence of apolar phase as the dispersed phase while the external phase was aqueous in nature (stained red). This indicated that the bigels were oil-in-water (i.e. organogel-in-hydrogel) type. The droplet size distribution was determined by Image J. The broad droplet size distribution in WG may be attributed to the coalescence of the droplets [142]. The coalescence is said to occur due to the lower viscosity of the aqueous whey powder phase. The average size of the droplets (figure 6.3d) in GG (4.12 ± 1.05 µm) and WG (4.94 ± 0.16 µm) was found to be greater than SG (3.62 ± 1.24 µm). This may be explained by the adsorption of gelatin and whey protein onto the emulsion droplet surface. Adsorption of proteins on the droplet surface may be attributed to the presence of both apolar and polar amino acids in the polypeptide backbone of the protein molecules [143]. This phenomenon of adsorption of proteins at the surface of the polar-apolar interface lead to an increase in the volume fraction of the emulsion droplets in GG and WG. It has been reported earlier in the literature that biphasic systems stabilized by proteins are highly prone to droplet coalescence. This is due to the interfacial membrane formed by the globular proteins which tend to break due to the generation of strong repulsive forces The span of the droplet size was in the range of 1-2.5 for all the sets of bigels [144]. The span factor of SG, GG and WG was found to be 1.60 ± 0.21, 1.52 ± 1.31 and 2.08 ± 2. 2, respectively. The span factor for GG bigels was lower than SG and WG. The span factor determines the uniformity of the droplet size [145].

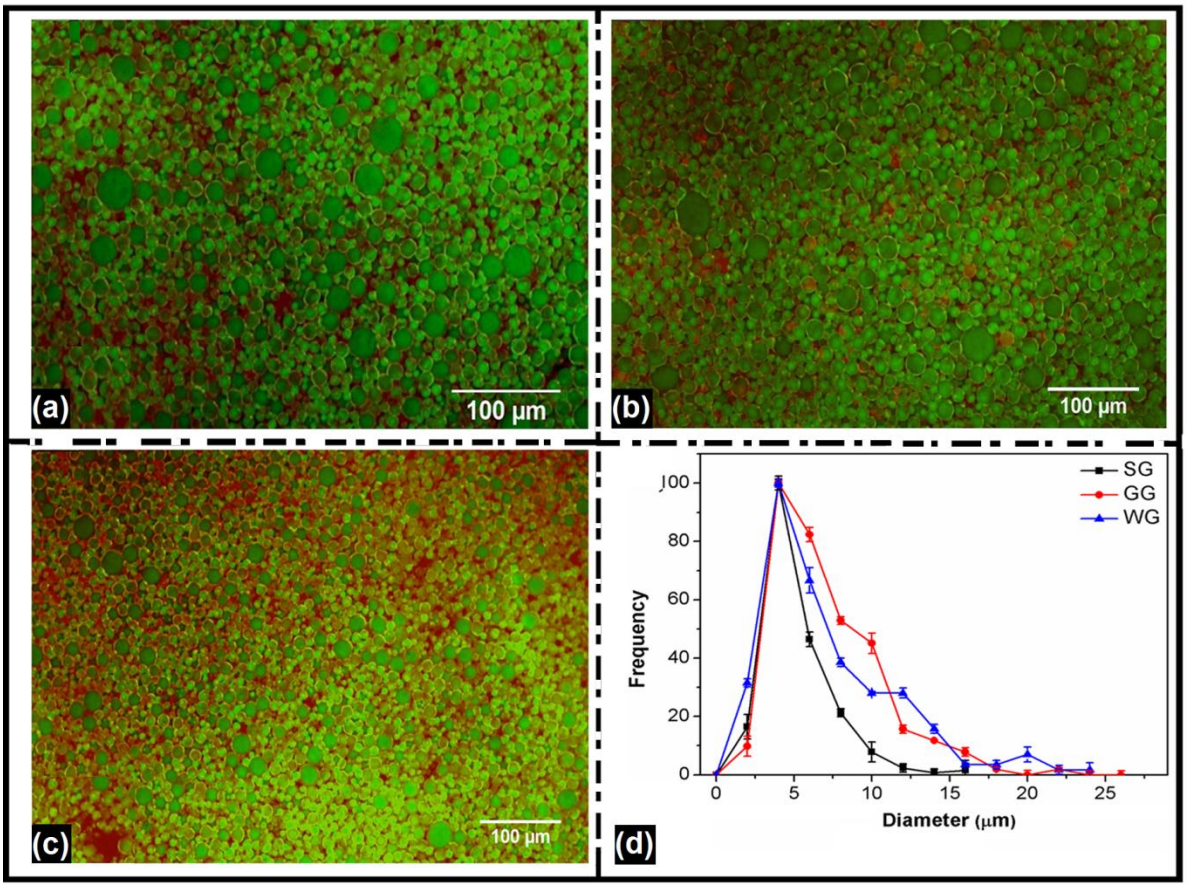

Figure 6.3: Fluorescence micrographs: (a) SG, (b) GG, (c) WG and (d) size distribution analyses of the bigels

6.3.3 FTIR analysis

The FTIR spectrograms of the proteins and the bigels have been shown in figure 6.4. Gelatin and whey powder showed characteristic bands of an amide linkage. The peaks at ~3304 cm^{-1} (NH stretching) and ~3080 cm^{-1} may be associated with the presence of amide group. The peak at 1470-1575 cm^{-1} suggested the presence of amide II bond. The peak in the range of 1640-1656 cm^{-1} may be associated with the presence of amide I band, responsible for the protein secondary structure. Any change in the peak position is associated with the conformational change in the native protein [146]. GG and WG contained all the peaks of amide I and amide II of gelatin and whey protein, respectively. This suggested that the proteins were present in their native state. The peak at ~1640 cm^{-1} in SG was associated with the bending vibrations of the water molecules. The vibrational band at 1741 cm^{-1} in SG was due to the stretching of the ester group CO in sorbitan monopalmitate. There was an increase in the intensity of the ester group CO stretching peaks in GG and WG. This may be accounted to the CO stretching vibrations due to the presence of glutamic acid and aspartic acid in gelatin and whey powder [147]. The presence of a broad peak at 3300-3550 cm^{-1} in

SG indicated strong intermolecular hydrogen bonding. There was a decrease in the intensity of OH stretching vibrations with a subsequent broadening of the peaks as the proteins were added to the bigels. This may be associated with the strong intermolecular hydrogen bonding amongst the NH group of the proteins and OH group of the water molecules [148]. The interaction was stronger in GG as compared to WG. Another possible interaction may be amongst the protein amines and the polar groups of sorbitan monopalmitate [149].

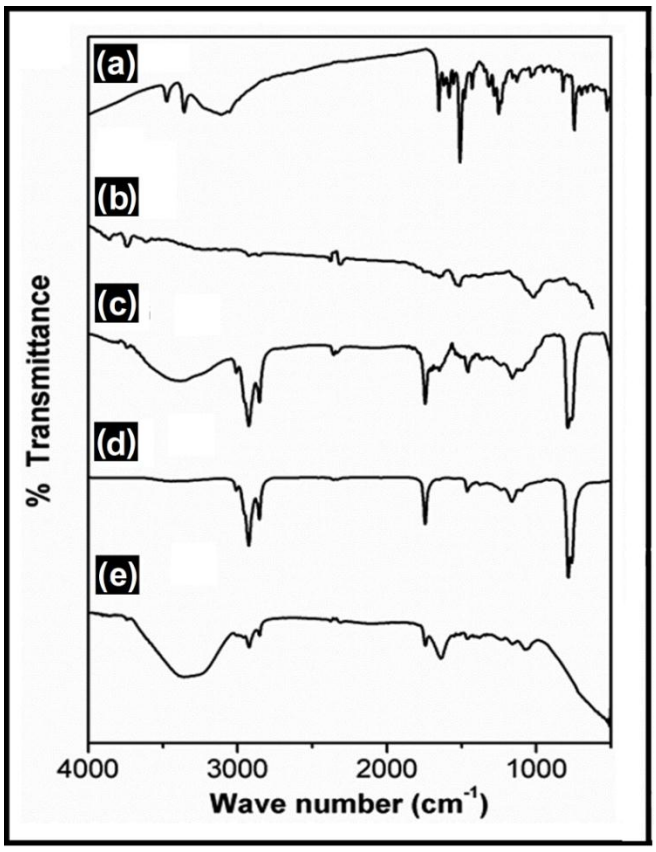

Figure 6.4: FTIR analysis (a) Gelatin (b) whey powder (c) WG (d) GG (e) SG

6.3.4 Viscosity analysis

The viscosity profiles of the bigels suggested non-Newtonian flow behavior (figure 6.5a-figure 6.5b). The non-Newtonian behavior has been reported to be an important parameter for topical and spreadable food formulations. The flow behavior of the bigels was predicted using the Ostwald-de Wale power law model.

The results indicated pseudoplastic flow behavior of the bigels with $n < 1$. The protein based bigels showed best fit (Table 6.3). The apparent viscosity of the bigels decreased in the order GG > WG > SG. The addition of the proteins increased the viscosity of the bigels. The movement of the droplets was reduced due to the presence of protein molecules at the interface. This resulted in the increase in the viscosity and the stability of the proteins based

bigels [143]. The increase in the viscosity may be associated with the intermolecular hydrogen bonding amongst the bigel components, as evident from the FTIR studies. The higher viscosity of the bigels containing proteins may be attributed to the presence of submicroscopic solid protein particles [150]. These submicroscopic solid protein particles swell in the presence of water. A higher viscosity of GG as compared to WG may be due to the occlusion of a large amount of water within the submicroscopic solid gelatin particles present in GG [151]. The droplet size of the formulations may have tailored the viscosity profile of the bigels. In general, the smaller the size of the droplets, the higher is the number of the particles and greater interaction amongst the droplets. This causes an increase in the viscosity [76]. Since the droplet size of GG was smaller than WG (Table 3), it was expected that the viscosity of GG would have been higher.

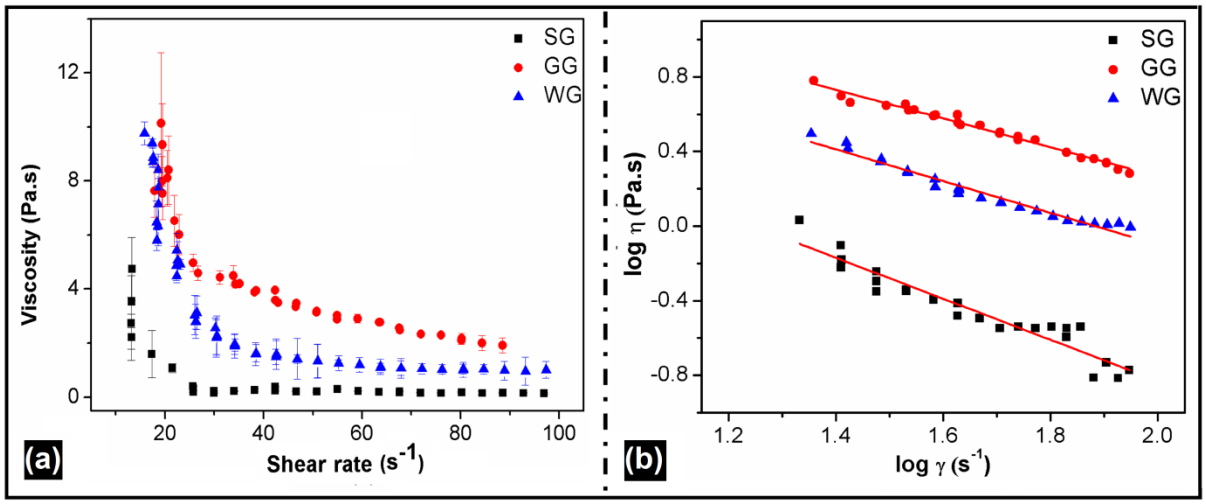

Figure 6.5: A plot of viscosity vs. shear rate of the bigels showing (a) shear thinning behavior and (b) power law fit

Table 6.2: Power law parameters

Sample code	n values	Correlation coefficient r^2
SG	0.5523	0.9023
GG	0.1195	0.9721
WG	0.1901	0.9635

6.3.5 Mechanical analysis

The presence of the proteins within soft materials may promote the formation of 3D matrices which, in turn, may help alter the mechanical properties (e.g. firmness, stickiness, spreadability, etc.) of the formulations. Figure 6.6a show the spreadability profile of the developed bigels. The value of the positive and the negative peaks corresponds to firmness

and adhesiveness (or stickiness) of the bigels, respectively. The firmness and the stickiness of the bigels decreased in the order of GG > WG > SG. It was seen that the addition of gelatin and whey powder increased the firmness and stickiness of the bigels. This may be due to the increased intermolecular hydrogen bonding when the protein molecules were incorporated (as confirmed by FTIR studies). The structural morphology of proteins is complex. When they are adsorbed onto the interface, they unfold and rearrange themselves exposing their hydrophobic functional groups that lead to aggregation and interactions, thereby increasing the firmness of the gels [152]. As reported earlier in literature the strength of the gel matrix is directly related to the viscosity of the gels. The above results show that GG bigels have a higher viscosity as compared to other bigels which might have contributed to its greater firmness [153].

The spreadability of the bigels was also calculated. Spreadability is defined as the reciprocal of work of shear [154]. The spreadability of the protein based bigels was less as compared to SG. The spreadability decreased in the order of SG > WG > GG. These results were in agreement with the viscosity studies. The k_1 and k_2 indicate the initial rate and extent of relaxation, respectively calculated from the normalized force vs. time profile (figure 6.6c).

Table 6.4 shows the stress relaxation parameters of the bigels. The rate of relaxation (k_1) was nearly equal in all the bigels. The extent of relaxation (k_2) was greater in protein-based bigels. An in-depth analysis of the stress relaxation was further carried out by determining S^*, F^* and percent stress relaxation values. For viscoelastic materials, the S^* value ranges from 0-1. The S^* values of the bigels were < 1. The F^* (asymptotic residual force) values for the bigels were ≈ 0.3. This indicated the viscoelastic behavior of the formulations.

The percent stress relaxation of the bigels decreased in the following order SG > WG > GG. As reported earlier, the percent stress relaxation for ideal elastic solid is 0, whereas, it is 100 for liquids [155]. The percent stress relaxation of the bigels was in the range of 65-70 suggesting viscoelastic nature of the bigels.

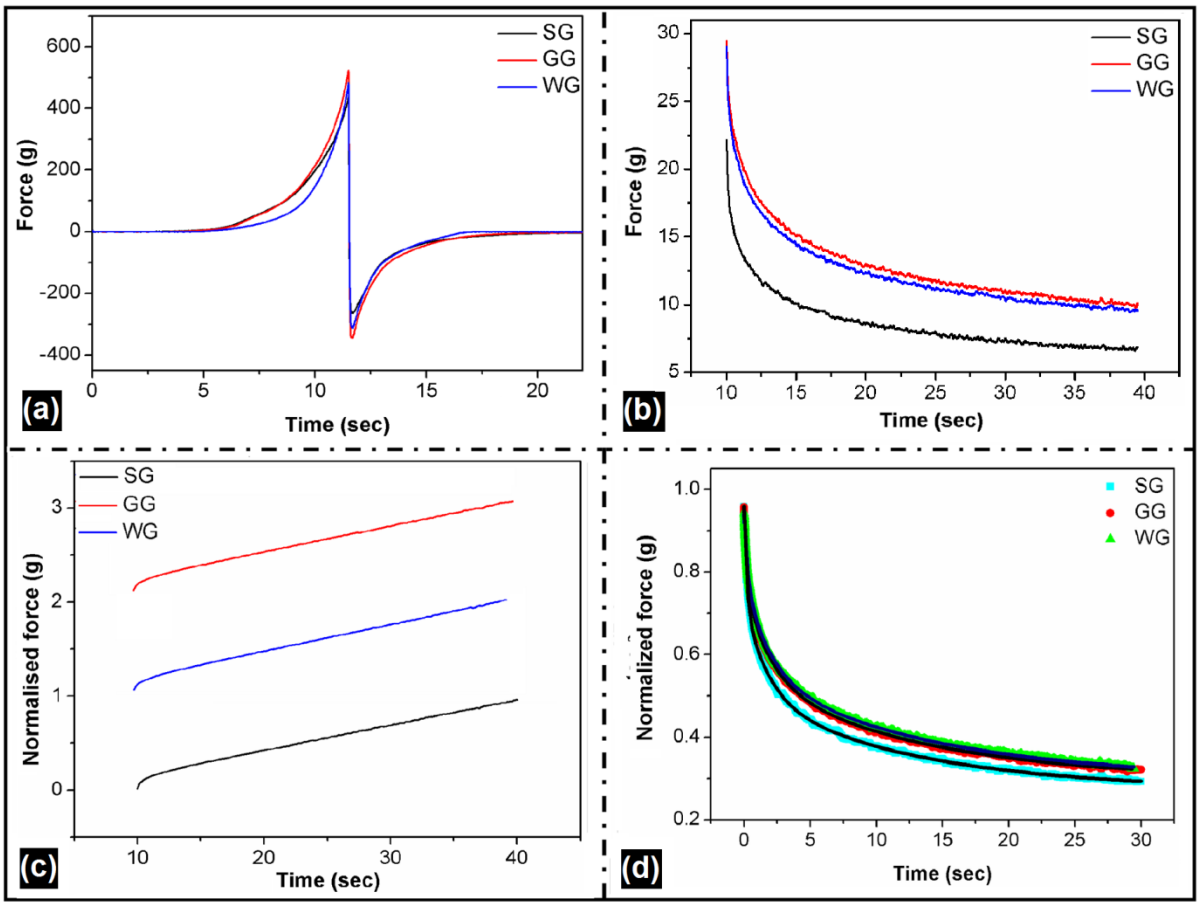

Figure 6.6: Mechanical properties of bigels (a) spreadability, (b) stress relaxation, (c) normalized force vs. time and (d) Wiechert model

Table 6.3: Mechanical properties of the bigels

Studies	Parameters	SG	GG	WG
Mechanical properties	Firmness (g)	435.2341 ± 2.7121	693.1212 ± 2.8211	468.0634 ± 2.7231
	Stickiness (g)	265.2723 ± 4.5732	449.0512 ± 4.1824	332.6913 ± 3.8931
	Spreadability $(g.sec)^{-1}$	0.0085 ± 0.0017	0.0011 ± 0.0009	0.0016 ± 0.0008
Stress relaxation study	Percent stress relaxation	69.1860 ± 1.2521	66. 5382 ± 3. 5172	68.1762 ± 3.0182
	K_1	0.1375	0.1567	0.1674
	K_2	0.0012	0.0282	0.0297
	S*	0.7501	0.7504	0.7468

Table 6.4: Wiechert model parameters of the bigels

Formulation code	τ_1	τ_2	τ_3	r^2
SG	0.1948	1.8739	13.6694	0.9992
GG	0.2473	1.7085	12.2699	0.9941
WG	0.2503	1.8856	12.8824	0.9954
Pre-exponential parameters				
	P_0	P_1	P_2	P_3
SG	0.2733	0.2732	0.2345	0.2276
GG	0.2982	0.2808	0.2806	0.2525
WG	0.2970	0.2716	0.2615	0.2202

The stress relaxation profiles were fitted as per the Weichert model having a spring and a dashpot. The spring and the dashpot represent the elastic and viscous components, respectively. This model describes the behavior of the protein based bigels with respect to different relaxation times. The use of n number of relaxation times gives a better fit to the model [156]. The Weichert model parameters were calculated. P_0 (residual stress) was higher in protein containing bigels, indicating higher solid-like nature of bigels. τ_1 (instantaneous relaxation time) was higher in GG and WG. On the other hand, the long-term relaxation times (τ_2 and τ_3) were higher in SG. Parameters like τ_2 and τ_3 provide information about the disintegration and breakage of polymer-polymer interactions. The long-term relaxation times τ_2 and τ_3 for the protein-based bigels was slightly lower than that of blank bigels. This indicated the formation of better and strong gel matrix in GG and WG. The coefficient of viscosities of all protein based bigels was higher than that of the normal bigels. This can be attributed to the formation of ordered triple helices during the heating and cooling process of bigel formation. These types of ordered triple helices are believed to give rise to crosslinks and junction zones which further resist to the stress applied to the gel matrix [157].

Table 6.5: Stress relaxation model fitting using Wiechert model

Formulation Code	Stress relaxation Model	Coefficient of viscosity of the dashpots
SG	$P(t) = 0.2733 + 0.2732e^{\frac{-t}{0.1948}} + 0.2345e^{\frac{-t}{1.8739}} + 0.2276e^{\frac{-t}{13.6694}}$	0.0532, 0.4394, 3.1111
GG	$P(t) = 0.2982 + 0.2808e^{\frac{-t}{0.2473}} + 0.2806e^{\frac{-t}{2.801}} + 0.2525e^{\frac{-t}{23.082}}$	0.0694, 0.4794, 3.0981
WG	$P(t) = 0.2970 + 0.2716e^{\frac{-t}{0.2503}} + 0.2615e^{\frac{-t}{1.8856}} + 0.2202e^{\frac{-t}{12.8824}}$	0.0679, 0.4930, 2.8367

6.3.6 Gel disintegration studies

The disintegration property of the bigels was determined using USP disintegration apparatus (Table 3). The disintegration times of SG, GG, and WG were found to be 55.0 ± 1.2 min, 37.0 ± 2.1 min and 27.0 ± 0.9 min, respectively. The results showed that the protein containing bigels disintegrated faster as compared to SG. The rapid solubilisation of the protein resulted in the faster disintegration of the protein bigels as compared to SG [158]. Amongst GG and WG, the disintegration of WG was faster. This may be due to the greater structural integrity of GG due to higher hydrogen bonding as confirmed by the FTIR studies.

6.3.7 Thermal analysis

The thermograms of the bigels have been shown in figure 6.7. The bigels showed melting temperature (T_m) at ~45 ºC. The broad endothermic peaks of SG, GG, and WG, may be associated with the loss of moisture present within the gels. The results suggested that the evaporation of the moisture from SG was at a much lower temperature as compared to GG and WG. This may be attributed to the increase in the intermolecular hydrogen bonding amongst the bigel components when the proteins (gelatin and whey powder) were incorporated within the gel. The increase in the melting point of GG and WG indicated improved thermal stability of GG and WG as compared to SG. The change in the enthalpy of the bigels decreased in the following order GG (422 J/g) > WG (272 J/g) > SG (220 J/g). The change in the enthalpy is associated (ΔH) with the increase in the intermolecular interactions (hydrogen bonding) amongst the bigel.

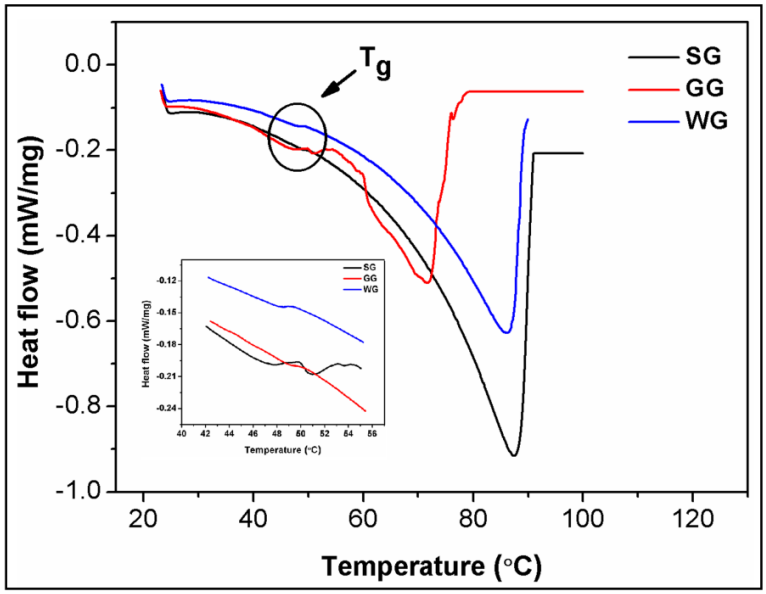

Figure 6.7: DSC profiles SG, GG, and WG

6.3.8 Electrical analysis

The electrical properties of the bigels were measured at room temperature. The presence of two semicircles in the Nyquist plot (figure 6.8a) may be attributed to the presence of both bulk and grain boundary effects. The intercept of the semicircles on the real axis gives a bulk resistance of the materials. There was a decrease in the bulk resistance (R_b) of the bigels as proteins were incorporated. This was due to the presence of the charged groups in proteins. The conductivity of GG was higher as compared to WG. The observed phenomenon may be due to the higher adsorption of SG at the electrode surface as compared to WG and GG. The dielectric constant (ε) profile has been shown in figure 6.8b. The presence of hydrophilic functional groups in the proteins resulted in the slightly higher ε of GG and WG. The variation in the AC conductivity of the bigels has been shown in figure 6.8c. The AC conductivity of GG and WG was higher than SG. The presence of protein in the gels contributed to an increase in the AC conductivity due to the hopping of charge carriers between the orbitals located at the residues of native protein [159]. The presence of the hydrophobic amino acids in whey protein led to a slight decrease in the AC conductivity. The variation of total AC conductivity σ' (ω) of the gels with frequency (ω) was expressed using Jonscher's power law model (figure 6.8c). The AC conductivity of the bigels increased with the frequency. The plateau in the high-frequency region (1000-10000 Hz) gave an indication of the DC conductivity of the bigels. The s values of SG, GG, and WG were found to be 0.24, 0.28, and 0.21, respectively.

The tan δ profile has been shown in figure 6.8d. All the bigels showed a single relaxation peak. There was a slight variation in the relaxation of the bigels. This may be due to the ionic transport process in the bulk.

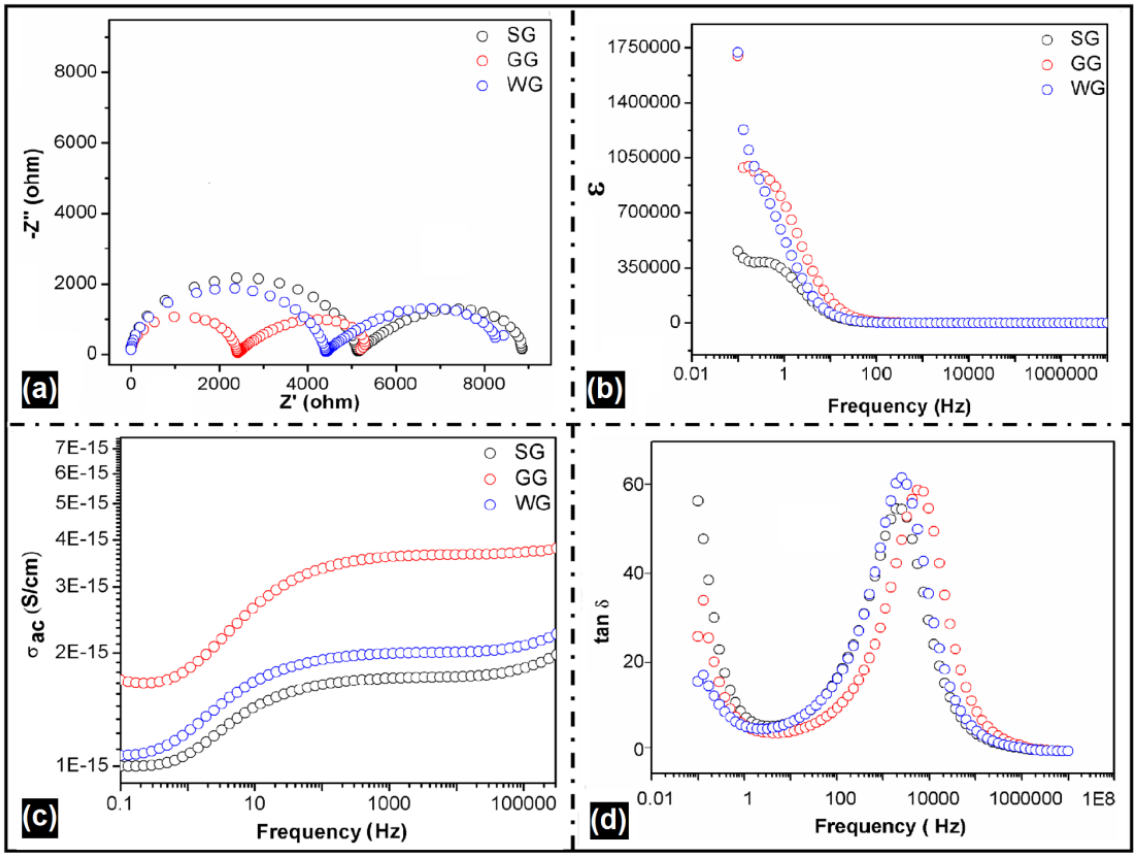

Figure 6.8: Electrical properties of the bigels, (a) Nyquist plot, (b) dielectric constant, (c) AC conductivity, and (d) tan δ profile

6.3.9 *In vitro* cytotoxicity of dialyzed formulation components

The results of the cytotoxicity tests of the bigels have been summarized in figure 6.9. The percent hemolysis of the bigels was less than 5 indicating their hemocompatibility (figure 6.9a). *In vitro* cytotoxicity test was carried out using HaCaT cells showed a higher cell viability index (figure 6.9b) in the case of GG as compared to SG and WG. The study suggested that the addition of the proteins to the gels improved the cytocompatibility. The variations in the cell viability were found to be significantly different ($p < 0.05$).

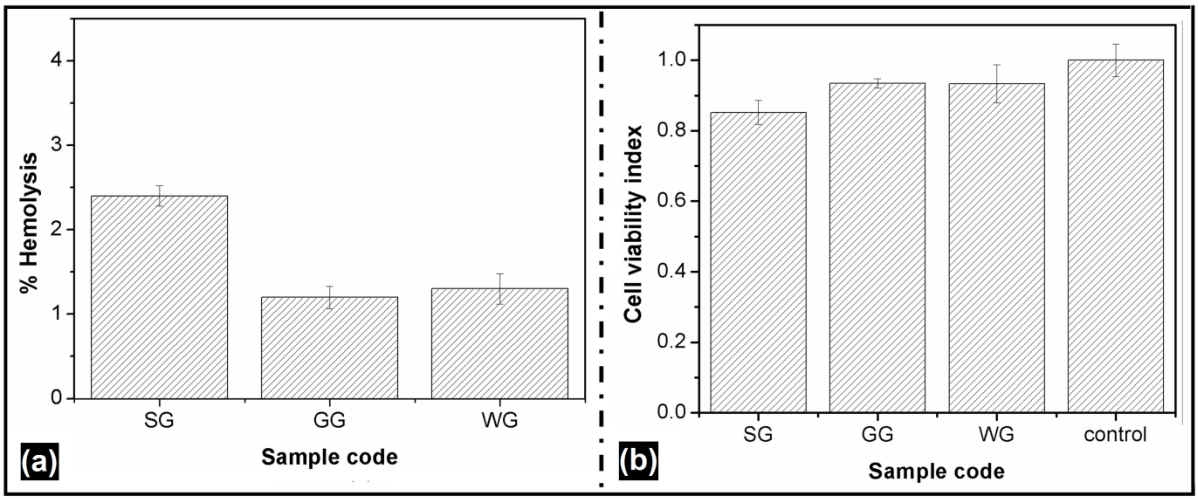

Figure 6.9: *In vitro* cytotoxicity of dialyzed formulation components (a) percent hemolysis and (b) cell viability index of SG, GG, and WG bigels

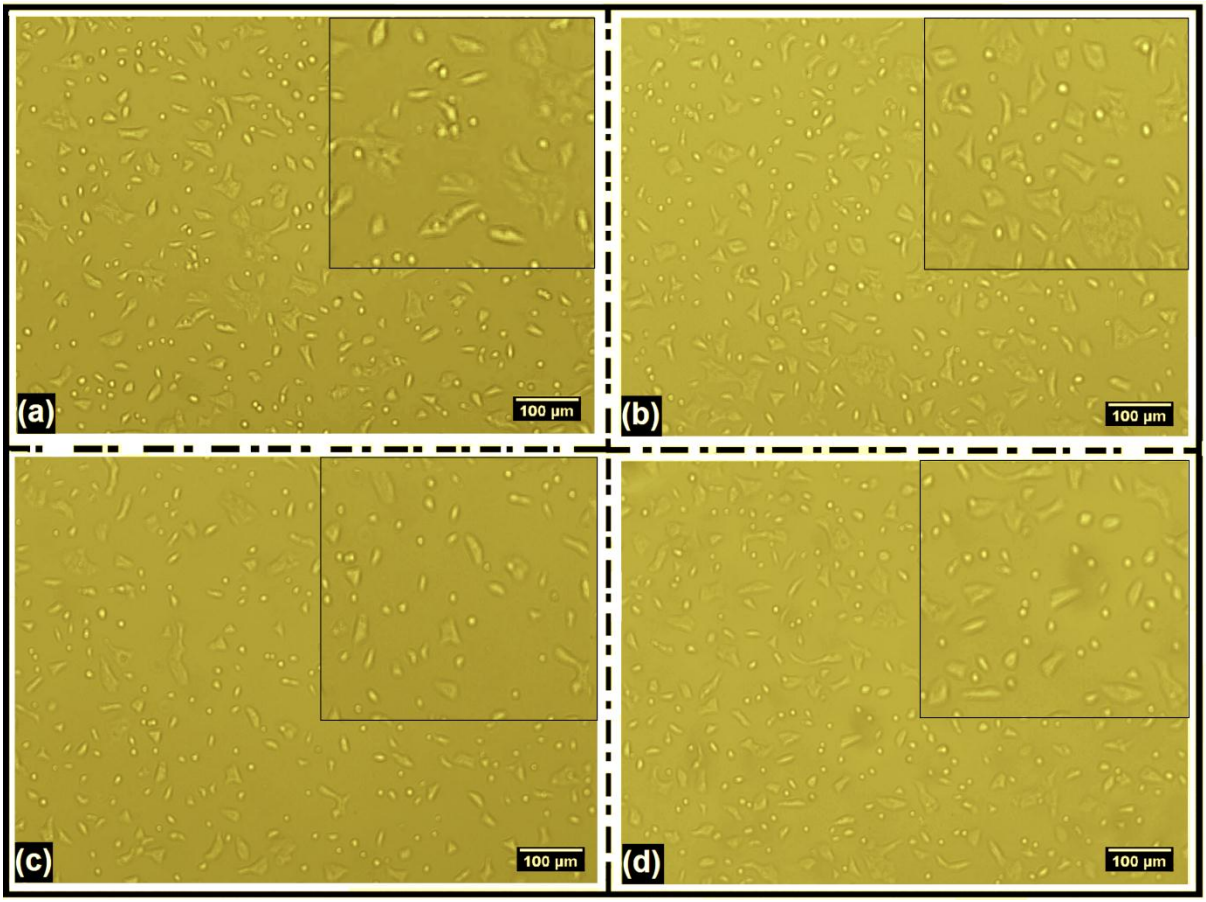

Figure 6.10: Micrographs of HaCaT cells (a) control, in the presence of leachates of bigels (b) SG, (c) GG and (d) WG bigels

6.3.10 *In vitro* antimicrobial studies

Antimicrobial activity of the metronidazole loaded bigels was carried out against the gram-negative bacterium, *E. coli*. MR (Metrogyl®) was used as the positive control. The study showed that SGM, GGM, and WGM had good antimicrobial activity against *E. coli*. The zone of inhibition was in the order of MR > GGM > WGM > SG (figure 6.11, table 6.6). This can be attributed to the faster diffusion of the drug from MR followed by GGM, WGM, and SGM, respectively. The *in vitro* drug release profile also showed release pattern in similar order. These results suggested that the developed formulations can prolong the release of the drug thus making them suitable for controlled delivery applications. The p values > 0.05 indicated comparable antimicrobial activity of the drug loaded bigels and Metrogyl® MR (Dosage form- gel, Dose-Apply, and rub in a thin film of Metrogyl gel twice daily to affected areas after washing) used as a reference. 1000 µg of the drug dose was used in all the cases for the test as well as for reference.

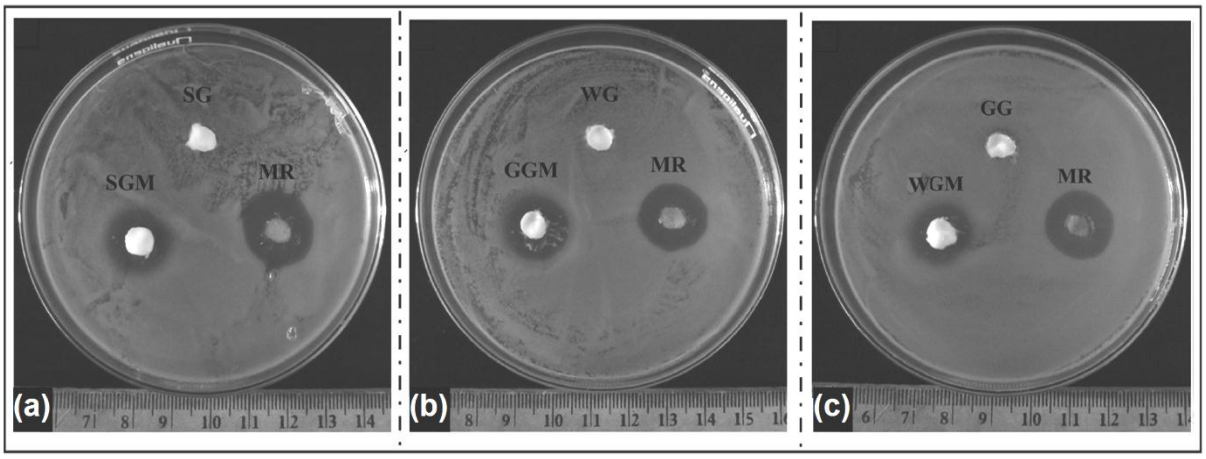

Figure 6.11: Antimicrobial activity of the bigels against *E. coli*. (a) SGM, (b) GGM and (c) WGM

Table 6.6: Zone of inhibitions of SGM, GGM, and WGM bigels

Sample code	Zone of inhibitions (cm) *E. coli*		
	Test	**MR**	**Blank (BL)**
SGM	1.45 ± 0.25	2.1 ± 0.62	-
GGM	1.72 ± 0.25	2.4 ± 0.53	-
WGM	1.51 ± 0.40	2.2 ± 0.73	-

6.3.11 *In vitro* drug release studies

The release profiles of metronidazole from SGM, GGM, and WGM have been shown in figure 6.12a and the release kinetics parameters have been tabulated in Table 6.7. The release profiles suggested 20.9%, 58.3% and 30.2% of metronidazole was released from SGM, GGM, and WGM, respectively, at the end of 12h. The release of the drug was compared with the marketed formulation of metronidazole. The marketed formulation (Metrogyl®) showed comparatively higher release (89.9%). The drug release from the bigels decreased in the order of GGM > WGM > SGM. The higher release from GGM can be explained by the dissolution of the gelatin molecules, which leaves behind pores which accelerate the release of the drug from the matrix [160].

This was expected, as the bulk resistance calculated from the impedance spectroscopy were in the same order of SG > WG > GG. In other words, the conductivity of the bigels was in the order of GG > WG > SG. In general, the formulations with higher conductivity usually show higher drug release profiles, if the sink conditions are properly maintained. The release profiles showed a burst release of metronidazole from MR. The burst release was lower in the developed bigels. The burst release was significantly higher in GGM amongst the prepared bigels but was significantly lower as compared to MR. The burst release of metronidazole from MR and GGM may be associated with the hydrophilic nature of the formulations. This study showed that the release of metronidazole may be tailored by altering the compositions of the bigels. The release of metronidazole from the bigels and MR followed Higuchi release kinetic model. This indicated diffusion mediated drug release from the formulations. The release exponent was calculated from the Korsmeyer-Peppas model to identify the mechanism of diffusion. The release exponent of GGM was less than 0.5 suggesting quasi-Fickian diffusion mechanism [161]. This may be attributed to the presence of tiny interstices of helical fibres of gelatin in GGM. The release exponent of SGM and WGM was greater than 0.5 indicating a combination of diffusion and erosion of the formulations as a probable mechanism of drug release. Marketed formulation of metronidazole Metrogyl® (Dosage form- gel, Dose-Apply, and rub in a thin film of Metrogyl gel twice daily to affected areas after washing) was used as a reference.

Figure 6.12c and table 6.7 showed that the release of metronidazole followed zero-order kinetics on the application of AC. Metronidazole release from the marketed formulation was almost equivalent to that of GGM bigels. The drug release from the marketed formulation under active condition was highest amongst all the bigels. The release of metronidazole was highest from GGM followed by WGM and SGM, respectively. The results can be explained

by the conductivity profile of the bigels. The release of the drug was higher when AC current was used as compared to the passive conditions (figure 6.12d). The percent increase in the release of metronidazole was found to be highest in SGM followed by WGM and GGM, respectively. This may be due to the easy diffusion of the drug from WGM and GGM, which resulted in the reduced efficiency of the iontophoretic system. The effect was more pronounced in SGM, where the diffusion of metronidazole was restricted (as seen from passive release profile). The mechanism of drug release from the bigels followed zero order mass transport on the application of current. The "n" value for the KP model was found to be in the range 0.5-1.

Table 6.7: Drug release kinetics from normal and iontophoretic setup

Formulation code	**Zero order model (r^2)**	**Higuchi model (r^2)**	**Best fit model**	**Korsmeyer-Peppas**		**Mechanism of drug release**
				(r^2)	**N**	
Passive drug delivery						
SGM	0.9602	0.9910	Higuchi	0.9901	0.6213	Diffusion
GGM	0.8012	0.9621	Higuchi	0.9902	0.3513	Diffusion
WGM	0.9182	0.9900	Higuchi	0.9811	0.7002	Diffusion
MR	0.9801	0.8801	Higuchi	0.9802	0.4700	Diffusion
Iontophoretic drug delivery						
SGM (Passive)	0.8512	0.9916	Higuchi	0.9228	0.7702	Diffusion
GGM (Passive)	0.5602	0.9808	Higuchi	0.9310	0.3813	Diffusion
WGM (Passive)	0.9700	0.9210	Higuchi	0.8802	0.4721	Diffusion
SGM (Active)	0.9931	0.9511	Zero order	0.8510	0.8304	Anomalous
GGM (Active)	0.9902	0.9600	Zero order	0.7291	0.8471	Anomalous
WGM (Active)	0.9912	0.9700	Zero order	0.6101	0.7521	Anomalous

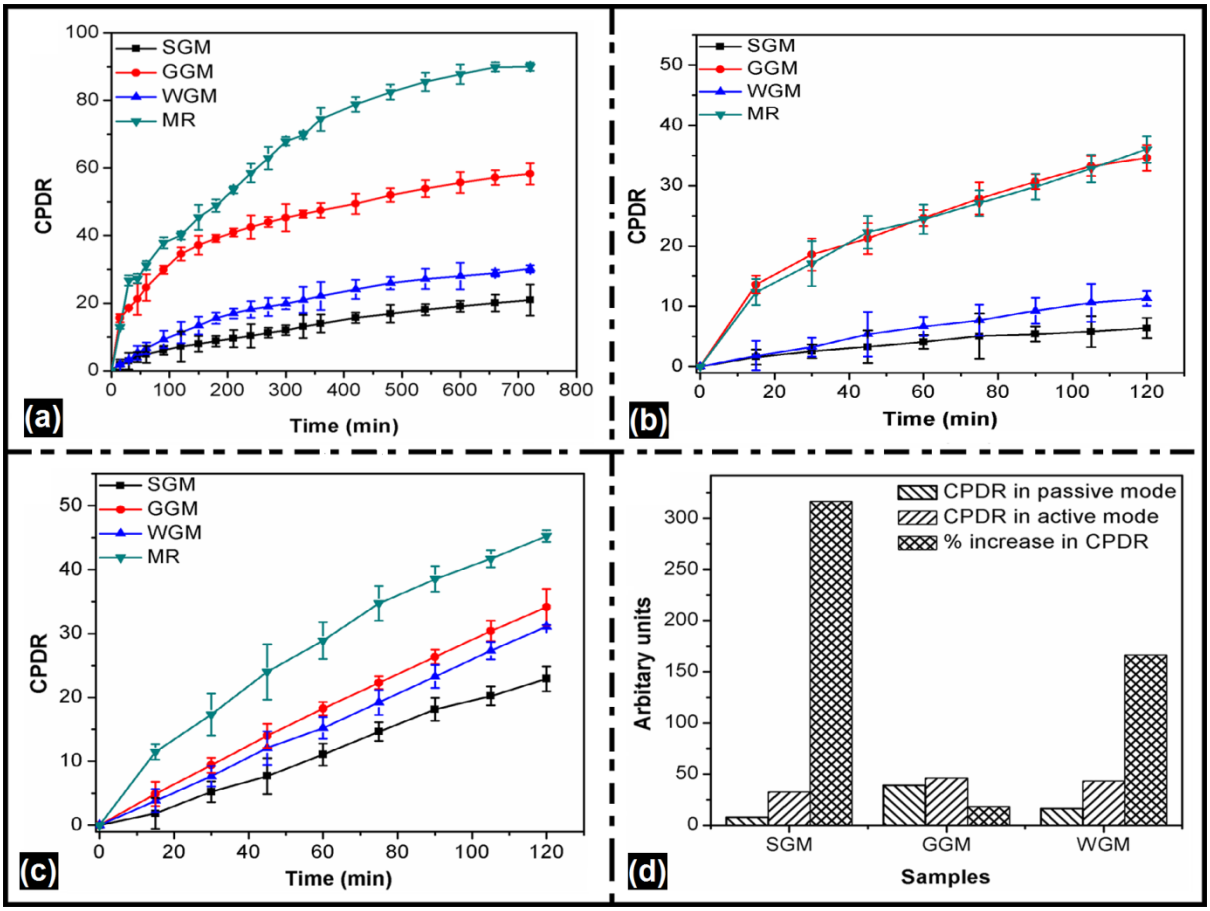

Figure 6.12: *In vitro* metronidazole release. (a) passive drug release, (b) passive drug release using iontophoretic drug release setup, (c) active drug release using iontophoretic drug release setup and (d) effect of iontophoresis over passive drug release

6.4 Major outcomes

- Fluorescence microscopy suggested that oleogels were present as the dispersed phase.
- The bigels containing whey powder and gelatin had a larger droplet size as compared to the blank bigel. This was attributed to the adsorption of the proteins on the droplet surface.
- The viscosity and firmness of the gelatin bigel were higher as compared to the whey powder bigel due to droplet size and intermolecular hydrogen bonding, respectively.
- The conductivity of proteins based bigel was reported to have a higher conductivity as compared to the blank bigels. This was due to the presence of hopping charge carriers. The higher conductivity of gelatin bigels with respect to whey powder based bigels was attributed to the lesser bulk resistance of these bigels.
- HaCaT cells showed good viability in the presence of the bigels indicating the biocompatibility of the bigels.
- The bigels showed good antimicrobial activity against *E. coli*.
- The higher release from gelatin-based bigels as compared to other bigels was due to the faster dissolution of the gelatin molecules. The faster dissolution of gelatin leaves behind pores which accelerated the release of the drug from the matrix. Controlled release of the drug from the whey powder gels was due to its ability to swell in the presence of water.

CHAPTER 7

Preparation and characterization of polysaccharides based bigels using emulgels of sunflower oil and sorbitan monopalmitate

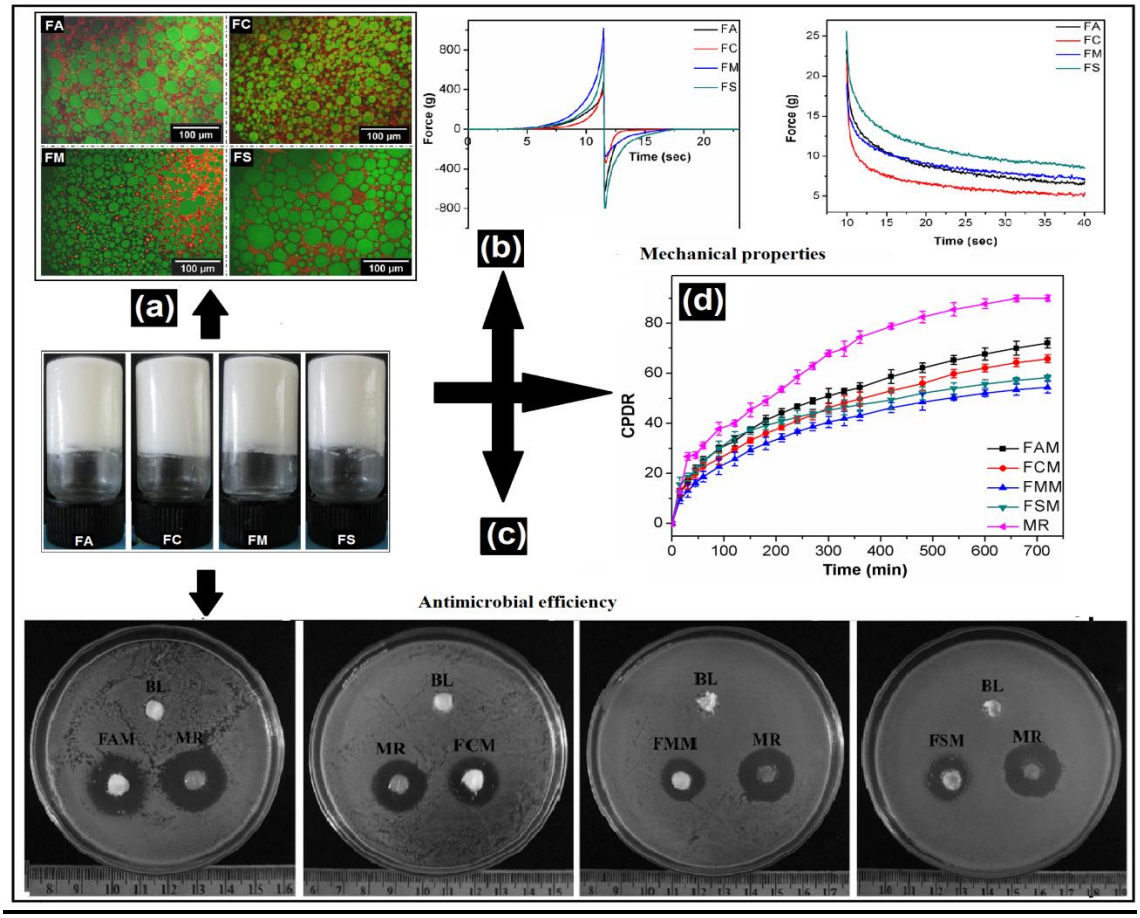

Graphical outline: (a) Fluorescence micrographs, (b) Mechanical properties, (c) antimicrobial activity, and (d) *in vitro* drug release behavior of polysaccharides based bigels.

Overview

The effect of various polysaccharides on the physical and mechanical properties of bigels was explored in depth. The bigels were prepared by mixing sorbitan monopalmitate-sunflower oil oleogels with the aqueous polysaccharide sols. A fluorescence microscope was used to analyze the microstructure of the bigels. The types of physicochemical interactions occurring within the bigels were analysed using an FTIR. The flow behavior of the gels was studied using viscometer. The bigels were further characterized for their mechanical and viscoelastic properties using a static mechanical tester. Gel disintegration studies were carried out at pH 7.4. A differential scanning calorimeter and a phase sensitive multimeter were used to determine the thermal and electrical properties of the bigels. The *in vitro* cytotoxicity studies of the bigels were carried using goat blood RBC and HaCaT cells. The antimicrobial efficiency of the bigels was investigated using *E.coli*. *In vitro* drug release studies were conducted under passive as well as active conditions at pH 7.4. The micrographs showed spherical droplets of oleogels in the continuous aqueous phase. The FTIR studies showed hydrogen bonding in the bigels. The bigels were viscoelastic in nature and exhibited shear-thinning behavior. The disintegration time of bigels containing starch and maltodextrin was found to be slower. The thermal profile showed the presence of more than one event. The bigels were electrically conductive. These bigels showed good antimicrobial efficacy. The release of metronidazole (model drug) from the bigels was diffusion mediated. The application of AC current to the bigels released the drug in a constant manner. The preliminary studies suggest that the developed bigels can be used effectively as controlled delivery matrices.

7.1 Introduction

Gelation of edible oil is a promising alternative that modifies the physical properties of the edible oil as compared to the chemical methods, which often results in the production of trans-fatty acids. However, structured edible oils are not consumed as such; instead, they are further formulated into food products. They are usually delivered in the form of emulsion systems such as margarine (w/o systems) or mayonnaises and dressings (o/w systems). Polysaccharides are naturally occurring polymers and may either be obtained from plant, animal or microbes [162]. Since the polysaccharides are biochemically similar to the extracellular matrix components of the human body, they are often found to be biocompatible in nature. Due to this reason, they have been extensively studied to develop food and pharmaceutical products. One of the most commonly used applications is the development of hydrogel-based matrices for controlled delivery of bioactive agents.

In this study, two classes of natural polysaccharides, *viz.* linear and branched, were chosen for formulating bigels. Sodium alginate and sodium carboxymethyl cellulose were used as the linear polysaccharide, whereas, starch soluble (potato starch) and maltodextrin were used as the branched polysaccharides. The stability, availability, renewability and low toxicity of these polymers make them attractive for various pharmaceutical and food applications. Sodium alginate is a natural anionic copolymer extracted from brown seaweed and algae composed of α-L-guluronic acid (G) and β-D-mannuronic acid (M) residues. The formation of a gelatinous barrier of alginate upon hydration acts as a diffusion barrier for many drugs and is an important phenomenon for controlled delivery of bioactive agents. Carboxymethyl cellulose is a semi-synthetic anionic water-soluble polysaccharide possessing β-(1→4)-D-glucopyranose units. It has been widely studied for biomedical applications. It is often available as sodium salt, and its viscosity-imparting tendency has been used to tailor the release properties of the drugs [163]. Soluble starch $(C_6H_{10}O_5)_n$ is one of the most abundant polymers in nature, comprising of glucose units with 'n' ranging from 300 to 1000. It is a mixture of linear polymer amylose and highly branched amylopectin. Maltodextrin is a neutral polysaccharide derived by enzymatic degradation of starch. Its film-forming property and ability to act as an osmotically bulk forming agent make it a suitable candidate for food and pharmaceutical applications

Keeping the facts above in mind, an attempt was made to develop polysaccharide based bigels for the controlled delivery of antibiotics (e.g. metronidazole).

7.2 Experimental

7.2.1 Preparation of polysaccharides based bigels

The compositions of the polysaccharide based bigels are mentioned in Table 7.1. 5 g of the prepared polysaccharide solution (50 °C) was added drop-wise to the 5 g of oleogel (50 °C). The mixture was thoroughly mixed at 12000 rpm until a milky white emulsion was formed. This mixture was then allowed to cool to room temperature to form bigels. Drug loaded bigels were prepared in a similar manner.

Table 7.1: Composition of the polysaccharide based bigels

Sample code	Polysaccharides % (w/w)				Sorbitan Mono palmitate % (w/w)	Sun flower oil % (w/w)	Metronidazole % (w/w)
	Sodium alginate	Sodium carboxy methyl cellulose	Maltodextrin	Starch soluble			
FA	0.5	-	-	-	9	41	-
FC	-	0.5	-	-	9	41	-
FM	-	-	0.5	-	9	41	-
FS	-	-	-	0.5	9	41	-
FAM	0.5	-	-	-	9	41	1
FCM	-	0.5	-	-	9	41	1
FMM	-	-	0.5	-	9	41	1
FSM	-	-	-	0.5	9	41	1

7.3 Results and discussion

7.3.1 Preparation of bigels

The backward extrusion profile (figure 7.1) of the sols suggested Newtonian flow behavior. The viscosities of sodium alginate, sodium CMC, maltodextrin and starch sols were found to be 0.01028 ± 0.00514 Poise, 0.01365 ± 0.00625 Poise, 0.00893 ± 0.004 Poise and 0.00798 ± 0.0035 Poise, respectively. When sodium alginate and carboxymethyl cellulose are dispersed in water, an electrolytic reaction occurs separating the alginate and carboxymethyl cellulose into sodium cations and polyanionic polymers. In addition to this, the water molecules and -

OH groups on the alginate and carboxymethyl cellulose molecules exhibit electric dipole moments which considerably enhance electrostatic interacting forces which increase the viscosity of sodium alginate and sodium carboxymethyl cellulose solutions as compared to soluble starch and maltodextrin.

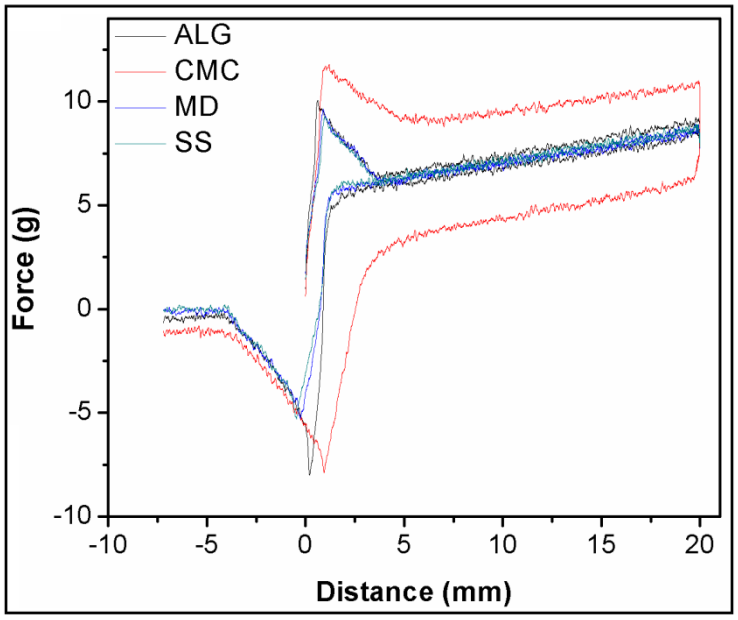

Figure 7.1: Viscosity profile of the polysaccharide sol from the backward extrusion method

Inverted-tube method was used to confirm the gel formation (Figure 7.2). The prepared bigels were found to be stable for >10 months under intermediate testing conditions. In this test, the bigels were kept under the specified conditions as mentioned above. The evaluation was based on visible signs of destabilization of bigels such as phase separation and changes in the color. A minimum of 3 batches of each sample was studied under these conditions. The pH of all the bigels was found to be in the range of 6-7.

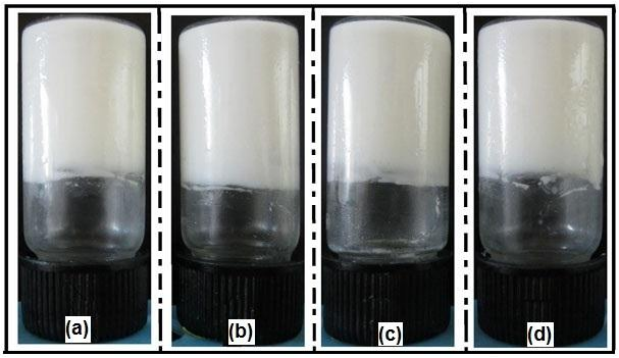

Figure 7.2: Inverted-tube for the confirmation of bigels formation (a) FA, (b) FC, (c) FM and (d) FS

Alginate belongs to a class of linear unbranched polysaccharides containing varying amounts of 1, 4′-linked β-D-mannuronic acid and α-L-guluronic acid residues. These homopolymeric regions of β-D-mannuronic acid blocks and α-L-guluronic acid blocks are inter dispersed with regions of alternating structure (β-D-mannuronic acid–α-L-guluronic acid blocks)[164]. The crosslinking and gelation of the polymers are mainly achieved by the exchange of sodium ions from the guluronic acids with the divalent cations, and the stacking of these guluronic groups to form the characteristic egg-box structure. Each alginate chain can dimerize to form junctions with many other chains as a result of which gel networks are formed rather than insoluble precipitates [164]. The bigels of sodium carboxymethyl cellulose are formed majorly due to the hydrogen bonding. The hydrogen bonding usually occurs due to the presence of hydroxyl groups [165].

Soluble starch $(C_6H_{10}O_5)_n$ is one of the most abundant polymers in nature, comprising of glucose units with "n" ranging from 300 to 1000. It is a mixture of linear polymer amylose and highly branched amylopectin. During the process of heating, the starch granules undergo gelatinization that causes a reorganization of the structure. Starch is organized in concentric alternating semi-crystalline and amorphous layers in the form of granules [166]. These granules vary in size. On heating water first starts entering the rings. These rings start swelling and at a certain degree, release the amylose units. On cooling, there is an interaction between the amylose units forming a gel network. The major interactions that bind both the components of the starch are hydrogen bonds and hydrate bridges. The amylopectin rearrangement occurs, later on, giving rigidity to the gel matrix [167]. The formation of maltodextrin gels is similar to that of the starch as it is a hydrolysed product of starch. The chemistry behind these gels is the formation of smaller crystallites from the nuclei (aggregates of double helices of amylose) thereby growing into a stronger gel. During this process, there is a conversion of helices to coil structure [168].

7.3.2 Microscopy and microstructural analysis

Figure 7.3 shows the presence of spherical droplets in a continuum phase. The droplets were green indicating the presence of oleogel as the dispersed phase. The presence of red color as the continuum phase suggested the presence of water as the external phase. The observations from the micrographs indicated the formation of an oil-in-water type of bigels. The average droplet size (or 50% of the droplets) of the dispersed phase in the bigels was in the range of 5.0-16.0 μm (Figure 2e). The average droplet size of the dispersed phase of FM was smaller as compared to the other bigels. The differences in the droplet sizes of the internal phase of

FM and FC were statistically insignificant ($p > 0.05$) while for the rest of the bigels showed $p < 0.05$ indicating that the droplet sizes were statistically different. A narrow size distribution of the dispersed phase droplet of FC and FM bigels was observed. These results may be due to the viscosity-imparting effect of carboxymethyl cellulose and maltodextrin [169]. FA and FS, on the other hand, showed a broad size distribution. This difference in the particle sizes of FS was due to the poor efficiency of starch granules to stabilize oil droplets, which may be accounted to the low surface hydrophobicity of the starch granules [170]. This, in turn, affects the droplet size distribution (DSD) of the final bigels. Due to the low hydrophobicity of starch, the droplets started to coalesce resulting in a wider DSD in FS. Alginate chains, on the other hand, readily form hydrogen bonds with the surrounding molecules which reduced the electrostatic repulsion [171]. This could have promoted droplet coalescence resulting in a broad size distribution in FA.

The span factor of FA, FC, FM and FS was 1.52 ± 2.14, 1.28 ± 1.51, 2.01 ± 1.86 and 2.91 ± 2.52, respectively. The span factor for FA and FC bigels was found to be lower than FM and FS. This indicated the formation of near uniform droplets in FA and FC.

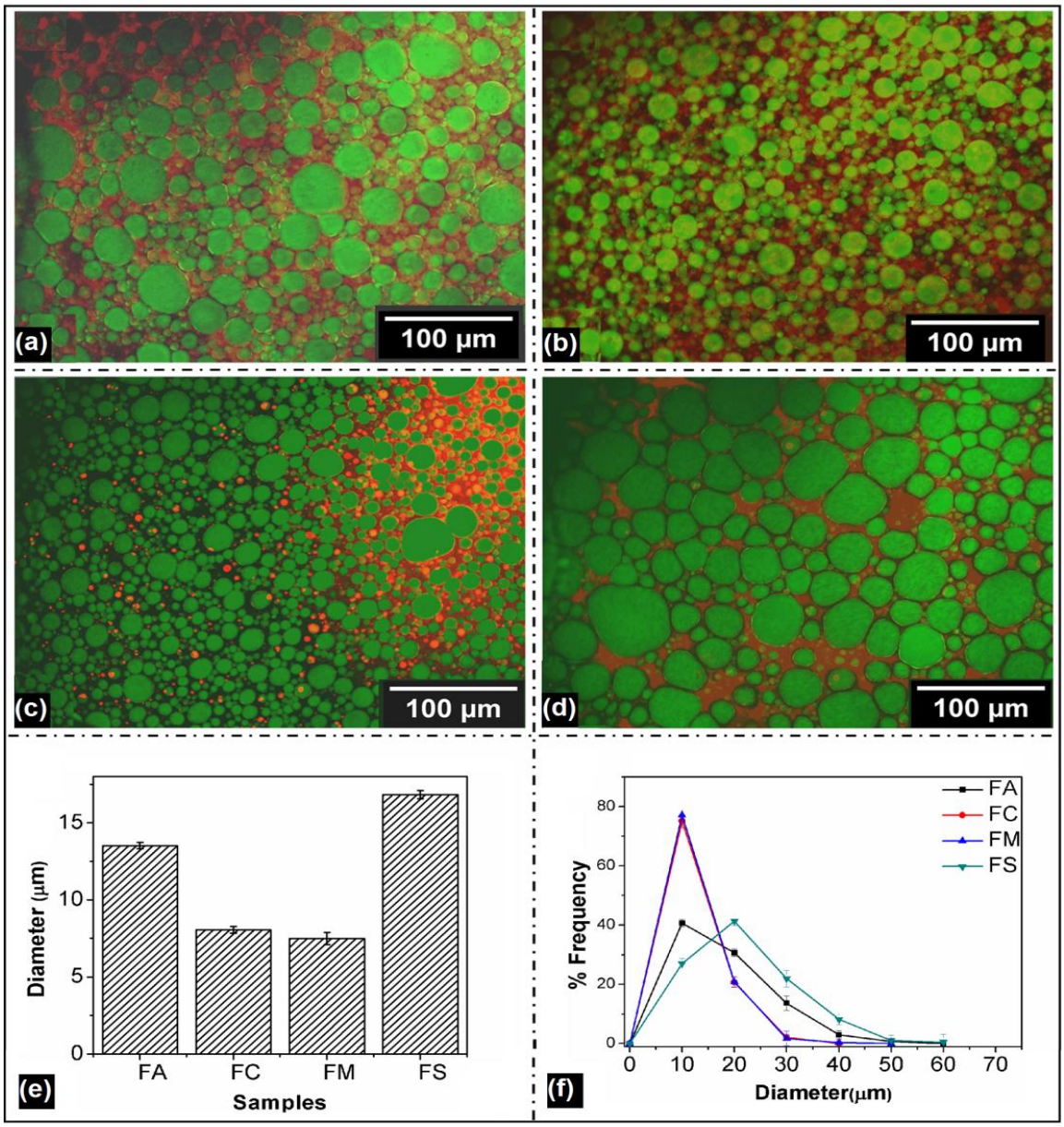

Figure 7.3: Fluorescence micrographs of: (a) FA, (b) FC, (c) FM, (d) FS, (e) average droplet size and (f) droplet size distribution

7.3.3 FTIR analysis

FTIR spectrum (figure 7.4a) of sodium alginate showed CO stretching vibrations at 1645 cm^{-1}. The free OH stretching vibrations were seen in the range of 3046-3301 cm^{-1}. The IR peak at 1460 cm^{-1} was due to COO^- groups. The FTIR spectrum of sodium carboxymethyl cellulose showed a sharp peak at 1146 cm^{-1} indicating the stretching vibrations due to the ether groups. The peaks at 2934 cm^{-1} and 2855 cm^{-1} were due to the CH stretching vibrations in CH_2 and CH groups. The FTIR bands at 1600 cm^{-1} and 1417 cm^{-1} were due to the stretching vibrations of COO^- groups. Starch soluble and maltodextrin showed characteristic

peaks at 859 cm^{-1} and 853 cm^{-1} indicating the presence of α-type glycosidic linkage. The polysaccharides showed a characteristic peak at 1023-1080 cm^{-1} which were due to the CO stretching vibrations (COC group of sugar ring). The disappearance of this peak in the bigels (figure 7.4b) indicated the breaking of the ring structure present in the polysaccharides due to the presence of molecular interactions in the bigels. The bigels showed a blue shift to a higher wavenumber from 3143 cm^{-1} to 3331cm^{-1}, 3320 cm^{-1} to 3358 cm^{-1}, 3275 cm^{-1} to 3363 cm^{-1} and 3281 cm^{-1} to 3363 cm^{-1} for FA, FC, FM and FS, respectively (figure 3b). The blue shift suggested stronger hydrogen bonding in the polysaccharides as compared to the bigels. An increase in the broadening of the peak in the range of 3000-3693 cm^{-1} in bigels was associated due to the overlapping of OH stretching vibrations of polysaccharides and water.

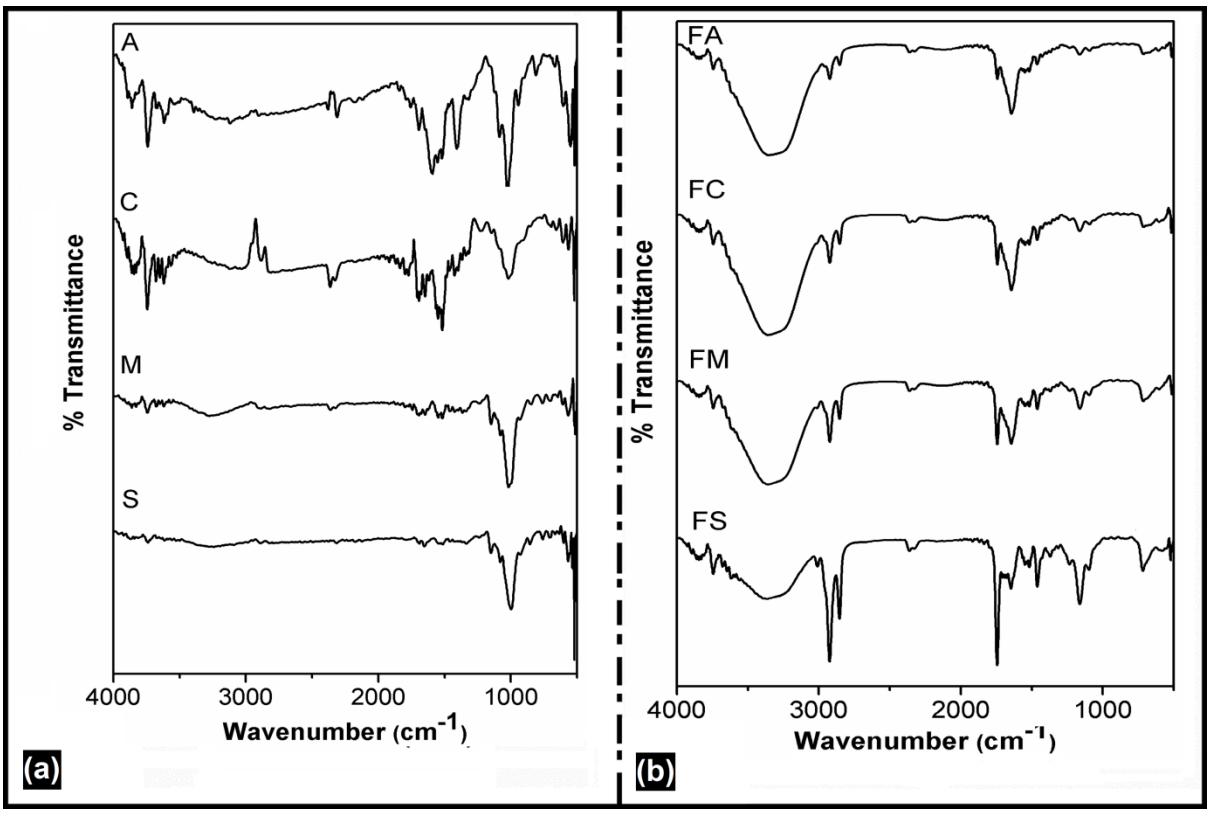

Figure 7.4: FTIR of (a) raw materials and (b) bigels

(A: Sodium alginate, C: Sodium carboxymethyl cellulose, M- Maltodextrin and S- soluble starch)

7.3.4 Viscosity analysis

The viscosity of the bigels decreased with the increase in the shear rate indicating shear thinning behavior. The viscosities of the bigels were in the order of FM ≈ FS > FA > FC (Figure 7.5a). The viscosity data were fitted to the power law equation as discussed in chapter 4.

The 'n' values were determined from the log-log plot of η and γ. The 'n' values were < 1. (Figure 7.5b, table 7.2). The viscosity of FM and FS were higher than the FA and FC bigels. The low viscosities of FA and FC may be associated with the interaction of the linear polysaccharides with the non-ionic surfactants. There have been studies related to the interaction of the anionic polymer with the non-ionic surfactants. Some part of the sodium CMC and sodium alginate might have interacted with the polar head group of the non-ionic surfactant (sorbitan monopalmitate). This exposed the non-polar groups, thereby, enhancing the overall hydrophobicity and possibly the interpolymer association [172-173]. The decrease in the relative viscosities for polymer-thickened systems can also be explained in terms of the viscosity ratio between the continuous phase viscosity (η_c) and the dispersed phase viscosity (η_d), i.e., η_c/η_d. [173]. The interaction between surfactant and the polysaccharide resulted in the decrease in the viscosity of the continuous phase. This resulted in the decrease in the viscosity of the bigels even though the viscosity of the polysaccharide sol was higher. It has also been reported earlier that the addition of lipids and surfactants make the starch granules more rigid, which might have resulted in the increase in the viscosity of FS. The higher viscosity of FM was due to the use of high-saccharified maltodextrin. The high-saccharified maltodextrin has been reported to swell to a high degree resulting in the thickening of the maltodextrin sol. This explained the higher viscosity of FM. The higher viscosity of FS was due to the amylose content within the starch molecules. Higher amylose content resulted in the higher viscosity which is due to the increased chain entanglement amongst the amylose chains. The higher viscosity of FM and FS is also associated with the branched structure of maltodextrin and starch. With the increase in the branching, the entanglement amongst the polysaccharide chains increased, resulting in the increase in the viscosity.

The inter-chain interaction amongst the linear polysaccharides was minimal. The inter-chain interaction refers to the presence of a helical structure of amylose and amylopectin as reported earlier in the literature [174]. The interactions that play a major role in these polymers are the hydrogen bonds. Strong hydrogen bonds stabilize the linear chain of sodium CMC along the direction of the chain thus maintaining and reinforcing the flat, linear, and rigid conformation of the chain. The axial and equatorial arrangement of all the aliphatic hydrogen groups and a polar hydroxyl group, respectively, render the complete cellulose chains hydrophobic with only the sides being hydrophilic and capable of forming hydrogen bonding. Thus, there are no intermolecular hydrogen bonding between the chains [175]. An opposite phenomenon is observed in the branched polysaccharides. In the case of branched

polysaccharides starch and maltodextrin, the amylose and amylopectin play an important role. The complex structure of these polymers predominates the other factors that affect the gel formation and viscosity. Amylose has a higher mobility and lower molecular weight as compared to amylopectin [176]. Amylose exists as a random coil in water. There might be an aggregation of amylose during the gel formation, which accounts for the lower viscosity of the alginate and sodium carboxymethyl cellulose based bigels [177].

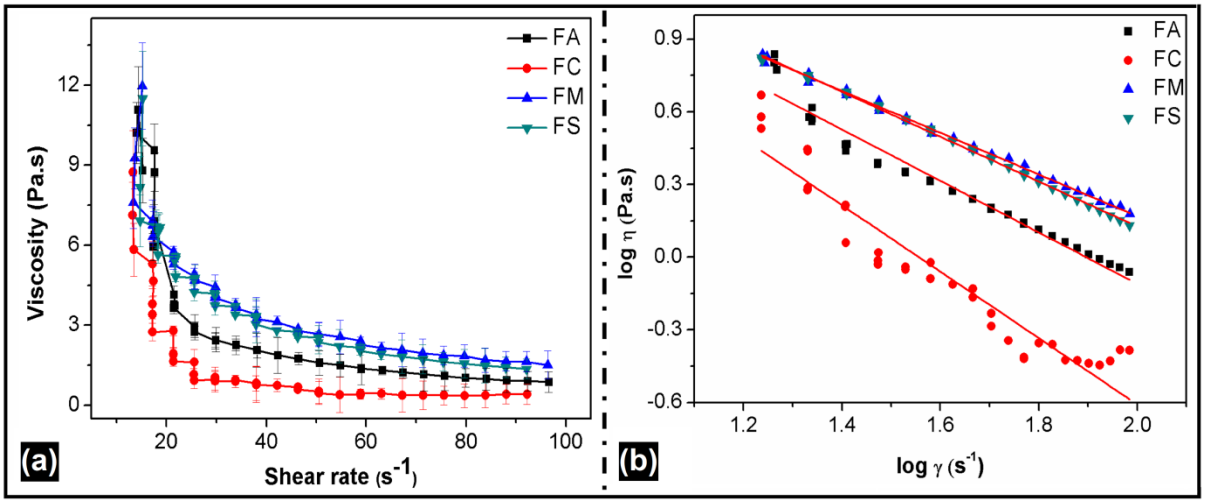

Figure 7.5: (a) Viscosity of the bigels and (b) power law fit of the bigels

Table 7.2: Power law parameters

Sample code	n values	Correlation coefficient r^2
FA	0.0912	0.9767
FC	0.5756	0.9123
FM	0.0870	0.9995
FS	0.1412	0.9968

7.3.5 Mechanical analysis

The effect of the polysaccharides on the mechanical property of the bigels was studied by performing spreadability studies (Table 7.3). Usually, firmness is dependent on the viscosity of the polymer used and its concentration. The firmness (Figure 7.6a) of bigels were in the order of FM > FS > FA > FC, respectively. The results were in agreement with the viscosity studies which suggested that the incorporation of the branched polysaccharide resulted in the increase in the strength of the bigels. The lower firmness of FS as compared to FM can be attributed to the decreased retrogradation of the starch (amylose and amylopectin) granules [178]. The amylose retrogradation, present in the starch, determines the initial hardness of the

bigels. The formation of amylose-lipid complexes reduces the availability of amylose for intermolecular hydrogen bonding thus reducing the firmness [179]. Many researchers have reported that amylose retrogradation is a fast process and takes place within minutes to hours in comparison to amylopectin, which takes almost hours to days. Amylose retrogradation is almost complete before the product is cooled to room temperature [180]. The spreadability of the branched polysaccharides based bigels was less as compared to that of linear polysaccharides based bigels. The stickiness of the bigels was also in the order of the firmness studies, except the stickiness of FM. The stickiness of FM was much lower than other bigels. This may be attributed to the stickiness-reducing effect of maltodextrin as reported earlier in the literature [181].

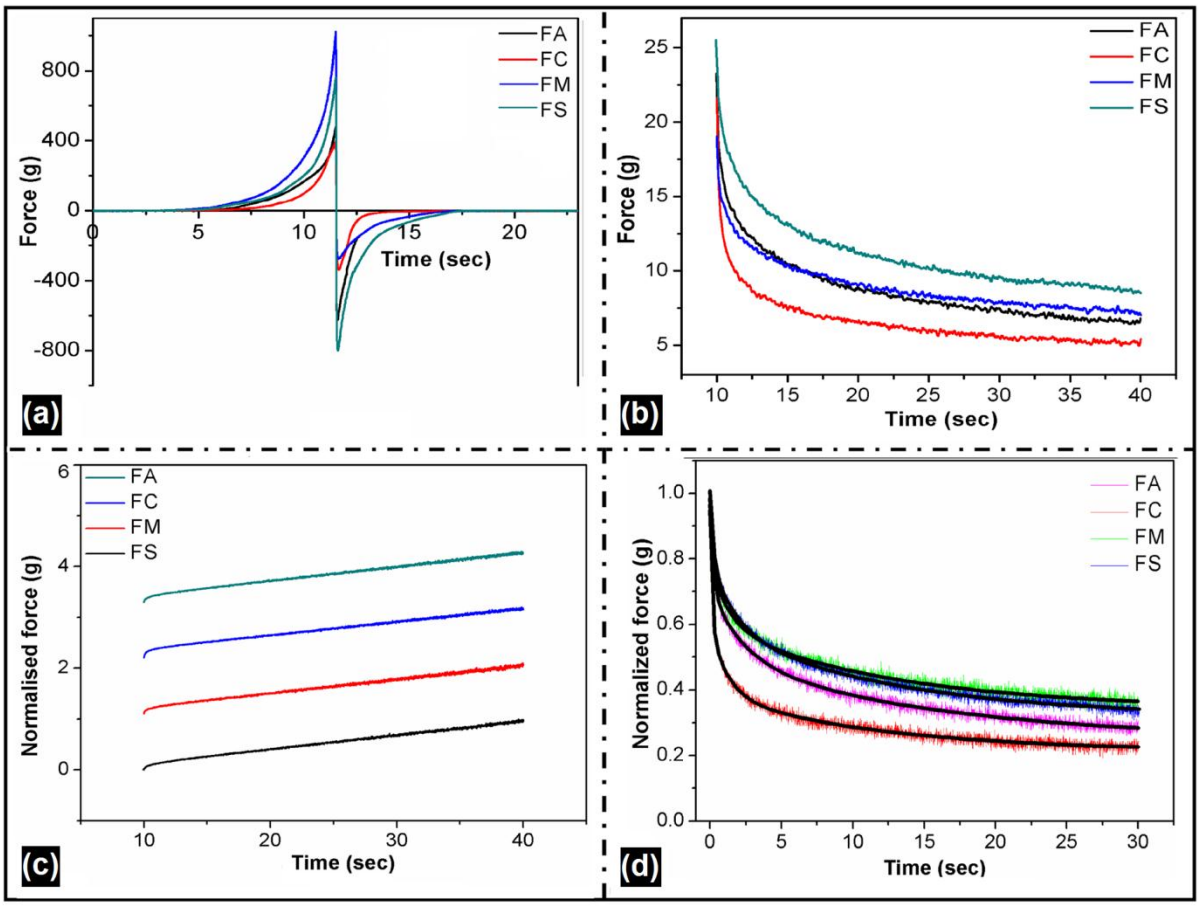

Figure 7.6: Mechanical analysis (a) spreadability, (b) stress relaxation, (c) normalised force vs. time and (d) Wiechert model

It was observed from the graph that the force reaches asymptotically to an equilibrium value instead of 0. This showed that these bigels behaved as a viscoelastic material.

It has been reported earlier that solid materials have higher k_2 values as compared to the soft or semi-solid formulations and showed a value close to unity [182]. However, no clear trend

could be discerned from both k_1 (rate) and k_2 (extent) values. Hence, the viscoelastic parameter (S^*) was subsequently quantified. The S^* values are in the range of 0-1 for viscoelastic materials. Viscoelastic materials with higher elastic behavior have S^* values closer to 1. The S^* values of all the bigels were < 1 indicating the viscoelastic property of these bigels. The differences between the S^* values was insignificant.

Percent stress relaxation was dependent on the properties of the polysaccharide incorporated in the bigels. The relaxation of the gels containing linear polysaccharides was much higher as compared to the branched polysaccharides. Greater relaxation of FA and FC bigels means that the bigels had more capacity to dissipate the applied stress (energy) as compared to FM and FS. The lower degree of relaxation in FM and FS can be explained by the complex structures of amylose and amylopectin units which are present in both starch and maltodextrin. The branching increases the number of polymer chain ends in comparison to linear polymers of same molecular weight. This restricts the chain relaxation process [183]. It was observed that the bigels with lower firmness showed greater relaxation as compared to the firmer bigels. The relaxation decreased in the order of FC > FA > FS > FM. Percent stress relaxation for ideal elastic solid corresponds to 0% while for liquid it is 100%. The percent stress relaxation for the bigels was in between 0% and 100% indicating their viscoelastic behavior.

The Weichert's model (figure 7.6d), was used to provide the relaxation behavior with respect to time. This relaxation model is similar to the viscoelastic model used to describe the shape recovery behavior after the application of stress. This model is used to describe the crosslinking stability and polymer segment mobility in the bigels [184]. The residual stress (P_0) is an indicator of the stability of the bigels. A decrease in the residual stress indicates the breaking of bonds in the polymer network. The residual stress was higher in the FM and FS (table 7.4). The P_0 values decreased in the following order of FM=FS> FA>FC. A lower percent stress relaxation was observed when branched polysaccharides were used. The relaxation times (τ) were in the order of $\tau_1 < \tau_2 < \tau_3$ and were in acceptance with the literature [107]. According to the earlier studies, each relaxation constant is associated with specific structural rearrangement. τ_1 is the shortest relaxation time constant and τ_3 is the longest relaxation time constant. τ_2 and τ_3 are the important parameters that decide the stability of the bigels and are associated with the polymer rearrangement occurring during the relaxation process [106].

The values of τ_2 and τ_3 correspond to the disentanglement and breakage of polymer interactions, respectively. The decrease in the values of τ_2 and τ_3 can be attributed to the

formation of better network and interaction amongst the polysaccharide chains in the bigels. It was also observed from the model that the τ_2 and τ_3 values of the branched polysaccharide based bigels were higher as compared to linear polysaccharides based bigels. These results confirm that the disorganization of the bigels containing branched polysaccharides is less as compared that containing linear polysaccharides when stress is applied. The coefficients of viscosities of all the bigels displayed a complex behavior. The results showed that the viscosity at particular stress value and relaxation time was dependent on the viscosity of the hydrogel phase in the bigels. These findings were in agreement with the backward extrusion study which showed that sodium CMC sol had a higher viscosity as compared to sodium alginate, maltodextrin, and soluble starch based sols.

Table 7.3: Mechanical properties of the gels

Studies	Parameters	FA	FC	FM	FS
Mechanical properties	Firmness (g)	682.4721± 3.1423	646.2832 ± 2.5287	1000.7623 ± 1.8211	729.4421 ± 3.1471
	Stickiness (g)	555.2812 ± 2.1503	472.0912 ± 3.1653	274.9421 ± 1.3282	800.2737 ± 2.1552
	Spreadability $(g.sec)^{-1}$	0.0021 ± 0.0013	0.0015 ± 0.0013	0.0007 ± 0.0005	0.0010 ± 0.0090
	K_1 (g)	0.1549 ± 0.0234	0.0948 ± 0.0054	0.1527 ± 0.0043	0.1666 ± 0.0347
	K_2 (g)	0.0285 ± 0.0142	0.0269 ± 0.0134	0.0278 ± 0.0123	0.0284 ± 0.0097
	S*	0.7505 ± 0.1232	0.7499 ± 0.2456	0.7502 ± 0.1386	0.7516 ± 0.2376
	Percent stress Relaxation	70.5202 ± 3.6585	76.1627 ± 1.4282	65.3332 ± 2.4792	65.6251 ± 1.4726

Table 7.4: Weichert model parameters of the bigels

Formulation code	τ_1	τ_2	τ_3	r^2
FA	0.3121	2.1421	12.3356	0.9812
FC	0.3565	1.7034	14.9398	0.9734
FM	0.3074	1.2911	12.1701	0.9781
FS	0.2563	1.1839	11.6969	0.9908
	Pre-exponential parameters			
	P_0	P_1	P_2	P_3
FA	0.2499	0.2698	0.2078	0.2579
FC	0.2124	0.2602	0.2762	0.3496
FM	0.3338	0.2788	0.2538	0.2586
FS	0.3011	0.2041	0.2092	0.2763

Table 7.5: Stress relaxation model fitting using Wiechert model

Formulation Code	Stress relaxation Model	Coefficient of viscosity of the dashpots
FA	$P(t) = 0.2499 + 0.2698e^{\frac{-t}{0.3121}} + 0.2078e^{\frac{-t}{2.1421}} + 0.2579e^{\frac{-t}{12.3356}}$	0.0842, 0.4451, 3.1813
FC	$P(t) = 0.2124 + 0.2602e^{\frac{-t}{0.3565}} + 0.2762e^{\frac{-t}{1.7034}} + 0.3496e^{\frac{-t}{14.9398}}$	0.0927, 0.4704, 5.2229
FM	$P(t) = 0.3338 + 0.2788e^{\frac{-t}{0.3074}} + 0.2538e^{\frac{-t}{1.2911}} + 0.2586e^{\frac{-t}{12.1701}}$	0.0857, 0.3276, 3.1471
FS	$P(t) = 0.3011 + 0.2041e^{\frac{-t}{0.2563}} + 0.2092e^{\frac{-t}{1.1839}} + 0.2763e^{\frac{-t}{11.6969}}$	0.0523, 0.2476, 3.2318

7.3.6 Gel disintegration studies

The disintegration times of FA, FC, FM and FS in pH 7.4 were 360 ± 1.26 min, 240 ± 1.53 min, 60 ± 0.98 min, 108 ± 1.12 min, and, respectively.The faster disintegration of FM bigels was associated with the increased solubility of maltodextrins. The slow disintegration of FA and FC was due to the formation of a thick, viscous layer of sodium alginate and carboxymethyl cellulose solutions around the oil droplets which hindered the diffusion of the

aqueous media within the gel matrix, which in turn, resulted in the slow disintegration of the bigels.

7.3.7 Thermal analysis

Figure 7.7 shows the DSC profiles of the bigels. The DSC profiles of all the bigels showed more than one endothermic peak indicating the presence of more than one thermal event. The endothermic peak in the range of 45-50 °C was due to the melting of sorbitan monopalmitate. The endothermic peak of FA and FC at 87.1 °C and 86.76 °C was due to the loss of the absorbed water associated with the hydrophilic group of sodium alginate and sodium carboxymethyl cellulose, respectively [185]. The endothermic peak for all the bigels between 90-102 °C may be associated with the evaporation of water present within the bigel matrix. Small endothermic peaks in the range of 105-120 °C for FM and FS were associated with the melting of amylose-lipid complexes formed by the interaction of amylose with the fatty acids present in sunflower oil and sorbitan monopalmitate [186]. Table 7.5 lists ΔH of the bigels. The branched polysaccharide based bigels, had a higher enthalpy than FA and FC. The higher enthalpy was associated with, the more stable gel formation. The enthalpy is the total heat energy uptake by the sample after suitable baseline correction during the transition [187].

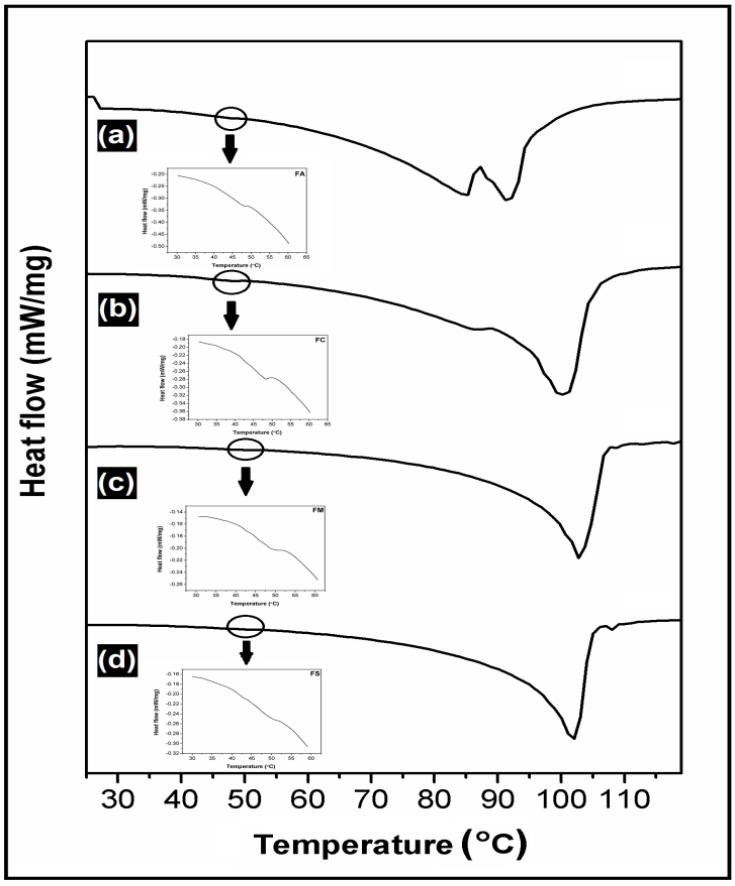

Figure 7.7: DSC profile of (a) FA, (b) FC, (c) FM and (d) FS

Table 7.6: DSC parameters of the gels

Sample code	ΔH (J/g)
FA	917.6
FC	1008
FM	923.2
FS	1088

7.3.8 Electrical analysis

Figure 7.8 shows the electrical properties of the bigels. The bulk resistance of the bigels was calculated from the Nyquist plot (figure 7.8a). FM showed highest bulk resistance as compared to the other polysaccharide based bigels. The bulk resistance of the bigels decreased in the following order FM > FS > FC > FA. The results suggested that bigels containing branched polysaccharides had higher bulk resistance. Figure 7.8b shows the variation of dielectric constant with frequency. A decrease in the dielectric constant was observed. This was attributed to the alignment of the dipoles in the direction of applied electric field at low frequency, however, at higher frequencies quick reversal of the dipole happens [188]. The AC conductivity increased with a rise in the frequency (figure 7.8c). AC conductivity of FM was lower than the other bigels. This may be attributed to the higher viscosity of the branched polysaccharides based bigels which might have altered the movement of the conducting ions. The plateau in the profile contributed to the DC conductivity of the gels.

The s-values obtained from the equation were in the range of 0 and 1. The‘s’ for FA, FC, FM and FS were 0.63, 0.63, 0.42 and 0.65, respectively. The variation of tan δ with frequency is shown in figure 9d. It was observed from the graph that the bigels exhibited a zero dielectric loss at higher frequencies The higher tan δ at lower frequencies was attributed to the conductivity relaxation of the polymers present in the bigels [189]. The relaxation was also associated with the flexibility of the polysaccharide chain. High values of dielectric loss are associated with grain boundary resistance, where higher energy is required for electron exchange. It was also observed from the above graph that the FC and FA showed two relaxation peaks. The two relaxation peaks may be called as α and β peaks. The α relaxation peak may be associated with the strong intra and inter molecular hydrogen bonding within the cellulose chains [190]. The β relaxation of cellulose is associated with the bound water molecules.

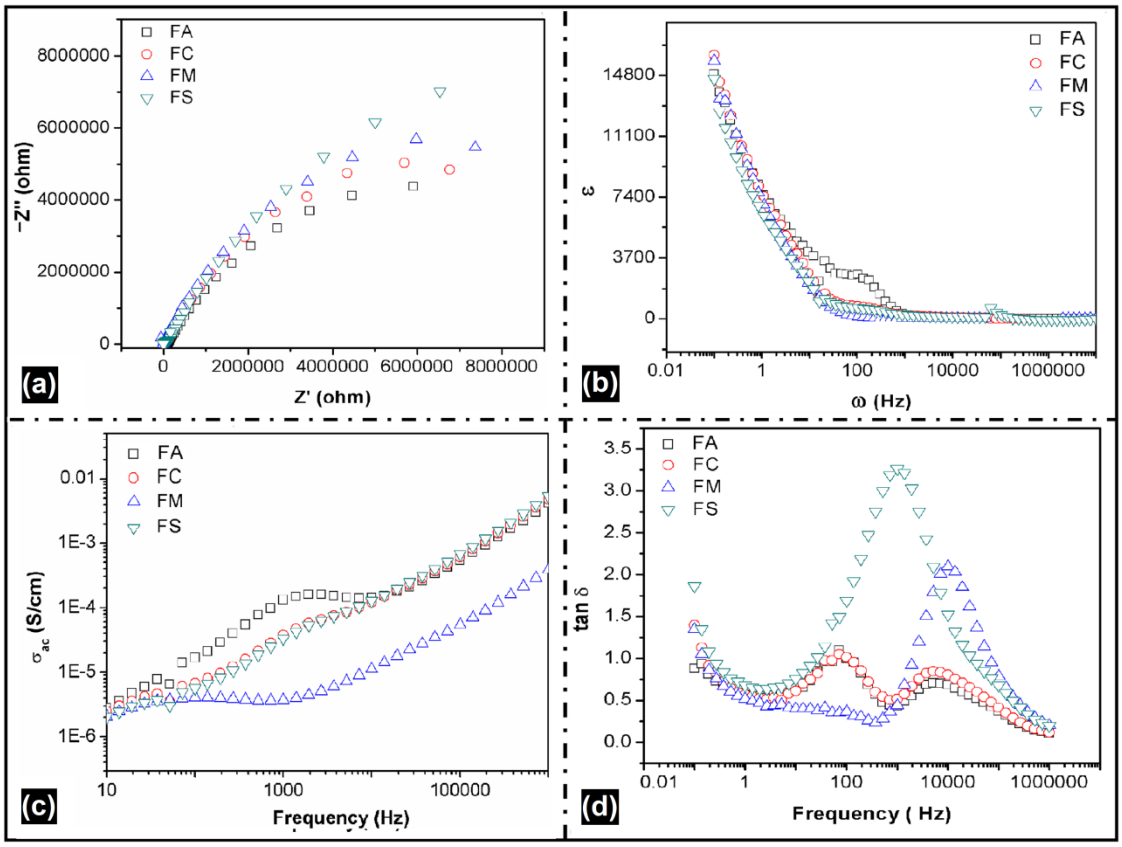

Figure 7.8: Impedance profile of the bigels (a) Nyquist plot, (b) dielectric constant vs. frequency, (c) AC conductivity, and (d) tan δ vs. frequency

7.3.9 *In vitro* cytotoxicity of dialyzed formulation components

The percent hemolysis and cell viability index of the HaCaT cells are shown in figure 7.9. The bigels were found to be highly hemocompatible, indicating the nontoxic nature (figure 7.9a) of the developed bigels. This nature of the bigels was expected because the components used for the preparation of the bigels are FDA approved. The cell viability was also dependent on the type of the polysaccharides used in the study (figure 7.9b). It was observed from the graph that FM and FS showed a slightly higher viability index as compared to FA and FC. The results were found to be statistically insignificant. This confirmed that the bigels were biocompatible. The cells remained unchanged in the presence of the bigels (figure 7.10).

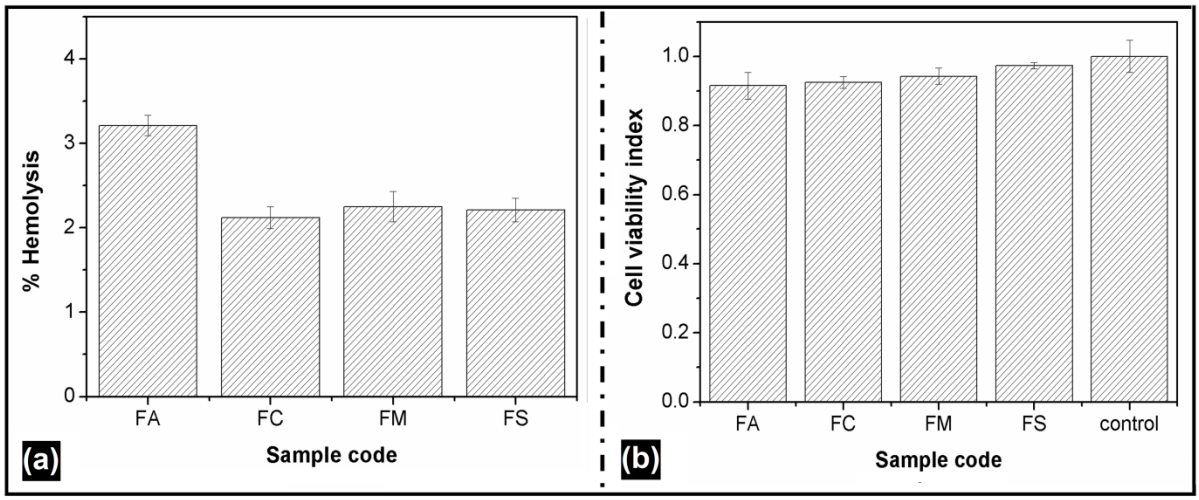

Figure 7.9: *In vitro* cytotoxicity of dialyzed formulation components (a) percent hemolysis and (b) cell viability index of polysaccharides based bigels

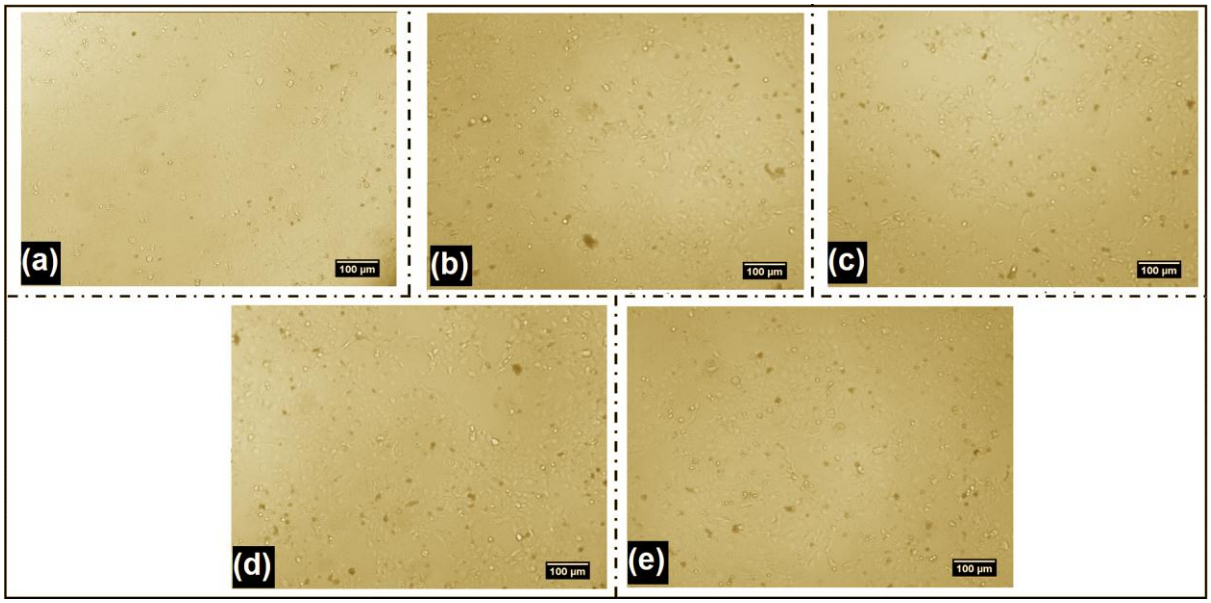

Figure 7.10: Micrographs of the cells (a) control, in the presence of leachates of bigels (b) FA, (c) FC, (d) FM and (e) FS

7.3.10 *In vitro* antimicrobial studies

The antimicrobial efficiency of the drug loaded bigels was tested against *E. coli* (Table 7.6). It was observed the marketed and the metronidazole loaded bigels showed nearly equal antimicrobial efficiency (Figure 7.11). The difference in the antimicrobial efficiency was insignificant ($p < 0.05$). The zone of inhibitions of the bigels containing branched polysaccharides was slightly lower. This can be accounted to the sustained release of the drug from the gel matrices, as was evident from the drug release studies. This indicated that the efficiency of bigels was nearly equal to the Metrogyl® (MR) (Dosage form-gel, Dose-Apply,

and rub in a thin film of Metrogyl gel twice daily to affected areas after washing) used as a reference. 1000 µg of the drug dose was used in all the cases for the test as well as for reference.

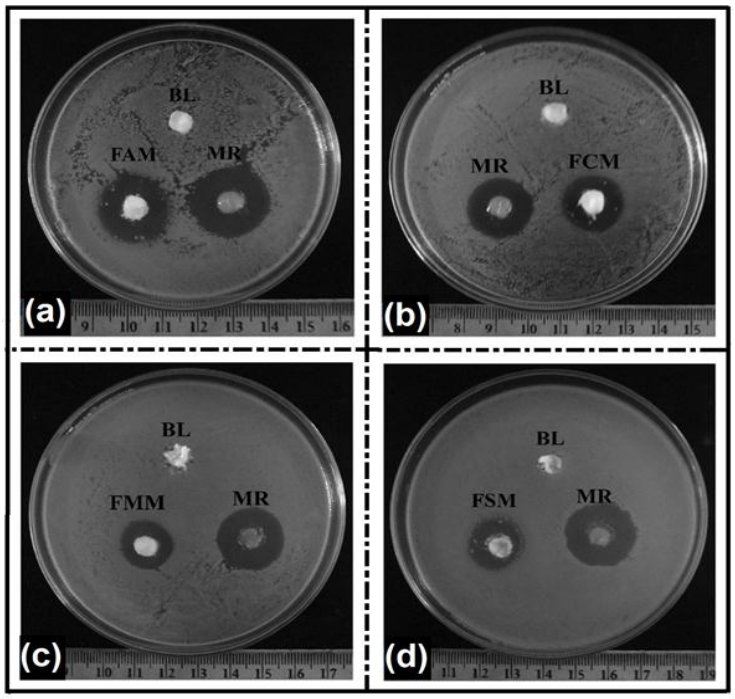

Figure 7 10: Zone of inhibitions of polysaccharide based bigels against *E. coli*

Table 7.7: Zone of inhibition of the metronidazole loaded bigels against *E. coli*

Sample code	Zone of inhibition (cm) *E. coli*		
	Test	**Marketed**	**BL**
FAM	2.2 ± 0.7	2.5 ± 0.5	-
FCM	2.2 ± 1.0	2.5 ± 0.6	-
FMM	2.6 ± 0.1	2.5 ± 0.1	-
FSM	2.4 ± 0.4	2.5 ± 0.7	-

7.3.11 *In vitro* drug release studies

The *in vitro* drug release profile of metronidazole from the prepared formulations and Metrogyl® (MR) (Dosage form-gel, Dose-Apply, and rub in a thin film of Metrogyl gel twice daily to affected areas after washing) has been shown in Figure 7.12a. MR showed 90.33% release of metronidazole in a span of 12 h. FAM, FCM, FSM and FMM showed 71.68%,

65.67% 57.97% and 53.87% release of metronidazole, respectively. The results indicated that the branched polysaccharides slowed down the diffusion of the metronidazole molecules to a greater extent as compared to the linear polysaccharides. This reduced the release of the drug molecules from the bigels containing branched polysaccharides. The effect of branching and controlled release properties of starch and maltodextrin on the drug release has been previously studied. The branching in these polysaccharides plays an important role in improving the strength of gel matrix, which in turn, influences the diffusion of the drugs. It is believed that a structure with a highly ordered organization is a good candidate for the controlled release of drugs [191]. Amylopectin and amylose present in these branched polysaccharides help in the formation and stabilization of the matrix structure. The highly branched amylopectin is expected to enhance an extensive interaction amongst the amylopectin molecules resulting in a viscous matrix capable of sustaining drug release. The linear chains in sodium CMC and sodium alginate, on the other hand, cannot make these types of arrangements due to the axially oriented conformations. The more efficiently the networks are formed, lesser is the diffusion of the molecule [192]. Faster release of metronidazole from FAM and FCM bigels may be attributed to the ionization of carboxylate groups. The ionization further increases the concentration of free H^+ inside the gel which facilitates the water intake by increasing the osmotic pressure. This causes a swelling of the bigel matrix thus ensuring a faster release of the drug [193-194].

An increase in the entanglement of the polymeric chains results in the increase in the physical crosslink points. This not only decreases the spaces available within the interpolymeric chains of the gelled matrices but also the hydration of the polymer matrices. This phenomenon, in turn, hindered the diffusion of the drug molecules within the matrices. The release of the drugs from the bigels followed Higuchi release kinetics while the release of drug from Metrogyl® followed zero order kinetics. This showed diffusion mediated transport of the drug from the bigels. The release exponent was calculated from the Korsmeyer-Peppas model. The release exponent was < 0.5 suggesting Fickian diffusion of the drug molecules (table 5). The differences in the release profile were statistically significant ($p > 0.05$).

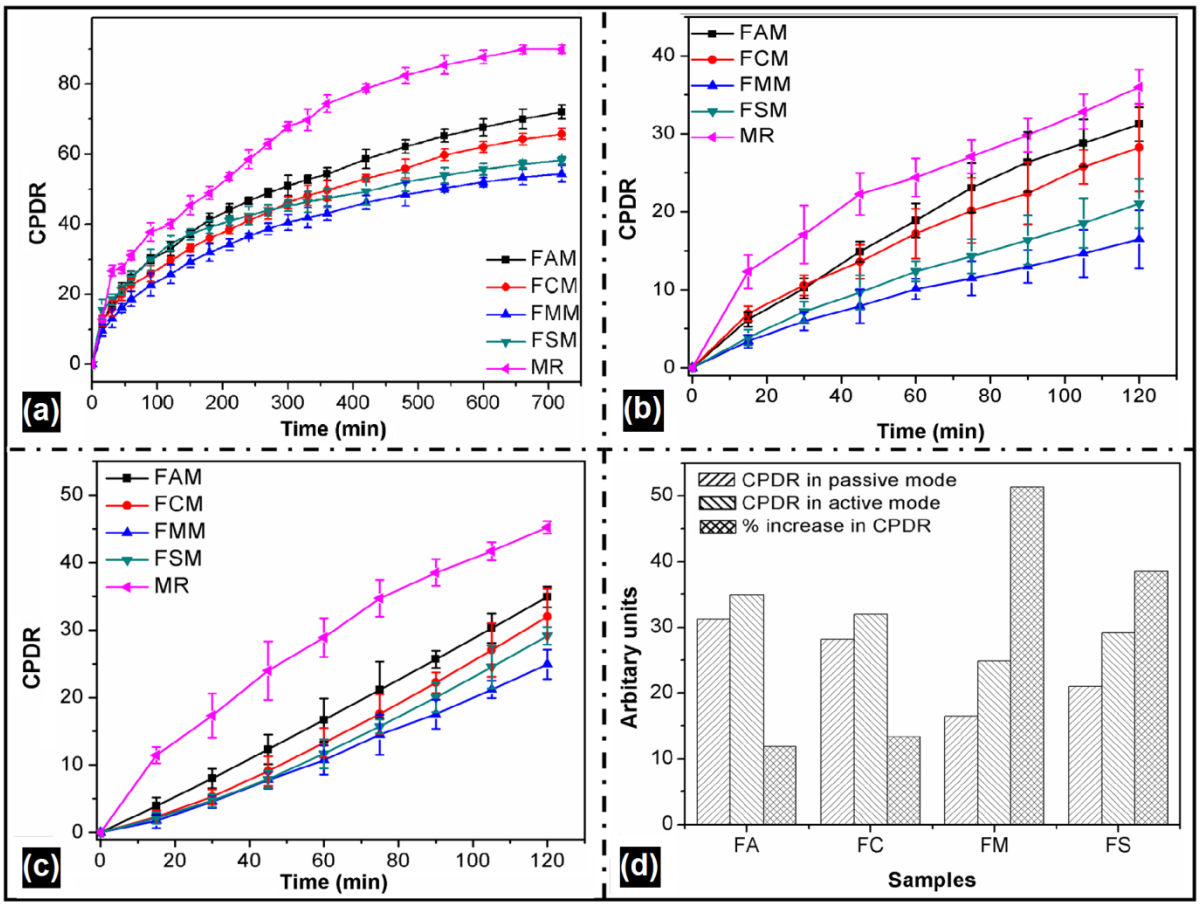

Figure 7.11: *In vitro* metronidazole release. (a) passive drug release, (b) passive drug release using iontophoretic drug release setup, (c) active drug release using iontophoretic drug release setup and (d) effect of iontophoresis over passive drug release

Table 7.8: Release kinetics of the metronidazole from polysaccharides based bigels

Formulation code	Zero order model (r^2)	Higuchi model (r^2)	Best fit model	Korsmeyer-Peppas		Mechanism of release
				(r^2)	n	
Passive drug delivery						
FAM	0.8821	0.9900	Higuchi	0.9812	0.4010	Diffusion
FCM	0.9001	0.9919	HIguchi	0.9792	0.4700	Diffusion
FMM	0.8513	0.9702	Higuchi	0.9810	0.4802	Diffusion
FSM	0.8002	0.9631	Higuchi	0.9830	0.4513	Diffusion
MR	0.9816	0.8801	Zero order	0.9812	0.4702	Diffusion
Iontophoretic drug delivery						
FAM (Passive)	0.9817	0.9910	Higuchi	0.9929	0.4901	Diffusion
FCM (Passive)	0.9712	0.9802	Higuchi	0.9923	0.4800	Diffusion
FMM (Passive)	0.9862	0.9900	Higuchi	0.9942	0.4901	Diffusion
FSM (Passive)	0.9828	0.9919	Higuchi	0.9953	0.4802	Diffusion
FAM (Active)	0.9901	0.9702	Zero order	0.9698	0.7501	Anomalous
FCM (Active)	0.9803	0.9503	Zero order	0.8900	0.7403	Anomalous
FMM (Active)	0.9912	0.9721	Zero order	0.8601	0.7002	Anomalous
FSM (Active)	0.9818	0.8482	Zero order	0.8802	0.7113	Anomalous

The effect of AC current on the drug release was studied. The results have been shown in figure 7.11c and table 7.7. It was observed that the mechanism of metronidazole release was zero-order when the AC current was applied. The marketed preparation of metronidazole showed a faster release of the drug under both active and passive condition. This suggested that metronidazole was released from the matrices at a constant rate [195]. The release at a constant rate indicates that the dissolution of the drug was the rate limiting step. The diffusion exponent (n-value) was calculated from the KP model. According to this model, n=0.5 (diffusion controlled drug release), n=1 (swelling controlled drug release). Values of n between 0.5 and 1.0 is an indicator for the superposition of both phenomena (anomalous transport), which was found in the bigels.

7.4 Major outcomes

- Bigels were prepared using polysaccharides and characterized as controlled delivery matrices.
- The addition of starch to the bigels increased the droplet size of the dispersed phase to a larger extent as compared to maltodextrin, sodium alginate and sodium CMC bigels.
- The bigels containing branched polysaccharides had a higher viscosity as compared to linear polysaccharides based bigels. The bigels showed a viscoelastic property.
- The mechanical properties of the bigels varied depending on the composition of the bigels. The bigels containing maltodextrin and starch showed higher firmness as compared to that of bigels containing linear polysaccharides.
- Drug release from the bigels containing soluble starch and maltodextrin-based bigels was lower as compared to bigels containing sodium alginate and sodium CMC.
- The drug loaded bigels showed similar antimicrobial efficiency with the marketed formulations of metronidazole.

CHAPTER 8

Preparation and characterization of natural gums based bigels using emulgels of sunflower oil and sorbitan monopalmitate

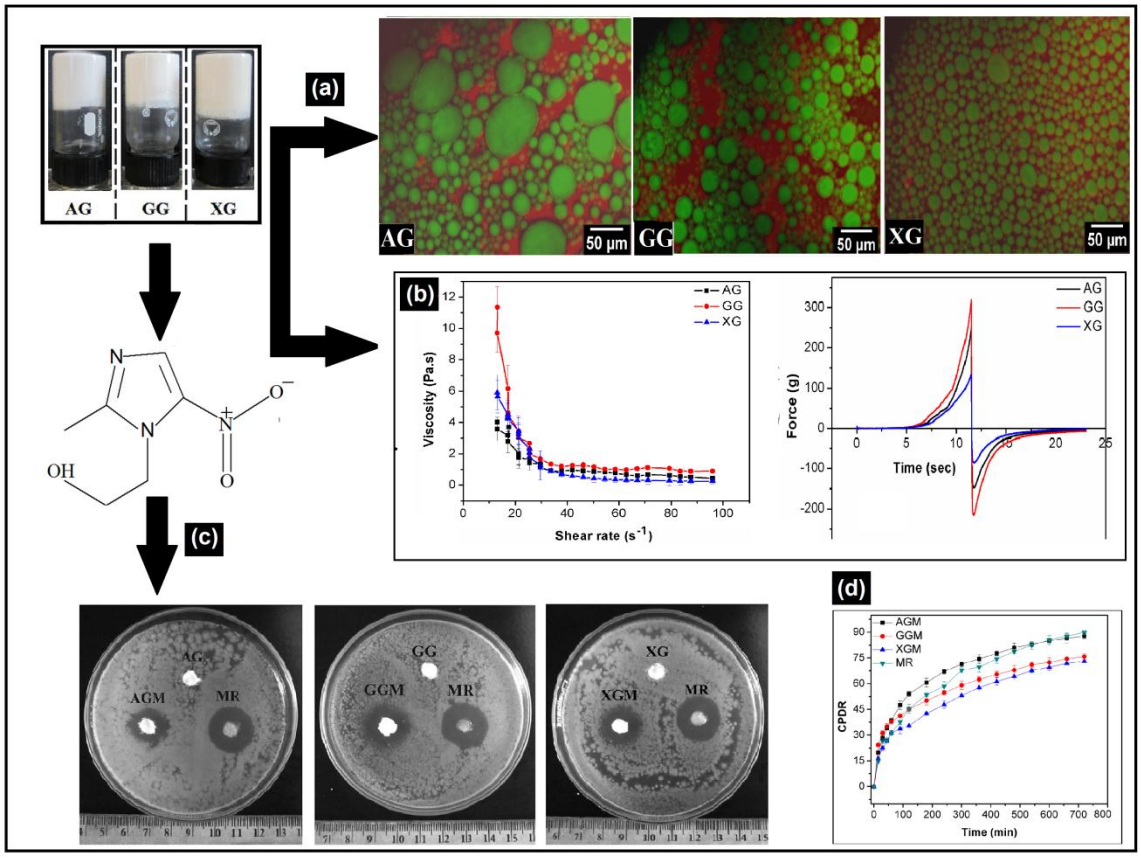

Graphical outline: (a) Fluorescence micrographs, (b) Mechanical properties, (c) antimicrobial activity and (d) *in vitro* drug release behavior.

Overview

In this chapter, sunflower oil-sorbitan monopalmitate-natural gum based bigels were prepared and thoroughly characterized. The bigels were prepared by mixing the oleogels of sunflower oil-sorbitan monopalmitate and the hydrogels of natural gums. The microstructure of the bigels was analyzed by fluorescence microscopy. The molecular interactions amongst the components of the bigels were studied by FTIR spectroscopy. The flow and mechanical behavior of the bigels were analyzed using viscometer and static mechanical tester, respectively. The gel disintegration studies were carried out at pH 7.4. The thermal and electrical properties of the bigels were evaluated using differential scanning calorimeter (DSC) and a phase sensitive multimeter, respectively. The efficiency of the bigels as a carrier for the delivery of metronidazole was explored. The antimicrobial efficiency and cytotoxicity studies of the bigels were checked against *E. coli* and HaCaT cells, respectively. *In vitro* drug release was carried out under physiological conditions. The fluorescence microscopy suggested the presence of oleogels as the internal phase. FTIR studies showed hydrogen bonding within the bigels as the major molecular interaction. The viscosity and mechanical studies indicated that the bigels were viscoelastic in nature. The disintegration of the bigels was dependent on the viscosity of the bigels. The melting endotherm of the bigels was observed at 45-52 °C. The bigels were electrically conductive. The viability index of HaCaT cells was good in the presence of the bigels. The *in vitro* drug release study suggested diffusion-mediated drug release. The drug loaded bigels showed near equal antimicrobial efficacy as compared to the available marketed formulation. The results suggested that the bigels had sufficient properties as *in vitro* delivery matrices.

8.1 Introduction

Gels based on edible oils are preferred over organic solvents due to consumer demands originating from health concerns. Edible oils, such as sunflower oil, soybean oil, groundnut oil and sesame oil are rich in ω- 6 polyunsaturated fatty acids and vitamin E. These classes of oils are important sources of fatty acids which are precursors of signaling molecules such as eicosanoids e.g. prostaglandins. These fatty acids control many physiological factors such as cholesterol level and blood pressure. Due to the presence of the unsaturated fatty acids, sunflower oil is prone to oxidation which results in a product of short shelf- life and low nutritional quality. Structuring of these types of oils in the form of oleogels, emulgels or bigels increases their acceptability for food and pharmaceutical applications [196]. These structured formulations also reduce the level of zero trans-fatty acids, thereby, improving the nutritional value. The major types of structuring agents of edible oils include low molecular weight organogelators such as aromatic rings, alkylamide, fatty acids steroid derivative and anthryl derivatives.

Mixing of oleogels with hydrogels forms a biphasic system that not only prevents the oxidative deterioration but also acts as effective carriers for the delivery of bioactive agents for biomedical, pharmaceutical, and nutraceutical applications. These types of formulations are termed as bigels, also called as biphasic gels. They offer a combined advantage of hydrogels as well as oleogels. Main advantages of these types of systems are that both lipophilic and hydrophilic agents can be delivered simultaneously. Enhanced hydration of the stratum corneum is an added advantage. These gels have a cooling and moisturizing effect [5]. Easy spreadability and water washability, when applied to the skin, makes them superior candidates over other formulations for topical applications. The objective of this chapter was to study the effect of natural gums on the properties of sunflower oil-sorbitan monopalmitate based bigels and check the efficiency of these systems as a delivery vehicle.

8.2 Experimental

8.2.1 Preparation and evaluation of natural gums based bigels

Accurately weighed amount of sorbitan monopalmitate (table 8.1) was first dissolved in sunflower oil (50 °C) to form a clear isotropic mixture of gelator and oil. Bigels were formed by the drop-wise addition of gum solution at 50 °C with a continuous stirring at 12000 rpm. The tubes were inverted to check any flow from the bigels. Metronidazole was used as a model drug for the preparation of drug loaded bigels.

Table 8.1: Composition of the natural gums based bigels

Sample code	Amount of Gum % (w/w)			Water % (w/w)	Sorbitan monopalmitate % (w/w)	Sunflower oil % (w/w)	Metronidazole % (w/w)
	Aacaia	Guar	Xanthan				
AG	0.6	-	-	49.4	9	41	-
GG	-	0.6	-	49.4	9	41	-
XG	-	-	0.6	49.4	9	41	-
AGM	0.6	-	-	49.4	9	40	1
GGM	-	0.6	-	49.4	9	40	1
XGM	-	-	0.6	49.4	9	40	1

8.3 Results and discussion

8.3.1 Preparation of bigels

The viscosities of the acacia, guar and xanthan gum sols (0.6 % w/w) were found to be 0.8637 ± 0.1454 mPa.s, 0.9310 ± 0.2642 mPa.s and 3.3182 ± 0.2463 mPa.s, respectively. The high viscosity of the xanthan gum sol may be attributed to its complex chemical structure. The molecules of xanthan gum form complex aggregates via hydrogen bonding resulting in polymer entanglement. This results in a higher viscosity of xanthan gum sol. This type of interaction is not significant in guar gum and acacia gum thus, a lower viscosity was observed.

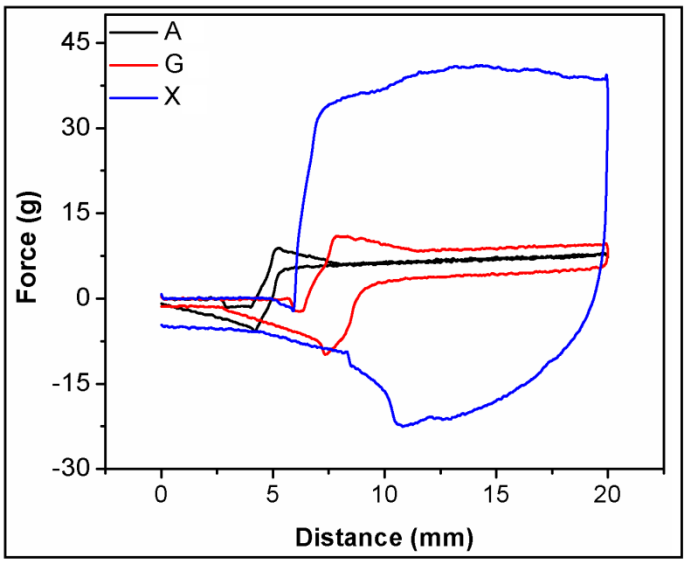

Figure 8.1: Backward extrusion of acacia, guar, and xanthan gum sol

A-Acacia gum, G-Guar gum and X-Xanthan gum.

The bigels appeared to be milky-white opaque in nature (figure 8.2). The bigels were stable even after 10 months. The pH of the bigels was in the range of 6-7.

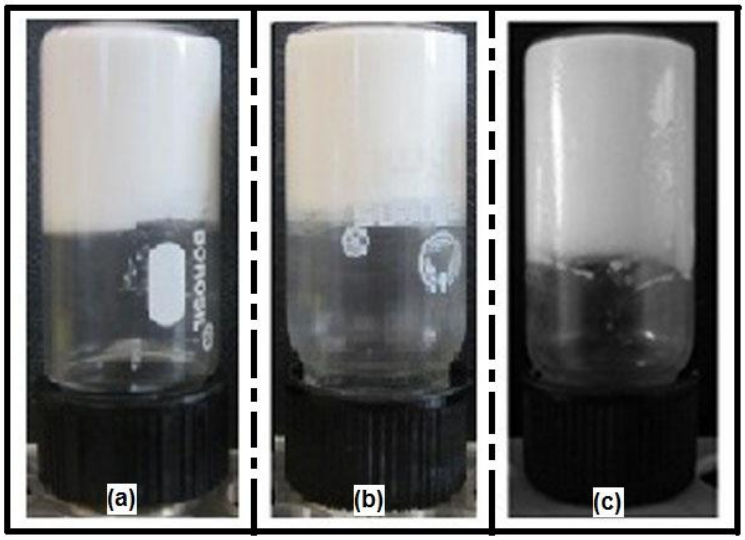

Figure 8.2: Inverted-tube method confirming the bigel formation (a) AG, (b) GG and (c) XG

The different chemical structure of the natural gums plays an important role in the formation of bigels. Xanthan gum contains β-D-(1-4) linked glucan backbone and short trisaccharide side chain. The trisaccharide side chain is composed of α-mannose, β-D- glucuronic acid and β-mannose on alternating glucose residues. During the heating, there is a change in the conformation of the gum. This conformational change leads to the intermolecular binding involving co-crystallization of the disordered chains xanthan gums giving rise to an ordered networked structure [197]. Guar gum contains a backbone of D-mannopyranosyl residues (M)

linked β-(1→4), and side chains of a single galactopyranosyl units (G) linked α-(1→6) [198]. The bigel formation is believed to occur due to the self-association of galactomannan chains [199]. Gum arabic (acacia gum) on the other hand, is a highly branched, branch-on-branch, complex acidic heteropolysaccharide with the (1→3)-β-D-galactopyranosyl units as the main chain and side chains containing L-arabinofuranosyl, L-rhamnopyranosyl, D-galactopyranosyl, and D-glucopyranosyl uronic acid units [200]. It is a protein-polysaccharide hybrid with the protein fraction playing a crucial part in the interfacial functionality and the formation of bigels. The major proteins found in acacia gum are arabinogalactan protein, arabinogalactan, and glycoprotein. On heating, the protein molecules of the gum start agglomerating. This agglomeration is a combination of both covalent and non-covalent interactions leading to the formation of bigels [201-202].

8.3.2 Microscopy and microstructural analysis

The fluorescence micrographs of the bigels confirmed the presence of the oleogel and hydrogel as the dispersed phase and the external phase, respectively (Figure 8.3). The observations from the micrographs indicated the formation of an oleogel-in-hydrogel type of bigels. The average droplet size of bigels was found to be in the range of 8.0-13.0 μm (Figure 3e). The average droplet size of the dispersed phase of XG was smaller than AG and GG. The differences in the droplet sizes of the internal phase of AG, GG, and XG were statistically insignificant ($p > 0.05$). A narrow size distribution of the dispersed phase droplet of XG was observed as compared to AG and GG. This may be explained by the higher viscosity of the aqueous solutions of xanthan gum, as determined from the backward extrusion study. The higher viscosity of the continuous phase prevents the liquid drainage between two colliding particles thus giving a smaller droplet size distribution [203]. The droplets AG and GG, on the other hand, showed a broad size distribution due to the presence of both large and small droplets. The span factor for AG, GG and XG was found to be 2.27 ± 1.14, 2.52 ± 0.47 and 1.96 ± 0.46, respectively. The span factor determines the uniformity of the droplet size [145]. The lower span factor of XG bigels suggested the presence of uniform droplets.

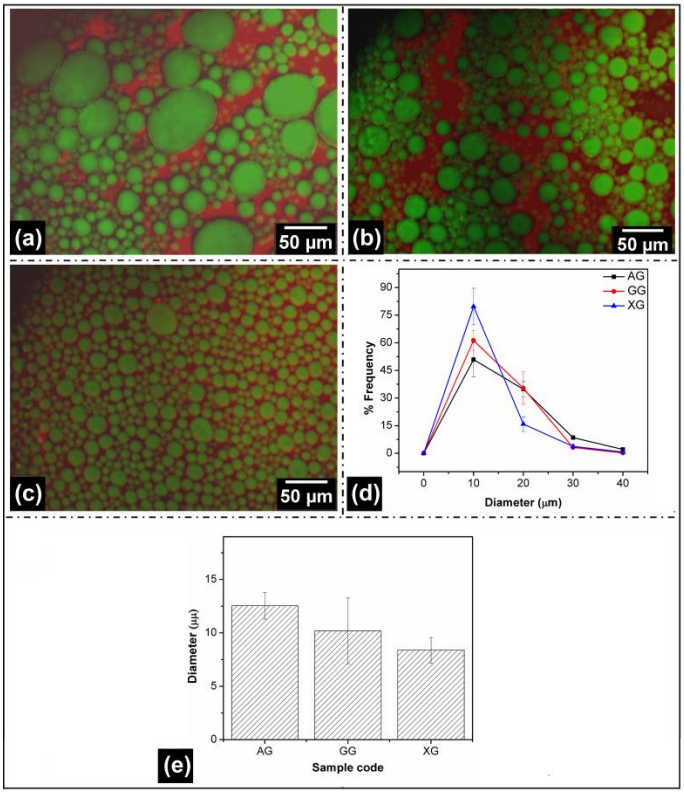

Figure 8.3: Fluorescence micrographs of: (a) AG, (b) GG, (c) XG, (d) droplet size distribution and (e) average droplet size

8.3.3 FTIR analysis

Figure 8.4 shows the FTIR spectra of the raw materials and the bigels. The fingerprint region for both the raw materials and bigels was in the wavenumber range of 880 cm^{-1} and 1500 cm^{-1}. The peaks in this region provided information about the carbohydrate specific bonds and functional groups. The major contribution was due to the sugar ring structure present in the gums. The peaks at 3420 cm^{-1}, 3337 $cm^{-1,}$ and 3450 cm^{-1} were assigned to OH stretching vibrations in acacia, guar and xanthan gums, respectively. The OH stretching vibrations observed in gum acacia was associated with the glucosidic ring. The symmetric and asymmetric stretching vibrations of CH_2 in acacia gum were observed at 2149.1 cm^{-1} and 2927.1 cm^{-1}, respectively. CO stretching vibrations (carbonyl group) of the saccharide were observed at 1611.2 cm^{-1}. Another peak at 1426.8 cm^{-1} was assigned to CO stretching vibrations of COO^- group. The CH_2 symmetrical stretching vibration in guar gum was observed at 2913 cm^{-1}. The peak at 1626 cm^{-1} in xanthan gum was associated with CO groups of pyruvate [204]. The COC absorption peak of acetal group was observed at 1065 cm^{-1}. The peaks at 1548 cm^{-1} were associated with CO asymmetric stretching vibrations of carboxylate anion in the xanthan gum side chain [205].

The IR spectra of the bigels showed a peak broadening in the wavenumber region of 2500 cm^{-1}-3500 cm^{-1}. The peak broadening in this region indicated a large number of hydroxyl groups available for hydrogen bonding in the bigels due to the presence of water. The extent of hydrogen bonding, in the bigels, was predicted by calculating the area under the curve (AUC) in the wavenumber range of 2500 cm^{-1} and 3500 cm^{-1}. The AUCs were 764.431, 947.316 and 1088.716 for AG, GG, and XG, respectively. This suggested that the degree of hydrogen bonding was in the order of XG > GG > AG.

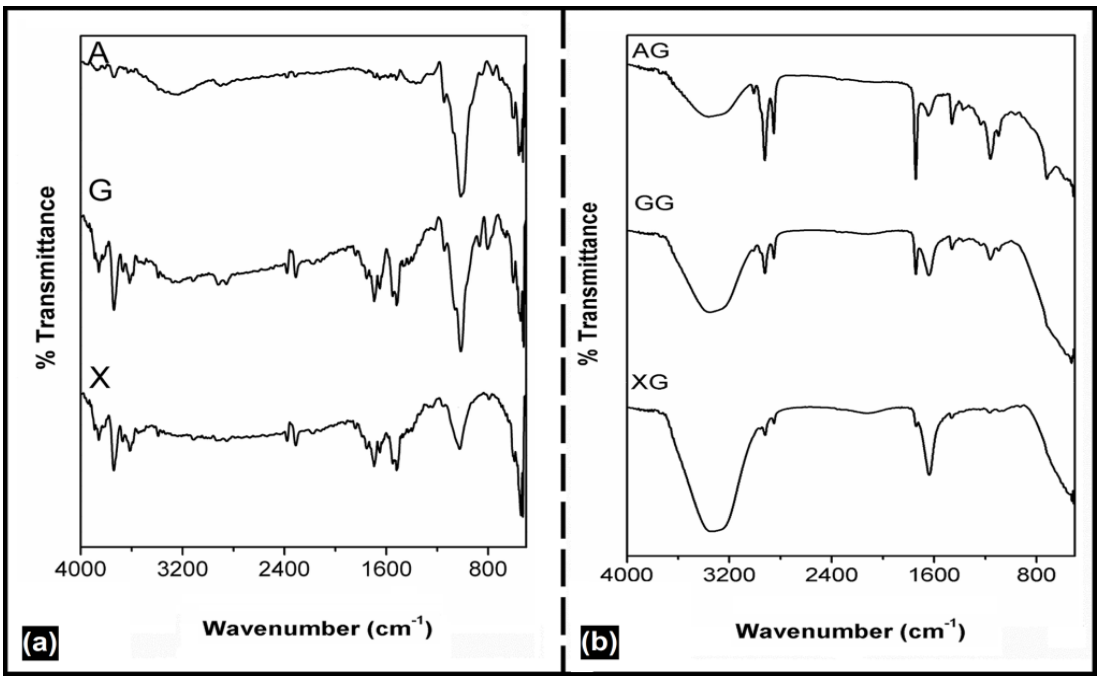

Figure 8.4: FTIR spectra of (a) raw materials: (A- Acacia gum, G- guar gum, X- xanthan gum and (b) bigels

8.3.4 Viscosity analysis

The viscosities of the bigels in low shear rate were in the order of GG > XG > AG (Figure 8.5a). At higher shear rates the viscosity was in the order of GG > AG > XG. The viscosity of XG was found to be lowest at high shear rates. The increased viscosity of XG at low shear rates may be due to the complex molecular structure and high molecular weight of xanthan gum as reported earlier in the literature [206]. The water absorption capacity of xanthan gum is high due to the existence of many free carboxyl groups. When the gum is dispersed in water, a conformational transition is observed. The transition usually occurs from a double helical structure to complex aggregates. These transitions occur through hydrogen bonds and polymer entanglement. Due to the formation of this complicated network and entanglements, the addition of xanthan gum resulted in higher viscosity and pseudoplastic behavior of XG at low shear rates. However, these entanglements progressively break at high shear rates. This is

attributed to the inherent property of xanthan gum [128]. It has been reported earlier in the literature that the hydrophobic interactions are strong forces and play a significant role in strengthening of the matrix. Some researchers have also proposed the hydrophobic interactions as the major driving forces that help in the adsorption of guar gum to the surfaces of the hydrophobic talc [207]. These interactions predominantly are difficult to break at both low and high shear rates. The low viscosity of XG at higher shear rates is because the chains in xanthan gum have a weak intermolecular association that tend to break at higher shear rates. The low viscosity of AG was attributed to the low hydraulic radius and lower intermolecular interactions in the solution of acacia gum [208].

The parameters for the power law fit of the bigels have been tabulated in Table 8.2, and the model fit has been shown in figure 8.5b. It was observed that n was < 1 indicating a pseudoplastic behavior (shear thinning).

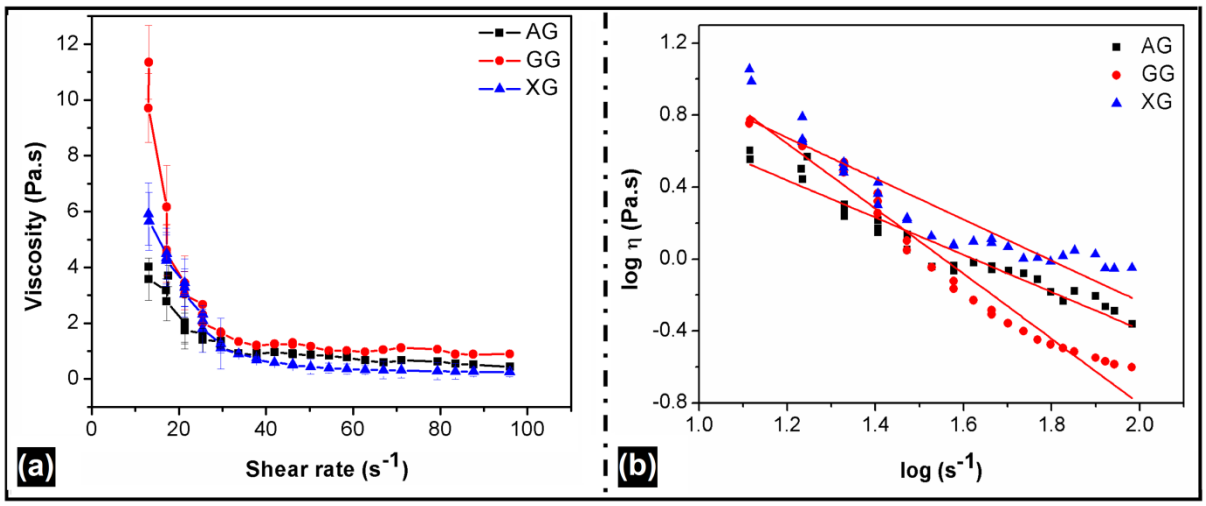

Figure 8.5: (a) Viscosity profile and (b) power law fit of the gum based bigels

Table 8.2: r^2 values of the power law fit

Sample code	n values	r^2 values
AG	0.1232	0.9356
GG	0.0367	0.9672
XG	0.1573	0.9012

8.3.5 Mechanical analysis

The results obtained from large-scale deformation studies have been summarized in table 8.3 and figure 8.6. The effect of the natural gums on the structural integrity of the bigels was studied from the firmness studies. The firmness (Figure 8.6a) of the bigels was in the order of GG > AG > XG, respectively. The results were in accordance with the viscosity studies at

higher shear rates, which suggested the presence of a strong network in GG and AG as compared to XG. The results can be explained by the higher hydrogen bonding in AG and GG gels as compared to XG gels. The firmness is also dependent on the composition of the gums. As guar gum is a galactomannan, the M/G ratio (mannose: galactose) has an important effect in the strengthening of gel matrix [209]. The M/G ratio corresponds to 2:1 for guar gum [210]. The dense arrangement and packing of mannan residues in GG promoted hydrogen bonding causing an increase in the firmness as compared to AG. The presence of galactomannan in guar gum has been used to increase the stiffness of many formulations including tablets and emulsions by improving chain entanglement and association at the molecular level [211]. The addition of galactomannan has been reported to increase the water binding capacity and gel strength [212].

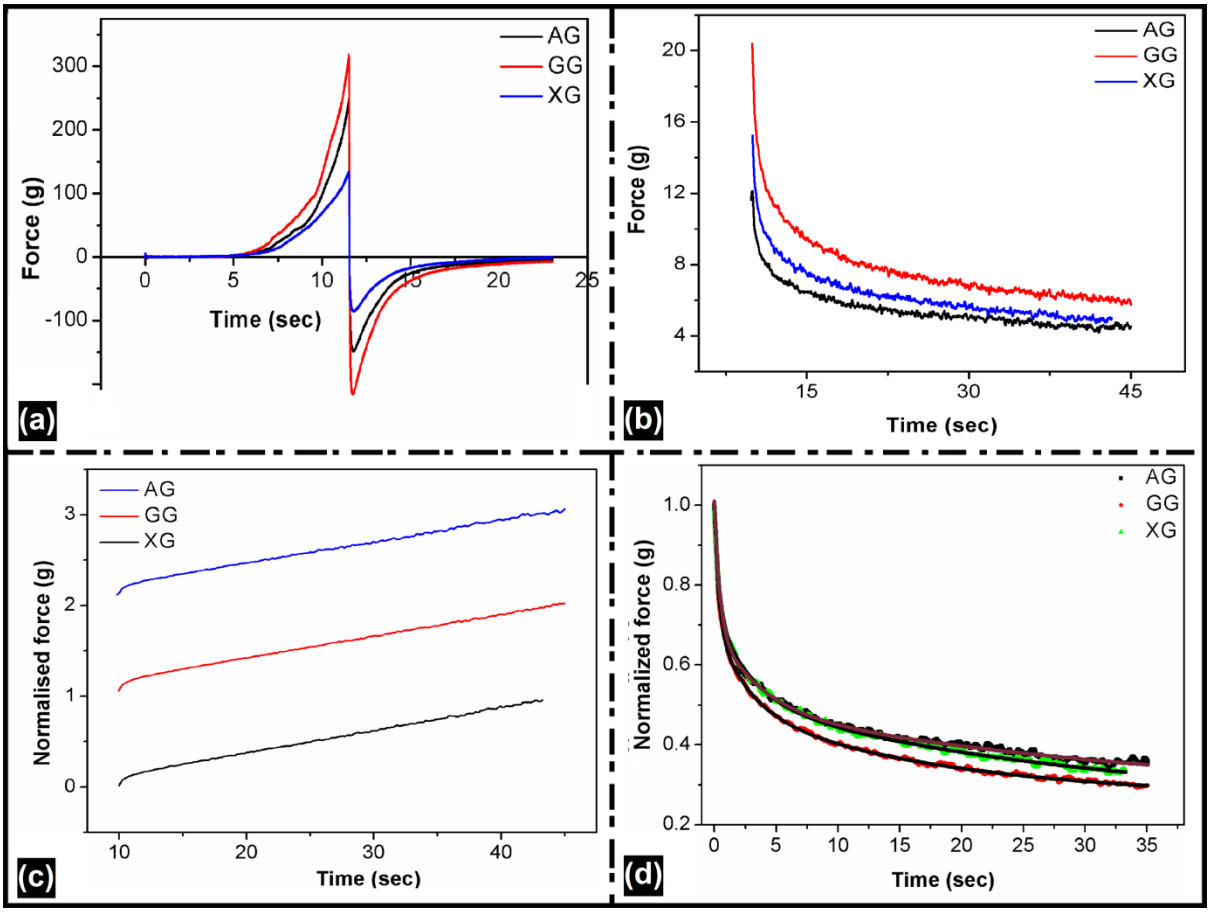

Figure 8.6: Texture properties of AG, GG and XG gels, (a) firmness, (b) stress relaxation, (c) normalised force vs. time and (d) Wiechert model

The conformation of xanthan gum has been reported to affect the rheological as well as the mechanical properties [213]. The electrostatic repulsion between the charged groups in xanthan gum gives rise to an elongated structure. This elongated structure causes xanthan

gum molecules to align themselves, results in the intermolecular association (hydrogen bonding) resulting in the formation of a weakly structured material [214]. The extension of the polymer may also result from the packing of the oleogels into the hydrogel matrix of xanthan gum. This further led to the lower firmness of XG as compared to AG and GG. Another reason for the lower firmness of XG may be accounted for the formation of hydration shells around the stiffer rods of xanthan gum due to the presence of free water [215]. The stickiness of the bigels was in the order of their firmness. Bigels with higher firmness showed lower spreadability.

The viscoelastic behavior of the bigels was studied from the stress relaxation study (Figure 8.6b). The stress relaxation data was fitted using modified Peleg's equation discussed in chapter 4. The percent stress relaxation parameters, k_1 (rate) and k_2 (extent), were calculated to analyze the viscoelastic properties (figure 8.6c). The rate of relaxation (k_1) decreased in the following order XG > GG > AG. It was reported earlier by Peleg and Normand (1983) that solid materials had higher k_2 values as compared to the soft or semi-solid formulations and showed a value close to unity. However, no clear trend could be discerned from these values. The viscoelastic parameter S^* was further calculated. A material is said to be viscoelastic if the S^* values range from 0-1. For viscoelastic materials having higher elastic component the S^* values are closer to 1. All the bigels showed S^* values < 1 indicating the viscoelastic property of the gels.

The bigels were classified as viscoelastic as the force reached asymptotically to an equilibrium value instead of 0. The percent stress relaxation decreased in the following order GG > XG > AG (Table 8.3). The greater relaxation means higher energy was dissipated during the relaxation process. The results showed that the energy dissipated was more in GG. As reported earlier, more energy is dissipated due to the friction where chain entanglement is predominant. Guar gum forms network through chain entanglements [216]. For the stress relaxation to occur, a breakup of the physical entanglements bonds is required [209]. The gels formed by entanglements form a flexible transient network which releases the stress, dissipating energy [217].

The semi flexible nature of xanthan and the tendency of self-aggregation and association dissipate less energy as a result of which lower %SR was observed for XG bigels as compared to AG bigels. As the guar gum is composed of galactomannan, which has been used as sieving matrices in many applications, the presence of voids in these natural sieves might have released the hydraulic pressure to a greater extent, thereby increasing the % SR as compared to XG bigels.

Table 8.3: Mechanical properties of the bigels

Studies	Parameters	AG	GG	XG
	Firmness (g)	249.8212 ± 3.7656	309.6623 ± 2.9896	135.4823 ± 2.6453
	Stickiness (g)	142.6324 ± 3.7678	213.3915 ± 2.6412	85.3715 ± 3.2135
	Spreadability $(g.sec)^{-1}$	0.0029 ± 0.0013	0.0020 ± 0.0015	0.0049 ± 0.0021
Stress relaxation	F^* (g)	4.6442	5.7058	5.0423
	K_1 (g)	0.1276	0.1283	0.1527
	K_2 (g)	0.0239	0.0244	0.0253
	S*	0.7818	0.7789	0.7693
	Percent stress relaxation	63.1572	71.8951	67.7962

To know the change in the stress with respect to time, the data was fitted to three relaxation Weichert model (figure 8.6d). The use of three element model describes the stress decay to an infinite time point. The residual stress (P_0) is an indicator of the stability of the bigels. A decrease in the residual stress indicates the breaking of bonds in the polymer network. The residual stress was higher in the GG and AG (Table 8.4). The P_0 values decreased in the following order GG > AG > XG. These values were in agreement with the firmness of the bigels. The Weichert model was used to describe the stress decay as a function of time. The relaxation times (τ) were in the order of $\tau_1 < \tau_2 < \tau_3$ and were in acceptance with the literature [107]. The sum of all pre-exponential factors was 1 indicating a good fit (table 8.5). The coefficients of viscosity of GG bigels was little higher than other AG and XG bigels at τ_1. These results were in agreement with the viscosity studies. During the long term, relaxation times τ_2 and τ_3 a complex phenomenon was observed. XG bigels showed a higher coefficient of viscosity which may be attributed to the rearrangement of xanthan chains from helix to coil and vice versa after the application of stress [218].

Table 8.4: Weichert model parameters of the bigels

Sample code	**τ_1**	**τ_2**	**τ_3**	**r^2**
AG	0.3722	2.8016	23.0825	0.9989
GG	0.3214	2.4769	16.5942	0.9968
XG	0.3346	2.8781	30.1967	0.9988
		Pre-exponential factors		
Sample code	**P_0**	**P_1**	**P_2**	**P_3**
AG	0.2522	0.2054	0.2312	0.3171
GG	0.2670	0.2981	0.2061	0.2362
XG	0.2450	0.2720	0.2284	0.2585

Table 8.5: Stress relaxation model fitting using Wiechert model

Formulation code	Stress relaxation model	Coefficient of viscosity of the dashpots
AG	$P(t) = 0.2522 + 0.2054e^{\frac{-t}{0.3722}} + 0.2312e^{\frac{-t}{2.8016}} + 0.317e^{\frac{-t}{23.0825}}$	0.0762, 0.6471, 7.3164
GG	$P(t) = 0.2670 + 0.2981e^{\frac{-t}{0.3214}} + 0.2061e^{\frac{-t}{2.4769}} + 0.2362e^{\frac{-t}{16.5942}}$	0.0951, 0.5101, 3.9167
XG	$P(t) = 0.2450 + 0.2720e^{\frac{-t}{0.3346}} + 0.2284e^{\frac{-t}{2.8781}} + 0.2585e^{\frac{-t}{30.1967}}$	0.0902, 0.6563, 7.7901

8.3.6 Gel disintegration studies

The disintegration time of AG, GG, and XG was found to be 25.5 ± 0.70 min, 50.5 ± 2.12 min and 53 ± 2.82 min, respectively (XG > GG > AG) at pH 7.4. Disintegration is fastened with the permeation of water into the gel matrix. As the viscosity of the xanthan gum sol was highest, the permeation of water was much lower in the viscous layer. The slow permeation of water in XG resulted in the increase in the disintegration time.

8.3.7 Thermal analysis

Figure 8.7 shows the DSC profiles of the gum based bigels. The values of ΔH decreased in the order of GG > XG > AG (table 8.6). Parameters like onset temperature (T_o) peak temperature (T_p) and conclusion temperature (T_c) were determined from the graph. There was a slight increase in T_o, T_p and T_c for GG as compared to AG and XG bigels. The melting enthalpy of GG was greater as compared to other gels indicating a higher thermal stability of GG. The ΔH of the system is also associated with the crystallinity, conformational change, and presence of ordered structure [219]. It reflects the effects of cumulative endothermic events, associated with the breaking of the hydrogen bonds [220]. The results were in agreement with the viscosity and the mechanical studies where GG gels were found to be firmer. As reported earlier, xanthan gum undergoes a thermally induced transition from an ordered state to a disordered arrangement (helix-coil). This resulted in the decrease of the ΔH values as compared to GG.

The decrease in the ΔH (Table 6) of XG as compared to GG and AG can also be accounted for the availability of water molecules in the gums [221]. This could be because xanthan gum retains more water molecules by hydrogen bonding. This was evident from the FTIR studies.

The high water binding capacity of xanthan gum lowers the energy required for crystal disorganization in XG. This, in turn, increases the kinetic energy and subsequently lowers the ΔH values [130].

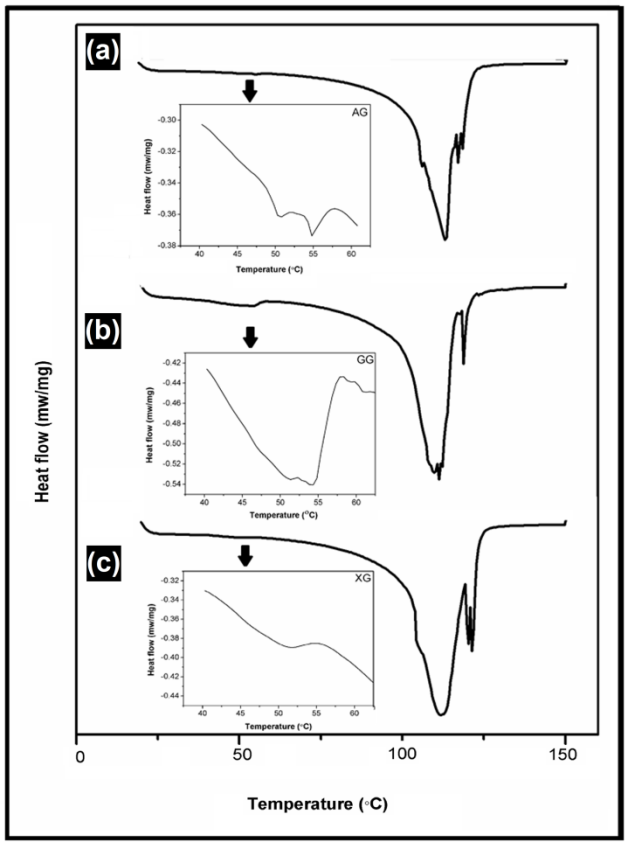

Figure 8.7: DSC profiles of (a) AG, (b) GG and, (c) XG bigels

Table 8.6: Thermal parameters studied from DSC

Sample code	T_o (°C)	T_p (°C)	T_c (°C)	ΔH (J/g)
AG	49.3	50.2	51.6	-0.114
GG	52.6	53.1	55.2	-1.858
XG	49.6	51.9	54.9	-0.429

8.3.8 Electrical analysis

Figure 8.8 shows the electrical properties of the bigels. The bulk resistance (Nyquist plot) of the gels decreased in the order of AG > GG > XG. AG was found to have highest bulk resistance as compared to the bigels. The resistance of GG was higher than XG. It has been reported earlier that the integral part of gum acacia structure contains proteins (2-3%). The gel formation over here requires a heat treatment. The heat treatment could have caused the aggregation of the protein molecules, thereby, increasing the bulk resistance of AG [222]. Figure 8.8b shows the variation of dielectric constant with frequency. A decrease in the

dielectric constant was observed as the frequency was increased. This was attributed to the alignment of the dipoles in the direction of the applied electric field at low frequencies, however, at higher frequencies, quick reversal of the dipoles happen [188]. The dielectric constant decreased with the increase in the frequency. FTIR studies indicated that XG showed higher hydrogen bonding. It has been reported earlier that the electron transfer across these hydrogen bonds is greatly increased due to the coupling of electron motions with those of the protons [223]. This resulted in the increased conductivity of XG as compared to AG and GG. The AC conductivity was explained by the universal power law equation (figure 8.8c). The plateau in the profile contributed to the DC conductivity of the gels. The s-values (dimensionless) obtained from the equation were in between 0 and 1. The s values for AG, GG, and XG were 0.20, 0.20 and 0.22, respectively.

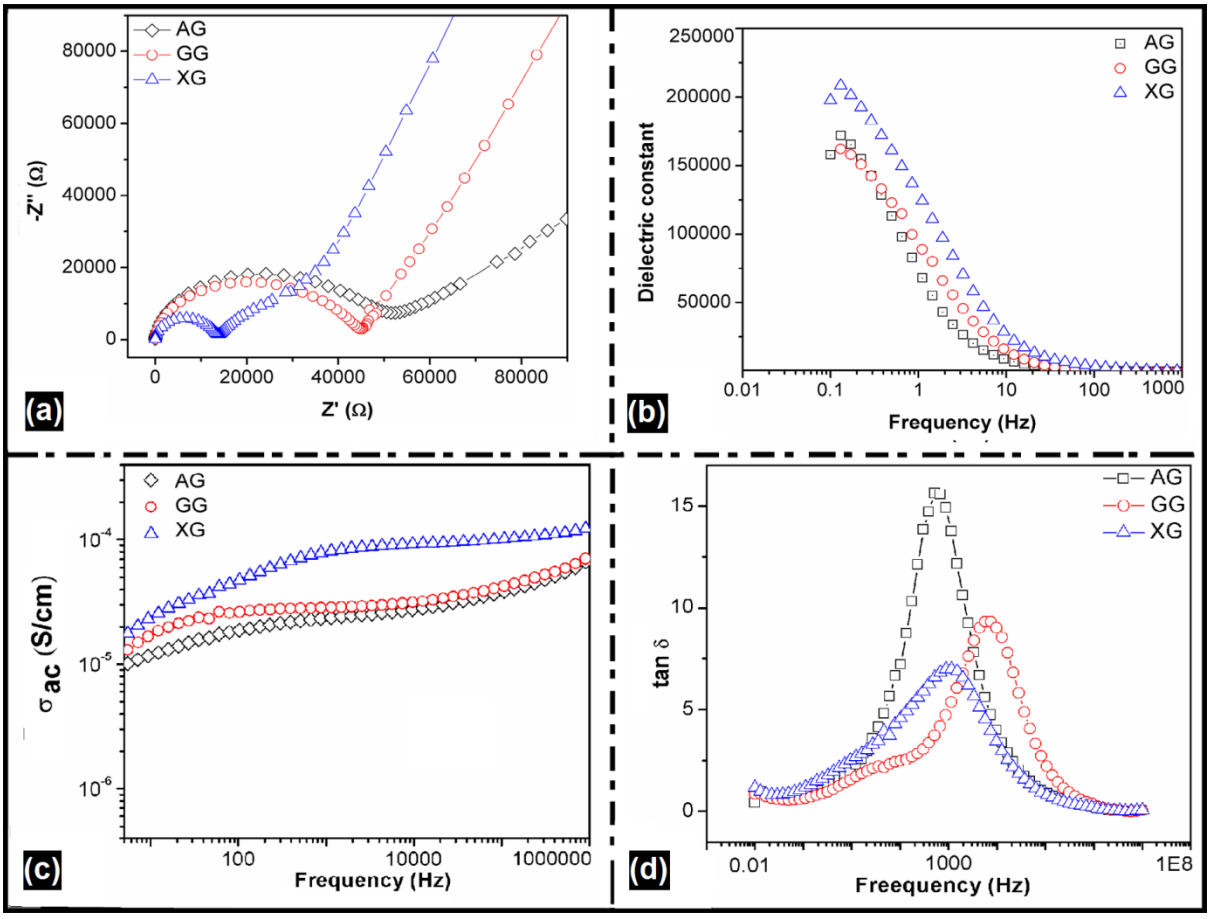

Figure 8.8: Impedance profile of gum based gels (a) Nyquist plot, (b) dielectric constant vs. frequency, (c) AC conductivity vs. frequency and (d) tan δ vs. frequency

The variation of tan δ with frequency is shown in figure 8.8d. The relaxation was also associated with the flexibility of the gum chain. High values of dielectric loss are associated

with grain boundary resistance, associated with more energy requirement for electron exchange. AG showed a higher dielectric loss as compared to GG and XG.

8.3.9 *In vitro* cytotoxicity of dialyzed formulation components

Figure 8.9 shows that the percent hemolysis of the bigels was found to be < 5. This indicated that the bigels were hemocompatible in nature. The cell viability index (figure 8.9b) was dependent on the type of the gums used. The cell viability index was in the order of XG > AG > GG. XG had a higher cytocompatibility. The differences were statistically significant ($p < 0.05$). This suggested that the bigels were biocompatible. There was no change in the structure of the cells (figure 8.10).

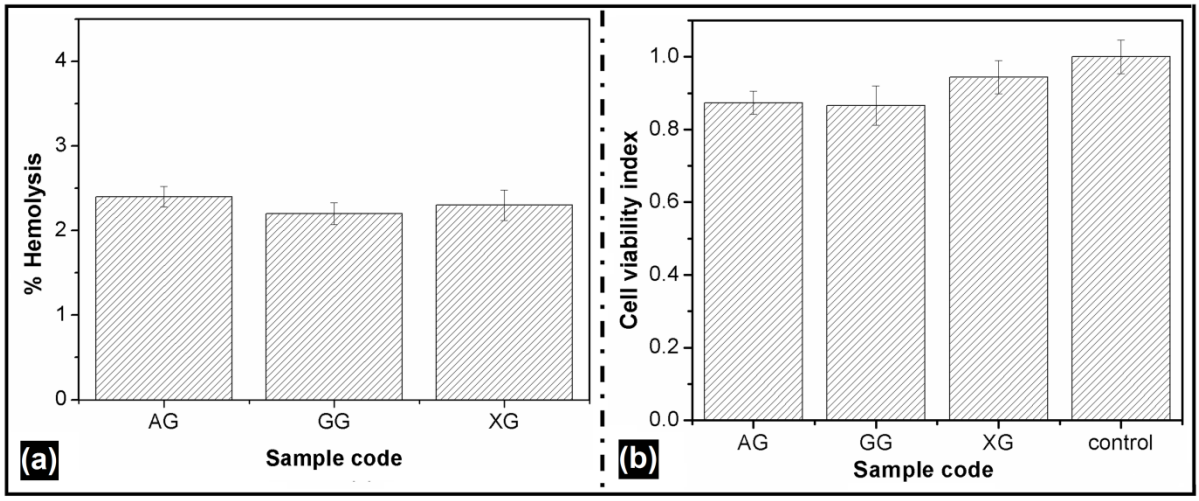

Figure 8.9: *In vitro* cytotoxicity of dialyzed formulation components (a) percent hemolysis and (b) *in vitro* cytotoxicity

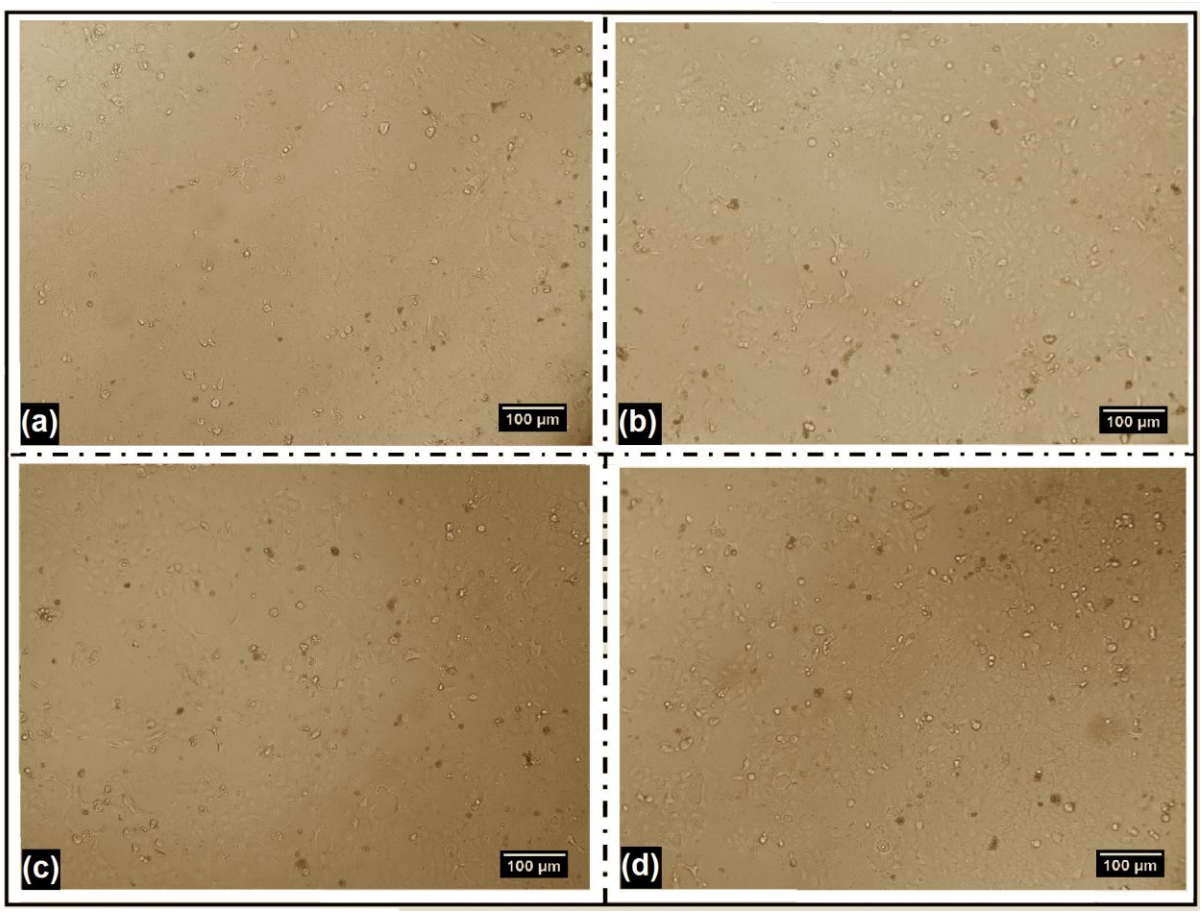

Figure 8.10: Micrographs of HaCaT cells (a) control, in the presence of the leachates of the bigels (b) AG, (c) GG and (d) XG

8.3.10 *In vitro* antimicrobial studies

The marketed formulation of metronidazole, Metrogyl®, MR (Dosage form- gel, Dose-Apply, and rub in a thin film of Metrogyl gel twice daily to affected areas after washing) was used as a reference to check the antimicrobial efficiency of the drug loaded bigels against *E. coli* (table 8.7). 1000 µg of the drug dose was used in all the cases for the test as well as for reference. The method was based on bore well technique. AG, GG, and XG were taken as negative controls. The antimicrobial efficiency of AGM was little higher as compared to the other bigels. The statistical analysis showed no significant difference amongst the antimicrobial activity of drug loaded bigels and MR ($p > 0.05$) suggesting that the efficiency of the drug loaded bigels was equal to MR.

Table 8.7: Zone of inhibition of the metronidazole loaded bigels against *E. coli* (BL- refers to bigels without drug)

Sample code	Zone of inhibition (cm) *E. coli*		
	Test	**Marketed**	**BL**
AGM	2.6 ± 0.1	2.5 ± 0.5	-
GGM	2.2 ± 1.0	2.5 ± 0.6	-
XGM	2.1 ± 1.7	2.5 ± 0.1	-

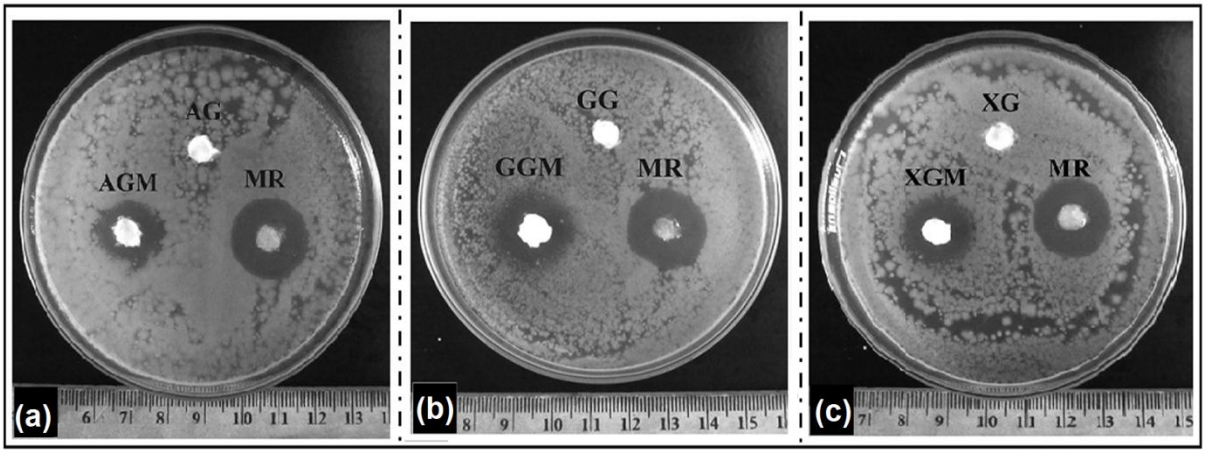

Figure 8.10: Antimicrobial efficiency of (a) AGM, (b) GGM, and (c)XGM bigels against *E. coli*

8.3.11 *In vitro* drug release studies

The *in vitro* release of metronidazole from the bigels and reference Metrogyl® MR (Dosage form- gel, Dose-Apply, and rub in a thin film of Metrogyl gel twice daily to affected areas after washing) has been shown in figure 8.12. MR showed 90.44% release of metronidazole in a span of 12 h. AGM, GGM and XGM showed 87.72%, 75.75%, and 73.04% release of metronidazole, respectively. The differences in the drug release from bigels were statistically significant ($p < 0.05$).

The drug release was affected by the viscosity of the gels to a larger extent [224]. The results from backward extrusion study showed that the xanthan gum sol had a higher viscosity. The slow permeation of water due to the high viscosity of xanthan gum in XG gels decreased the wettability and particle aggregation thereby decreasing the dissolution efficiency of XGM bigels. Another factor that contributed to the slow release of metronidazole from the XGM was caused by less swelling of xanthan gum in the external hydrogel matrix due to the elastic

retraction of the acetyl side chains [225]. Apart from the viscosity of the bigels, faster release of metronidazole from AGM was also attributed to the rapid swelling of acacia gum in pH > 6.5. The rapid swelling of AGM in pH 7.4 might have disrupted the gel structure by increasing the porosity and water uptake. This was also evident from the faster disintegration of the bigels containing acacia gum. This resulted in a faster release of the drug from AGM as compared to GGM and XGM [226].

Various models like Higuchi, Zero and Peppas models were used to predict the kinetics of drug release (table 8.8). The r^2 values were found to be better in Higuchi model indicating that the release of the drug was a diffusion-mediated process. The results showed $n \leq 0.5$ indicating a Fickian or pseudo Fickian release of metronidazole [227].

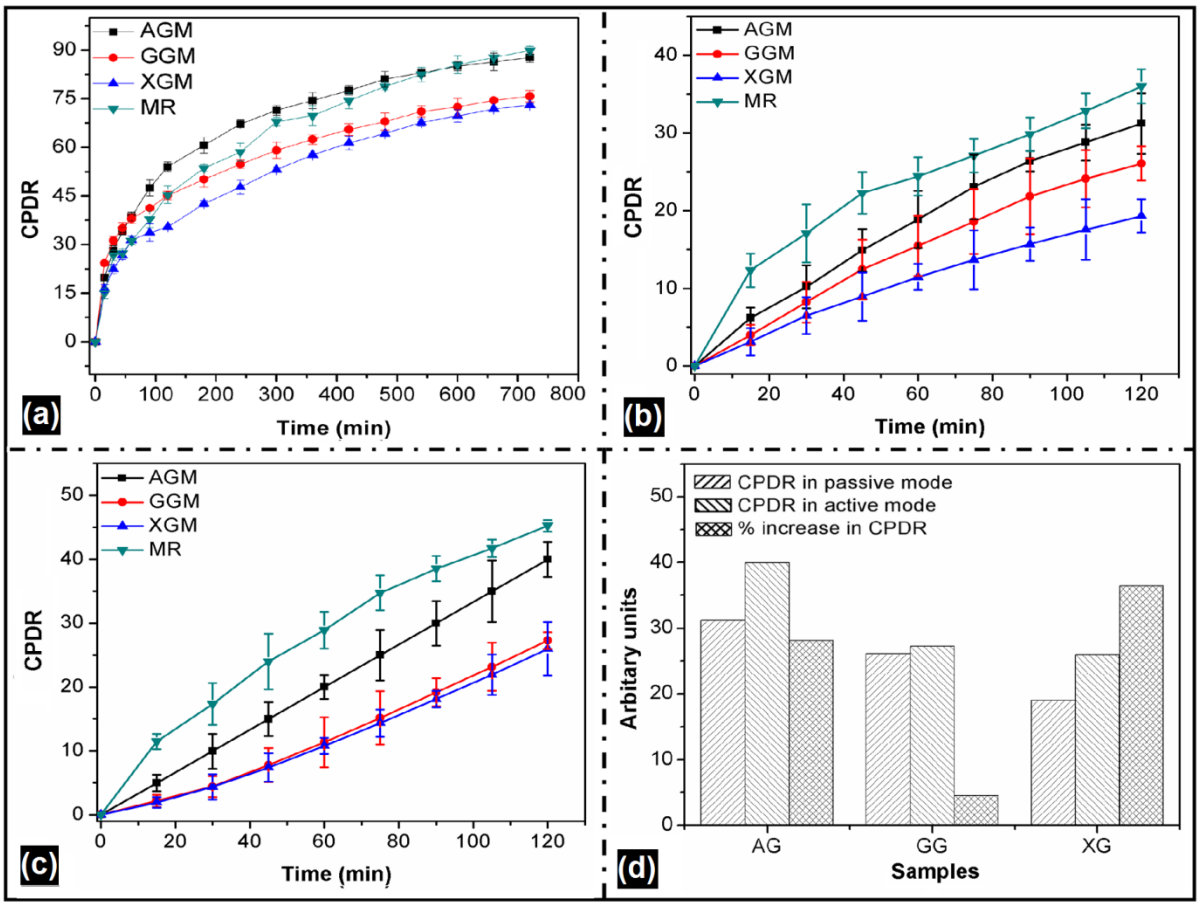

Figure 8.11: *In vitro* drug release of metronidazole from AGM, GGM, and XGM bigels (a) 12 h release under passive condition, (b) 2 h release under passive condition, (c) active release for 2h and (d) percentage rise in the drug release

The effect of AC current on the drug release is shown in figure 11b and table 8.8. It was observed that the mechanism of metronidazole release was zero-order when the AC current was applied. This suggests that metronidazole was released from the matrices at a constant

rate. According to this mechanism, the ingress of water into the polymer matrix causes the relaxation of the polymer chains. The relaxation process was the rate controlling step in the release. The relaxation of the polysaccharide chains in the bigels increases the mobility of the active compounds and finally expanding the gel volume resulting in the release of the drugs [228]. The 'n' values for the bigels were in the range of 0.5 and 1 indicating the superposition of both diffusion and relaxation of the polysaccharides responsible for the release of the drugs. Drug release from the marketed preparation showed a similar pattern as carried out under normal condition.

Table 8.8: Release kinetics of metronidazole from of AGM, GGM and XGM bigels

Formulation code	Zero order model (r^2)	Higuchi model (r^2)	Best fit model	Korsmeyer-Peppas		Mechanism of release
				(r^2)	N	
Passive drug delivery						
AGM	0.8012	0.9591	Higuchi	0.9900	0.4500	Diffusion
GGM	0.8123	0.9942	Higuchi	0.9701	0.2800	Diffusion
XGM	0.8863	0.9921	Higuchi	0.9711	0.3700	Diffusion
MR	0.9891	0.8815	Zero order	0.9721	0.4712	Diffusion
Iontophoretic drug delivery						
AGM (Passive)	0.9849	0.9900	Higuchi	0.9923	0.4801	Diffusion
GGM (Passive)	0.9802	0.9917	Higuchi	0.9650	0.5001	Diffusion
XGM (Passive)	0.9731	0.9802	Higuchi	0.9902	0.4800	Diffusion
AGM (Active)	0.9912	0.9814	Zero order	0.9210	0.7903	Anomalous
GGM (Active)	0.9901	0.9830	Zero order	0.8702	0.7502	Anomalous
XGM (Active)	1.0012	0.9882	Zero order	0.9711	0.7810	Anomalous

8.4 Major outcomes

- The bigels containing acacia gum and guar gum showed greater firmness and stickiness as compared to bigels containing xanthan gum.
- FTIR studies showed the formation of physical bigels indicating hydrogen bonding as an important driving force behind the gelation.
- The viscosity of the bigels decreased as the shear rate was increased, indicating a pseudoplastic flow.
- The mechanical studies revealed the viscoelastic nature of the bigels.
- The antimicrobial activity of the gum based bigels was comparable to that of marketed formulation
- The release from these bigels was diffusion controlled. The addition of gums to the bigels slightly lowered the drug release as compared to the marketed preparation of metronidazole.

CHAPTER 9

Preparation and characterization of synthetic polymers based bigels using emulgels of sunflower oil and sorbitan monopalmitate

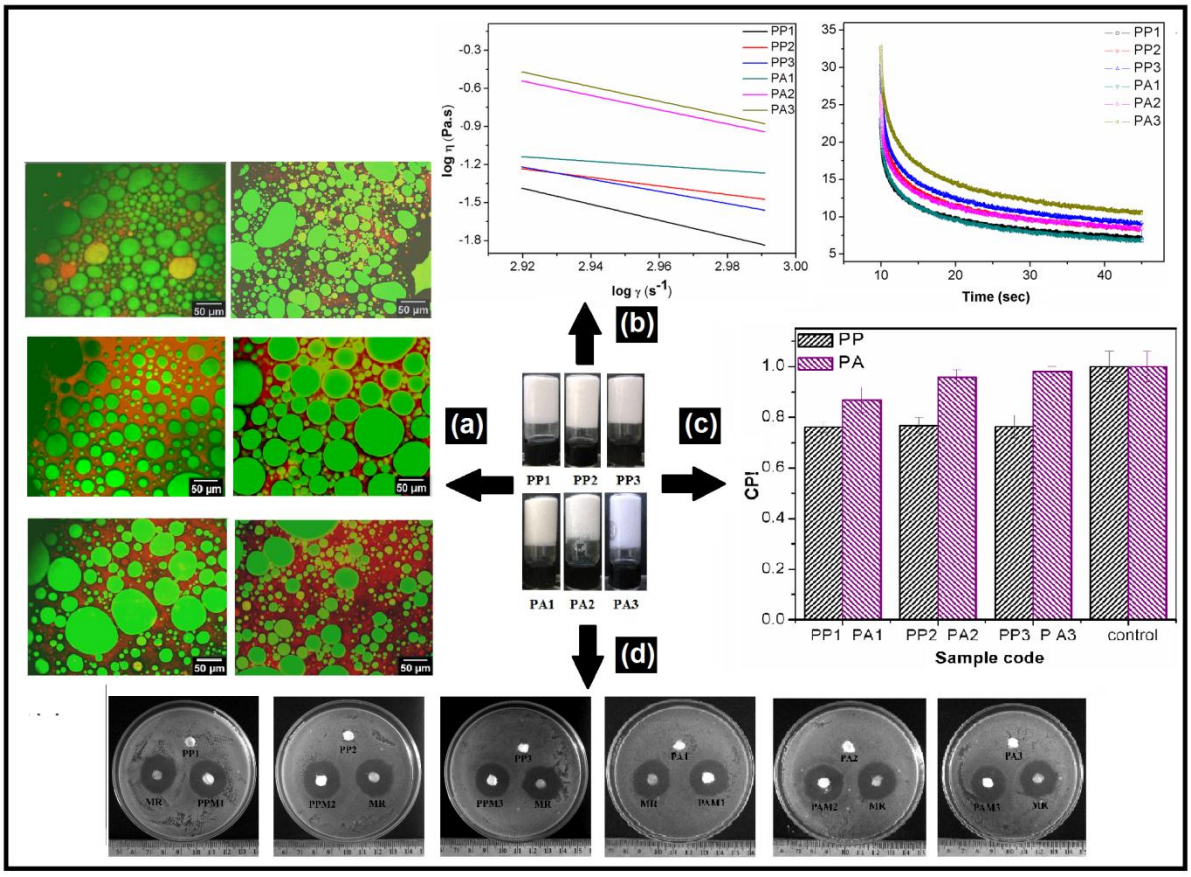

Graphical outline: (a) Fluorescence micrographs, (b) mechanical properties, (c) CPI, and (d) antimicrobial efficacy of synthetic polymer based bigels.

Overview

Bigels of sunflower oil, sorbitan monopalmitate and water soluble synthetic polymers (e.g. polyvinyl alcohol and polyvinyl pyrrolidone) were prepared and explored as matrices for the controlled delivery of metronidazole. Fluorescence microscope was used to characterize the microstructure of the bigels. Static mechanical tester was used to study the mechanical properties of the bigels. Ostwald-de Wale power law was used to predict the flow behavior of the bigels. Phosphate buffer pH 7.4 was used to determine the gel disintegration time. Thermal and electrical properties of the bigels were studied by DSC and phase sensitive multimeter, respectively. The efficiency of these bigels as a delivery vehicle for antimicrobial agents was assessed *in vitro* using *E. coli*. The cytotoxicity studies were conducted *in vitro* using HaCaT cell line. The microstructure of the bigels showed the presence of hydrogel as a continuous phase and oleogels as the dispersed form. The bigels were viscoelastic in nature and showed a pseudoplastic flow behavior. The addition of PVA to the bigels prolonged the disintegration time as compared to PVP. There was no change in the melting point of sorbitan monopalmitate even after the addition of the synthetic polymers. The synthetic polymers affected the conductivity of the bigels to a larger extent. An increase in the polymer concentration resulted in the decrease in the drug release. The bigels showed a high cell viability index indicating their biocompatible nature. The drug loaded bigels showed equivalent inhibitory zones against *E. coli* as compared to the commercially available formulations.

9.1 Introduction

Oleogels are semisolid systems which contain immobilized edible oil in an organogelator matrix. They have been used as a dermatological base. Health concerns originating from the use of gels of organic solvents have initiated an in- depth research on edible oils. Edible oil, like sunflower oil, is rich in ω- 6 polyunsaturated fatty acids and vitamin E. It has been used in the production of margarine. Oleogels prepared by structuring the edible oils provide desired textural properties. There are many structuring agents available currently, which can tailor the properties of the oleogels. Mixing oleogels with hydrogels forms biphasic systems which are known as bigels [5]. Bigels are soft solids that belong to a class of interfacially jammed emulsion gels. These classes of biphasic gels are relatively unexplored and have been gaining attention in food as well as pharmaceutical industries due to their tunable mechanical properties. These gels have combined advantages of hydrogels as well as oleogels. Apart from the pharmaceutical applications, bigels can also be used as delivery carriers for nutraceuticals [229]. Bigels containing water soluble synthetic polymers are being used for the delivery of the pharmaceutical agents. The commonly used non-ionic synthetic polymers are polyvinylpyrrolidone (PVP) and polyvinyl alcohol (PVA). PVP belongs to a class of amphiphilic synthetic polymers. The molecular weight of PVP ranges from 2500 to 3000000 and is often classified by the K value, calculated using Fikentscher's equation. PVP K30, utilized in the present study, had a molecular weight of 50000 [230]. It has been used in many formulations for preparing nanoparticles, liposomes, and diblock polymer micelles for the delivery of drugs. PVP is a non-ionic linear polymer that can be used as hydrophobisizer and stabilizer to prevent oxidation and decrease chemical instability [231]. The good solubility, non-toxicity, biodegradability and excellent affinity to various polymers and resins have widened its application in medicine, pharmaceuticals, cosmetics, food, printing inks, textiles, and many other fields. PVP has been considered as a suitable component for the preparation of semi-IPN hydrogel with satisfactory swelling behavior and pH sensitivity, which has been explored in drug delivery systems [232]. However, the inferior fragile mechanical properties and low swelling capability of PVP has limited its application in hydrogel preparation. This problem can be avoided by blending the hydrogels with another polymer, such as polysaccharides [12]. PVA is biocompatible in nature and can be readily functionalized. It is a polyhydroxy polymer that has been used in many practical applications because of its easy availability and biodegradability. It is one of the very few vinyl polymers which is soluble in water [233]. These classes of polymers have good stabilizing property for

various multiphase systems enabling them to be used as a property modifier in the present study.

The changes in the properties of the bigels using water soluble synthetic polymers have not been explored so far. The present study was conducted to compare the properties of the bigels containing the above-mentioned synthetic polymers and check their suitability for the delivery of metronidazole.

9.2 Experimental

9.2.1 Preparation of the synthetic polymer based bigels

The composition of the synthetic polymer based bigels is mentioned in table 9.1. The bigels were prepared using various concentrations of PVA and PVP solutions. Rest of the procedure was same as mentioned in the previous chapters.

Table 9.1: Composition of the PVA and PVP bigel

Sample code	Sorbitan monopalmitate % (w/w)	Sunflower oil % (w/w)	Polymer % (w/w)		Water % (w/w)	Metronidazole % (w/w)
			PVA	PVP		
PP1	9	41	-	1	49	-
PP2	9	41	-	3	47	-
PP3	9	41	-	5	45	-
PA1	9	41	1	-	49	-
PA2	9	41	3	-	47	-
PA3	9	41	5	-	45	-
PPM1	9	40	-	1	49	1
PPM2	9	40	-	3	47	1
PPM3	9	40	-	5	45	1
PAM1	9	40	1	-	49	1
PAM2	9	40	3	-	47	1
PAM3	9	40	5	-	45	1

9.3 Results and discussion

9.3.1 Preparation of the bigels

The backward extrusion profile (figure 9.1) of the sols suggested Newtonian flow behavior. There was a slight difference in the viscosities of the polymer sols. The viscosities of the PP1, PP2, PP3, PA1, PA2 and PA3 were found to be 0.0822 ± 0.0456 Poise, 0.0853 ± 0.0128 Poise, 0.9017 ± 0.0223 Poise, 0.0831 ± 0.0123 Poise, 0.0872 ± 0.1065 Poise and 0.9063 ±

0.2466 Poise, respectively. The viscosities of the polymer solutions were dependent on the concentration of the polymer used. An increase in the polymer concentration resulted in the increase in the viscosity. The viscosity of the PVA solution was slightly higher than PVP solution. This was attributed to the high molecular weight of PVA as compared to PVP. The mechanism of bigels formation from the synthetic polymers is attributed to the hydrogen bonding. The molecular formula of PVA is $[CH_2CH\ (OH)]_n$. The PVA bigels are formed majorly by cross-linkings between interchains by hydrogen bonding [234-235]. These interactions are basically due to the polycondensation of the -OH group of PVA with any OH groups or alkyl groups, driven thermally during the preparation of bigels. These crosslinks further lead to the crystallisation of PVA molecules in the bigels [236-237].

The molecular formula of PVP is $(C_6H_9NO)_n$. It has a pyrrolidone attached to the vinyl group. Each PVP unit has two vacancies due to uncoupled electrons at the oxygen atom of the carbonyl group for hydrogen bonding. The presence of PVP in the gels increase the hydrogen bonding in the gel network [238]. Apart from hydrogen bonding the hydrophobic interactions of the side chains with that of span 40 lead to the formation of a rigid gel matrix [239].

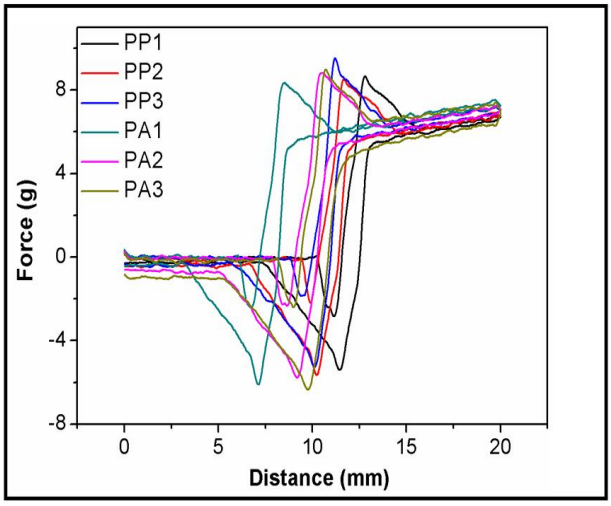

Figure 9.1: Backward extrusion of the polymer sol

The formation of the bigels was confirmed by inverted-tube method (Figure 9.2). All bigels were milky-white and non-greasy to touch, often associated with hydrogels. There were no visible signs of destabilization or color change for >10 months in the bigels.

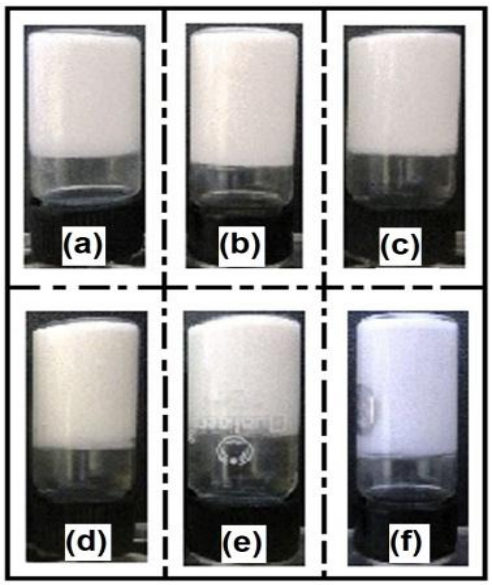

Figure 9.2: Inverted-tube method to confirm bigel formation (a) PP1, (b) PP2, (c) PP3, (d) PA1, (e) PA2 and (f) PA3

9.3.2 Microscopy and microstructural analysis

The fluorescence micrographs confirmed the presence of oleogels dispersed as droplets (colored green droplets) (figure 9.3). The continuous phase was aqueous in nature (red colored). The droplets were spherical in shape. The micrographs suggested the formation of oleogel-in- hydrogel type of bigels. The average droplet size (50% of the droplets) was in the range of 8.0-13.0 μm (Figure 9.3e). The average droplet size of the dispersed phase of PA bigels was smaller than PP bigels. The differences in the droplet sizes of the internal phase of PA and PP bigels were statistically significant ($p < 0.05$). The larger droplet size of PP bigels may be attributed interchain self-aggregation of PVP chains [240]. The droplet size distribution was narrower in PA bigels as compared to the PP bigels. These observations may be explained by the emulsion stabilizing property of PVA [241]. The span of the droplet size was in the range of 1-2.5 for all the bigels. The span factor for PP1, PP2 and PP3 bigels was 2.12± 0.13, 2.18 ± 0.21 and 1.75 ± 0. 16, respectively. The span factor for PA1, PA2 and PA3 was found to be 1.98 ± 0.42, 1.85 ± 0.65 and 1.61± 0.42 respectively. The span factor determines the uniformity of the droplet size [145]. It was found that span factor of PA bigels was comparatively less than PP bigels showing the formation of more uniform droplets.

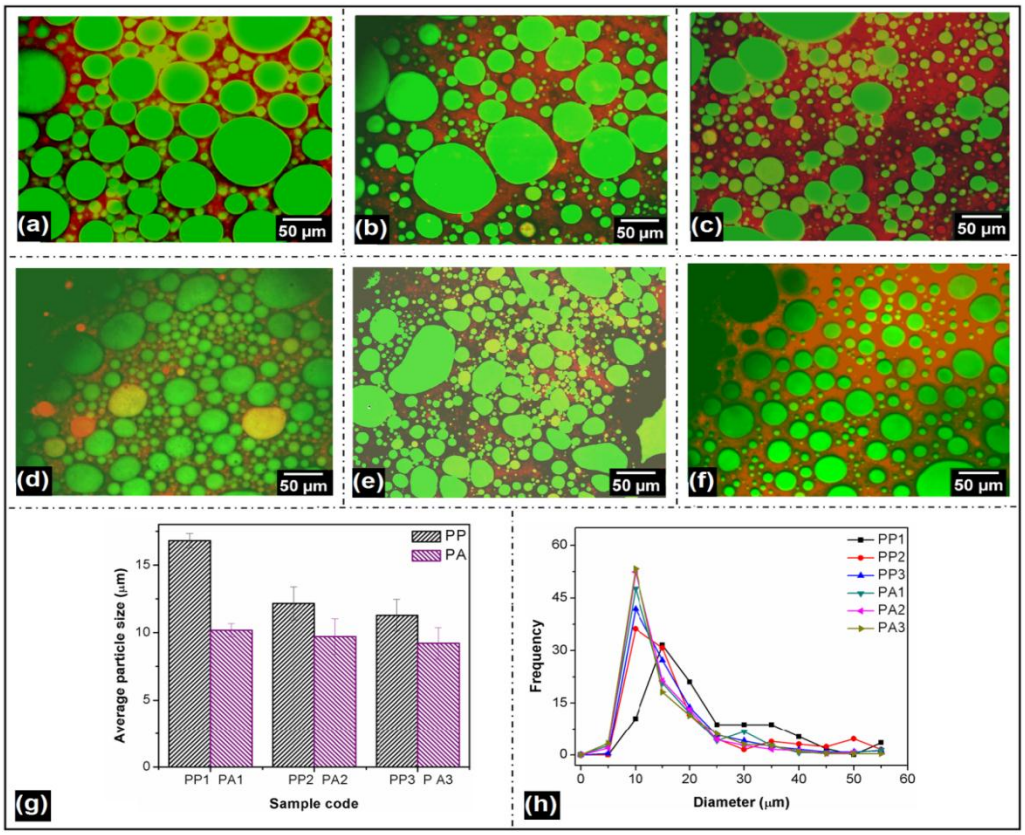

Figure 9.3: Fluorescent micrographs of (a) PP1, (b) PP2, (c) PP3, (d) PA1, (e) PA2, (f) PA3, (g) average particle size distribution and (h) frequency vs. diameter

9.3.3 FTIR analysis

FTIR of PVA (figure 9.4a) showed broad C–H alkyl stretching vibrations at 2850-3000 cm^{-1}. The absorption peak of strong OH stretching vibrations of the free alcohol group was seen at 3600-3650 cm^{-1} and the absorption peak due to the hydrogen bonded OH groups was observed at 3200-3570 cm^{-1}. The hydrophilic forces in PVA chains present in PA bigels give rise to intramolecular and intermolecular hydrogen bondings. The PA bigels showed significant change in the peak intensity as the PVA content was increased. The carbonyl absorption (C=O) in the PA bigels due to sorbitan monopalmitate and sunflower oil molecules was seen at 1716 cm^{-1}. With the rise in the PVA content from PA1 to PA3, this peak became less intense. This may be associated with the involvement of C=O groups present in sorbitan monopalmitate and sunflower oil in the formation of hydrogen bonds. The peak at 1652 cm^{-1} was associated with the C-C stretching vibrations of vinyl groups in PVA chains. This peak was also intensified with the increase in the PVA content from PA1 to PA3. This was also accompanied by the increased intensity of OH stretching vibrations in the

region of 3000-3500 cm^{-1}. This suggested an increase in the hydrogen bonding within the formulations.

The FTIR of PVP (figure 9.4b) showed an absorption peak at 1647 cm^{-1} which was due to the C=O groups attached to the pyrrole ring. The C-N stretching vibrations were seen at 1572 cm^{-1}. The characteristic absorption peak at 1465 cm^{-1} in PVP molecules was due to C-H bending vibrations [232]. The C-H stretching vibrations in PP bigels shifted to 2973 cm^{-1}. The C=O absorption peak associated with sorbitan monopalmitate and sunflower oil molecules in PP bigels was shifted to 1732 cm^{-1}, indicating the interaction of this group with the PVP molecules. The hydrogen bonding in the PP bigels was also associated with the shifting of the C=O absorption peaks in PVP to a lower frequency in the bigels. The hydrogen bonding also increased with the increase in the PVP concentration in the PP bigels.

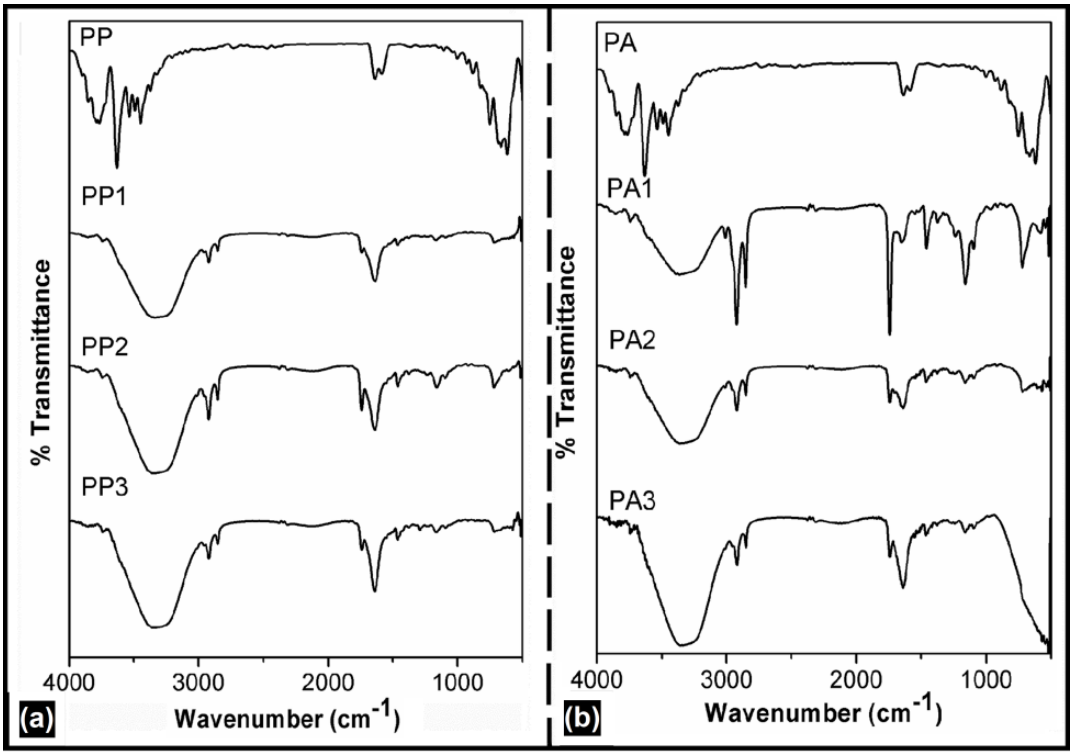

Figure 9.4: FTIR spectra of (a) PA and (b) PP bigels

9.3.4 Viscosity analysis

Figure 9.5a shows the viscosity profiles of PP and PA bigels. It was observed that PA bigels had a higher viscosity as compared to PP bigels. The viscosity of the bigels increased with the increase in the polymer concentration. The flow behavior of the bigels was estimated using Ostwald-de Wale power law mathematical model.

It was clear from the figure the model fitting that the bigels exhibited a shear-thinning phenomena ($r^2 \approx 0.99$) (table 9.2). This indicated that the viscosity of the bigels progressively

decreased with the increase in the shear rate (figure 9.5b). The 'n' value was found to be < 1 (from model fitting) indicating a non-Newtonian shear-thinning flow behavior. This type of phenomenon is necessary for the efficient delivery of drugs, as this property enables the formation of a thin layer of the formulation over the skin surface. This helps in enhancing the topical absorption of the drug. Apart from the above, long-term stability during storage is achieved. This is due to the higher viscosity at low shear rates, which reduces the chances of phase separation. The shear- thinning behavior was attributed to the progressive breaking of the hydrogen bonds under the influence of shear stress. This phenomenon resulted in the flow of the bigels, thereby, making the bigels flow. As evident from the results of the FTIR, all the bigels showed the presence of hydrogen bonding, which was disrupted when shear stress was applied. This may explain the pseudoplastic behavior of the bigels. The intermolecular forces play an important role in determining the viscosity of a system. It has been reported earlier, that more hydrogen bonds per molecule of the polymer enable the formation of strong three-dimensional networks between the molecules [242]. This resulted in the higher viscosity of the bigels at low shear rates.

The magnitude of the viscosity decreased was in the order of PA3 > PA2 > PA1 > PP3 > PP2 > PP1. This observation can be related to the droplet size. The decrease in the droplet size might have decreased the mean separation distance between the droplets which increased the aggregation of the droplets. This aggregation finally led to an increased viscosity of the bigels.

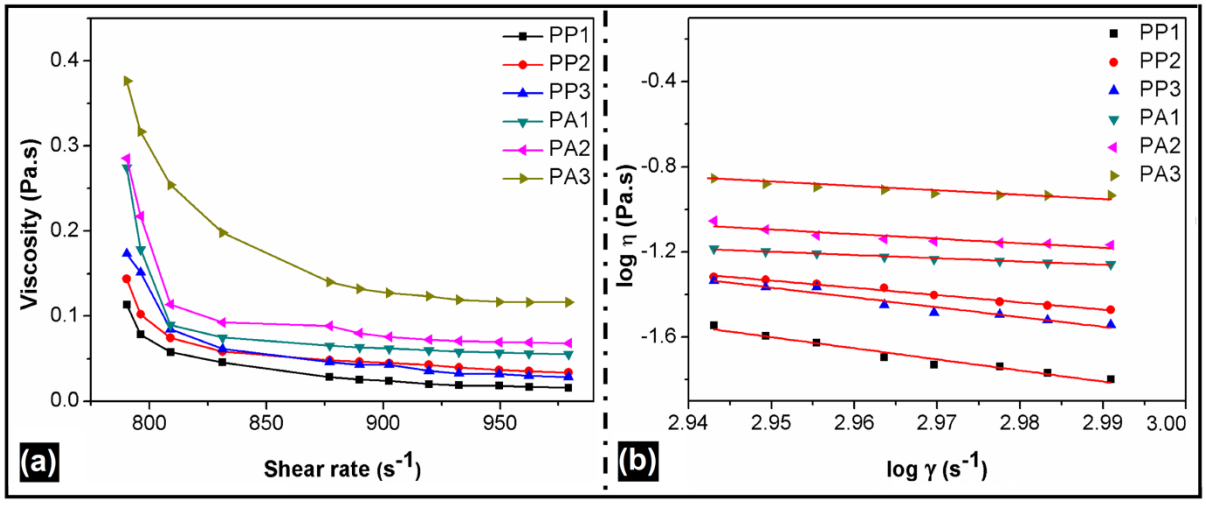

Figure 9.5: Flow behavior of PA and PP bigels (a) viscosity and (b) power law fit

Table 9.2: Power law fit of the bigels

Sample code	n-values	r^2 values
PP1	0.1361	0.9862
PP2	0.2123	0.9907
PP3	0.6912	0.9912
PA1	0.8797	0.9832
PA2	0.7462	0.9764
PA3	0.6719	0.9991

9.3.5 Mechanical analysis

The results of the mechanical analysis have been summarized in Table 9.3, figure 9.6. These results were in agreement with the viscosity studies. The firmness of PP bigels was less as compared to the PA bigels. It has been reported earlier that addition of PVP decreases the strength of chitosan blends due to its fragile nature [243]. The stickiness of the PA bigels was more as compared to PP bigels. The stickiness of the bigels may also be related to the concentration of the polymer. The absorption capacity of water by PVA is higher than PVP. This provides an adhesive force, to form liquid bridges leading to particle aggregates. Firmness was also dependent on the concentration of the polymer. As the polymer concentration increased, the aggregation and interaction increased leading to a rigid gel matrix and thus increased the firmness of the bigels [244]. The work of shear was calculated in terms of total force required to carry out the shearing process. It is a characteristic feature of semisolid formulations. It provides information about the spreadability of the formulations. Work of shear is inversely proportional to spreadability. The spreadability of PP bigels was found to be higher as compared to PA bigels. This parameter was found to be dependent on the concentration of the polymer in the bigels. It was observed that the spreadability decreased with the increase in the polymer concentration. The spreadability of the formulations was in the following order PP1 > PP2 > PP3 for PP bigels and PA1 > PA2 > PA3 for PA bigels. The work of shear and firmness of the bigels were in direct relation to each other.

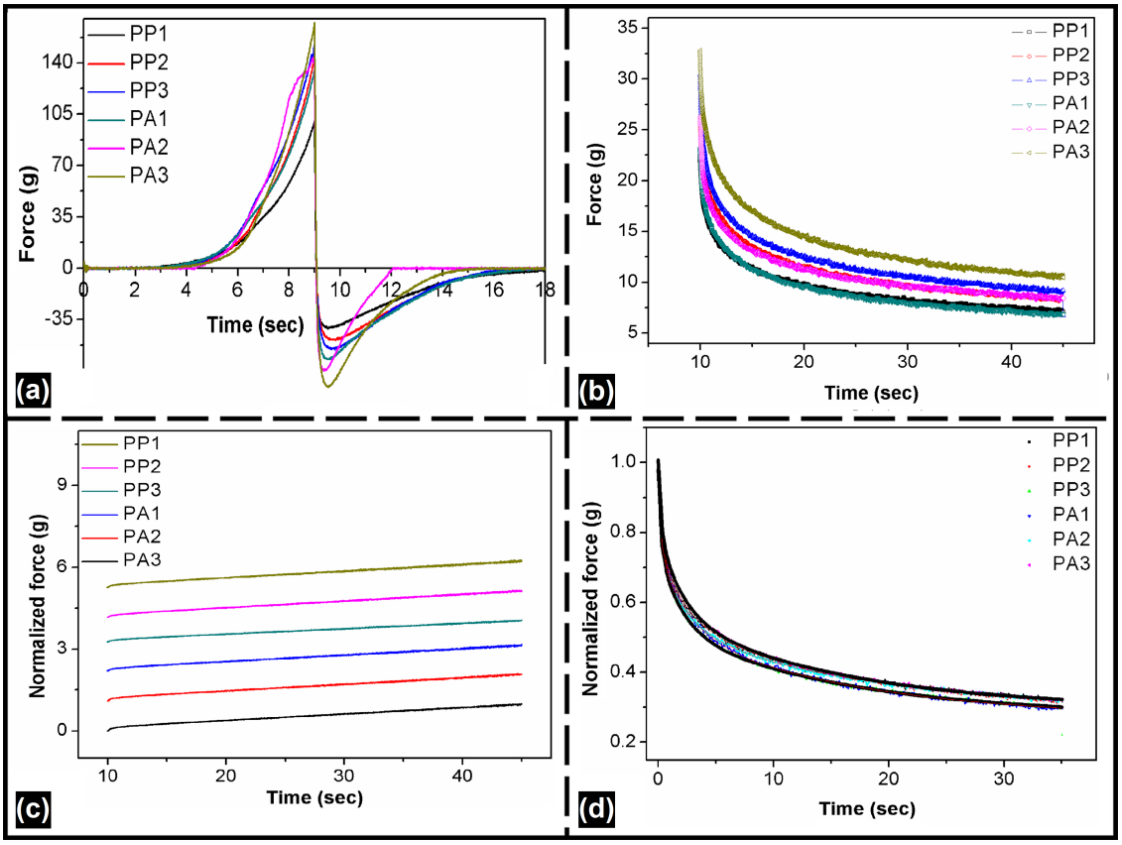

Figure 9.6: Mechanical analysis (a) spreadability (b) stress relaxation (c) normalized force vs. time and (d) Weichert model

The stress relaxation studies were carried out to evaluate the viscoelastic properties of the bigels (Figure 9.6d). It was observed from the graph that the force reached asymptotically to an equilibrium value instead of 0. The k_1 (rate) and k_2 (extent) parameters were calculated from Peleg and Normand equation to determine the viscoelastic properties of the bigels. According to Peleg and Normand (1983), solid materials have k_2 values close to unity. However, a clear trend was not observed from these values.

Hence, other viscoelastic parameters such as S^* and F^* were further quantified. For viscoelastic materials, the S^* value ranges from 0-1. Materials with higher elastic behavior have S^* values closer to 1. The S^* values of all the bigels (PA and PP) were < 1, indicating the viscoelastic property of the bigels. There was a marginal decrease in the F^* values with the increase in the PVP content. On the contrary, an increase in the PVA content resulted in the increase in the F^* values.

The percent stress relaxation decreased with the increase in the polymer concentration. It was also observed that the percent stress relaxation in PP bigels was little higher as compared to PA bigels. For stress relaxation to occur, the polymer should move across easily. The movement of the polymer also depends on the firmness of the bigels. It was found that PA

bigels were firmer as compared to PP bigels. Hence, a lesser percent stress relaxation was observed in PA bigels. The percent stress relaxation was reduced with the increase in the polymer concentration. As reported earlier, the hydrophobic alkyl chain ends of PP forms a tiny hydrophobic region and facilitates the formation of the regular polymeric network. An increase in the polymer concentration results in the increase in the formation of physical crosslinks, which is responsible for the decrease in the percent stress relaxation. In the case of PA bigels, strong hydrogen bonding plays an important role in the percent stress relaxation of the bigels.

A greater relaxation means a higher energy was dissipated as the stress was applied. Percent stress relaxation for ideal elastic solid corresponds to 0% while for liquid it is 100%. The percent stress relaxation for the bigels was in the range of 65%-70% indicating their liquid-predominant nature.

Table 9.3: Texture properties of the bigels

Studies	Parameters	PP1	PP2	PP3	PA1	PA2	PA3
Mechanical properties	Firmness (g)	100.3162 ± 1.2624	144.5031± 2.6946	152.7306 ± 3.8587	135.2157 ± 2.7676	167.4576 ± 1.6378	176.6132 ± 6.6132
	Spreadability ($g^{-1}.sec^{-1}$)	0.0068 ± 0.0031	0.0058 ± 0.0011	0.0056 ± 0.0021	0.0044 ± 0.0017	0.0041 ± 0.0012	0.0037 ± 0.0016
	Stickiness (g)	41.2681 ± 7.1752	49.0972 ± 6.8233	55.5994 ± 7.9325	62.2336 ± 3.2172	70.1957 ± 4.1236	81.208 ± 2.1756
Stress relaxation	F^* (g)	0.3173	0.3147	0.2923	0.2217	0.291	0.3216
	K_1 (g)	0.1361	0.0611	0.0948	0.0251	0.0246	0.0234
	K_2 (g)	0.0247	0.0227	0.0269	0.0241	0.0246	0.0243
	S*	0.7794	0.7784	0.7786	0.3892	0.3899	0.3900
	Percent stress relaxation	69.6873	68.6651	68.1908	68.8571	67.8392	67.5590

The Peleg's model, as reported, was unable to provide a complete picture of the relaxation. To have an in-depth knowledge, the data was fitted to three Maxwell elements Weichert viscoelastic model (figure 9.6d). This decay in stress over time was explained by this model. The profile of stress relaxation shows that initially the decay in stress with time was fast followed by a slow dissipation of stress. The relaxation times τ_1, τ_2, and τ_3 represent the various process of polymer rearrangement occurring within the bigels when stress is applied. The residual stress (P_0) is an indicator of the stability of the bigels. A decrease in the residual stress indicates the breaking of the associative bonds in the polymer network [245]. The residual stress was higher in the formulations with higher polymer content (Table 9.4). It was observed from the study that the stability of the PA bigels was more as compared to PP bigels. The easier structural rearrangements of the PVP and the PVA chains resulted in the higher stress decay as the polymer concentration was increased. The relaxation times (τ) were in the order of $\tau_1 < \tau_2 < \tau_3$ and were in acceptance with the literature [107]. According to the earlier studies, each relaxation constant is associated with the specific structural rearrangement. τ_1 is the shortest relaxation time constant and τ_3 is the longest relaxation time constant. τ_2 and τ_3 are the important parameters that decide the stability of the bigels and are associated with the polymer rearrangement occurring during the relaxation process [106]. Since the values of τ_2 and τ_3 correspond to the disentanglement and breakage of the polymer interactions under the applied stress. The decrease in the value of τ_2 and τ_3 can be attributed to the formation of better network and interaction amongst the polymer chains in the bigels. The τ_2 and τ_3 values decreased with the increase in the polymer concentration (table 9.4). It was also observed from the model that the τ_2 and τ_3 values of the PA bigels were lower as compared to the PP bigels. This indicated that the interactions in the PA bigels were much stronger than the PP bigels. These results were in agreement with the firmness results of the bigels. The coefficient of viscosity (Table 9.5) of the dashpots decreased with an increase in the polymer concentration. These results were in accordance with the above backward extrusion and viscosity studies.

Table 9.4: Weichert model parameters of PA and PP bigels

Sample code	τ_1	τ_2	τ_3	r^2
PP1	0.6857	3.3103	19.6001	0.9910
PP2	0.3982	1.9861	15.2442	0.9870
PP3	0.1957	1.9319	14.9492	0.9880
PA1	0.2469	2.2921	16.2933	0.9890
PA2	0.1923	1.9411	14.9392	0.9901
PA3	0.1857	1.8397	14.3976	0.9931

Pre-exponential factors

Sample code	P_0	P_1	P_2	P_3
PP1	0.2816	0.2876	0.2345	0.1963
PP2	0.2889	0.2492	0.1835	0.2850
PP3	0.2933	0.2341	0.2341	0.2563
PA1	0.2936	0.2695	0.2371	0.2000
PA2	0.2941	0.2181	0.2490	0.2388
PA3	0.2988	0.2624	0.3162	0.1226

Table 9.5: Stress relaxation model fitting using Wiechert model

Formulation Code	Stress relaxation Model	Coefficient of viscosity of the dashpots
PP1	$P(t)=0.2816 + 0.2876e^{\frac{-t}{0.6857}} + 0.2345e^{\frac{-t}{3.3103}} + 0.1963e^{\frac{-t}{19.6001}}$	0.1972, 0.7762, 3.8474
PP2	$P(t)=0.2889 + 0.2492e^{\frac{-t}{0.3982}} + 0.1835e^{\frac{-t}{1.9861}} + 0.2850e^{\frac{-t}{15.2442}}$	0.0991, 0.3644, 4.3445
PP3	$P(t)=0.2933 + 0.2341e^{\frac{-t}{0.1957}} + 0.2341e^{\frac{-t}{1.9319}} + 0.2563e^{\frac{-t}{14.9492}}$	0.0458, 0.4522, 3.8314
PA1	$P(t)=0.2936 + 0.2695e^{\frac{-t}{0.2469}} + 0.2371e^{\frac{-t}{2.2921}} + 0.2000e^{\frac{-t}{16.2933}}$	0.0665, 0.5434, 3.2586
PA2	$P(t)=0.2941 + 0.2181e^{\frac{-t}{0.1923}} + 0.2490e^{\frac{-t}{1.9411}} + 0.2388e^{\frac{-t}{14.9392}}$	0.0419, 0.4833, 3.5674
PA3	$P(t)=0.2988 + 0.2624e^{\frac{-t}{0.1857}} + 0.3162e^{\frac{-t}{1.8397}} + 0.1226e^{\frac{-t}{14.3976}}$	0.0487, 0.5817, 1.7650

9.3.6 Gel disintegration studies

The gel disintegration studies of PA1, PA2, PA3, PP1, PP2 and PP3 was found to be 105 ± 0.54 sec, 113 ± 1.12 sec, 120 ± 0.24 sec, 60 ± 1.24 sec, 95 ± 2.54, 98 ± 1.67 sec, respectively. These results were in agreement with the viscosity of the polymer sol and the mechanical properties of the bigels. The higher viscosity of PA bigels hindered the permeation of the solvent. This caused a slower disintegration of the PA bigels as compared to that of the PP bigels. These results were also in agreement with the mechanical and rheological properties of the bigels.

9.3.7 Thermal analysis

The DSC profiles of the bigels are shown in figure 9.7, table 9.6. The effect of the polymers on the change in the enthalpy (ΔH) was calculated. The ΔH value of PP3 bigels was higher as compared to the PA3 bigels. The decrease in the ΔH value of PA3 as compared to PP3 can be explained by the interaction of the water molecules with the PVA chains [221]. PVA in PA bigels retains more water molecules. This is due to more hydrophilic nature of PVA as compared to PVP. High water retaining capacity of PVA in PA bigels lowers the energy required for crystal disorganization. This increases the mobility of the polymer chains within the bigels during heating. This, in turn, increases the kinetic energy and finally lowers the ΔH values [130]. The heating cycle in the DSC showed another endothermic peak (40-44 °C), with a positive heat flow indicating the melting of the sorbitan monopalmitate molecules in the bigels.

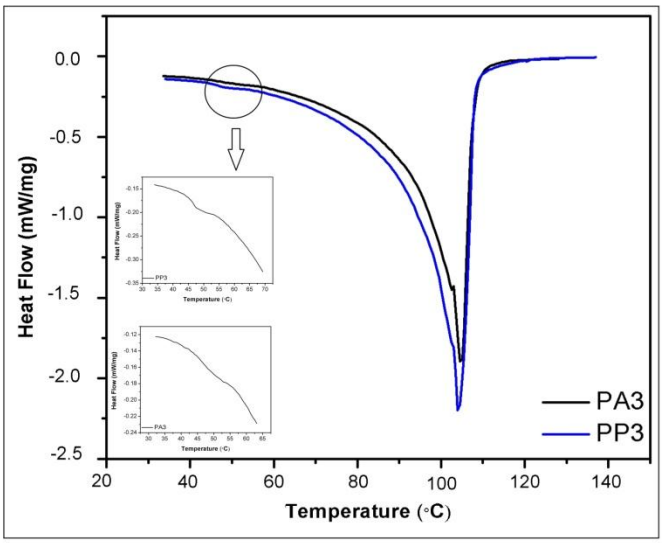

Figure 9.7: DSC profile of PA3 and PP3 bigels

Table 9.6: Thermal parameters studied from DSC

Sample code	ΔH (J/g)
PA	751.9
PP	923.8

9.3.8 Electrical analysis

The Nyquist plot of the bigels has been shown in figure 9.8. The bulk resistance was obtained from the intercept of the semicircle with the real axis in the low-frequency region. It was observed that the bulk resistance of the bigels was in the order of PP3 > PP2 ≈ PP1 ≈ PA3 > PA2 > PA1 (figure 9.8a). This may be attributed to the fact that an increase in the PVP content increased the hydrophobicity of the bigels. This may be attributed to the presence of nonpolar methylene and methine groups in PVP.

The dielectric constant (ε) is a measure of the stored charge in the bigels (figure 9.8b). A reduction in the 'ε' was observed at higher frequencies. This can be explained by the electrode polarization at low frequency. However, the polarization effect was minimized at high frequencies.

The 'ε' values of PA bigels were higher than PP bigels. It has been reported earlier that PVA has a very high dielectric constant with a value > 1000 kV/mm. These results were in accordance with the earlier reported literature, where aqueous PVP solution has been reported to have lower 'ε' values as compared PVA solution. The PVA chains have flexible side groups with a polar rotating bond with an intense dielectric α-transition [246]. The OH groups of PVA are capable of both accepting and donating protons. This promotes interactions of the water molecules with a large number of PVA monomers as compared to PVP. This strong hydrogen bonding orients the PVA chains present in the PA bigels to increase the net polarization. The low ε values of PP are due to the dominance of the strong hydrophobic effect in PVP as compared to the hydrophilic interactions amongst the carboxyl groups of PVP monomers and water molecules. Another factor that led to the decrease in ε values may be the difference in the orientation of randomly coiled flexible PVP chain segments in the external aqueous phase of the bigels [247].

The AC conductivity σ' (ω) profiles of the bigels have been shown in figure 9.8c. The AC conductivity was in the order of PA1 > PA2 > PA3 = PP1 = PP2 = PP3. The PA bigels contain PVA in the external phase, and hence, the properties of these bigels predominantly depend on the PVA molecules. PVA has a tendency to swell in the presence of water. This property of the polymer results in the formation of the ion transfer channels, which play an

important role in imparting ionic conductivity [248]. This resulted in an increase in the AC conductivity of PA bigels as compared to the PP bigels. The AC conductivity of the PA bigels was inversely proportional to that of the concentration of the polymer. The results of AC conductivity of the bigels were in support of the results of the bulk resistance (DC impedance) and ε. The PP bigels, on the other hand, did not much variation in the AC conductivity.

The loss factor (tan δ) represents the dissipation of energy in the dielectric system. The variation of tan δ with frequency is shown in figure 9.8d. It was observed from the graph that the samples exhibited a zero dielectric loss at higher frequencies. The higher tan δ at lower frequencies was due to the relaxation of the polymers in the bigels. The relaxation is associated with the flexibility of the polymer chain. High values of dielectric loss are associated with grain boundary resistance, thereby requiring more energy for electron exchange. As the PVA concentration was increased, the bigels became less conductive due to the increase in the local viscosity, which in turn, increased the dielectric loss [249].

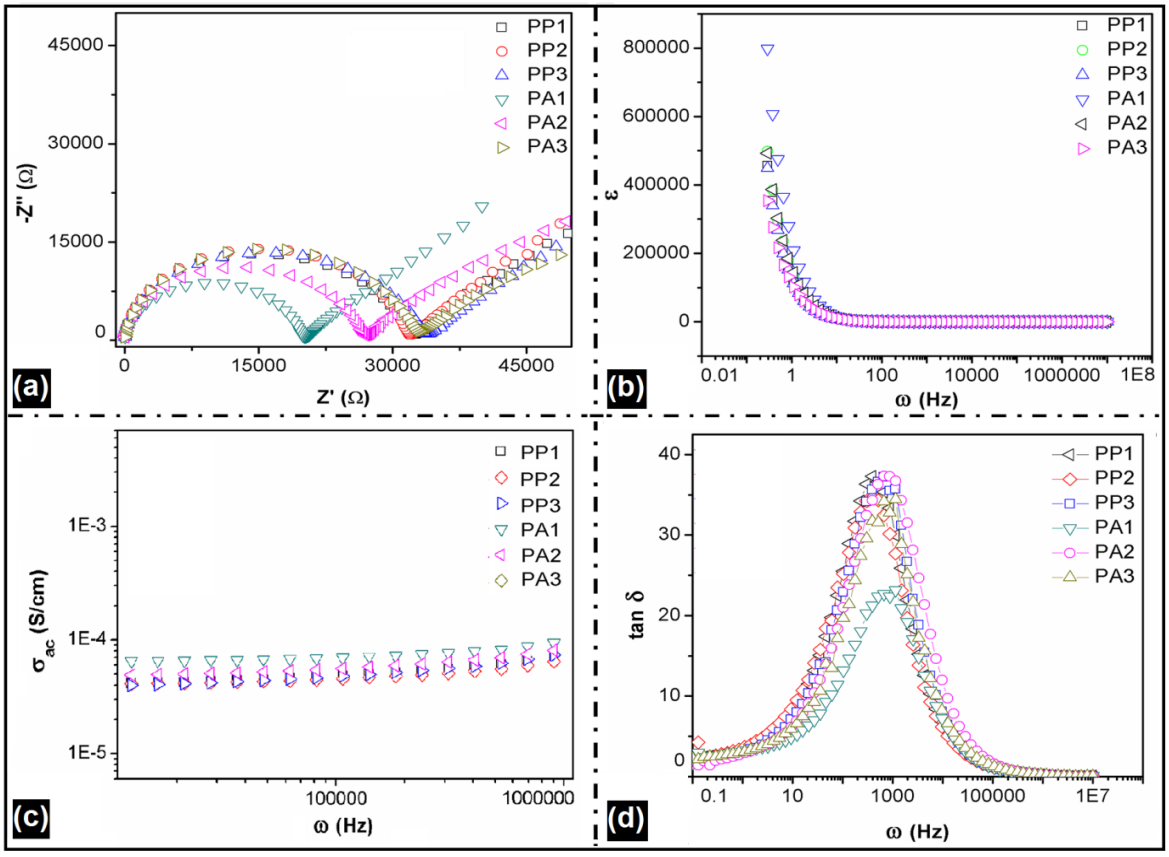

Figure 9.8: Electrical properties of PA and PP (a) Nyquist plot, (b) variation of dielectric constant with frequency, (c) AC conductivity vs. frequency and (d) tan δ vs. frequency

9.3.9 *In vitro* cytotoxicity of dialyzed formulation components

The percent hemolysis of the goat RBC was in the range of 0-2% (figure 9.9a). This suggested non-hemolytic nature of the bigels as per the ASTM F756-00, 2000 (American Society for Testing and Materials) protocol [250].

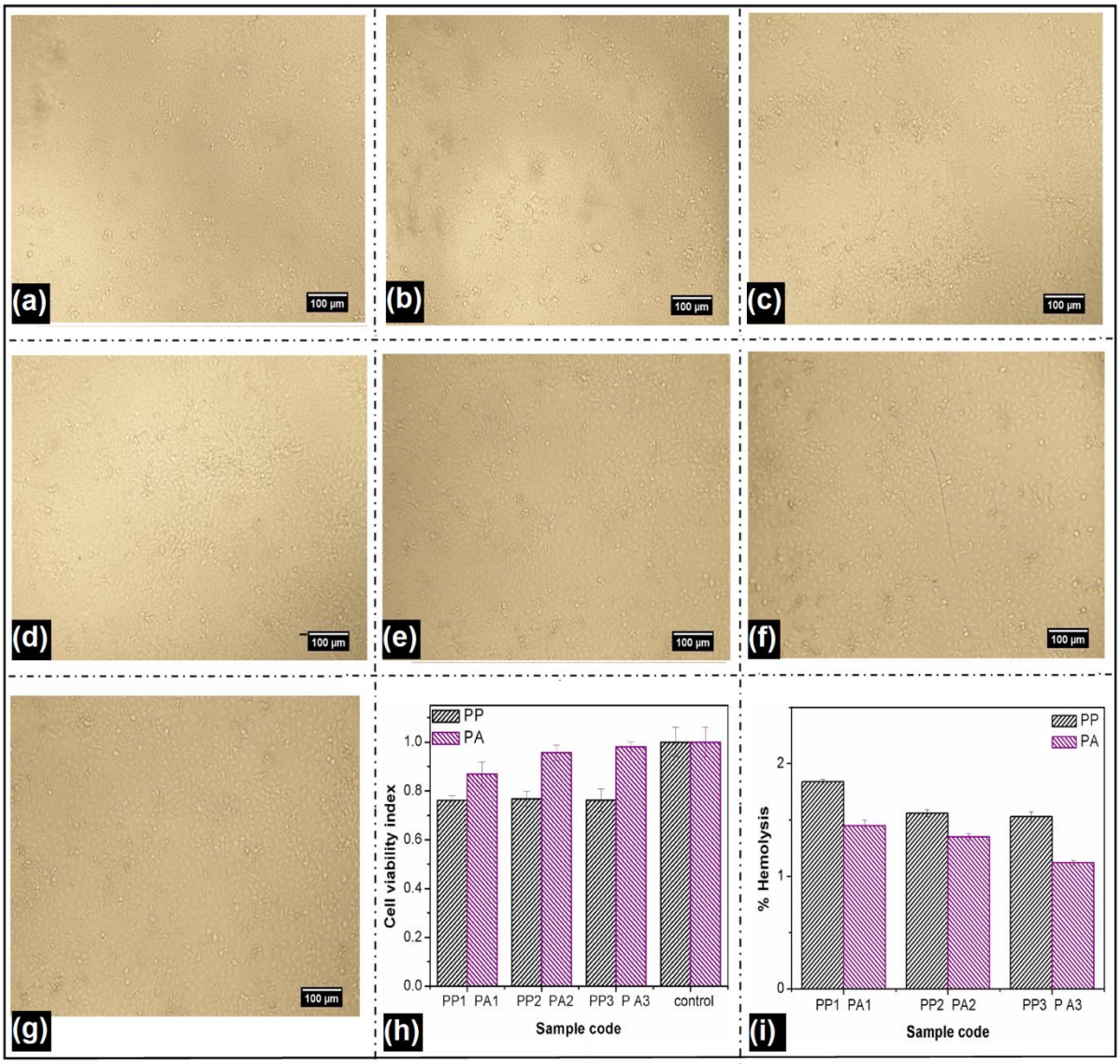

Figure 9.9: *In vitro* cytotoxicity of dialyzed formulation components of PA and PP bigels (a) micrographs of control, (b) cells in the presence of PA1, (c) PA2, (d) PA3, (e) PP1, (f) PP2, (g) PP3, (h) cell viability index and (i) percent hemolysis.

The cytotoxicity studies were performed by MTT assay. The MTT (3-(4,5-dimethylthiazol-2-yl)-2,5-diphenyltetrazolium bromide) assay is a simple colorimetric assay to measure cytotoxicity, cell viability. The viability of HaCaT cells in the presence of leachates of PP and PA bigels is shown in figure 9.9b. The cell viability index of PA bigels was concentration dependent and was found to be higher in the presence of leachates of PA bigels as compared

to PP bigels. The cell viability varied in the order of PA3 > PA2 > PA1. On the contrary, the viability index of the PP bigels was same. The cell viability index of PP bigels was significantly lower than the control. The difference was statistically significant ($p < 0.05$). The structure of the cells was maintained in the presence of leachates.

9.3.10 *In vitro* antimicrobial studies

The antimicrobial efficiency of the drug loaded bigels (PPM1, PPM2, PPM3, PAM1, PAM2, and PAM3) was carried out against *E. coli* (Table 9.7). Marketed formulation of metronidazole Metrogyl®, MR (Dosage form-gel, Dose-Apply, and rub in a thin film of Metrogyl gel twice daily to affected areas after washing) was used as a reference. 1000 µg of the drug dose was used in all the cases for the test as well as for reference. PP1, PP2, PP3, PA1, PA2 and PA3 were taken as negative controls. It was observed that the efficiency of MR and metronidazole loaded bigels showed nearly equal antimicrobial efficiency (figure 9.10). The statistical analysis showed no significant difference between the bigels and MR ($p > 0.05$) This suggested that the antimicrobial effectiveness of the bigels was nearly equal to MR and thus, can act as efficient carriers for the delivery of antibiotics.

Table 9.7: Zone of inhibition of the metronidazole loaded bigels against *E. coli*

Sample code	Zone of inhibitions (cm) *E. coli*		
	Test	**MR**	**Blank**
PPM1	2.6 ± 0.1	2.6 ± 0.5	-
PPM2	2.4 ± 0.1	2.6 ± 0.6	-
PPM3	2.3 ± 0.7	2.5 ± 0.1	-
PAM1	2.6 ± 0.1	2.6 ± 0.2	-
PAM2	2.5 ± 0.1	2.6 ± 0.6	-
PAM3	2.3 ± 0.7	2.5 ± 0.2	-

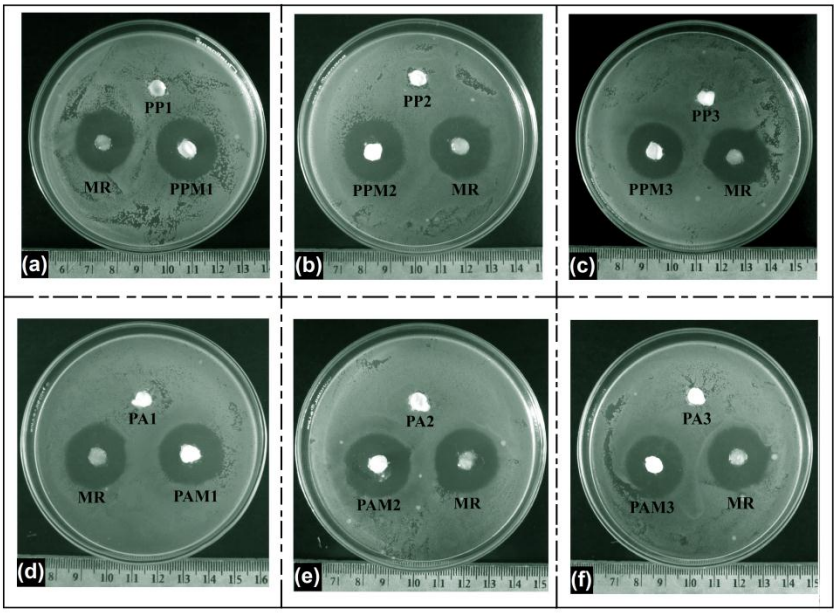

Figure 9.10: Antimicrobial activity of metronidazole loaded PP and PA bigels

9.3.11 *In vitro* drug release studies

In vitro drug release of metronidazole from PA and PP bigels has been shown in figure 9.11. Marketed formulation of metronidazole Metrogyl® MR (Dosage form-gel, Dose-Apply, and rub in a thin film of Metrogyl gel twice daily to affected areas after washing) was used as a reference. There was 63.65%, 60.42%, 53.96%, 51.97%, 42.91% and 38.08% drug release from PPM1, PPM2, PPM3, PAM1, PAM2 and PAM3, respectively at the end of 12h. The release rate of metronidazole was slightly decreased with an increase in the polymer content. PAM bigels showed lower drug release as compared to PPM bigels. According to the viscosity and mechanical experiments, the presence of PVA resulted in the formation of more viscous and stronger gels. Strong and viscous bigels reduced the drug release to a larger extent. The results from the viscosity studies showed that PA bigels had a higher viscosity as compared to PP bigels. The earlier It has also been reported earlier that PVA macromolecular chains form a compact network that hinders the diffusion of the macromolecules [251]. Another factor that led to the slower release of the drug from the bigels was attributed to the stabilizing effect of PVA. As reported earlier, a higher PVA concentration yields a more stable emulsion. This hinders the mass transfer of the active component from the formulations [252]. It has been reported earlier that PVP increases the surface wettability and also the water penetration into the matrix, thus giving a faster release of drug from the PP bigels [253].

The kinetics of *in vitro* release was predicted by fitting the cumulative percentage drug release data to various models such as zero-order and Higuchi. The mechanism of the release was predicted by fitting the data to Korsmeyer–Peppas model. The correlation coefficient (r^2) and n-value (calculated from the slope) has been tabulated in Table 9.8. Based on the results, it was found that the r^2 values were better in Higuchi model indicating diffusion as a process governing criterion for the drug release. The mechanism of diffusion was further evaluated from the 'n' value (release exponent) of Korsmeyer-Peppas model. The results showed $n \leq 0.5$ indicating Fickian or pseudo-Fickian diffusion of metronidazole from the bigels. The pseudo-Fickian release is considered as a complex release mechanism which is dependent on various other factors such as swelling and erosion of polymers, the porosity of the matrix and drug diffusion rate.

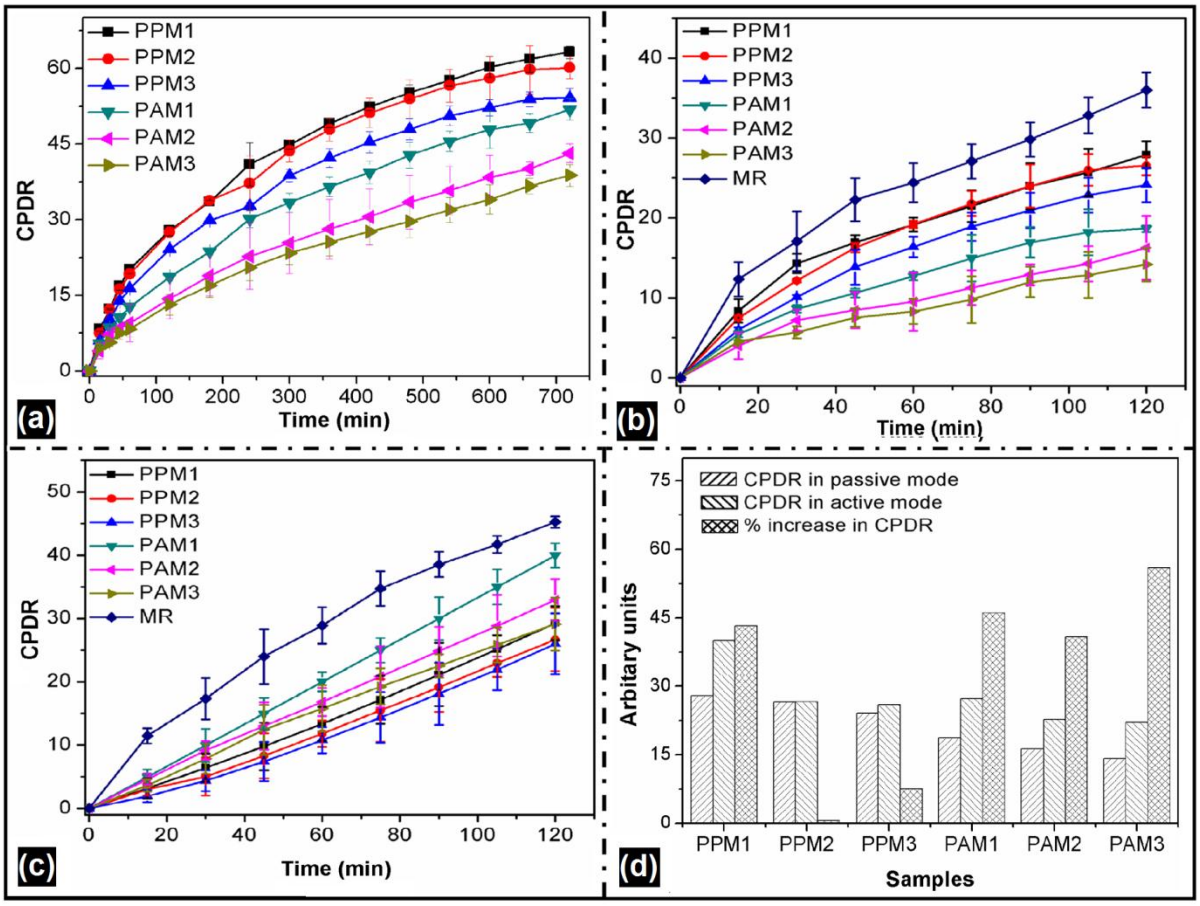

Figure 9.11: *In vitro* metronidazole release (a) passive drug release, (b) passive drug release using iontophoretic drug release setup, (c) active drug release using iontophoretic drug release setup and (d) Effect of iontophoresis over passive drug release.

Figure 9.11b and Figure 9.11c shows iontophoretic release profile of metronidazole. The mechanism of drug release was found to be zero order under active condition. This phenomenon indicated the presence of both diffusion as well as molecular relaxation that governed the release of drugs through the matrix. Here the rate-controlling step is the relaxation process of the macromolecules after absorption of the water molecules. The drug release under the active condition is dependent on the bulk resistance of the bigels. The bulk resistance of the PA bigels was more as compared to PP the bigels. This high conductivity of the PA bigels formed conducting channels which acted as the major driving force behind the faster drug release. The ‘n’ values of the Korsmeyer-Peppas model were in the range of 0.5 and 1.0. This indicated the anomalous transport of the drug which was a superposition of both diffusion and other mechanism playing an important role in the transport of the macromolecule.

Table 9.8: Release kinetics of metronidazole from PA and PP bigels (Metrogyl® denoted as MR)

Formulation code	Zero order model (r^2)	Higuchi model (r^2)	Best fit model	Korsmeyer-Peppas		Mechanism of release
				(r^2)	N	
Passive drug delivery						
PPM1	0.9101	0.9991	Higuchi	0.9928	0.5000	Diffusion
PPM2	0.9120	0.9921	Higuchi	0.9962	0.5000	Diffusion
PPM3	0.9021	0.9992	Higuchi	0.9912	0.5000	Diffusion
PAM1	0.9421	0.9972	Higuchi	0.9912	0.5000	Diffusion
PAM2	0.9601	0.9931	Higuchi	0.9937	0.5000	Diffusion
PAM3	0.9603	0.9912	Higuchi	0.9901	0.5000	Diffusion
MR	0.9811	0.8800	Zero order	0.9734	0.4702	Difusion
Iontophoretic drug delivery						
PPM1 (Passive)	0.9184	0.9911	Higuchi	0.9812	0.5000	Diffusion
PPM2 (Passive)	0.8521	0.9811	Higuchi	0.9854	0.4612	Diffusion
PPM3 (Passive)	0.9312	0.9983	Higuchi	0.9904	0.5001	Diffusion
PAM1 (Passive)	0.9212	0.9821	Higuchi	0.9905	0.4500	Diffusion
PAM2 (Passive)	0.9401	0.9900	Higuchi	0.9910	0.4823	Diffusion
PAM3 (Passive)	0.9700	0.9802	Higuchi	0.9981	0.4805	Diffusion
PPM1 (Active)	0.9821	0.9702	Zero-order	0.9718	0.6811	Anomalous
PPM2 (Active)	0.9800	0.9621	Zero-order	0.9721	0.6102	Anomalous
PPM3 (Active)	0.9903	0.9701	Zero-order	0.9810	0.6800	Anomalous
PAM1 (Active)	0.9922	0.9721	Zero-order	0.9621	0.6601	Anomalous
PAM2 (Active)	0.9901	0.9500	Zero-order	0.9821	0.6901	Anomalous
PAM3 (Active)	0.9812	0.9302	Zero-order	0.9801	0.6200	Anomalous

9.4 Major outcomes

- The bigels containing PVA showed greater firmness as compared to the bigels containing PVP.
- The mechanical studies revealed the viscoelastic behavior of the bigels.
- The viscosity of the bigels increased with the increase in the concentration of PVA and PVP. The bigels showed shear thinning behavior.
- The electrical properties showed that the conductivity of the PVA bigels was higher as compared to the PVP bigels.
- The cell viability index of the bigels increased with the increase in the PVA concentration.
- The inclusion of PVA resulted in a much slower release of the drug as compared to the PVP bigels and marketed formulation under active condition.

CHAPTER 10

Summary and Conclusion

10.1 Summary and conclusion

The thesis provides a broad investigation on the promising role of bigels in the delivery of poorly soluble drugs, and their use as matrices in iontophoresis. The bigels were prepared using different proteins, polysaccharides, and synthetic polymers. They were then characterized thoroughly. The comparison between various types of bigels is shown in table 10.1. From the above study, it was concluded that the effectiveness of interfacial jamming and stabilization of these multiphase systems was dependent on the type and concentration of polymer used in the study. The major conclusions drawn are

- The particle size of protein based bigels was found to be smaller as compared to that of polysaccharides, gums, and synthetic polymers based bigels. The particle size of protein based bigels varied from 4-5 µm as compared to other polymers based bigels where the size ranged from 7-17 µm.
- The effect of proteins, polysaccharides, gums and synthetic polymers on the viscosity profile was not significant. All the bigels exhibited a pseudoplastic flow behavior.
- The bigels containing polysaccharides like maltodextrin and starch showed higher firmness than other polymer based bigels. The synthetic polymers and xanthan gum based bigels were found to be less firm as compared to other bigels. The starch-based bigels were found to have more stickiness values.
- The synthetic polymer based bigels were found to be less sticky as compared to protein, polysaccharides, and natural gums based bigels. The spreadability of starch and maltodextrin-based bigels were least amongst all other bigels. Although the protein based bigels had little higher spreadability as compared to that of starch and maltodextrin-based bigels, their spreadability was lower as compared to other polysaccharides, natural gum, and synthetic polymer based bigels.
- All the bigels showed a viscoelastic behavior.
- There was no change in the stability of all the bigels even though after 10 months as per ICH guidelines.
- A slow release of metronidazole as compared to marketed formulation was obtained in all the bigels containing proteins, polysaccharides, natural gums and synthetic polymers. Release behavior of the drug from the whey protein based bigels was more controlled as compared to all other bigels. Drug release from gum based bigels was comparatively higher than that of proteins, polysaccharides, and synthetic polymers based bigels but quite slower than available marketed formulation of the same drug.

- Application of AC current to the bigels led to the release of drug in a constant manner, thus making them suitable candidates for iontophoresis.
- Although there was not much difference in the antimicrobial efficiency of different types of bigels, the antimicrobial activity of all the drug loaded bigels was comparable with that of the marketed formulations of metronidazole.
- The *in vitro* cytotoxicity studies of the bigels showed that they can be well tolerated. Based on above results it can be concluded that the physical and mechanical properties, stability, drug release, and antimicrobial efficiency were closely related to the type of polymers used in the study.
- From the above study, it was concluded that the protein and starch based bigels served as a good carrier for the controlled delivery of metronidazole.
- Furthermore, the low expenses incurred during the preparation of bigels can also help in the development of suitable cost effective biomaterial to be used in both pharmaceutical and biomedical industries.

Table 10.1: Comparative account of the bigel formulations

Sample code	Size distribution (μm)	Texture studies			Bulk resistance (Ω)	*In vitro* drug release	cell viability index
		Firmness (g)	Stickiness (g)	Spreadability ($g^{-1}sec^{-1}$)			
				Emulgels			
GW	3.3245 ± 0.8123	172.1127 ± 4.1175	84.9208 ± 4.1854	0.0009 ± 0.0081	21545.9712	43.1228 ± 0.5612	0.8521± 0.0342
				Bigels			
SG	3.6214 ± 1.2473	435.2341 ± 2.7121	265.2723 ± 4.5732	0.0085 ± 0.0017	5202.3145	76.2123 ± 3.5231	0.8602 ± 0.0342
GG	4.1264 ± 1.0572	693.1756 ± 2.8731	449.0512 ± 4.15824	0.0011 ± 0.0009	2407.7221	58.3173 ± 0.1321	0.8521 ± 0.0132
WG	4.9492 ± 0.16722	468.0634 ± 2.7231	332.6913 ± 3.8931	0.0016 ± 0.0008	4469.1226	30.2275 ± 1.0421	0.9331 ± 0.0543
FA	13.3712 ± 0.7972	682.4721± 3.1423	555.2812 ± 2.1503	0.0021 ± 0.0013	31968.2817	71.6889 ± 1.9312	0.9151 ± 0.0385
FC	7.9146 ± 0.2183	646.2832 ± 2.5287	472.0912 ± 3.1653	0.0015 ± 0.0013	40743.8674	65.6773± 1.5521	0.9253 ± 0.0172
FM	7.7724 ± 0.31278	1000.7623 ± 1.8211	274.9421 ± 1.3282	0.0007 ± 0.0005	19222.7321	53.8782 ± 2.3765	0.9425 ± 0.0238
FS	16.6213 ± 0.2479	729.4421 ± 3.1471	800.27 37± 2.1552	0.0010 ± 0.0090	12327.6284	57.9712 ± 1.0721	0.9730 ± 0.0238
AG	12.5561 ± 2.4354	249.8212 ± 3.7656	142.6324 ± 3.7678	0.0029 ± 0.0013	51516.8821	87.7292 ± 1.4167	0.8734 ± 0.0087
GAG	10.1923 ± 2.1473	309.6623 ± 2.9896	213.3915 ± 2.6412	0.0020 ± 0.0015	36406.4812	75.7561± 1.6728	0.8658± 0.0537
XG	8.2921 ± 3.1467	135.4823 ± 2.6453	85.3715 ± 3.2135	0.0049 ± 0.0021	23812.3045	73.0492 ± 0.4182	0.9440 ± 0.0461
PA	10.1827 ± 0.4916	135.2157 ± 2.7676	62.2336 ± 3.2172	0.0044 ± 0.0017	20104.8267	51.9712 ± 2.1419	0.8683 ± 0.0491
PP	16.8173 ± 0.5326	100.3162 ± 1.2624	41.2681 ± 7.1752	0.0068 ± 0.0031	33463.1284	63.6527 ± 1.2192	0.7611 ± 0.0285

GW: Sorbitan monopalmitate and sunflower oil based emulgels **SG: Blank bigels** **GG-Gelatin based bigels** **WG- Whey protein based bigels** **FA- Alginate based bigels** **FC- Carboxymethyl cellulose based bigels** **FM- Maltodextrin based bigels** **FS- Starch based bigels** **AG-Acacia gum based bigels** **GAG-Guar gum based bigels** **XG-Xanthan gum based bigels** **PA-Polyvinly alcohol basedbigels** **PP- Polyvinyl pyrrolidone based bigels**

REFERENCES

1. Paolino, D., et al., *Drug Delivery Systems, Encyclopedia of Medical Devices and Instrumentation*. 2006, John Wiley & Sons, Inc.
2. Dash, S., et al., *Kinetic modeling on drug release from controlled drug delivery systems.* Acta Poloniae Pharmaceutica-Drug Research, 2010. **67**(3): p. 217-23.
3. Huang, X. and C.S. Brazel, *On the importance and mechanisms of burst release in matrix-controlled drug delivery systems.* Journal of Controlled Release, 2001. **73**(2–3): p. 121-136.
4. Rehman, K. and M.H. Zulfakar, *Recent advances in gel technologies for topical and transdermal drug delivery.* Drug development and industrial pharmacy, 2014. **40**(4): p. 433-440.
5. Ibrahim, M.M., S.A. Hafez, and M.M. Mahdy, *Organogels, hydrogels and bigels as transdermal delivery systems for diltiazem hydrochloride.* Asian Journal of Pharmaceutical Sciences, 2013. **8**(1): p. 48-57.
6. Almeida, I., et al., *Moisturizing effect of oleogel/hydrogel mixtures.* Pharmaceutical development and technology, 2008. **13**(6): p. 487-494.
7. Rehman, K., M.C.I. Mohd Amin, and M.H. Zulfakar, *Development and physical characterization of polymer-fish oil bigel (Hydrogel/Oleogel) system as a transdermal drug delivery vehicle.* Journal of oleo science, 2014. **63**(10): p. 961-970.
8. Sawalha, H., et al., *The Influence of concentration and temperature on the formation of γ-Oryzanol+β-Sitosterol tubules in edible oil organogels.* Food biophysics, 2011. **6**(1): p. 20-25.
9. Nielloud, F., *Pharmaceutical Emulsions and Suspensions: Revised and Expanded*. 2000: CRC Press.
10. Zhao, D., et al., *Nonionic triblock and star diblock copolymer and oligomeric surfactant syntheses of highly ordered, hydrothermally stable, mesoporous silica structures.* Journal of the American Chemical Society, 1998. **120**(24): p. 6024-6036.
11. Dassanayake, L.S.K., D.R. Kodali, and S. Ueno, *Formation of oleogels based on edible lipid materials.* Current Opinion in Colloid & Interface Science. 2011. **16**(5): p. 432-439.

12. Wang, M., et al., *Radiation synthesis of PVP/CMC hydrogels as wound dressing.* Nuclear Instruments and Methods in Physics Research Section B: Beam Interactions with Materials and Atoms, 2007. **265**(1): p. 385-389.
13. Gaucher, G., et al., *Block copolymer micelles: preparation, characterization and application in drug delivery.* Journal of Controlled Release, 2005. **109**(1–3): p. 169-188.
14. Cho, M.J., *Esters of metronidazole and compositions containing them*. 1984, EP Patent 0,127,274.
15. Pichayakorn, W. and P. Boonme, *Evaluation of cross-linked chitosan microparticles containing metronidazole for periodontitis treatment.* Materials Science and Engineering: C, 2013. **33**(3): p. 1197-1202.
16. Shimizu, H., et al., *Effectiveness of iontophoresis with alternating current (AC) in the treatment of patients with palmoplantar hyperhidrosis.* The Journal of dermatology, 2003. **30**(6): p. 444.
17. Ogami, S., et al., *Pentazocine transport by square-wave AC iontophoresis with an adjusted duty cycle.* Journal of medical and dental sciences, 2008. **55**(1): p. 15-27.
18. Barel, A.O., M. Paye, and H.I. Maibach, *Handbook of cosmetic science and technology*. 2009: Informa healthcare Nueva York.
19. Abdallah, D.J. and R.G. Weiss, *Organogels and low molecular mass organic gelators.* Advanced Materials, 2000. **12**(17): p. 1237-1247.
20. Hoffman, A.S., *Hydrogels for biomedical applications.* Advanced drug delivery reviews, 2002. **54**(1): p. 3-12.
21. Chang, R.-K., et al., *Generic development of topical dermatologic products: formulation development, process development, and testing of topical dermatologic products.* The AAPS journal, 2013. **15**(1): p. 41-52.
22. Almeida, I.F. and M.F. Bahia, *Evaluation of the physical stability of two oleogels.* International journal of pharmaceutics, 2006. **327**(1): p. 73-77.
23. Kumar, R. and O.P. Katare, *Lecithin organogels as a potential phospholipid-structured system for topical drug delivery: a review.* Aaps Pharmscitech, 2005. **6**(2): p. E298-E310.
24. Tokuyama, H. and Y. Kato, *Preparation of thermosensitive polymeric organogels and their drug release behaviors.* European polymer journal, 2010. **46**(2): p. 277-282.
25. Pisal, S., et al., *Effect of organogel components on in vitro nasal delivery of propranolol hydrochloride.* Aaps Pharmscitech, 2004. **5**(4): p. 92-100.

26. Göpferich, A., *Mechanisms of polymer degradation and erosion.* Biomaterials, 1996. **17**(2): p. 103-114.
27. Sinha, V. and M.P. Kaur, *Permeation enhancers for transdermal drug delivery.* Drug development and industrial pharmacy, 2000. **26**(11): p. 1131-1140.
28. Bonacucina, G., et al., *Colloidal soft matter as drug delivery system.* Journal of Pharmaceutical Sciences, 2009. **98**(1): p. 1-42.
29. Bastiat, G., et al., *Tyrosine-based rivastigmine-loaded organogels in the treatment of Alzheimer's disease.* Biomaterials, 2010. **31**(23): p. 6031-6038.
30. Vintiloiu, A., et al., *In situ-forming oleogel implant for rivastigmine delivery.* Pharmaceutical research, 2008. **25**(4): p. 845-852.
31. Kantaria, S., G.D. Rees, and M.J. Lawrence, *Formulation of electrically conducting microemulsion-based organogels.* International Journal of Pharmaceutics, 2003. **250**(1): p. 65-83.
32. Gupta, P.N., et al., *Non-invasive vaccine delivery in transfersomes, niosomes and liposomes: a comparative study.* International journal of pharmaceutics, 2005. **293**(1): p. 73-82.
33. Willimann, H., et al., *Lecithin organogel as matrix for transdermal transport of drugs.* Journal of pharmaceutical sciences, 1992. **81**(9): p. 871-874.
34. Peppas, N., et al., *Hydrogels in pharmaceutical formulations.* European Journal of Pharmaceutics and Biopharmaceutics, 2000. **50**(1): p. 27-46.
35. Mohd Amin, M.C.I., et al., *Synthesis and characterization of thermo-and pH-responsive bacterial cellulose/acrylic acid hydrogels for drug delivery.* Carbohydrate Polymers, 2012. **88**(2): p. 465-473.
36. Cho, E., J.S. Lee, and K. Webb, *Formulation and characterization of poloxamine-based hydrogels as tissue sealants.* Acta Biomaterialia, 2012. **8**(6): p. 2223-2232.
37. Peppas, N.A., et al., *Hydrogels in pharmaceutical formulations.* European Journal of Pharmaceutics and Biopharmaceutics, 2000. **50**(1): p. 27-46.
38. Manosroi, A., et al., *Transfollicular enhancement of gel containing cationic niosomes loaded with unsaturated fatty acids in rice (Oryza sativa) bran semi-purified fraction.* European journal of pharmaceutics and biopharmaceutics, 2012. **81**(2): p. 303-313.
39. Maver, U., et al., *Novel hybrid silica xerogels for stabilization and controlled release of drug.* International journal of pharmaceutics, 2007. **330**(1): p. 164-174.

40. Sui, R., A.S. Rizkalla, and P.A. Charpentier, *Synthesis and formation of silica aerogel particles by a novel sol-gel route in supercritical carbon dioxide.* The Journal of Physical Chemistry B, 2004. **108**(32): p. 11886-11892.
41. García-González, C.A., M. Alnaief, and I. Smirnova, *Polysaccharide-based aerogels—Promising biodegradable carriers for drug delivery systems.* Carbohydrate Polymers, 2011. **86**(4): p. 1425-1438.
42. Guenther, U., I. Smirnova, and R. Neubert, *Hydrophilic silica aerogels as dermal drug delivery systems–Dithranol as a model drug.* European journal of pharmaceutics and biopharmaceutics, 2008. **69**(3): p. 935-942.
43. Ulker, Z. and C. Erkey, *An emerging platform for drug delivery: Aerogel based systems.* Journal of Controlled Release, 2014. **177**: p. 51-63.
44. Mehling, T., et al., *Polysaccharide-based aerogels as drug carriers.* Journal of Non-Crystalline Solids, 2009. **355**(50–51): p. 2472-2479.
45. Giray, S., et al., *Controlled drug delivery through a novel PEG hydrogel encapsulated silica aerogel system.* Journal of biomedical materials research Part A, 2012. **100**(5): p. 1307-1315.
46. Smirnova, I., et al., *Dissolution rate enhancement by adsorption of poorly soluble drugs on hydrophilic silica aerogels.* Pharmaceutical development and technology, 2004. **9**(4): p. 443-452.
47. Mehling, T., et al., *Polysaccharide-based aerogels as drug carriers.* Journal of Non-Crystalline Solids, 2009. **355**(50): p. 2472-2479.
48. Giray, S., et al., *Controlled drug delivery through a novel PEG hydrogel encapsulated silica aerogel system.* Journal of biomedical materials research Part A, 2012. **100A**(5): p. 1307-1315.
49. Smirnova, I., et al., *Dissolution rate enhancement by adsorption of poorly soluble drugs on hydrophilic silica aerogels.* Pharmaceutical development and technology, 2005. **9**(4): p. 443-452.
50. Veronovski, A., Ž. Knez, and Z. Novak, *Preparation of multi-membrane alginate aerogels used for drug delivery.* The Journal of Supercritical Fluids, 2013. **79**: p. 209-215.
51. Marin, M.A., R.R. Mallepally, and M.A. McHugh, *Silk fibroin aerogels for drug delivery applications.* The Journal of Supercritical Fluids, 2014. **91**: p. 84-89.

52. Del Gaudio, P., et al., *Design of alginate-based aerogel for nonsteroidal anti-inflammatory drugs controlled delivery systems using prilling and supercritical-assisted drying.* Journal of Pharmaceutical Sciences, 2013. **102**(1): p. 185-194.
53. Betz, M., et al., *Preparation of novel whey protein-based aerogels as drug carriers for life science applications.* The Journal of Supercritical Fluids, 2012. **72**: p. 111-119.
54. Valo, H., et al., *Drug release from nanoparticles embedded in four different nanofibrillar cellulose aerogels.* European journal of pharmaceutical sciences, 2013. **50**(1): p. 69-77.
55. Radin, S., et al., *In vivo tissue response to resorbable silica xerogels as controlled-release materials.* Biomaterials, 2005. **26**(9): p. 1043-1052.
56. Li, Z.-Z., et al., *Fabrication of porous hollow silica nanoparticles and their applications in drug release control.* Journal of Controlled Release, 2004. **98**(2): p. 245-254.
57. Sabri, F., et al., *In vivo ultrasonic detection of polyurea crosslinked silica aerogel implants.* PloS one, 2013. **8**(6): p. e66348.
58. Kortesuo, P., et al., *Silica xerogel as an implantable carrier for controlled drug delivery—evaluation of drug distribution and tissue effects after implantation.* Biomaterials, 2000. **21**(2): p. 193-198.
59. Kortesuo, P., et al., *In vitro release of dexmedetomidine from silica xerogel monoliths: effect of sol-gel synthesis parameters.* International journal of pharmaceutics, 2001. **221**(1–2): p. 107-114.
60. Munusamy, P., et al., *Targeted drug delivery using silica xerogel systems to treat diseases due to intracellular pathogens.* Materials Science and Engineering: C, 2009. **29**(8): p. 2313-2318.
61. Kortesuo, P., et al., *Sol-gel-processed sintered silica xerogel as a carrier in controlled drug delivery.* Journal of Biomedical Materials Research, 1999. **44**(2): p. 162-167.
62. Quintanar-Guerrero, D., et al., *Silica xerogels as pharmaceutical drug carriers.* Expert opinion on drug delivery, 2009. **6**(5): p. 301-312.
63. Wu, Z., et al., *Controlled release of lidocaine hydrochloride from the surfactant-doped hybrid xerogels.* Journal of Controlled Release, 2005. **104**(3): p. 497-505.

64. Ahola, M.S., et al., *In vitro release of heparin from silica xerogels.* Biomaterials, 2001. **22**(15): p. 2163-2170.
65. Fonseca, L.S.d., et al., *Nanocapsule@xerogel microparticles containing sodium diclofenac: A new strategy to control the release of drugs.* International journal of pharmaceutics, 2008. **358**(1–2): p. 292-295.
66. Lee, E.-J., et al., *Membrane of hybrid chitosan–silica xerogel for guided bone regeneration.* Biomaterials, 2009. **30**(5): p. 743-750.
67. Dickinson, E., *Hydrocolloids as emulsifiers and emulsion stabilizers.* Food Hydrocolloids, 2009. **23**(6): p. 1473-1482.
68. Aland, S. and A. Voigt, *Simulation of common features and differences of surfactant-based and solid-stabilized emulsions.* Colloids and Surfaces A: Physicochemical and Engineering Aspects, 2012. **413**(0): p. 298-302.
69. Solans, C., N. Azermar, and J. Parra, *High-internal-phase-volume emulsions in water/nonionic surfactant/hydrocarbon systems*, in *Trends in Colloid and Interface Science II*. 1988, Springer. p. 224-227.
70. Peng, J., et al., *Water-in-oil gel emulsions from a cholesterol derivative: Structure and unusual properties.* Journal of Colloid and Interface Science, 2009. **336**(2): p. 780-785.
71. Kunieda, H., et al., *Spontaneous formation of highly concentrated water-in-oil emulsions (gel-emulsions).* Langmuir, 1996. **12**(9): p. 2136-2140.
72. Anton, M., et al., *Filler effects of oil droplets on the rheology of heat-set emulsion gels prepared with egg yolk and egg yolk fractions.* Colloids and Surfaces B: Biointerfaces, 2001. **21**(1–3): p. 137-147.
73. Solans, C., J. Esquena, and N. Azemar, *Highly concentrated (gel) emulsions, versatile reaction media.* Current Opinion in Colloid & Interface Science, 2003. **8**(2): p. 156-163.
74. Zhang, X., R. Zhao, and W. Qian, *Preparation of an emulgel for treatment of aphthous ulcer on the basis of carbomers.* Journal of Clinical Pharmacology, 1995. **30**: p. 417-418.
75. Mohamed, M.I., *Optimization of chlorphenesin emulgel formulation.* The AAPS journal, 2004. **6**(3): p. 81-87.
76. Park, U.S., et al. *Assessment of a new skin brightening emulgel containing glycolic acid, lactic acid, kojic acid, arbutin, and UVA/UVB filters in females with melasma*.

in *Journal of The American Academy of Dermatology*. 2012: Mosby-Elsevier 360 Park Avenue South, Newyork, NY 10010-1710 USA.

77. Brisco, C.M. and J.O. Trimble, *Phase stable lecithin organogel composition*. 2008, Google Patents.
78. Jesitus, J., *Research begins to unlock mysteries behind AD, psoriasis in children.* 2012.
79. Fripiat, J. and J. Uytterhoeven, *Hydroxyl content in silica gel "Aerosil".* The Journal of Physical Chemistry, 1962. **66**(5): p. 800-805.
80. Das, M.K. and A.B. Ahmed, *Formulation and ex vivo evaluation of rofecoxib gel for topical application.* Acta Poloniae Pharmaceutica-Drug Research, 2007. **64**(5): p. 461-7.
81. Fortini, A., *Clustering and gelation of hard spheres induced by the Pickering effect.* Physical Review E, 2012. **85**(4): p. 040401.
82. Newton, D.W., C.H. Becker, and G. Torosian, *Physical and chemical characteristics of water-soluble, semisolid, anhydrous bases for possible ophthalmic use.* Journal of pharmaceutical sciences, 1973. **62**(9): p. 1538-1542.
83. Couffin-Hoarau, A.-C., et al., *In situ-Forming Pharmaceutical Organogels Based on the Self-Assembly of L-Alanine Derivatives.* Pharmaceutical research, 2004. **21**(3): p. 454-457.
84. Wu, Z.L. and J.P. Gong, *Hydrogels with self-assembling ordered structures and their functions.* NPG Asia Mater, 2011. **3**: p. 57-64.
85. Mcintyre, R.A., *Common nano-materials and their use in real world applications.* Science progress, 2012. **95**(1): p. 1-22.
86. Schwertfeger, F., D. Frank, and M. Schmidt, *Hydrophobic waterglass based aerogels without solvent exchange or supercritical drying.* Journal of Non-Crystalline Solids, 1998. **225**: p. 24-29.
87. Gesser, H. and P. Goswami, *Aerogels and related porous materials.* Chemical Reviews, 1989. **89**(4): p. 765-788.
88. Asija, R., *Emulgel: A novel approach to topical drug delivery.* Journal of Biomedical and Pharmaceutical Research, 2013. **2**(6): **2**(6): p. 91-94.
89. Ashara, K.C., et al., *Microemulgel: an overwhelming approach to improve therapeutic action of drug moiety.* Saudi Pharmaceutical Journal, 2014. In press.

90. Studart, A.R., H.C. Shum, and D.A. Weitz, *Arrested Coalescence of Particle-coated Droplets into Nonspherical Supracolloidal Structures†.* The Journal of Physical Chemistry B, 2009. **113**(12): p. 3914-3919.
91. Nagarkar, S.P. and S.S. Velankar, *Morphology and rheology of ternary fluid–fluid–solid systems.* Soft matter, 2012. **8**(32): p. 8464-8477.
92. Jansen, F. and J. Harting, *From Bijels to Pickering emulsions: A lattice Boltzmann study.* Physical Review E, 2011. **83**(4): p. 046707.
93. Tavacoli, J.W., et al., *Novel, Robust, and Versatile Bijels of Nitromethane, Ethanediol, and Colloidal Silica: Capsules, Sub-Ten-Micrometer Domains, and Mechanical Properties.* Advanced Functional Materials, 2011. **21**(11): p. 2020-2027.
94. Witt, J.A., D.R. Mumm, and A. Mohraz, *Bijel reinforcement by droplet bridging: a route to bicontinuous materials with large domains.* Soft Matter, 2013. **9**(29): p. 6773-6780.
95. Di Michele, L., et al., *Aggregation dynamics, structure, and mechanical properties of bigels.* Soft matter, 2014. **10**(20): p. 3633-3648.
96. Stratford, K., et al., *Colloidal jamming at interfaces: A route to fluid-bicontinuous gels.* Science, 2005. **309**(5744): p. 2198-2201.
97. Rehman, K. and M.H. Zulfakar, *Recent advances in gel technologies for topical and transdermal drug delivery.* Drug development and industrial pharmacy, 2013. **40**(4): p. 433-440.
98. Shen, L., et al., *Humidity responsive asymmetric free-standing multilayered film.* Langmuir, 2010. **26**(22): p. 16634-16637.
99. Behera, B., et al., *Mechanical properties and delivery of drug/probiotics from starch and non-starch based novel bigels: A comparative study.* Starch-Stärke, 2014. **66**(9-10): p. 865-879.
100. Abe, H., et al., *Adhesion of Gels by Silica Particle.* The Journal of Physical Chemistry B, 2014. **118**(9): p. 2518-2522.
101. Firoozmand, H. and D. Rousseau, *Tailoring the morphology and rheology of phase-separated biopolymer gels using microbial cells as structure modifiers.* Food Hydrocolloids, (0).
102. Morley, T. and J.R.W. Fisher, *Method of producing a composition from an oleogel and an aqueous gel and the composition*. 2011, Google Patents.

103. Lee, M.N. and A. Mohraz, *Hierarchically porous silver monoliths from colloidal bicontinuous interfacially jammed emulsion gels.* Journal of the American Chemical Society, 2011. **133**(18): p. 6945-6947.
104. Cates, M.E. and P.S. Clegg, *Bijels: a new class of soft materials.* Soft Matter, 2008. **4**(11): p. 2132-2138.
105. Varrato, F., et al., *Arrested demixing opens route to bigels.* Proceedings of the National Academy of Sciences, 2012. **109**(47): p. 19155-19160.
106. Maria, H.J., et al., *Stress relaxation behavior of organically modified montmorillonite filled natural rubber/nitrile rubber nanocomposites.* Applied Clay Science, 2014. **87**: p. 120-128.
107. Bellido, G. and D. Hatcher, *Asian noodles: Revisiting Peleg's analysis for presenting stress relaxation data in soft solid foods.* Journal of food engineering, 2009. **92**(1): p. 29-36.
108. Sadough, S., M. Rahmani, and V. Pouyafar, *Rheological behavior, microstructure and hardness of A356 aluminum alloy in semisolid state using backward extrusion process.* Transactions of Nonferrous Metals Society of China, 2010. **20**: p. s906-s910.
109. Moharamzadeh, K., et al., *Cytotoxicity of resin monomers on human gingival fibroblasts and HaCaT keratinocytes.* dental materials, 2007. **23**(1): p. 40-44.
110. Jain, R., et al., *Novel UV spectrophotometer methods for quantitative estimation of metronidazole and furazolidone using mixed hydrotropy solubilization.* Arabian Journal of Chemistry, 2013.
111. Pasquali, R.C., N. Sacco, and C. Bregni, *Stability of Lipogels with Low Molecular Mass Gelators and Emollient Oils.* Journal of Dispersion Science and Technology, 2010. **31**(4): p. 482-487.
112. Ren, X., et al., *Gelation and fluorescent organogels of a complex of perylenetetracarboxylic tetraacid with cationic surfactants.* Colloids and Surfaces A: Physicochemical and Engineering Aspects, 2011. **375**(1-3): p. 156-162.
113. Schaink, H., et al., *Crystal network for edible oil organogels: possibilities and limitations of the fatty acid and fatty alcohol systems.* Food Research International, 2007. **40**(9): p. 1185-1193.
114. Tolasa, S., C.M. Lee, and S. Cakli, *Physical and Oxidative Stabilization of Omega-3 Fatty Acids in Surimi Gels.* Journal of food science, 2010. **75**(3): p. C305-C310.

115. Cottens, S., et al., *Pharmaceutical compositions*. 2007, US Patent App. 20,070/208,075.
116. Shaikh, I., et al., *Aceclofenac Organogels: In Vitro and In Vivo Characterization.* Current Drug Delivery, 2009. **6**(1): p. 1-7.
117. Li, W.-S., et al., *Glycine and l-glutamic acid-based dendritic gelators.* Tetrahedron, 2007. **63**(36): p. 8794-8800.
118. Sahoo, S., et al., *Organogels: Properties and Applications in drug delivery.* Designed Monomers & Polymers, 2010. **14**(2): p. 95-108.
119. Muik, B., et al., *Two-dimensional correlation spectroscopy and multivariate curve resolution for the study of lipid oxidation in edible oils monitored by FTIR and FT-Raman spectroscopy.* Analytica Chimica Acta, 2007. **593**(1): p. 54-67.
120. Zhang, D., Y. Shen, and G.A. Somorjai, *Studies of surface structures and compositions of polyethylene and polypropylene by IR+ visible sum frequency vibrational spectroscopy.* Chemical Physics Letters, 1997. **281**(4): p. 394-400.
121. Ifuku, S., et al., *Preparation and characterization of redox cellulose Langmuir–Blodgett films containing a ferrocene derivative.* Journal of Polymer Science Part A: Polymer Chemistry, 2005. **43**(21): p. 5023-5031.
122. Pérez-Mateos, M., P. Montero, and M.C. Gómez-Guillén, *Formulation and stability of biodegradable films made from cod gelatin and sunflower oil blends.* Food Hydrocolloids, 2009. **23**(1): p. 53-61.
123. Tahoun, S.A. and M. Mortland, *Complexes of montmorillonite with primary, secondary, and tertiary amides: ii. coordination of amides on the surface of montmorillonite.* Soil Science, 1966. **102**(5): p. 314-321.
124. Yilgor, I., et al., *FTIR investigation of the influence of diisocyanate symmetry on the morphology development in model segmented polyurethanes.* Polymer, 2006. **47**(11): p. 4105-4114.
125. Gellman, S.H., et al., *Conformation-directing effects of a single intramolecular amide-amide hydrogen bond: variable-temperature NMR and IR studies on a homologous diamide series.* Journal of the American Chemical Society, 1991. **113**(4): p. 1164-1173.
126. Luo, X., et al., *Supramolecular organogels formed by monochain derivatives of succinic acid.* Journal of Colloid and Interface Science, 2009. **329**(2): p. 372-375.
127. Evan, M., *Annular extrudate swell of pseudoplastic and viscoplastic fluids.* Journal of Non-Newtonian Fluid Mechanics, 2007. **141**(2-3): p. 138-147.

128. Comba, S. and R. Sethi, *Stabilization of highly concentrated suspensions of iron nanoparticles using shear-thinning gels of xanthan gum.* Water Research, 2009. **43**(15): p. 3717-3726.
129. Fang, P., R.M. Manglik, and M.A. Jog, *Characteristics of laminar viscous shear-thinning fluid flows in eccentric annular channels.* Journal of Non-Newtonian Fluid Mechanics, 1999. **84**(1): p. 1-17.
130. Aguirre-Cruz, A., et al., *Effect of carboxymethylcellulose and xanthan gum on the thermal, functional and rheological properties of dried nixtamalised maize masa.* Carbohydrate Polymers, 2005. **62**(3): p. 222-231.
131. Murdan, S., et al., *Water-in-sorbitan monostearate organogels (water-in-oil gels).* Journal of pharmaceutical sciences, 1999. **88**(6): p. 615-619.
132. Mohamad, M. and R. Jan, *Evaluation of Release Mechanism from Transdermal Matrix System of Aceclofenac.* International Journal of Research in Pharmaceutical and Biomedical Sciences. **3**(2): p. 675-678.
133. Costa, P. and J.M. Sousa Lobo, *Modeling and comparison of dissolution profiles.* European journal of pharmaceutical sciences, 2001. **13**(2): p. 123-133.
134. Dickinson, E. and S.-T. Hong, *Influence of water-soluble nonionic emulsifier on the rheology of heat-set protein-stabilized emulsion gels.* Journal of agricultural and food chemistry, 1995. **43**(10): p. 2560-2566.
135. González-Martínez, C., et al., *Influence of substituting milk powder for whey powder on yoghurt quality.* Trends in Food Science & Technology, 2002. **13**(9–10): p. 334-340.
136. Bryant, C.M. and D.J. McClements, *Molecular basis of protein functionality with special consideration of cold-set gels derived from heat-denatured whey.* Trends in Food Science & Technology, 1998. **9**(4): p. 143-151.
137. Verheul, M. and S.P. Roefs, *Structure of particulate whey protein gels: effect of NaCl concentration, pH, heating temperature, and protein composition.* Journal of agricultural and food chemistry, 1998. **46**(12): p. 4909-4916.
138. Verheul, M. and S. Roefs, *Structure of whey protein gels, studied by permeability, scanning electron microscopy and rheology.* Food Hydrocolloids, 1998. **12**(1): p. 17-24.

139. Segtnan, V.H. and T. Isaksson, *Temperature, sample and time dependent structural characteristics of gelatine gels studied by near infrared spectroscopy.* Food Hydrocolloids, 2004. **18**(1): p. 1-11.
140. Karim, A.A. and R. Bhat, *Fish gelatin: properties, challenges, and prospects as an alternative to mammalian gelatins.* Food Hydrocolloids, 2009. **23**(3): p. 563-576.
141. Clark, A.H., et al., *Structural and mechanical properties of agar/gelatin co-gels. Small-deformation studies.* Macromolecules, 1983. **16**(8): p. 1367-1374.
142. Watthanapimol, S., *Physical and chemical stability of fish oil-in-water emulsions prepared with preheated WPI and maltodextrins.* 2011. Master's Thesis. 2011.
143. Batista, A.P., et al., *Colored Food Emulsions—Implications of Pigment Addition on the Rheological Behavior and Microstructure.* Food Biophysics, 2006. **1**(4): p. 216-227.
144. McClements, D.J., *Protein-stabilized emulsions.* Current Opinion in Colloid & Interface Science, 2004. **9**(5): p. 305-313.
145. Nuyttens, D., et al., *Effect of nozzle type, size and pressure on spray droplet characteristics.* Biosystems Engineering, 2007. **97**(3): p. 333-345.
146. Goy-López, S., et al., *Physicochemical Characteristics of Protein–NP Bioconjugates: The Role of Particle Curvature and Solution Conditions on Human Serum Albumin Conformation and Fibrillogenesis Inhibition.* Langmuir, 2012. **28**(24): p. 9113-9126.
147. Barth, A., *The infrared absorption of amino acid side chains.* Progress in biophysics and molecular biology, 2000. **74**(3-5): p. 141-173.
148. Mishra, R., A.B.A. Majeed, and A. Banthia, *Development and characterization of pectin/gelatin hydrogel membranes for wound dressing.* International Journal of Plastics Technology, 2011: p. 1-14.
149. Du, Y., X. Du, and S. George, *Mechanism of pyridine-catalyzed SiO2 atomic layer deposition studied by Fourier transform infrared spectroscopy.* The Journal of Physical Chemistry C, 2007. **111**(1): p. 219-226.
150. 144. Loeb, J., *The reciprocal relation between the osmotic pressure and the viscosity of gelatin solutions.* The Journal of general physiology, 1921. **4**(1): p. 97-112.
151. Loeb, J., *donnan equilibrium and the physical properties of proteins : iv. viscosity-Continued.* The Journal of general physiology, 1921. **4**(1): p. 73-95.
152. Wilde, P., et al., *Proteins and emulsifiers at liquid interfaces.* Advances in Colloid and Interface Science, 2004. **108–109**: p. 63-71.

153. Johnston-Banks, F., *Gelatine*, in *Food gels*. 1990, Springer. p. 233-289.
154. Javanmard, M., et al., *Characteristics of gelling agent substituted fruit jam: studies on the textural, optical, physicochemical and sensory properties.* International Journal of Food Science & Technology, 2012. **47**(9): p. 1808-1818.
155. Wu, M.Y., et al., *Rheology of Fiber-Enriched Steamed Bread: Stress Relaxation and Texture Profile Analysis.* Journal of Food and Drug Analysis, 2012. **20**(1): p. 133-142.
156. Krupička, A., M. Johansson, and A. Hult, *Viscoelasticity in polymer films on rigid substrates.* Macromolecular Materials and Engineering, 2003. **288**(2): p. 108-116.
157. Badii, F. and N.K. Howell, *Fish gelatin: Structure, gelling properties and interaction with egg albumen proteins.* Food Hydrocolloids, 2006. **20**(5): p. 630-640.
158. Le Tien, C., et al., *Development of biodegradable films from whey proteins by cross-linking and entrapment in cellulose.* Journal of agricultural and food chemistry, 2000. **48**(11): p. 5566-5575.
159. Ye, Y.-J. and J. Ladik, *Theory of hopping conductivity in pig insulin.* Physical Review B, 1993. **48**(8): p. 5120-5126.
160. Dong, Z., Q. Wang, and Y. Du, *Alginate/gelatin blend films and their properties for drug controlled release.* Journal of Membrane Science, 2006. **280**(1–2): p. 37-44.
161. El-Leithy, E., et al., *Optimization and characterization of diclofenac sodium microspheres prepared by a modified coacervation method.* Drug discoveries & therapeutics, 2010. **4**(3): p. 208-216.
162. Wingender, J., T.R. Neu, and H.-C. Flemming, *What are bacterial extracellular polymeric substances?*, in *Microbial extracellular polymeric substances*. 1999, Springer. p. 1-19.
163. Pal, K., et al., *Hydrogel-Based Controlled Release Formulations: Designing Considerations, Characterization Techniques and Applications.* Polymer-Plastics Technology and Engineering, 2013. **52**(14): p. 1391-1422.
164. Gombotz, W.R. and S.F. Wee, *Protein release from alginate matrices.* Advanced drug delivery reviews, 2012. **64, Supplement**: p. 194-205.
165. Chang, C. and L. Zhang, *Cellulose-based hydrogels: Present status and application prospects.* Carbohydrate Polymers, 2011. **84**(1): p. 40-53.
166. Copeland, L., et al., *Form and functionality of starch.* Food Hydrocolloids, 2009. **23**(6): p. 1527-1534.

167. Funami, T., et al., *Effects of non-ionic polysaccharides on the gelatinization and retrogradation behavior of wheat starch ☆.* Food Hydrocolloids, 2005. **19**(1): p. 1-13.

168. Loret, C., et al., *Rheological characterisation of the gelation behaviour of maltodextrin aqueous solutions.* Carbohydrate Polymers, 2004. **57**(2): p. 153-163.

169. Mun, S., D.J. McClements, and J. Surh, *Influence of maltodextrin addition on the freeze-dry stability of β-lactoglobulin-based emulsions with controlled electrostatic and/or steric interactions.* Food Science and Biotechnology, 2011. **20**(4): p. 1143-1150.

170. Timgren, A., et al., *Emulsion stabilizing capacity of intact starch granules modified by heat treatment or octenyl succinic anhydride.* Food Science & Nutrition, 2013. **1**(2): p. 157-171.

171. Bonino, C.A., et al., *Electrospinning alginate-based nanofibers: From blends to crosslinked low molecular weight alginate-only systems.* Carbohydrate Polymers, 2011. **85**(1): p. 111-119.

172. Tanaka, R., et al., *Interaction of hydrophobically modified hydroxyethyl cellulose with various added surfactants.* Macromolecules, 1992. **25**(4): p. 1304-1310.

173. Różańska, S., et al., *Extensional Viscosity and Stability of Oil-in-water Emulsions with Addition Poly (ethylene oxide).* Procedia Engineering, 2012. **42**: p. 733-741.

174. Mora-Gutierrez, A. and I.C. Baianu, *Carbon-13 nuclear magnetic resonance studies of chemically modified waxy maize starch, corn syrups, and maltodextrins. Comparisons with potato starch and potato maltodextrins.* Journal of agricultural and food chemistry, 1991. **39**(6): p. 1057-1062.

175. Kortstee, A.J., et al., *Expression of Escherichia coli branching enzyme in tubers of amylose-free transgenic potato leads to an increased branching degree of the amylopectin.* The Plant Journal, 1996. **10**(1): p. 83-90.

176. Cheetham, N.W. and L. Tao, *Variation in crystalline type with amylose content in maize starch granules: an X-ray powder diffraction study.* Carbohydrate Polymers, 1998. **36**(4): p. 277-284.

177. Wyman, C.E., et al., *Hydrolysis of cellulose and hemicellulose.* Polysaccharides: Structural diversity and functional versatility, 2005. **1**: p. 1023-1062.

178. Sandhu, K.S. and M. Kaur, *Studies on noodle quality of potato and rice starches and their blends in relation to their physicochemical, pasting and gel textural properties.* LWT-Food Science and Technology, 2010. **43**(8): p. 1289-1293.

179. Wang, S. and L. Copeland, *Molecular disassembly of starch granules during gelatinization and its effect on starch digestibility: a review.* Food &Function, 2013. **4**(11): p. 1564-1580.
180. Bertolini, A., *Starches: characterization, properties, and applications*. 2009: CRC Press. Boca Raton, FL, p. 1-19.
181. Silalai, N. and Y.H. Roos, *Mechanical α-relaxations and stickiness of milk solids/maltodextrin systems around glass transition.* Journal of the Science of Food and Agriculture, 2011. **91**(14): p. 2529-2536.
182. Peleg, M. and M. Normand, *Comparison of two methods for stress relaxation data presentation of solid foods.* Rheologica Acta, 1983. **22**(1): p. 108-113.
183. Tabtiang, A., S. Lumlong, and R.A. Venables, *The influence of preparation method upon the structure and relaxation characteristics of poly(methyl methacrylate)/clay composites.* European Polymer Journal, 2000. **36**(12): p. 2559-2568.
184. Lin, J. and L. Chen, *The mechanical-viscoelastic model and WLF relationship in shape memorized linear ether-type polyurethanes.* Journal of Polymer Research, 1999. **6**(1): p. 35-40.
185. Saleem, M., D.R. Kotadia, and R.V. Kulkarni, *Effect of Formulation Variables on Dissolution of Water-Soluble Drug from Polyelectrolyte Complex Beads.* Dissolution Technologies, 2012. **19**(4): p. 21-28.
186. Zobel, H., S. Young, and L. Rocca, *Starch gelatinization: An X-ray diffraction study.* Cereal Chem, 1988. **65**(6): p. 443-446.
187. Epand, R., et al., *Formation of a new stable phase of phosphatidylglycerols.* Biophysical journal, 1992. **63**(2): p. 327-332.
188. Singh, K.P. and P.N. Gupta, *Study of dielectric relaxation in polymer electrolytes.* European Polymer Journal, 1998. **34**(7): p. 1023-1029.
189. Wong, Y.J., J. Hassan, and M. Hashim, *Dielectric properties, impedance analysis and modulus behavior of CaTiO3 ceramic prepared by solid state reaction.* Journal of Alloys and Compounds, 2013. **571**(0): p. 138-144.
190. Yang, G., L. Zhang, and Y. Liu, *Structure and microporous formation of cellulose/silk fibroin blend membranes: I. Effect of coagulants.* Journal of Membrane Science, 2000. **177**(1–2): p. 153-161.
191. Dumoulin, Y., et al., *Cross-linked amylose as matrix for drug controlled release. X-ray and FT-IR structural analysis.* Carbohydrate Polymers, 1998. **37**(4): p. 361-370.

192. Onofre, F., Y.-J. Wang, and A. Mauromoustakos, *Effects of structure and modification on sustained release properties of starches.* Carbohydrate Polymers, 2009. **76**(4): p. 541-547.
193. Abd El-Ghaffar, M.A., et al., *pH-sensitive sodium alginate hydrogels for riboflavin controlled release.* Carbohydrate Polymers, 2012. **89**(2): p. 667-675.
194. Kulkarni, R.V. and B. Sa, *Novel pH-sensitive interpenetrating network hydrogel beads of carboxymethylcellulose-(polyacrylamide-grafted-alginate) for controlled release of ketoprofen: Preparation and characterization.* Current Drug Delivery, 2008. **5**(4): p. 256-264.
195. Ofokansi, K.C. and F.C. Kenechukwu, *Formulation Development and Evaluation of Drug Release Kinetics from Colon-Targeted Ibuprofen Tablets Based on Eudragit RL 100-Chitosan Interpolyelectrolyte Complexes.* ISRN pharmaceutics, 2013. **2013**.
196. Yılmaz, E. and M. Öğütcü, *Properties and Stability of Hazelnut Oil Organogels with Beeswax and Monoglyceride.* Journal of the American Oil Chemists' Society, 2014. **91**(6): p. 1007-1017.
197. Williams, P., et al., *Mixed gels formed with konjac mannan and xanthan gum.* Food polymers, gels and colloids, 199, RSC Special Publication No. 82 Cambridge. p. 339-348.
198. Sandolo, C., et al., *Dynamo-mechanical and rheological characterization of guar gum hydrogels.* European polymer journal, 2007. **43**(8): p. 3355-3367.
199. Fitzsimons, S.M., D.M. Mulvihill, and E.R. Morris, *Large enhancements in thermogelation of whey protein isolate by incorporation of very low concentrations of guar gum.* Food Hydrocolloids, 2008. **22**(4): p. 576-586.
200. Zohuriaan-Mehr, M., et al., *Gum arabic–acrylic superabsorbing hydrogel hybrids: Studies on swelling rate and environmental responsiveness.* Journal of Applied Polymer Science, 2006. **102**(6): p. 5667-5674.
201. Dickinson, E., *Interfacial structure and stability of food emulsions as affected by protein–polysaccharide interactions.* Soft matter, 2008. **4**(5): p. 932-942.
202. Gulrez, S.K., G.O. Phillips, and S. Al-Assaf, *Hydrogels: methods of preparation, characterisation and applications*. 2011: INTECH Open Access Publisher. p. 117-150.

203. Jafari, S.M., et al., *Re-coalescence of emulsion droplets during high-energy emulsification.* Food Hydrocolloids, 2008. **22**(7): p. 1191-1202.
204. Su, L., et al., *Chemical modification of xanthan gum to increase dissolution rate.* Carbohydrate Polymers, 2003. **53**(4): p. 497-499.
205. Moosavi-Nasab, M., S. Pashangeh, and M. Rafsanjani, *Effect of fermentation time on xanthan gum production from sugar beet molasses.* World Academy of Science, Engineering and Technology: p. 68-2010.
206. Chaisawang, M. and M. Suphantharika, *Effects of guar gum and xanthan gum additions on physical and rheological properties of cationic tapioca starch.* Carbohydrate Polymers, 2005. **61**(3): p. 288-295.
207. Roberts, D.D., et al., *Effects of sucrose, guar gum, and carboxymethylcellulose on the release of volatile flavor compounds under dynamic conditions.* Journal of agricultural and food chemistry, 1996. **44**(5): p. 1321-1326.
208. Tsai, R.-Y., et al., *Chitosan/pectin/gum Arabic polyelectrolyte complex: Process-dependent appearance, microstructure analysis and its application.* Carbohydrate polymers, 2014. **101**: p. 752-759.
209. Wientjes, R., et al., *Linear viscoelastic behavior of enzymatically modified guar gum solutions: Structure, relaxations, and gel formation.* Macromolecules, 2001. **34**(17): p. 6014-6023.
210. Mannion, R.O., et al., *Xanthan/locust bean gum interactions at room temperature.* Carbohydrate Polymers, 1992. **19**(2): p. 91-97.
211. Silveira, J.L.M. and T.M.B. Bresolin, *Pharmaceutical use of galactomannans.* Química Nova, 2011. **34**(2): p. 292-299.
212. Arda, E., S. Kara, and Ö. Pekcan, *Synergistic effect of the locust bean gum on the thermal phase transitions of κ-carrageenan gels.* Food Hydrocolloids, 2009. **23**(2): p. 451-459.
213. Copetti, G., et al., *Synergistic gelation of xanthan gum with locust bean gum: a rheological investigation.* Glycoconjugate journal, 1997. **14**(8): p. 951-961.
214. Song, K.-W., H.-Y. Kuk, and G.-S. Chang, *Rheology of concentrated xanthan gum solutions: oscillatory shear flow behavior.* Korea-Australia Rheology Journal, 2006. **18**(2): p. 67-81.
215. Maurer, S., A. Junghans, and T.A. Vilgis, *Impact of xanthan gum, sucrose and fructose on the viscoelastic properties of agarose hydrogels.* Food Hydrocolloids, 2012. **29**(2): p. 298-307.

216. Ptaszek, P. and M. Grzesik, *Viscoelastic properties of maize starch and guar gum gels.* Journal of Food Engineering, 2007. **82**(2): p. 227-237.
217. Raghavan, S.R. and J.F. Douglas, *The conundrum of gel formation by molecular nanofibers, wormlike micelles, and filamentous proteins: gelation without cross-links?* Soft Matter, 2012. **8**(33): p. 8539-8546.
218. Westra, J., *Rheology of carboxymethyl cellulose with xanthan gum properties.* Macromolecules, 1989. **22**(1): p. 367-370.
219. Alamri, M.S., A.A. Mohamed, and S. Hussain, *Effects of alkaline-soluble okra gum on rheological and thermal properties of systems with wheat or corn starch.* Food Hydrocolloids, 2013. **30**(2): p. 541-551.
220. Suresh Kumar, K., et al., *Studies on the functional properties of protein concentrate of Kappaphycus alvarezii (Doty) Doty – An edible seaweed.* Food Chemistry, 2014. **153**(0): p. 353-360.
221. Chaisawang, M. and M. Suphantharika, *Pasting and rheological properties of native and anionic tapioca starches as modified by guar gum and xanthan gum.* Food Hydrocolloids, 2006. **20**(5): p. 641-649.
222. Gulrez, S.K., S. Al-Assaf, and G.O. Phillips, *Hydrogels: methods of preparation, characterisation and applications.* Progress in molecular and environmental bioengineering—from analysis and modeling to technology applications. InTech, Winchester, 2011: p. 117-150.
223. Kanungo, I., et al., *Influence of PCL on the material properties of collagen based biocomposites and in vitro evaluation of drug release.* Materials Science and Engineering: C, 2013. **33**(8): p. 4651-4659.
224. Varshosaz, J., N. Tavakoli, and F. Kheirolahi, *Use of hydrophilic natural gums in formulation of sustained-release matrix tablets of tramadol hydrochloride.* Aaps Pharmscitech, 2006. **7**(1): p. E168-E174.
225. Jaipal, A., et al., *Interaction of calcium sulfate with xanthan gum: Effect on in vitro bioadhesion and drug release behavior from xanthan gum based buccal discs of buspirone.* Colloids and surfaces B: Biointerfaces, 2013. **111**: p. 644-650.
226. Avadi, M.R., et al., *Preparation and characterization of insulin nanoparticles using chitosan and Arabic gum with ionic gelation method.* Nanomedicine: Nanotechnology, Biology and Medicine, 2010. **6**(1): p. 58-63.

227. Naik, D.R. and J.P. Raval, *Amorphous polymeric binary blend pH-responsive nanoparticles for dissolution enhancement of antiviral drug.* Journal of Saudi Chemical Society, 2012. In press.
228. Siepmann, J. and N.A. Peppas, *Modeling of drug release from delivery systems based on hydroxypropyl methylcellulose (HPMC).* Advanced drug delivery reviews, 2001. **48**(2–3): p. 139-157.
229. Behera, B., et al., *Mechanical properties and delivery of drug/probiotics from starch and non-starch based novel bigels: A comparative study.* Starch-Stärke, 2014. **66** (1-10): p. 865-879.
230. Leuner, C. and J. Dressman, *Improving drug solubility for oral delivery using solid dispersions.* European Journal of Pharmaceutics and Biopharmaceutics, 2000. **50**(1): p. 47-60.
231. Qiao, J., et al., *Alkaline solid polymer electrolyte membranes based on structurally modified PVA/PVP with improved alkali stability.* Polymer, 2010. **51**(21): p. 4850-4859.
232. Wang, W. and A. Wang, *Synthesis and swelling properties of pH-sensitive semi-IPN superabsorbent hydrogels based on sodium alginate-g-poly(sodium acrylate) and polyvinylpyrrolidone.* Carbohydrate Polymers, 2010. **80**(4): p. 1028-1036.
233. Chiellini, E., et al., *Biodegradation of poly (vinyl alcohol) based materials.* Progress in Polymer Science, 2003. **28**(6): p. 963-1014.
234. Takeshita, H., et al., *Spinodal Decomposition and Syneresis of PVA Gel.* Macromolecules, 2001. **34**(22): p. 7894-7898.
235. Kobayashi, M., et al., *Structural study of poly(vinyl alcohol) in the gel state by high-resolution solid-state 13C NMR spectroscopy.* Macromolecules, 1995. **28**(19): p. 6677-6679.
236. Nakane, K., et al., *Properties and structure of poly (vinyl alcohol)/silica composites.* Journal of Applied Polymer Science, 1999. **74**(1): p. 133-138.
237. Kanaya, T., et al., *Structure of poly (vinyl alcohol) gels studied by wide-and small-angle neutron scattering.* Macromolecules, 1994. **27**(20): p. 5609-5615.
238. Wang, B., et al., *Amperometric enzyme electrode for the determination of hydrogen peroxide based on sol–gel/hydrogel composite film.* Analytica Chimica Acta, 2000. **407**(1–2): p. 111-118.

239. Chari, K., *The structure of the PVP SDS complex in water.* Journal of Colloid and Interface Science, 1992. **151**(1): p. 294-296.

240. Paudel, A., E. Nies, and G. Van den Mooter, *Relating Hydrogen-Bonding Interactions with the Phase Behavior of Naproxen/PVP K 25 Solid Dispersions: Evaluation of Solution-Cast and Quench-Cooled Films.* Molecular Pharmaceutics, 2012. **9**(11): p. 3301-3317.

241. Sahoo, S.K., et al., *Residual polyvinyl alcohol associated with poly (D, L-lactide-co-glycolide) nanoparticles affects their physical properties and cellular uptake.* Journal of Controlled Release, 2002. **82**(1): p. 105-114.

242. Arpornpong, N., et al., *Ethanol-in-palm oil/diesel microemulsion-based biofuel: Phase behavior, viscosity, and droplet size.* Fuel, 2014. **132**(0): p. 101-106.

243. Yeh, J.T., et al., *Synthesis, characterization, and application of PVP/chitosan blended polymers.* Journal of Applied Polymer Science, 2006. **101**(2): p. 885-891.

244. Jones, D.S., A.D. Woolfson, and A.F. Brown, *Textural, viscoelastic and mucoadhesive properties of pharmaceutical gels composed of cellulose polymers.* International journal of pharmaceutics, 1997. **151**(2): p. 223-233.

245. Mbhele, Z., et al., *Fabrication and characterization of silver-polyvinyl alcohol nanocomposites.* Chemistry of Materials, 2003. **15**(26): p. 5019-5024.

246. Mohamed, S.A., et al., *Effect of ethylene carbonate as a plasticizer on CuI/PVA nanocomposite: Structure, optical and electrical properties.* Journal of Advanced Research, 2014. **5**(1): p. 79-86.

247. Sengwa, R.J. and S. Sankhla, *Dielectric dispersion study of coexisting phases of aqueous polymeric solution: Poly(vinyl alcohol)+poly(vinyl pyrrolidone) two-phase systems.* Polymer, 2007. **48**(9): p. 2737-2744.

248. Sang, S., et al., *Influences of Bentonite on conductivity of composite solid alkaline polymer electrolyte PVA-Bentonite-KOH-H_2O.* Electrochimica Acta, 2007. **52**(25): p. 7315-7321.

249. Kumari, N., V. Kumar, and S.K. Singh, *Synthesis, structural and dielectric properties of Cr3+ substituted Fe3O4 nano-particles.* Ceramics International, 2014. **40**(8, Part A): p. 12199-12205.

250. Leitão, A.F., et al., *Hemocompatibility study of a bacterial cellulose/polyvinyl alcohol nanocomposite.* Colloids and Surfaces B: Biointerfaces, 2013. **111**: p. 493-502.

251. Şanlı, O., N. Ay, and N. Işıklan, *Release characteristics of diclofenac sodium from poly(vinyl alcohol)/sodium alginate and poly(vinyl alcohol)-grafted-*

poly(acrylamide)/sodium alginate blend beads. European Journal of Pharmaceutics and Biopharmaceutics, 2007. **65**(2): p. 204-214.

252. Yang, Y.-Y., T.-S. Chung, and N. Ping Ng, *Morphology, drug distribution, and in vitro release profiles of biodegradable polymeric microspheres containing protein fabricated by double-emulsion solvent extraction/evaporation method.* Biomaterials, 2001. **22**(3): p. 231-241.

253. Patel, V., B. Prajapati, and M. Patel, *Design and characterization of chitosan-containing mucoadhesive buccal patches of propranolol hydrochloride.* Acta pharmaceutica, 2007. **57**(1): p. 61-72.

ANNEXURE-1

Materials used

Materials used	Specification
Sorbitan monopalmitate (Span 40)	MW: 402.64 Hydroxyl value: 270-305 Saponification value 140-155 Identity (IR) Passes test
Gelatin	Maximum limits of impurities Calcium: 0.2% Chloride: 0.2%
Sodium alginate	Viscosity- 1% w/v solution, 25 °C : 5.5 ± 2 cps
Maltodextrin	dextrose equivalent, DE < = 20% Maximum limits of impurities Total protein 0.1%% Heavy metals (as Pb) 0.005%
Carboxymethyl cellulose sodium salt	Assay (as Na; on dried basis) 6.5-10.0% pH value (1% w/v water) 6.0-8.0 Viscosity- 1% w/v solution, 20 °C: 1100-1900 cps Maximum limits of impurities Chloride: 0.25% Arsenic: 0.0003% Heavy metals (as Pb): 0.0020% Loss on drying: 10% Sulphated ash (on dried substance): 20.0-33.3%
Starch soluble	pH value (2% water) 6-7.5 Sensitivity passes test Loss on drying (105 °C) ≤ 10% Sulfated ash ≤ 0.35%
Acacia gum	Loss on drying NMT 15.0% Ash NMT 6.0%
Xanthan gum pure (food grade)	Loss on drying 15.0% Odour feeble no desabreable Particle size :100-200 mesh Ash: 6.5-16.0% pH of 1 % sol. In water 6.0-8.0 Nitrogen 1.5% Pyruvic acid 2.40% Heavy metals (as lead) 0.001% Lead (Pb) 0.0005% Arsenic(As) 0.0002%
PVP K30	Assay of Nitrogen(N): 11.5% to 12.8% Maximum limits of impurities Heavy metals (as Pb): 0.001% Loss on drying: 5.0% K value (Intrinsic velocity): 29-32

PVA	MW: 115000 Maximum limits of impurities Chloride(Cl): 0.001% Viscosity: 4-6 cps (4% aqueous solution, 20 °C
Nutrient broth	Peptic digest of animal tissue 5 g/l Sodium chloride 5 g/l Beef extract 1.50 g/l Yeast extract 1.50 g/l Final pH (at 25 °C) 7.4±0.2
Nutrient agar	Peptic digest of animal tissue 5 g/l Sodium chloride 5 g/l Beef extract 1.50 g/l Yeast extract 1.50 g/l Agar 15.00 g/l Final pH (at 25 °C) 7.4±0.2

THESIS DISSEMINATION

PUBLICATIONS-JOURNALS

Published papers

1. **Behera B.**; Sagiri S. S.; Pal K.*; Srivastava A., Modulating the physical properties of sunflower oil and sorbitan monopalmitate-based organogels. *Journal of Applied Polymer Science.* **2013,** *127* (6), 4910-17.
2. **Behera B.**; Sagiri S. S.; Singh V. K.; Pal K.*; Anis A., Mechanical properties and delivery of drug/probiotics from starch and non-starch based novel bigels: A comparative study. *Starch – Stärke.* **2014,** *66* (9-10), 865-79.
3. **Behera B.**; Sagiri S. S.; Pal K.*; Pramanik K.; Usman Ali Rana; Imran Shaki; Arfat Anis, Sunflower oil and protein based novel bigels as matrices for drug delivery applications- Characterization and in vitro antimicrobial efficiency. *Polymer - Plastics Technology and Engineering*. 2015. *54*(8), 837-850.
4. **Behera, B.**; Dey S.; Sharma V.; K. Pal*, Rheological and viscoelastic properties of novel sunflower oil-span 40-biopolymer based bigels and their role as functional material in the delivery of antimicrobial agents. *Advances in Polymer Technology*. 2015, 34(2).
5. **Behera, B.;** Singh V. K.; Kulanthaivel S.; Bhattacharya M. K.; Paramanik K.; Banerjee I.; Pal K.*; Physical and Mechanical properties of sunflower oil and synthetic polymers based bigels for the delivery of nitroimidazole antibiotic-A therapeutic approach for controlled drug delivery. *European polymer journal*. 2015, 64, 253-264.
6. **Behera B.;** Biswal D.; Uvanesh K.; Srivastava A. K.; Bhattacharya M. K.; Paramanik K.; Pal K.*; Modulating the properties of sunflower oil based novel emulgels using castor oil fatty acid ester: Prospects for topical antimicrobial drug delivery. *Colloids and Surfaces* .2015, 128, 155-164.

BIOGRAPHY

Beauty Behera received her B. Pharm degree in 2006 from Delhi Institute of Pharmaceutical Sciences and Research (DIPSAR), New Delhi. She did her M.Pharm (Pharmacuetics) from Indian Institute of Technology, Banaras Hindu University, Varanasi, (IIT, BHU) India. Currently she is pursuing her Ph.D. in Biotechnology and Medical Engineering from National Institute of Technology Rourkela, India. Her research interests include drug, probiotics delivery and development of biomaterials for pharmaceutical and nutraceutical applications

Personal details

Father's name:	Mr. K.C Behera
Mother's name:	Mrs. Arti Bala Behera
Date of Birth:	02nd Mar. 1985
Gender:	Female
Nationality:	Indian
Languages known:	English, Hindi, Oriya and Bengali
Permanent Address	N-40 Hargobind Enclave, Rajpur Khurd Extn., New Delhi-110068